

# Performance Evaluation of Arizona's LTPP SPS-5 Project: Strategic Study of Rehabilitation of Asphalt Concrete Pavements



Arizona Department of Transportation Research Center



# **Performance Evaluation of Arizona's LTPP SPS-5 Project: Strategic Study of Rehabilitation of Asphalt Concrete Pavements**

**SPR-396-5  
June 2015**

**Prepared by:**

Peter N. Schmalzer  
Nichols Consulting Engineers  
1885 S. Arlington Avenue, Suite 111  
Reno, NV 89509-3370

Steven M. Karamihas  
The University of Michigan Transportation Research Institute  
2901 Baxter Road  
Ann Arbor, MI 48109

Timin Punnackal  
Hans Meyer  
Kevin Senn  
Jason Puccinelli  
Nichols Consulting Engineers  
1885 S. Arlington Avenue, Suite 111  
Reno, NV 89509-3370

**Published by:**

Arizona Department of Transportation  
206 S. 17th Avenue  
Phoenix, AZ 85007  
in cooperation with  
US Department of Transportation  
Federal Highway Administration

This report was funded in part through grants from the Federal Highway Administration, US Department of Transportation. The contents of this report reflect the views of the authors, who are responsible for the facts and the accuracy of the data, and for the use or adaptation of previously published material, presented herein. The contents do not necessarily reflect the official views or policies of the Arizona Department of Transportation or the Federal Highway Administration, US Department of Transportation. This report does not constitute a standard, specification, or regulation. Trade or manufacturers' names that may appear herein are cited only because they are considered essential to the objectives of the report. The US government and the State of Arizona do not endorse products or manufacturers.

## Technical Report Documentation Page

1. Report No. FHWA-AZ-15-396(5)		2. Government Accession No		3. Recipient's Catalog No.	
4. Title and Subtitle Performance Evaluation of Arizona's LTPP SPS-5 Project: Strategic Study of Rehabilitation of Asphalt Concrete Pavements				5. Report Date June 2015	
				6. Performing Organization Code	
7. Author(s) Peter N. Schmalzer, Steven M. Karamihas, Timin Punnackal, Hans Meyer, Kevin Senn, Jason Puccinelli				8. Performing Organization Report No.	
9. Performing Organization Name and Address Nichols Consulting Engineers 1885 S. Arlington Avenue Suite 111 Reno, NV 89509-3370				10. Work Unit No. (TRAI5)	
				11. Contract or Grant No. SPR 000-1(147) 396	
12. Sponsoring Agency Name and Address Arizona Department of Transportation 206 S. 17th Avenue Phoenix, AZ 85007				13. Type of Report and Period Covered FINAL REPORT	
				14. Sponsoring Agency Code	
15. Supplementary Notes Prepared in cooperation with the US Department of Transportation, Federal Highway Administration.					
16. Abstract As part of the Long Term Pavement Performance (LTPP) Program, the Arizona Department of Transportation (ADOT) constructed 11 Specific Pavement Study-5 (SPS-5) test sections on Interstate 8 near Casa Grande. The SPS-5 project studied a variety of different rehabilitation methods for asphalt concrete pavements. The project was opened to traffic in 1990 and monitored at regular intervals until it was placed out of study in 2009. Surface distress, profile, and deflection data collected throughout the life of the pavement were used to evaluate the performance of rehabilitation methods using unique combinations of minimal and intensive surface preparation, virgin and recycled asphalt, and thick and thin overlay thicknesses. This report documents the analyses conducted as well as practical findings and lessons learned that will be of interest to ADOT.					
17. Key Words LTPP, pavement performance, rehabilitation, profile, distress, FWD, flexible, AC, deflections, roughness, backcalculation		18. Distribution Statement Document is available to the U.S. public through the National Technical Information Service, Springfield, VA, 22161		23. Registrant's Seal	
19. Security Classification Unclassified	20. Security Classification Unclassified	21. No. of Pages 178	22. Price		

# SI\* (MODERN METRIC) CONVERSION FACTORS

## APPROXIMATE CONVERSIONS TO SI UNITS

Symbol	When You Know	Multiply By	To Find	Symbol
<b>LENGTH</b>				
in	inches	25.4	millimeters	mm
ft	feet	0.305	meters	m
yd	yards	0.914	meters	m
mi	miles	1.61	kilometers	km
<b>AREA</b>				
in <sup>2</sup>	square inches	645.2	square millimeters	mm <sup>2</sup>
ft <sup>2</sup>	square feet	0.093	square meters	m <sup>2</sup>
yd <sup>2</sup>	square yard	0.836	square meters	m <sup>2</sup>
ac	acres	0.405	hectares	ha
mi <sup>2</sup>	square miles	2.59	square kilometers	km <sup>2</sup>
<b>VOLUME</b>				
fl oz	fluid ounces	29.57	milliliters	mL
gal	gallons	3.785	liters	L
ft <sup>3</sup>	cubic feet	0.028	cubic meters	m <sup>3</sup>
yd <sup>3</sup>	cubic yards	0.765	cubic meters	m <sup>3</sup>
NOTE: volumes greater than 1000 L shall be shown in m <sup>3</sup>				
<b>MASS</b>				
oz	ounces	28.35	grams	g
lb	pounds	0.454	kilograms	kg
T	short tons (2000 lb)	0.907	megagrams (or "metric ton")	Mg (or "t")
<b>TEMPERATURE (exact degrees)</b>				
°F	Fahrenheit	5 (F-32)/9 or (F-32)/1.8	Celsius	°C
<b>ILLUMINATION</b>				
fc	foot-candles	10.76	lux	lx
fl	foot-Lamberts	3.426	candela/m <sup>2</sup>	cd/m <sup>2</sup>
<b>FORCE and PRESSURE or STRESS</b>				
lbf	poundforce	4.45	newtons	N
lbf/in <sup>2</sup>	poundforce per square inch	6.89	kilopascals	kPa

## APPROXIMATE CONVERSIONS FROM SI UNITS

Symbol	When You Know	Multiply By	To Find	Symbol
<b>LENGTH</b>				
mm	millimeters	0.039	inches	in
m	meters	3.28	feet	ft
m	meters	1.09	yards	yd
km	kilometers	0.621	miles	mi
<b>AREA</b>				
mm <sup>2</sup>	square millimeters	0.0016	square inches	in <sup>2</sup>
m <sup>2</sup>	square meters	10.764	square feet	ft <sup>2</sup>
m <sup>2</sup>	square meters	1.195	square yards	yd <sup>2</sup>
ha	hectares	2.47	acres	ac
km <sup>2</sup>	square kilometers	0.386	square miles	mi <sup>2</sup>
<b>VOLUME</b>				
mL	milliliters	0.034	fluid ounces	fl oz
L	liters	0.264	gallons	gal
m <sup>3</sup>	cubic meters	35.314	cubic feet	ft <sup>3</sup>
m <sup>3</sup>	cubic meters	1.307	cubic yards	yd <sup>3</sup>
<b>MASS</b>				
g	grams	0.035	ounces	oz
kg	kilograms	2.202	pounds	lb
Mg (or "t")	megagrams (or "metric ton")	1.103	short tons (2000 lb)	T
<b>TEMPERATURE (exact degrees)</b>				
°C	Celsius	1.8C+32	Fahrenheit	°F
<b>ILLUMINATION</b>				
lx	lux	0.0929	foot-candles	fc
cd/m <sup>2</sup>	candela/m <sup>2</sup>	0.2919	foot-Lamberts	fl
<b>FORCE and PRESSURE or STRESS</b>				
N	newtons	0.225	poundforce	lbf
kPa	kilopascals	0.145	poundforce per square inch	lbf/in <sup>2</sup>

\*SI is the symbol for the International System of Units. Appropriate rounding should be made to comply with Section 4 of ASTM E380. (Revised March 2003)

# Contents

<b>EXECUTIVE SUMMARY .....</b>	<b>1</b>
<b>CHAPTER 1. INTRODUCTION .....</b>	<b>3</b>
<b>CHAPTER 2. SPS-5 DEFLECTION ANALYSIS.....</b>	<b>15</b>
Normalized Deflections .....	16
AASHTO 1993 Analysis.....	19
Backcalculation .....	59
Deflection Analysis Key Findings .....	85
<b>CHAPTER 3. SPS-5 DISTRESS ANALYSIS .....</b>	<b>87</b>
AC Distress Types.....	87
Research Approach.....	88
Overall Performance Trend Observations .....	89
Distress Analysis Key Findings .....	101
<b>CHAPTER 4. SPS-5 ROUGHNESS ANALYSIS .....</b>	<b>107</b>
Profile Data Synchronization .....	107
Data Extraction .....	108
Cross Correlation .....	108
Longitudinal Distance Measurement .....	110
Data Quality Screening .....	111
Summary Roughness Values.....	118
Profile Analysis Tools .....	124
Distress Surveys and Maintenance Records.....	131
Detailed Observations .....	131
Profile Analysis Key Findings .....	131
<b>CHAPTER 5. CONCLUSIONS AND RECOMMENDATIONS .....</b>	<b>137</b>
Deflection Analysis .....	137
Distress Analysis .....	138
Profile Analysis.....	138
<b>REFERENCES.....</b>	<b>141</b>
<b>APPENDIX A: CONSTRUCTION DEVIATIONS .....</b>	<b>143</b>
<b>APPENDIX B: SITE WORK HISTORY .....</b>	<b>145</b>
<b>APPENDIX C: ROUGHNESS VALUES .....</b>	<b>148</b>
<b>APPENDIX D: DETAILED OBSERVATIONS.....</b>	<b>153</b>

## List of Figures

Figure 1. Location of Arizona SPS-5 Test Sections .....	4
Figure 2. Layout of the SPS-5 Project.....	5
Figure 3. Existing Asphalt Concrete Pavement Cross Section Before SPS-5 Project Construction (from Hossain et al. 1996) .....	7
Figure 4. Subgrade Resilient Modulus versus Station, Section 040507.....	24
Figure 5. Subgrade Resilient Modulus versus Date, Section 040507.....	24
Figure 6. $SN_{eff}$ versus Station, Section 040507.....	25
Figure 7. $SN_{eff}$ versus Date, Section 040507.....	26
Figure 8. Subgrade Resilient Modulus versus Station, Section 040504.....	27
Figure 9. Subgrade Resilient Modulus versus Date, Section 040504.....	28
Figure 10. $SN_{eff}$ versus Station, Section 040504.....	29
Figure 11. $SN_{eff}$ versus Date, Section 040504.....	29
Figure 12. Subgrade Resilient Modulus versus Station, Section 040503.....	31
Figure 13. Subgrade Resilient Modulus versus Date, Section 040503.....	31
Figure 14. $SN_{eff}$ versus Station, Section 040503.....	32
Figure 15. $SN_{eff}$ versus Date, Section 040503.....	32
Figure 16. $M_r$ versus Station, Section 040508.....	34
Figure 17. $M_r$ versus Date, Section 040508 .....	35
Figure 18. $SN_{eff}$ versus Station, Section 040508.....	35
Figure 19. $SN_{eff}$ versus Date, Section 040508.....	36
Figure 20. $M_r$ versus Station, Section 040509.....	38
Figure 21. $M_r$ versus Date, Section 040509 .....	38
Figure 22. $SN_{eff}$ versus Station, Section 040509.....	39
Figure 23. $SN_{eff}$ versus Date, Section 040509.....	39
Figure 24. $M_r$ versus Station, Section 040502.....	41
Figure 25. $M_r$ versus Date, Section 040502 .....	41
Figure 26. $SN_{eff}$ versus Station, Section 040502.....	42
Figure 27. $SN_{eff}$ versus Date, Section 040502.....	42
Figure 28. $M_r$ versus Station, Section 040506.....	44
Figure 29. $M_r$ versus Date, Section 040506 .....	44
Figure 30. $SN_{eff}$ versus Station, Section 040506.....	45
Figure 31. $SN_{eff}$ versus Date, Section 040506.....	45
Figure 32. $M_r$ versus Station, Section 040505.....	47
Figure 33. $M_r$ versus Date, Section 040505 .....	47
Figure 34. $SN_{eff}$ versus Station, Section 040505.....	48
Figure 35. $SN_{eff}$ versus Date, Section 040505.....	48
Figure 36. $M_r$ versus Station, Section 040559.....	50
Figure 37. $M_r$ versus Date, Section 040559 .....	50
Figure 38. $SN_{eff}$ versus Station, Section 040559.....	51
Figure 39. $SN_{eff}$ versus Date, Section 040559.....	51

Figure 40. $M_r$ versus Station, Section 040560.....	53
Figure 41. $M_r$ versus Date, Section 040560 .....	53
Figure 42. $SN_{eff}$ versus Station, Section 040560.....	54
Figure 43. $SN_{eff}$ versus Date, Section 040560.....	54
Figure 44. $M_r$ versus Station, Section 040501.....	56
Figure 45. $M_r$ versus Date, Section 040501 .....	56
Figure 46. $SN_{eff}$ versus Station, Section 040501.....	57
Figure 47. $SN_{eff}$ versus Date, Section 040501.....	57
Figure 48. Subgrade Modulus Increase versus $SN_{eff}$ Increase.....	81
Figure 49. Measured versus Synthetic Deflection Basins .....	83
Figure 50. Hysteresis Plot, Section 040507 (Stiff Layer Phenomenon).....	85
Figure 51. Hysteresis Plot, Section 040559 (Stiff Layer Phenomenon Not Observed) .....	85
Figure 52. Structural and Environmental Distress Trends in Section 040501 .....	91
Figure 53. Structural and Environmental Distress Trends in Section 040502 .....	91
Figure 54. Structural and Environmental Distress Trends in Section 040503 .....	91
Figure 55. Structural and Environmental Distress Trends in Section 040504 .....	91
Figure 56. Structural and Environmental Distress Trends in Section 040505 .....	92
Figure 57. Structural and Environmental Distress Trends in Section 040506 .....	92
Figure 58. Structural and Environmental Distress Trends in Section 040507 .....	92
Figure 59. Structural and Environmental Distress Trends in Section 040508 .....	92
Figure 60. Structural and Environmental Distress Trends in Section 040509 .....	93
Figure 61. Structural and Environmental Distress Trends in Section 040559 .....	93
Figure 62. Structural and Environmental Distress Trends in Section 040560 .....	93
Figure 63. 2002 Structural Performance of All SPS-5 Sections .....	94
Figure 64. 2002 Environmental Performance of All SPS-5 Sections .....	95
Figure 65. 2005 Structural Performance of SPS-5 Core Sections.....	95
Figure 66. 2005 Environmental Performance of SPS-5 Core Sections.....	96
Figure 67. 2002 Rutting Index Summary of All SPS-5 Sections .....	96
Figure 68. 2005 Rutting Index Summary of SPS-5 Core Sections.....	97
Figure 69. Fatigue Cracking and AC Material Thicknesses.....	98
Figure 70. Consistency in Longitudinal Distance Measurement.....	110
Figure 71. IRI Progression of Section 040501 .....	118
Figure 72. IRI Progression of Section 040502 .....	119
Figure 73. IRI Progression of Section 040503 .....	119
Figure 74. IRI Progression of Section 040504 .....	120
Figure 75. IRI Progression of Section 040505 .....	120
Figure 76. IRI Progression of Section 040506 .....	121
Figure 77. IRI Progression of Section 040507 .....	121
Figure 78. IRI Progression of Section 040508 .....	122
Figure 79. IRI Progression of Section 040509 .....	122
Figure 80. IRI Progression of Section 040559 .....	123
Figure 81. IRI Progression of Section 040560 .....	123

Figure 82. PSD of Section 040502 Profiles (Left Side).....	125
Figure 83. PSD of Section 040508 Profiles (Left Side).....	126
Figure 84. Raw Profiles of Section 040509 .....	127
Figure 85. Filtered Profiles of Section 040509 .....	128
Figure 86. Long-Wavelength Profiles of Section 040560.....	128
Figure 87. Roughness Profile of Section 040503 (25-ft Base Length).....	130
Figure 88. Roughness Profiles of Section 040509 (10-ft Base Length) .....	130
Figure C-1. Comparison of HRI to MRI. ....	1499
Figure D-1. Roughness Profiles of Section 040506 (10-ft Base Length).....	162

## List of Tables

Table 1. Arizona SPS-5 Project Layout, Post-Rehabilitation.....	6
Table 2. Summary of SPS-5 Test Sections (from Hossain et al. 1996) .....	7
Table 3. Summary of Preconstruction Distress in Travel Lane .....	8
Table 4. Summary of Section Performance .....	9
Table 5. Climatic Information for SPS-5 .....	12
Table 6. Traffic Loading Summary.....	13
Table 7. FWD Test Dates by Section .....	15
Table 8. Normalized Deflections .....	17
Table 9. Summary of AASHTO 1993 Analysis of FWD Data .....	21
Table 10. Preconstruction $SN_{eff}$ Variation by Overlay Material .....	22
Table 11. Preconstruction $SN_{eff}$ Variation by Overlay Thickness .....	22
Table 12. Preconstruction $SN_{eff}$ Variation by Level of Surface Preparation.....	23
Table 13. Layer Structure, Section 040507 .....	23
Table 14. Layer Structure, Section 040504 .....	27
Table 15. Layer Structure, Section 040503 .....	30
Table 16. Layer Structure, Section 040508 .....	33
Table 17. Layer Structure, Section 040509 .....	37
Table 18. Layer Structure, Section 040502 .....	40
Table 19. Layer Structure, Section 040506 .....	43
Table 20. Layer Structure, Section 040505 .....	46
Table 21. Layer Structure, Section 040559 .....	49
Table 22. Layer Structure, Section 040560 .....	52
Table 23. Layer Structure, Section 040501 .....	55
Table 24. $SN_{eff}$ Increase by Overlay Material .....	58
Table 25. $SN_{eff}$ Increase by Overlay Thickness .....	58
Table 26. $SN_{eff}$ Increase by Level of Surface Preparation.....	59
Table 27. Summary of $SN_{eff}$ Increase by Experimental Factor .....	59
Table 28. Layer Models for Backcalculation, Section 040507.....	61
Table 29. Backcalculation Results, Section 040507 .....	62
Table 30. Layer Models for Backcalculation, Section 040504.....	63
Table 31. Backcalculation Results, Section 040504 .....	64
Table 32. Layer Models, Section 040503 .....	65
Table 33. Backcalculation Results, Section 040503 .....	65
Table 34. Layer Models, Section 040508 .....	66
Table 35. Backcalculation Results, Section 040508 .....	67
Table 36. Layer Models, Section 040509 .....	67
Table 37. Backcalculation Results, Section 040509 .....	68
Table 38. Layer Models, Section 040502 .....	69
Table 39. Backcalculation Results, Section 040502 .....	70
Table 40. Layer Models, Section 040506 .....	71

Table 41. Backcalculation Results, Section 040506 .....	71
Table 42. Layer Models, Section 040505 .....	72
Table 43. Backcalculation Results, Section 040505 .....	73
Table 44. Layer Models, Section 040559 .....	74
Table 45. Backcalculation Results, Section 040559 .....	74
Table 46. Layer Models, Section 040560 .....	75
Table 47. Backcalculation Results, Section 040560 .....	76
Table 48. Layer Model, Section 040501.....	77
Table 49. Backcalculation Results, Section 040501 .....	77
Table 50. Measured and Temperature-Corrected AC Moduli .....	78
Table 51. Nonlinearity of AB Modulus .....	78
Table 52. Nonlinear Layer Parameters .....	79
Table 53. Nonlinear Backcalculation Results .....	79
Table 54. Postconstruction $SN_{eff}$ Increase .....	80
Table 55. Measured and Synthetic Deflection Basins.....	82
Table 57. Flexible Pavement Distress Types and Failure Mechanisms .....	88
Table 58. MDS Dates by Section .....	90
Table 59. Core Section Performance Against Structural Distresses .....	103
Table 60. Core Section Performance Against Environmental Distresses.....	103
Table 61. Profile Measurement Visits of the SPS-5 Site.....	107
Table 62. Selected Repeats of Section 040501 .....	112
Table 63. Selected Repeats of Section 040502 .....	112
Table 64. Selected Repeats of Section 040503 .....	113
Table 65. Selected Repeats of Section 040504 .....	113
Table 66. Selected Repeats of Section 040505 .....	114
Table 67. Selected Repeats of Section 040506 .....	114
Table 68. Selected Repeats of Section 040507 .....	115
Table 69. Selected Repeats of Section 040508 .....	115
Table 70. Selected Repeats of Section 040509 .....	116
Table 71. Selected Repeats of Section 040559 .....	116
Table 72. Selected Repeats of Section 040560 .....	117
Table 73. Summary of Roughness Behavior .....	134
Table C-1. Roughness Values .....	1499

## List of Abbreviations, Acronyms, and Symbols

AASHTO	American Association of State Highway and Transportation Officials
AB	aggregate base
AC	asphalt concrete
ADOT	Arizona Department of Transportation
ADS	automated distress survey
ARAC	asphalt rubber asphalt concrete
DCP	dynamic cone penetrometer
ESAL	equivalent single-axle load
FHWA	Federal Highway Administration
FWD	falling weight deflectometer
HMA	hot-mix asphalt
HMAC	hot-mix asphalt concrete
HRI	Half-car Roughness Index
IRI	International Roughness Index
LTPP	Long Term Pavement Performance
MDS	manual distress survey
MEPDG	<i>Mechanistic-Empirical Pavement Design Guide</i>
ML	midlane
MP	milepost
$M_r$	resilient modulus
MRI	Mean Roughness Index
N/A	not available, not applicable
NWP	non-wheel path
OGFC	open-graded friction course
OWP	outer wheel path
PSD	power spectral density
RAP	recycled asphalt pavement
RMSE	root mean square error
RN	Ride Number
SHRP	Strategic Highway Research Program
SM	select material
$SN_{eff}$	effective structural number
SPS	Specific Pavement Study
SPT	Standard Penetration Test
WP	wheel path

## **Acknowledgments**

The project team would like to acknowledge the Arizona Department of Transportation for sponsoring this project. In addition, the authors thank the Arizona Transportation Research Center and the Technical Advisory Committee for their input, and thank Mr. Christ Dimitroplos for his leadership. The comprehensive information stored in the Long Term Pavement Performance Program database allowed this research to be conducted.

## EXECUTIVE SUMMARY

As part of the Long Term Pavement Performance (LTPP) Program, the Arizona Department of Transportation (ADOT) constructed 11 Specific Pavement Study-5 (SPS-5) test sections on Interstate 8 (I-8) near Casa Grande. The SPS-5 experiment was designed to study the effect of specific maintenance/rehabilitation treatments on asphalt concrete (AC) pavement performance. This project consisted of two sets of test sections: nine core sections matching similar projects constructed by other highway agencies and two supplemental sections to investigate alternative design characteristics selected by ADOT. Construction of all 11 sections was completed in April 1990, and 10 of the sections (all except the control section) were not placed out of study until a major rehabilitation in January 2009. Some years earlier, in October 1996, the control section had been placed out of study first, having reached the end of its service life and consequently needing reconstruction.

This report provides general information about the project location, including climate, traffic, and subgrade conditions, as well as details about the layer configurations of each test section. All 11 of the SPS-5 test sections were constructed consecutively and so were exposed to the same traffic-loading, climate, and subgrade conditions. This allows direct comparisons among unique combinations of surface preparation, overlay material, and overlay thicknesses without the confounding effects introduced by different in situ conditions.

By comparing changes in effective structural numbers and structural distresses, both the deflection and distress analyses concluded that (1) thick (5-inch) AC overlays performed better than thin (2-inch) AC overlays, (2) virgin AC overlays performed better than recycled AC overlays, and (3) test sections that had received intensive surface preparation performed better than those that had received minimal surface preparation. The distress analysis concluded that the use of 5-inch overlays was the most critical rehabilitation feature in improving the structural performance of a pavement. Additionally, the distress analysis concluded that the use of virgin AC was the most critical rehabilitation feature in improving a pavement's resistance to environmental distresses.

Key findings from the deflection analysis were largely based on the results obtained using the AASHTO 1993 analysis method. An elastic layer backcalculation was also performed as part of the deflection analysis. However, the elastic layer backcalculation produced highly variable and unreasonable results that should be used with appropriate discretion. Profile analysis results showed that roughness and roughness progression alone cannot be used to represent the health of a test section. Several test sections did not exhibit changes in roughness in proportion to the amount of fatigue cracking they displayed.

All sections received pavement maintenance consisting of two to three fog seals and one crack seal. These maintenance events can mask the extent and severity of actual distresses in the pavement in the short term. However, in this study the impact of maintenance work on distresses was not significant and was considered negligible.

This long-term study of pavement performance in Arizona was initiated to help develop improvements to pavement design and retrofit procedures. Including profile analysis, falling weight deflectometer, and distress analysis, forensic analyses on the LTPP samples documented the performance range of various pavements. Combined with ADOT's Pavement Management Services (PMS) data and then compared to pavement prediction models to improve pavement design methodologies, the LTPP data sets were used to calibrate to local conditions the American Association of State Highways and Transportation Officials (AASHTO) Mechanistic-Empirical Pavement Design method, which improves pavement design and will lead to more reliable and cost-effective pavements.

## CHAPTER 1. INTRODUCTION

Understanding the contribution of maintenance and rehabilitation procedures to long-term pavement performance can be extremely valuable to pavement managers looking to optimize resources and improve overall performance. The objectives of this research were to document the overall performance trends of the Specific Pavement Study-5 (SPS-5) project, identify key differences in performance among the various rehabilitation techniques, and document key findings that would be useful to the Arizona Department of Transportation (ADOT).

This report provides the results of surface distress, deflection, and profile analyses for the Long Term Pavement Performance (LTPP) Program SPS-5 site on Interstate 8 (I-8) near Casa Grande, Arizona. The SPS-5 project (040500) studied the effect of specific maintenance and rehabilitation treatments on asphalt concrete (AC) pavement performance. The project consisted of 11 test sections—nine core sections and two supplemental sections. The nine core sections represented the standard experimental matrix that the Strategic Highway Research Program (SHRP) required. ADOT added the two supplemental test sections to evaluate features that were not included in the SHRP experiment design. In this report, the test sections are generally referred to by their six-digit SHRP project ID numbers (for example, 040501), but some figures and tables use ADOT's numbering system, which omits the first two digits (for example, 0501).

In eight of the nine core SPS-5 test sections (all except the control section), two types of surface preparation were used:

- **Minimal preparation**, which included partial patching, full-depth patching, and milling of an existing surface friction course (to a depth of less than 1 inch).
- **Intensive preparation**, which included removing and replacing existing crack sealing, performing crack sealing, removing and replacing existing partial and full-depth patching, performing additional partial and full-depth patching, and milling to a depth such that the final surface was at least 0.5 inch above or below an interface between material layers (Hossain et al. 1996). The depth of material removed by milling, excluding any surface friction course, was replaced with an equal thickness of virgin AC. This material was not counted as part of the overlay thickness.

The ninth core section was a control section that received only the routine maintenance required to keep the roadway in a safe and functional condition. Four of the SHRP test sections received either a 2- or 5-inch-thick virgin asphalt overlay. The other four sections received either a 2- or 5-inch-thick recycled asphalt overlay.

The two ADOT supplemental sections used the same types of surface preparation as the SPS-5 test sections used, but different overlay materials and thicknesses. Section 040559 received an inverted overlay consisting of 3 inches of recycled overlay placed on 3 inches of virgin AC. Section 040560 received an asphalt rubber asphalt concrete (ARAC) overlay.

The SPS-5 project was located on eastbound I-8 in Pinal County (see Figure 1) and was incorporated in ADOT rehabilitation project IR-8-2(91), which extended from milepost (MP) 147.60 to MP 160.87, approximately 17 miles southwest of Casa Grande.

The SPS-5 project was constructed in a two-mile segment of this 13-mile rehabilitation project (from MP 159.01 to MP 161). The soil was covered with various desert-type brush and small trees. Each test section (except Section 040560) was 500 ft in length, which does not include transitional segments between sections and destructive sampling areas outside the monitoring limits. Average elevation of the project was 1071 ft, with latitude of 32° 50' and longitude of -112° 00'. Figures 1 and 2 show the location and layout of the SPS-5 project, and Table 1 lists the test section properties.



(Courtesy of Google Maps)

**Figure 1. Location of Arizona SPS-5 Test Sections**

**SHRP SPS-5 TEST SECTION LAYOUT  
040500 CASA GRANDE, ARIZONA  
I-8 EASTBOUND**

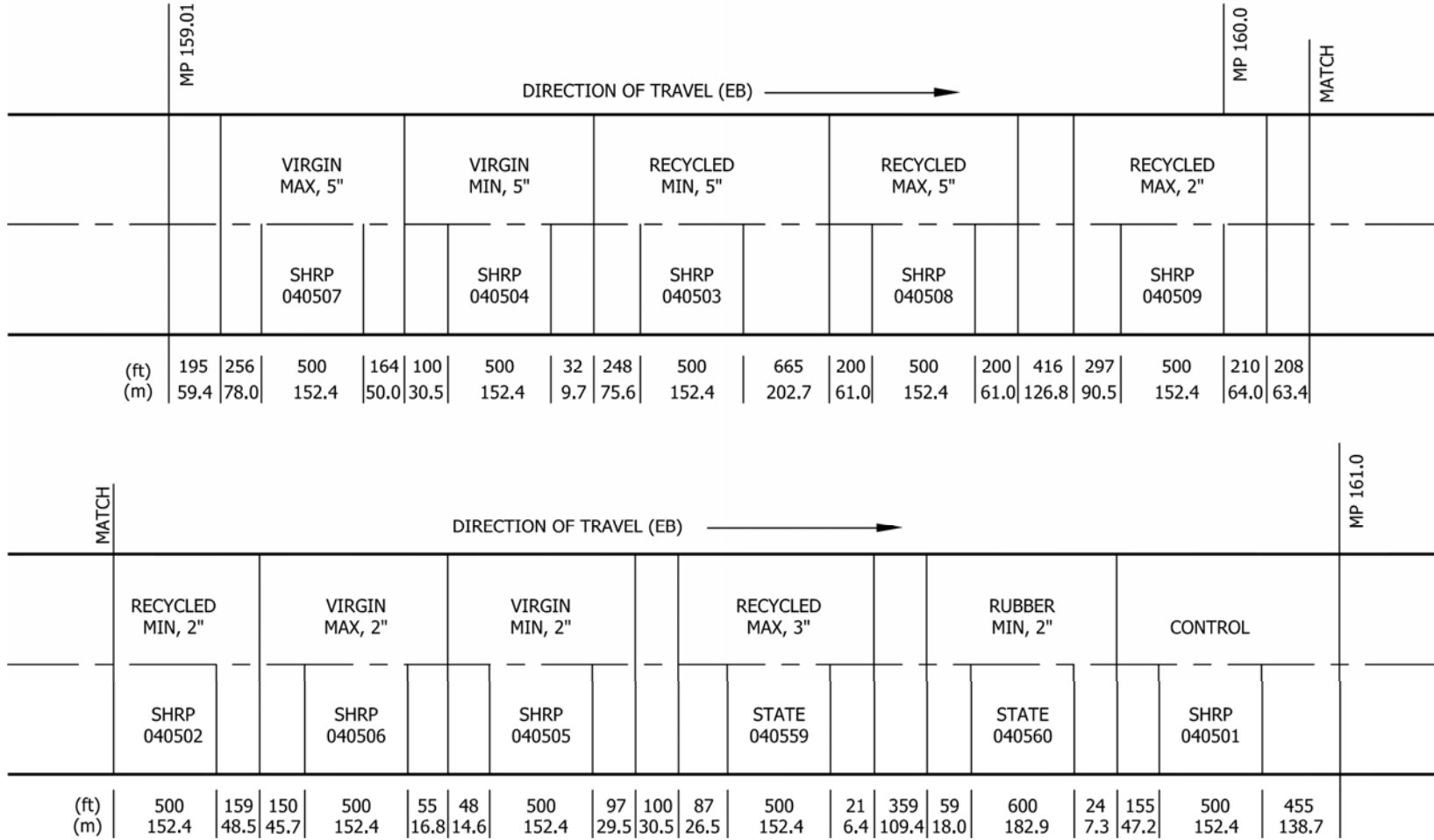


**Figure 2. Layout of the SPS-5 Project**

**Table 1. Arizona SPS-5 Project Layout, Post-Rehabilitation**

Station		SHRP ID	ADOT ID	Asphalt Concrete		Base		Subgrade
(ft)	(m)			Thickness (inches)	Type	Thickness (inches)	Type	Type
0	0	040507	1	3.7	existing AC	20.7	coarse-soil aggregate mix	silty gravel with sand
500	152			2.7	virgin AC fill			
				4.1	virgin AC overlay			
764	233	040504	1	3.8	existing AC	17.6	coarse-soil aggregate mix	silty gravel with sand
1264	385			4.8	virgin AC overlay			
1544	471	040503	1	3.0	existing AC	16.6	coarse-soil aggregate mix	silty gravel with sand
2044	623			4.7	recycled AC overlay			
2909	887	040508	1	4.2	existing AC	15.0	coarse-soil aggregate mix	silty gravel with sand
3409	1039			2.4	virgin AC fill			
				4.1	recycled AC overlay			
4322	1317	040509	1	2.4	existing AC	14.8	coarse-soil aggregate mix	silty gravel with sand
4822	1470			2.6	virgin AC fill			
				1.3	recycled AC overlay			
5240	1597	040502	1	2.6	existing AC	14.7	coarse-soil aggregate mix	silty gravel with sand
5740	1750			2.7	recycled AC overlay			
6049	1844	040506	1	4.3	existing AC	12.8	coarse-soil aggregate mix	silty gravel with sand
6549	1996			2.8	virgin AC fill			
				2.4	virgin AC overlay			
6652	2028	040505	1	2.7	existing AC	12.8	coarse-soil aggregate mix	silty gravel with sand
7152	2180			2.8	virgin AC overlay			
7436	2266	040559	1	1.7	existing AC	13.2	coarse-soil aggregate mix	silty gravel with sand
7936	2419			3.0	virgin AC fill			
				3.0	recycled AC overlay			
8375	2553	040560	1	4.1	existing AC	14.0	coarse-soil aggregate mix	silty gravel with sand
8975	2736			2.2	ARAC overlay			
9154	2790	040501	1	4.1	existing AC	14.2	coarse-soil aggregate mix	silty gravel with sand
9654	2943			0.9	OGFC			

Before the SPS-5 project was constructed, the roadway was 38 ft wide with two travel lanes that were each 12 ft wide bounded by a 10-ft outside shoulder and a 4-ft inside shoulder. The pavement section consisted of 8 inches of select material (SM), 6 inches of aggregate base (AB) and 4.5 inches of asphalt concrete (AC). The existing surface course was an open-graded friction course (OGFC) of 0.5 inch. A typical cross section of the road before construction is shown in Figure 3 (Hossain et al. 1996).

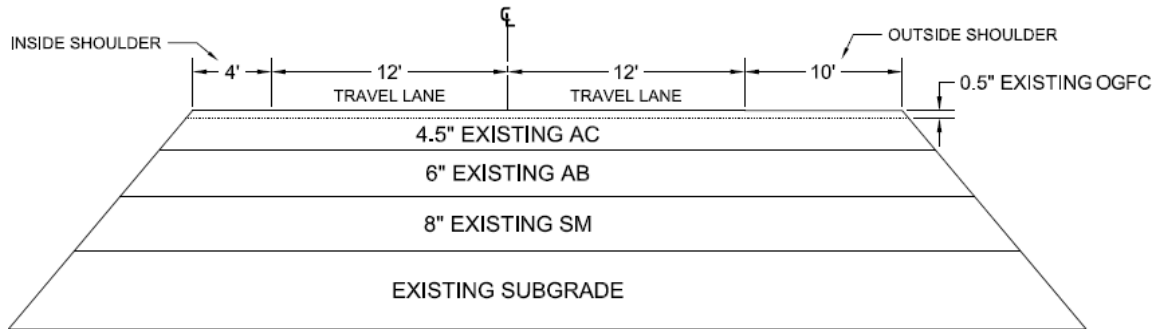


**Figure 3. Existing Asphalt Concrete Pavement Cross Section Before SPS-5 Project Construction (from Hossain et al. 1996)**

As mentioned previously, this project consisted of 11 test sections. Table 2 summarizes the features of each section.

**Table 2. Summary of SPS-5 Test Sections (from Hossain et al. 1996)**

SHRP ID	Location		Length (ft)	Surface Preparation <sup>1</sup>	Overlay Material	Overlay Thickness (inches)
	From	To				
040507	0+00	5+00	500	Intensive	Virgin	5
040504	7+64	12+64	500	Minimal	Virgin	5
040503	15+44	20+44	500	Minimal	Recycled	5
040508	29+09	34+09	500	Intensive	Recycled	5
040509	43+22	48+22	500	Intensive	Recycled	2
040502	52+40	57+40	500	Minimal	Recycled	2
040506	60+49	65+49	500	Intensive	Virgin	2
040505	66+52	71+52	500	Minimal	Virgin	2
040559	74+36	79+36	500	Intensive	Recycled	3
040560	83+75	89+75	600	Minimal	ARAC	2
040501	91+54	96+54	500	Routine maintenance	None	None (control)

<sup>1</sup> Minimal preparation: (1) milling off existing OGFC (less than 1 inch) and (2) partial and full-depth patching. Intensive preparation: (1) milling off existing OGFC and a portion of existing AC (from 1.9 to 3.5 inches), (2) removing and replacing existing crack sealing and partial and full-depth patching, and (3) performing additional crack sealing and partial and full-depth patching.

Researchers encountered some construction issues during the milling of Section 040502. The first passes with the milling machine did not completely remove the friction course, and the remaining material was badly stripped. Crews also encountered difficulties with using a 6-ft milling machine as opposed to a machine that could span the entire 12-ft lane. See Appendix A for a complete list of construction deviations.

Before the SPS-5 experiment was constructed, researchers reviewed the existing distresses in the travel lane of the test sections. Table 3 provides a summary of this review, which shows the overall poor condition of the pavement. The majority of the distress in each section was block cracking. Fatigue cracking was also observed in every section. The control section, 040501, did not receive an overlay and deteriorated to a very poor condition. Section 040501 was placed out of study within six years because it required reconstruction.

**Table 3. Summary of Preconstruction Distress in Travel Lane**

SHRP ID	Fatigue Cracking (ft <sup>2</sup> )	Block Cracking (ft <sup>2</sup> )	Longitudinal Cracking (ft)	Transverse Cracking (ft)
040501	966	5820	0	0
040502	1110	5484	0	0
040503	541	6073	0	0
040504	229	4148	40	242
040505	125	4582	61	221
040506	661	5876	0	0
040507	620	6021	0	0
040508	475	6283	0	0
040509	327	6274	0	0
040559	1139	5715	0	0
040560	384	7928	0	0

Notes:

1. All distress measurements were taken with an automated distress survey using a lane width of 15 ft.
2. Sections 040501 through 040559 were 500 ft long; Section 040560 was 600 ft long.

Table 4 provides a summary of falling weight deflectometer (FWD) deflection measurements, fatigue and block cracking levels, and International Roughness Index (IRI) values for the core test sections. (Fatigue and block cracking were measured with both automated distress surveys [ADS] and manual distress surveys [MDS].) These values indicate the condition of each section before receiving an AC overlay (preconstruction), after receiving the overlay (postconstruction), and during the last survey taken before each section was placed out of study. This table helps illustrate the overall performance of

the test sections, which is discussed in greater detail in Chapters 2, 3, and 4 of this report. These chapters discuss the deflection, distress, and roughness analyses conducted for this project.

**Table 4. Summary of Section Performance**

SHRP ID	Survey Event	Survey Dates <sup>1</sup>	Deflections <sup>2</sup>		Fatigue Cracking (ft <sup>2</sup> )	Block Cracking (ft <sup>2</sup> )	IRI (inches/mi)
			D0 (mils)	D60 (mils)			
040501 <sup>3</sup>	Preconstruction	1/19/1990 (FWD), 11/29/1989 (ADS), 2/5/1990 (IRI)	12.7	1.1	966	5820	78
	Postconstruction	1/16/1991 (FWD), 1/15/1991 (MDS), 9/21/1990 (IRI)	14.9	1.1	1992	4000	79
	Last survey	9/13/1996 (FWD), 10/20/1994 (MDS), 2/23/1993 (IRI)	9.7	0.8	2781	3272	86
040502	Preconstruction	1/18/1990 (FWD), 11/29/1989 (ADS), 2/5/1990 (IRI)	10.7	0.8	1110	5484	127
	Postconstruction	1/16/1991 (FWD), 10/19/1994 (MDS), 9/21/1990 (IRI)	5.7	0.7	4	0	86
	Last survey	9/15/2008 (FWD), 9/15/2008 (MDS), 9/11/2008 (IRI)	9.6	0.9	3684	2550	244
040503	Preconstruction	1/18/1990 (FWD), 11/29/1989 (ADS), 2/5/1990 (IRI)	12.9	0.9	541	6073	107
	Postconstruction	1/15/1991 (FWD), 10/18/1994 (MDS), 9/21/1990 (IRI)	6.4	0.7	0	0	60
	Last survey	12/10/2003 (FWD), 12/5/2005 (MDS), 9/11/2008 (IRI)	7.2	1.3	104	0	146
040504	Preconstruction	1/18/1990 (FWD), 11/29/1989 (ADS), 2/5/1990 (IRI)	10.7	0.8	229	4148	98
	Postconstruction	1/15/1991 (FWD), 10/18/1994 (MDS), 9/21/1990 (IRI)	3.8	0.6	0	0	76
	Last survey	12/10/2003 (FWD), 12/5/2005 (MDS), 9/11/2008 (IRI)	2.9	0.7	2	0	108

1 Manual distress survey (MDS) used a lane width of 12 ft; automated distress survey (ADS) used a lane width of 15 ft.

2 D0: Deflection of the pavement under the center of the loading plate. D60: Deflection of the pavement 60 inches from the center of the loading plate.

3 Section did not receive an overlay and was placed out of study within 6 years.

4 Section length was 600 ft.

Table 4. Summary of Section Performance (Continued)

SHRP ID	Survey Event	Survey Dates <sup>1</sup>	Deflections <sup>2</sup>		Fatigue Cracking (ft <sup>2</sup> )	Block Cracking (ft <sup>2</sup> )	IRI (inches/mi)
			D0 (mils)	D60 (mils)			
040505	Preconstruction	1/19/1990 (FWD), 11/29/1989 (ADS), 2/5/1990 (IRI)	11.3	1.1	125	4582	162
	Postconstruction	1/16/1991 (FWD), 10/25/1994 (MDS), 9/21/1990 (IRI)	6.1	0.8	183	0	81
	Last survey	9/15/2008 (FWD), 9/15/2008 (MDS), 9/11/2008 (IRI)	9.5	0.9	4285	1206	131
040506	Preconstruction	1/19/1990 (FWD), 11/29/1989 (ADS), 2/5/1990 (IRI)	16.1	1.0	661	5876	110
	Postconstruction	1/16/1991 (FWD), 10/20/1994 (MDS), 9/21/1990 (IRI)	4.5	0.7	0	0	65
	Last survey	9/15/2008 (FWD), 9/15/2008 (MDS), 9/11/2008 (IRI)	8.9	1.3	65	0	134
040507	Preconstruction	1/18/1990 (FWD), 11/29/1989 (ADS), 2/5/1990 (IRI)	8.3	0.7	620	6021	116
	Postconstruction	1/14/1991 (FWD), 10/18/1994 (MDS), 9/21/1990 (IRI)	2.8	0.6	0	0	82
	Last survey	12/10/2003 (FWD), 12/5/2005 (MDS), 9/11/2008 (IRI)	1.6	0.4	0	0	98
040508	Preconstruction	1/18/1990 (FWD), 11/29/1989 (ADS), 2/5/1990 (IRI)	10.8	0.7	475	6283	98
	Postconstruction	1/15/1991 (FWD), 10/19/1994 (MDS), 9/21/1990 (IRI)	4.8	0.6	0	0	60
	Last survey	12/10/2003 (FWD), 12/5/2005 (MDS), 9/11/2008 (IRI)	5.7	1.1	0	0	87

1 Manual distress survey (MDS) used a lane width of 12 ft; automated distress survey (ADS) used a lane width of 15 ft.

2 D0: Deflection of the pavement under the center of the loading plate. D60: Deflection of the pavement 60 inches from the center of the loading plate.

3 Section did not receive an overlay and was placed out of study within 6 years.

4 Section length was 600 ft.

Table 4. Summary of Section Performance (Continued)

SHRP ID	Survey Event	Survey Dates <sup>1</sup>	Deflections <sup>2</sup>		Fatigue Cracking (ft <sup>2</sup> )	Block Cracking (ft <sup>2</sup> )	IRI (inches/mi)
			D0 (mils)	D60 (mils)			
040509	Preconstruction	1/18/1990 (FWD), 11/29/1989 (ADS), 2/5/1990 (IRI)	8.9	0.8	327	6274	151
	Postconstruction	1/16/1991 (FWD), 10/19/1994 (MDS), 9/21/1990 (IRI)	5.1	0.7	0	0	65
	Last survey	9/15/2008 (FWD), 9/15/2008 (MDS), 9/11/2008 (IRI)	9.7	1.0	910	0	286
040559	Preconstruction	1/19/1990 (FWD), 11/29/1989 (ADS), 2/5/1990 (IRI)	13.0	1.3	1139	5715	131
	Postconstruction	1/16/1991 (FWD), 10/20/1994 (MDS), 9/21/1990 (IRI)	5.9	1.1	0	0	73
	Last survey	12/12/2003 (FWD), 12/12/2003 (MDS), 9/11/2008 (IRI)	6.6	1.9	0	0	111
040560 <sup>4</sup>	Preconstruction	1/19/1990 (FWD), 11/29/1989 (ADS), 2/5/1990 (IRI)	12.0	1.2	384	7928	116
	Postconstruction	1/16/1991 (FWD), 10/20/1994 (MDS), 9/21/1990 (IRI)	12.6	1.2	0	0	50
	Last survey	12/12/2003 (FWD), 12/12/2002 (MDS), 9/11/2008 (IRI)	10.6	1.2	1955	0	140

1 Manual distress survey (MDS) used a lane width of 12 ft; automated distress survey (ADS) used a lane width of 15 ft.

2 D0: Deflection of the pavement under the center of the loading plate. D60: Deflection of the pavement 60 inches from the center of the loading plate.

3 Section did not receive an overlay and was placed out of study within 6 years.

4 Section length was 600 ft.

The climate for the SPS-5 project is considered to be a dry, no-freeze environment by LTPP definitions. Table 5 provides environmental details about the area. The temperature and precipitation information was derived from data collected at nearby weather stations and represents 38 years of recorded data. The humidity data was summarized from 22 years of virtual weather station data.

**Table 5. Climatic Information for SPS-5**

	<b>38-year Average</b>	<b>38-year Maximum</b>	<b>38-year Minimum</b>
Annual average daily mean temperature (°F)	71	73	68
Annual average daily maximum temperature (°F)	87	90	85
Annual average daily minimum temperature (°F)	54	57	51
Absolute maximum annual temperature (°F)	115	120	110
Absolute minimum annual temperature (°F)	24	30	16
Number of days per year above 90° F	172	190	144
Number of days per year below 32° F	20	39	5
Annual average freezing index (°F-days)	0	0	0
Annual average precipitation (inches)	8.7	16.4	3.2
Annual average daily mean solar radiation (W/ft <sup>2</sup> )	N/A	N/A	N/A
Annual average daily maximum relative humidity (%)	52	61	43
Annual average daily minimum relative humidity (%)	20	24	16

N/A: No data available.

Table 6 provides a summary of the total equivalent single-axle loads (ESALs) computed from traffic loading information collected at the SPS-5 site. For 1990 to 1992, and from 1994 to 1996, no traffic monitoring data were available. For these years, ADOT provided estimates for ESAL values. In 2000, neither monitored nor estimated ESAL values were available. The ADOT traffic estimates are provided to illustrate the expected traffic growth as modeled by the agency, but these values do not necessarily correlate with monitored traffic data. For example, the estimated ESAL values provided by ADOT in 2001 and 2002 were two to three times larger than the monitored values.

**Table 6. Traffic Loading Summary**

<b>Year</b>	<b>Monitored ESALs</b>	<b>Estimated ESALs</b>
1990	N/A	250,000
1991	N/A	180,000
1992	N/A	220,000
1993	148,400	N/A
1994	N/A	200,000
1995	N/A	200,000
1996	N/A	200,000
1997	256,200	N/A
1998	347,200	N/A
1999	407,400	N/A
2000	N/A	N/A
2001	335,400	761,000
2002	269,000	880,000
2003	298,800	N/A
2004	390,100	N/A
2005	369,500	N/A
2006	246,500	N/A
2007	263,200	N/A
2008	371,700	N/A

N/A: No data available.

Three analyses were conducted to evaluate pavement performance of the SPS-5 project. Chapters 2, 3, and 4 of this report describe these three analyses—deflection, distress, and roughness. Each chapter provides a description of the research approach along with performance comparisons among test sections, overall trends, a summary of the results, and key findings.

In 2008, the Federal Highway Administration (FHWA) initiated a forensic evaluation of four of the nine test sections (040502, 040505, 040506, and 040509). The objectives of this forensic investigation were to: (1) identify causes of pavement failure and investigate associated distress mechanisms, (2) examine pavement structural and functional performance, (3) measure within-section layer thicknesses and material properties, and (4) test end-state physical properties. Destructive and nondestructive tests were conducted, including coring, trenching, dynamic cone penetrometer (DCP) testing, Standard Penetration Tests (SPT), laboratory testing of materials, distress surveys, transverse profiles, longitudinal profiles, and falling weight deflectometer (FWD) tests (Nichols Consulting Engineers, unpublished data, 2010).



## CHAPTER 2. SPS-5 DEFLECTION ANALYSIS

Prior to construction, each SPS-5 test section consisted of approximately 5 inches of asphalt concrete (AC) on 15 inches of aggregate base (AB). Construction procedures varied across the sections, with one control section receiving no treatment and other sections receiving various combinations of milling and overlay with different types of AC materials as discussed in Chapter 1.

One round of FWD testing was performed on each test section approximately three months before construction. Another round of FWD testing was performed approximately nine months after construction. Each section then received further FWD testing every one to five years until it went out of study. Section 040501 (the control section) received the least testing—a total of five rounds—as it went out of study first. The sections investigated in the forensic study in 2008 received 12 rounds of FWD testing. The remaining sections received 11 rounds of FWD testing. Table 7 shows the dates when each section received FWD testing.

**Table 7. FWD Test Dates by Section**

Test Date	0501	0502	0503	0504	0505	0506	0507	0508	0509	0559	0560
1/18/1990-1/19/1990	✓	✓	✓	✓	✓	✓	✓	✓	✓	✓	✓
1/14/1991-1/16/1991	✓	✓	✓	✓	✓	✓	✓	✓	✓	✓	✓
10/2/1991-10/3/1991	✓	✓	✓	✓	✓	✓	✓	✓	✓	✓	✓
10/18/1994-10/20/1994	✓	✓	✓	✓	✓	✓	✓	✓	✓	✓	✓
9/11/1996-9/13/1996	✓	✓	✓	✓	✓	✓	✓	✓	✓	✓	✓
11/12/1997-11/14/1997		✓	✓	✓	✓	✓	✓	✓	✓	✓	✓
12/9/1998-12/10/1998		✓	✓	✓	✓	✓	✓	✓	✓	✓	✓
12/13/1999-12/14/1999		✓	✓	✓	✓	✓	✓	✓	✓	✓	✓
12/16/2000-12/18/2000		✓	✓	✓	✓	✓	✓	✓	✓	✓	✓
12/10/2002-12/12/2002		✓	✓	✓	✓	✓	✓	✓	✓	✓	✓
12/10/2003-12/12/2003		✓	✓	✓	✓	✓	✓	✓	✓	✓	✓
9/15/2008		✓			✓	✓			✓		

The preconstruction round of testing was performed in January 1990. At that time, the LTPP FWD guidelines were still under development, and there are some differences between data collected before construction and subsequent data. The most noteworthy difference is the test point interval—for the preconstruction testing, the interval was nominally 100 ft, while for subsequent testing the interval was nominally 50 ft. Also, only three replicate drops were conducted at each drop height during preconstruction testing, as opposed to four replicates for later testing.

In 1999, another change was made to the FWD testing procedure. Two sensors were added to the FWD: one sensor at 48 inches from the center of the loading plate and one at -12 inches.

### **NORMALIZED DEFLECTIONS**

Table 8 presents average normalized deflections measured by the center sensor (D0) of the FWD and the sensor at 60 inches from the center (D60) for both the midlane (ML) and outer wheel path (OWP). This data is for drop height 2, which is nominally 9000 lb, then normalized to exactly 9000 lb using the following equation:

$$d_n = \frac{d_m \times P}{9000} \quad (\text{Eq. 1})$$

Where  $d_n$  = normalized deflection (mils)  
 $d_m$  = measured deflection (mils)  
 $P$  = drop load (pounds)

Normalized deflection is the simplest method of analyzing FWD data. While its utility in analyzing pavement structures is limited, this method does offer an easy way to make qualitative comparisons, which can be very helpful in identifying areas to focus on in more sophisticated and time-consuming analyses. The issues raised in the following discussion of the normalized deflection data will be revisited later in this report.

The deflection reading at 60 inches from center (D60) should be sensitive only to the stiffness of the subgrade. The zone of influence of an FWD test can be approximated as a 45-degree cone with its apex at the center of the load plate. Since the thickness (including AC and AB) of the thickest test section in this project (Section 040507) was 29.9 inches, any deflection reading from a sensor with an offset of greater than 30 inches would be assumed to be independent of the pavement layers. For most tests in this data set, only two sensors have an offset of greater than 30 inches—those at 36 and 60 inches. Since 36 inches is still close to the zone of influence, the sensor at 60 inches was selected to represent the subgrade.

**Table 8. Normalized Deflections**

Section <sup>1</sup>	Test Date <sup>2</sup>	Surface Preparation	AC Thickness (inches)	Midlane		Outer Wheel Path	
				D0 (mils)	D60 (mils)	D0 (mils)	D60 (mils)
040507	1/18/1990	Intensive	5.0	8.3	0.8	13.3	0.8
	1/14/1991		9.2	2.8	0.6	3.0	0.5
	12/10/2003			1.6	0.4	1.8	0.4
040504	1/18/1990	Minimal	5.0	10.7	0.8	12.3	0.8
	1/15/1991		9.2	3.8	0.6	4.2	0.6
	12/10/2003			2.9	0.5	3.8	0.5
040503	1/18/1990	Minimal	5.0	13.0	0.9	18.1	1.0
	1/15/1991		8.9	6.4	0.7	8.3	0.7
	12/10/2003			7.2	0.9	9.4	0.8
040508	1/18/1990	Intensive	5.4	10.8	0.8	15.1	0.9
	1/15/1991		9.2	4.9	0.6	5.1	0.6
	12/10/2003			5.7	0.8	5.5	0.6
040509	1/18/1990	Intensive	5.4	8.9	0.8	14.0	0.8
	1/16/1991		6.5	5.1	0.7	6.6	0.6
	9/15/2008			9.8	0.8	13.8	0.9
040502	1/18/1990	Minimal	5.1	10.7	0.8	13.7	0.7
	1/16/1991		6.4	5.7	0.7	7.0	0.7
	9/15/2008			9.6	0.7	14.4	0.7
040506	1/19/1990	Intensive	4.9	16.2	1.0	15.7	1.1
	1/16/1991		8.2	4.5	0.7	4.8	0.7
	9/15/2008			8.9	0.9	9.9	0.9
040505	1/19/1990	Minimal	5.0	11.3	1.1	15.5	1.2
	1/16/1991		6.9	6.2	0.8	7.5	0.8
	9/15/2008			9.5	0.8	13.4	0.8
040559	1/19/1990	Intensive	5.2	13.1	1.3	15.2	1.3
	1/16/1991		7.7	5.9	1.1	6.5	1.0
	12/12/2003			6.6	1.5	5.9	1.2
040560	1/19/1990	Minimal	5.0	12.1	1.2	17.5	1.3
	1/16/1991		6.3	12.6	1.2	16.6	1.3
	12/12/2003			10.6	1.0	15.1	1.0
040501	1/19/1990	N/A	5.0	12.7	1.1	16.2	1.2
	1/16/1991			14.9	1.1	16.4	1.1
	9/13/1996			9.8	0.8	12.3	0.8

1 Sections are listed in order of physical position at the test site.

2 Three FWD test dates are listed for each section: (1) before construction, (2) the first FWD test performed after construction, and (3) the last test available for that section.

From the D60 measurements, it is apparent that the subgrade is very stiff. In many cases, the D60 readings are less than 1 mil, which is problematic because the random error inherent in the geophones used to measure these deflections is stated by the manufacturer to be  $\pm 0.08$  mil. In some cases this represents 20 percent of the D60 measurement. This indicates that for subsequent analyses, data from the higher load levels should be used to reduce the effect of random error. While the 9000-lb load level is typically used in pavement design because it represents half of an 18-kip ESAL (i.e., one set of tires on an axle loaded to 18,000 lb), for thick sections on stiff subgrades such as this, the ability to determine the subgrade response independently of the pavement structure at this load level is hampered by the precision of the deflection measurement devices.

Some of the changes between preconstruction and postconstruction D60 measurements are quite large, especially for Sections 040507, 040504, and 040508. These are the thickest pavement sections, but they are also all located toward the beginning of the project layout. The most likely causes for changes in apparent subgrade stiffness are changes in moisture content or stress state. Thicker and stiffer pavements decrease the deviator stress and increase the confining pressures in the subgrade, which for most subgrade materials will increase stiffness. So it is reasonable that the thickest sections also exhibit the greatest increase in subgrade modulus.

Deflection data for both the ML and OWP are presented in Table 8. Typically, FWD data is used to make fatigue-related predictions about pavement performance (either explicitly in mechanistic design methods, or implicitly in empirical methods), so the data from the OWP, which undergoes direct loading, is most relevant. It is expected that the D0 deflections in the OWP will be higher than those in the ML because the D0 deflections are sensitive to pavement stiffness. These differences increase as the pavement deteriorates. It is also expected that there will be little difference between the ML and OWP measurements in the D60 data since this data should only be sensitive to the subgrade, which is not generally considered to undergo fatigue-related changes in stiffness. In addition, as the zone of influence of a load applied to the pavement surface increases in diameter with increasing depth, the deflection response of the deeper layers is less sensitive to small changes in the point of application of the load, which reduces the apparent distinction between subgrade properties measured in the ML and OWP.

In the preconstruction data, the average normalized D0 deflection measurement is 23 percent higher in the OWP than in the ML. This difference decreases to 14 percent after construction. In the sections that received intensive surface preparation, the difference between OWP and ML decreases to 10 percent, while in the sections that received minimal preparation, the difference decreases to only 18 percent. In the preconstruction D60 data, the OWP measurement is 4 percent higher than the ML value. After construction, the OWP is 4 percent lower than the ML. For the sections that received intensive preparation, the OWP is 9 percent lower than the ML, while for those that received minimal preparation, the OWP is 2 percent higher than the ML. Again, this discrepancy between the trends in the D60 data and expectations may be due to the influence of random error on very small measurements, or could indicate that the D60 data are not free of influence from the pavement layers as they were assumed to be.

## AASHTO 1993 ANALYSIS

The FWD data were analyzed using the procedure described in the 1993 *AASHTO Guide for Design of Pavement Structures* (AASHTO 1993). For this analysis, the FWD load and deflection data collected at the same location and nominal load were averaged before subsequent processing. Data for the OWP and drop height 4 (16,000 lb nominal) were used. Subgrade resilient modulus was calculated using the following equation for the sensor at 60 inches:

$$M_r = \frac{0.24 \times P}{r \times d_r} \quad (\text{Eq. 2})$$

Where  $P$  = load (pounds)  
 $r$  = sensor offset (inches)  
 $d_r$  = deflection (inches) at offset  $r$

This subgrade resilient modulus value does not include the 0.33 correction that is commonly applied when the results of FWD analysis are used for pavement design.

The effective pavement modulus is the modulus that represents the entire structure of the pavement above the subgrade. Researchers calculated this value iteratively using the following equation:

$$d_0 = 1.5pa \left[ \frac{1}{M_r \sqrt{1 + \left( \frac{D}{a} \sqrt{\frac{E_p}{M_r}} \right)^2}} + \frac{1 - \frac{1}{\sqrt{1 + \left( \frac{D}{a} \right)^2}}}{E_p} \right] \quad (\text{Eq. 3})$$

Where  $d_0$  = center deflection (inches)  
 $p$  = load plate pressure (psi)  
 $a$  = load plate radius (inches)  
 $D$  = total thickness of pavement layers (inches)  
 $M_r$  = subgrade resilient modulus (psi)  
 $E_p$  = effective pavement modulus (psi)

The effective structural number,  $SN_{eff}$ , was calculated using the following equation:

$$SN_{eff} = 0.0045 \times t \times \sqrt[3]{E_p} \quad (\text{Eq. 4})$$

Where  $t$  = pavement thickness (inches)  
 $E_p$  = effective pavement modulus (psi)

The AC component of the pavement structure has a temperature-dependent stiffness. The AB component does not. Because the effective pavement modulus includes both AC and AB components, temperature correction is somewhat problematic. The AASHTO 1993 guide includes a simple empirical method (Figure 5.6 on page III-99) for adjusting  $d_0$  based on the AC mid-depth temperature and the thickness of the AC layer. For this adjustment, mid-depth temperatures measured during the FWD test were used where available. BELLS2 temperature estimates were used where actual measurements were not available, including all of the preconstruction data (Lukanen et al. 2000).

The radius of relative stiffness,  $a_e$ , was calculated using the following equation:

$$a_e = \sqrt{a^2 + \left( D \sqrt[3]{\frac{E_p}{M_r}} \right)^2} \quad (\text{Eq. 5})$$

Where  $a_e$  = radius of the stress bulb at the subgrade-pavement interface (inches)  
 $a$  = FWD load plate radius (inches)  
 $D$  = total thickness of pavement layers (inches)  
 $E_p$  = effective pavement modulus (psi)  
 $M_r$  = subgrade resilient modulus (psi)

The AASHTO 1993 guide recommends using a sensor with an offset of at least  $0.7a_e$  when calculating resilient modulus according to Equation 5.

Researchers also calculated the structural number of the pavement solely using layer thicknesses and an assumed layer coefficient of 0.4 for AC and 0.12 for AB. This parameter,  $SN_0$ , represents the expected upper bound for  $SN_{eff}$ .

A summary of the results of the AASHTO 1993 analysis is presented in Table 9. Detailed discussion of the results for each test section is provided later in this chapter.

**Table 9. Summary of AASHTO 1993 Analysis of FWD Data**

Section	Surface Preparation	SN <sub>0</sub>	Test Date	M <sub>r</sub> (psi)	SN <sub>eff</sub> Raw	SN <sub>eff</sub> Corrected	0.7a <sub>e</sub> (inches)
040507	Intensive	5.08	1/18/1990	45,133	4.60	4.52	21
		7.27	1/14/1991	67,212	9.45	9.18	37
			12/10/2003	91,834	13.03	10.36	38
040504	Minimal	4.11	1/18/1990	47,376	4.08	4.08	19
		5.79	1/15/1991	62,843	7.22	7.63	32
			12/10/2003	70,926	7.93	7.50	30
040503	Minimal	3.99	1/18/1990	37,852	3.33	3.43	17
		5.55	1/15/1991	53,188	5.21	5.47	24
			12/10/2003	47,233	4.96	5.16	24
040508	Intensive	3.96	1/18/1990	44,978	3.32	3.47	17
		5.48	1/15/1991	61,842	6.19	6.40	27
			12/10/2003	56,234	5.83	6.15	26
040509	Intensive	4.58	1/18/1990	46,196	3.43	3.53	17
		5.16	1/16/1991	61,912	5.06	5.00	21
			9/15/2008	48,223	3.68	4.36	22
040502	Minimal	3.80	1/18/1990	52,447	3.42	3.45	16
		4.32	1/16/1991	54,531	4.69	4.71	21
			9/15/2008	49,538	3.56	4.67	21
040506	Intensive	3.50	1/19/1990	34,317	2.85	2.93	15
		4.82	1/16/1991	51,580	5.31	5.55	25
			9/15/2008	35,830	3.91	5.27	26
040505	Minimal	4.14	1/19/1990	29,400	2.82	2.80	15
		5.12	1/16/1991	44,479	4.24	4.54	21
			9/15/2008	45,717	3.44	4.39	20
040559	Intensive	3.66	1/19/1990	26,859	3.00	3.40	19
		4.66	1/16/1991	35,416	4.62	5.25	26
			12/12/2003	29,965	4.71	5.29	28
040560	Minimal	4.28	1/19/1990	28,141	3.04	3.16	17
		4.96	1/16/1991	28,867	3.14	3.63	20
			12/12/2003	39,150	3.47	3.65	18
040501	N/A	3.70	1/19/1990	30,790	3.32	3.28	17
			1/16/1991	30,744	3.10	3.25	17
			9/13/1996	41,966	3.36	4.25	20

Although the results for each section will be discussed below, it should be noted that there is a significant trend in preconstruction SN<sub>eff</sub> over the entire project. Preconstruction SN<sub>eff</sub> is greatest at Section 040507 (located at the beginning of the project), then gradually decreases to its lowest point at

Section 040505, and then increases slightly toward Section 040501. Section 040507 has a preconstruction  $SN_{eff}$  of 4.52, whereas for Section 040505 it is 2.80. This trend in  $SN_{eff}$  is similar to the trend in AB thickness, which is 20.7 inches for Section 040507 and 12.8 inches for Section 040505.

This large variability in preconstruction  $SN_{eff}$  poses problems for evaluating the project according to the experimental design. The experimental design was based on the assumption that the preconstruction structure and condition was essentially identical for each section. If this assumption is correct, then performance differences between sections can be ascribed solely to differences in construction. For example, Sections 040504 and 040505 both received minimal surface preparation and virgin AC overlays. The difference in construction is the thickness of the overlay. A naive analysis would ascribe the difference in performance solely to the thickness of the overlay. However, Section 040504 has a preconstruction  $SN_{eff}$  of 4.08, whereas it is 2.80 for Section 040505. If the difference in preconstruction structure is ignored, the effect of overlay thickness will be overemphasized.

Tables 10, 11, and 12 show the variability in preconstruction  $SN_{eff}$  by experimental factor.

**Table 10. Preconstruction  $SN_{eff}$  Variation by Overlay Material**

Cell	Overlay Material	
	Virgin	Recycled
Intensive, Thick	4.52	3.47
Intensive, Thin	2.93	3.53
Minimal, Thick	4.08	3.43
Minimal, Thin	2.8	3.45
Average	3.58	3.47

**Table 11. Preconstruction  $SN_{eff}$  Variation by Overlay Thickness**

Cell	Overlay Thickness	
	Thick	Thin
Virgin, Intensive	4.52	2.93
Virgin, Minimal	4.08	2.8
Recycled, Intensive	3.47	3.53
Recycled, Minimal	3.43	3.45
Average	3.88	3.18

**Table 12. Preconstruction SN<sub>eff</sub> Variation by Level of Surface Preparation**

Cell	Surface Preparation	
	Intensive	Minimal
Virgin, Thick	4.52	4.08
Virgin, Thin	2.93	2.8
Recycled, Thick	3.47	3.43
Recycled, Thin	3.53	3.45
Average	3.61	3.44

Preconstruction SN<sub>eff</sub> varies most with overlay thickness and least with overlay material. For analyses of this project that do not take preconstruction structural variability into account, a significant overemphasis of the effect of thicker overlays, and some overemphasis of the effect of intensive surface preparation and use of virgin material, should be expected.

**Section 040507**

Section 040507 is in the intensive maintenance, thick virgin overlay cell of the experimental matrix. It is physically located at the beginning of the project. The pre- and postconstruction layer structure as listed in Table TST\_L05B of the LTPP database is shown in Table 13.

**Table 13. Layer Structure, Section 040507**

Construction No.	Layer No.	Material Type	Thickness (inches) <sup>1</sup>
1	4	OGFC	0.7
	3	HMAC	4.3
	2	AB, 5.8% passing #200	20.7
	1	A-2-4, Silty gravel with sand	
2 – 4 <sup>2</sup>	6	Virgin HMAC Overlay	4.1
	5	Virgin HMAC Overlay	2.7
	3	HMAC	2.4
	2	AB, 5.8% passing #200	20.7
	1	A-2-4, Silty gravel with sand	

1 Depth of milling: 2.6 inches.

2 Does not include fog seals, which are considered structurally insignificant.

Construction was performed from May 16 to 24, 1990, and consisted of milling 2.6 inches of the original surface and placing a 6.8-inch overlay in three lifts. During the milling operation, the original asphalt

material exhibited extensive stripping. This section was also fog-sealed on May 28, 1998, and April 16, 2003.

$M_r$  calculated using the AASHTO 1993 procedure is shown in Figures 4 and 5. Figure 4 shows  $M_r$  versus station for the preconstruction, postconstruction, and final tests. Figure 5 shows the average  $M_r$  for each test date.

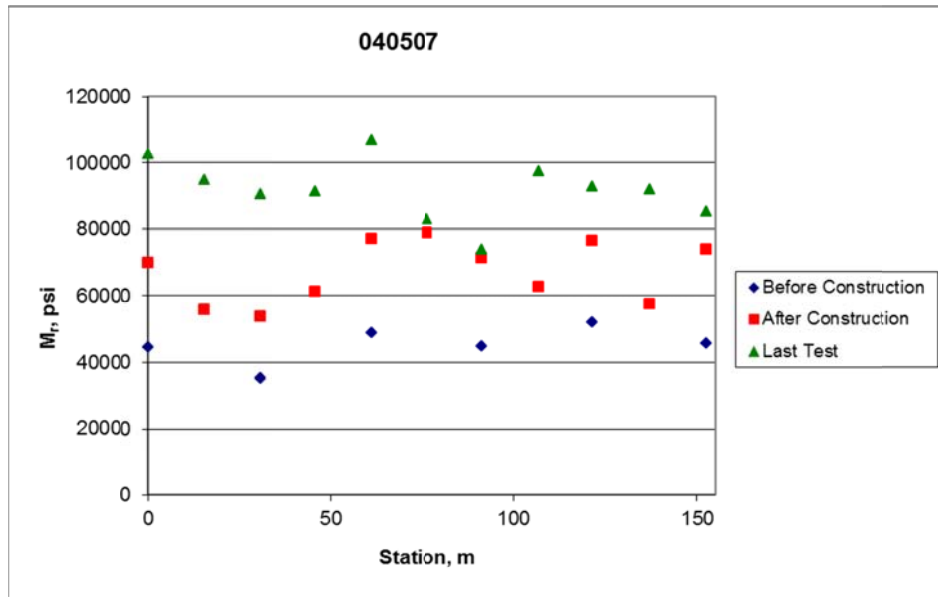


Figure 4. Subgrade Resilient Modulus versus Station, Section 040507

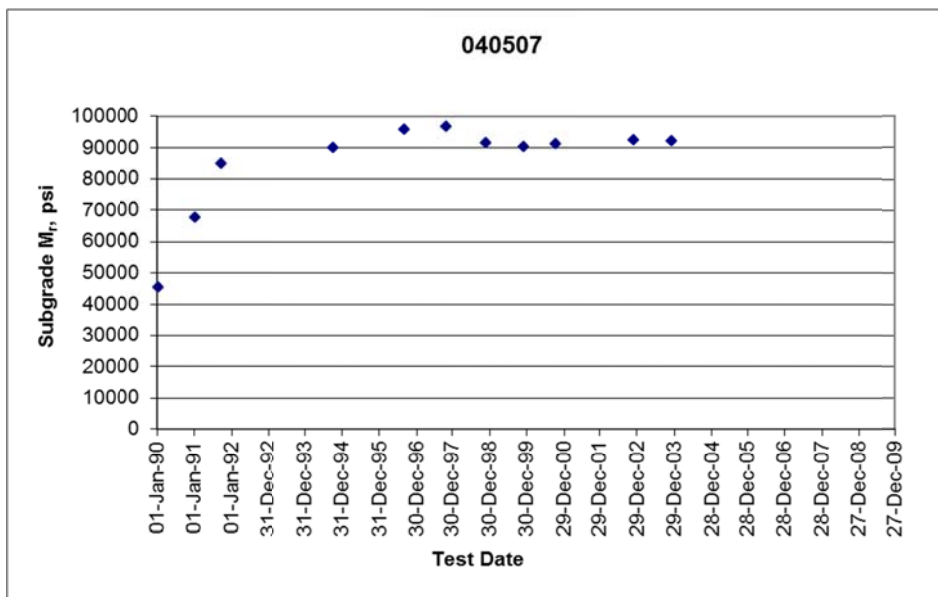


Figure 5. Subgrade Resilient Modulus versus Date, Section 040507

The behavior of this subgrade is unusual. The preconstruction  $M_r$  is 45,000 psi, which is high for subgrades in general, but within the reasonable range for an A-2-4 material. However, the postconstruction  $M_r$  increases to 90,000 psi, which is above the typical range for a subgrade. This result is stable across over a decade of data collection, which rules out operator or equipment error. This subgrade modulus was calculated using the sensor at 60 inches, whereas  $0.7a_e$  is no more than 42 inches for any of these tests, indicating that the result should not be influenced by the stiffness of the pavement structure.

Investigators checked for the influence of bedrock or other stiff layers using the  $1/r$  method (Rohde and Scullion 1990). This method requires data from at least three sensors at or beyond a 36-inch offset, which is only available for data collected after 1998. These plots show a slight decrease in slope at the 48-inch sensor, but the x-intercept for the line plotted through the 36-inch and 48-inch sensors is very close to 0, indicating a very large depth to bedrock, which means the bedrock should not be influencing the results.

The preconstruction test result could be dismissed as an outlier, but the sections at the other end of the project exhibit stable and typical  $M_r$  over time. This leaves two possible conclusions: Either the subgrade response changed after construction of this section, or the subgrade response at this site cannot be adequately modeled using standard techniques. This phenomenon is discussed further later in this chapter.

Figures 6 and 7 show  $SN_{eff}$  for this section versus station and time. The  $SN_{eff}$  values in these figures are temperature-corrected using the methodology described in the previous section.

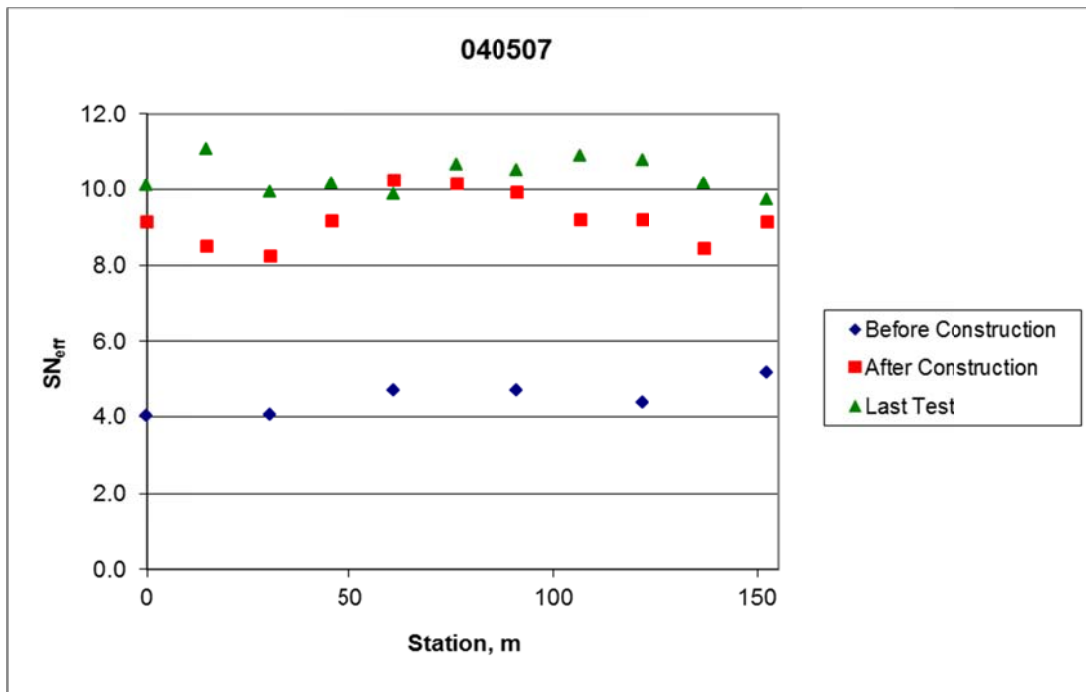
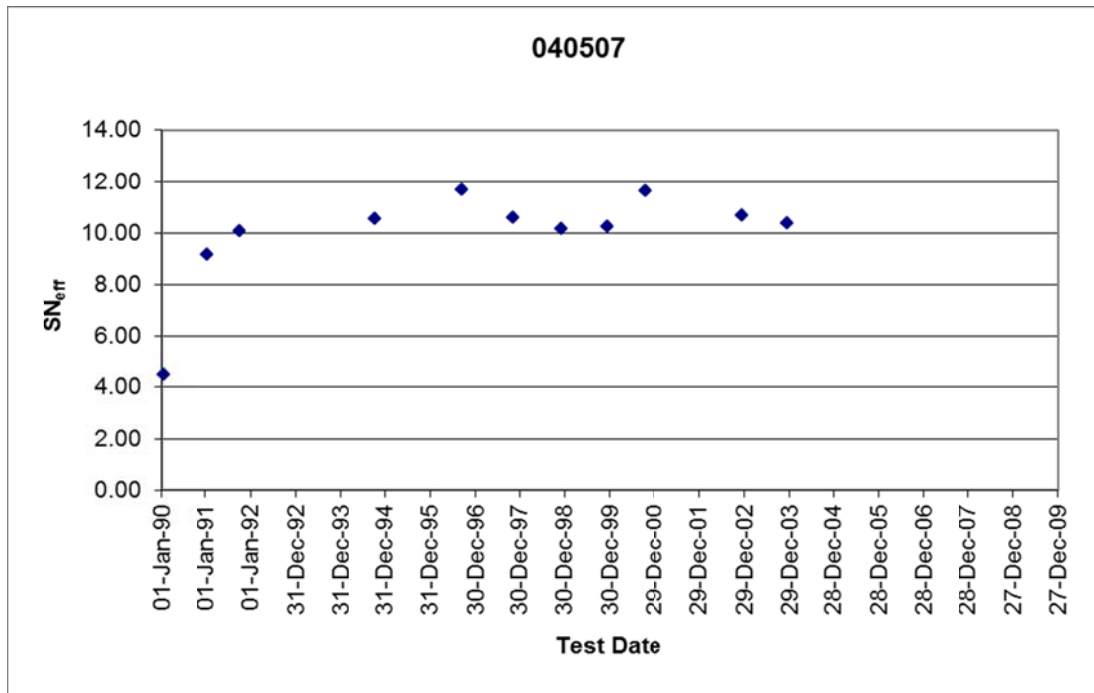


Figure 6.  $SN_{eff}$  versus Station, Section 040507



**Figure 7. SN<sub>eff</sub> versus Date, Section 040507**

The plot of immediate postconstruction SN<sub>eff</sub> values versus station shows a similar trend to the immediate postconstruction M<sub>r</sub> versus station plot, indicating that SN<sub>eff</sub> and M<sub>r</sub> are not fully independent, at least for that test date. The preconstruction SN<sub>eff</sub> is 4.60, which is reasonable considering the pavement structure. The average postconstruction SN<sub>eff</sub> is 10.7, which is considerably higher than would be expected given the pavement structure. As with the subgrade, the pavement structure at this section is much stiffer than expected. The SN<sub>eff</sub> versus date plot does not indicate deterioration of the pavement.

#### **Section 040504**

Section 040504 is in the minimal surface preparation, thick virgin overlay cell of the experimental matrix. The major difference between this section and Section 040507 according to the experimental design is the depth of the mill-and-fill. The pre- and postconstruction layer structure as listed in Table TST\_L05B of the LTPP database is shown in Table 14.

**Table 14. Layer Structure, Section 040504**

Construction No.	Layer No.	Material Type	Thickness (inches) <sup>1</sup>
1	4	OGFC	0.7
	3	HMAC	4.3
	2	AB, 4.8% passing #200	17.6
	1	A-2-4, Clayey sand with gravel	
2 – 5 <sup>2</sup>	5	Virgin HMAC overlay	4.8
	3	HMAC	4.3
	2	AB, 4.8% passing #200	17.6
	1	A-2-4, Clayey sand with gravel	

1 Depth of milling: 0.7 inch.

2 Does not include fog seals, which are considered structurally insignificant.

As compared with Section 040507, the thickness of AC is 0.1 inch less, and less of it is new overlay. The thickness of AB is 3.1 inches less.

Construction was performed from May 16 to 24, 1990. This section received fog seals on May 28, 1998, and April 16, 2003, and crack sealing on May 1, 2002.

$M_r$  calculated using the AASHTO 1993 procedure is shown in Figures 8 and 9. Figure 8 shows  $M_r$  versus station for the preconstruction, postconstruction, and final tests. Figure 9 shows the average  $M_r$  for each test date.

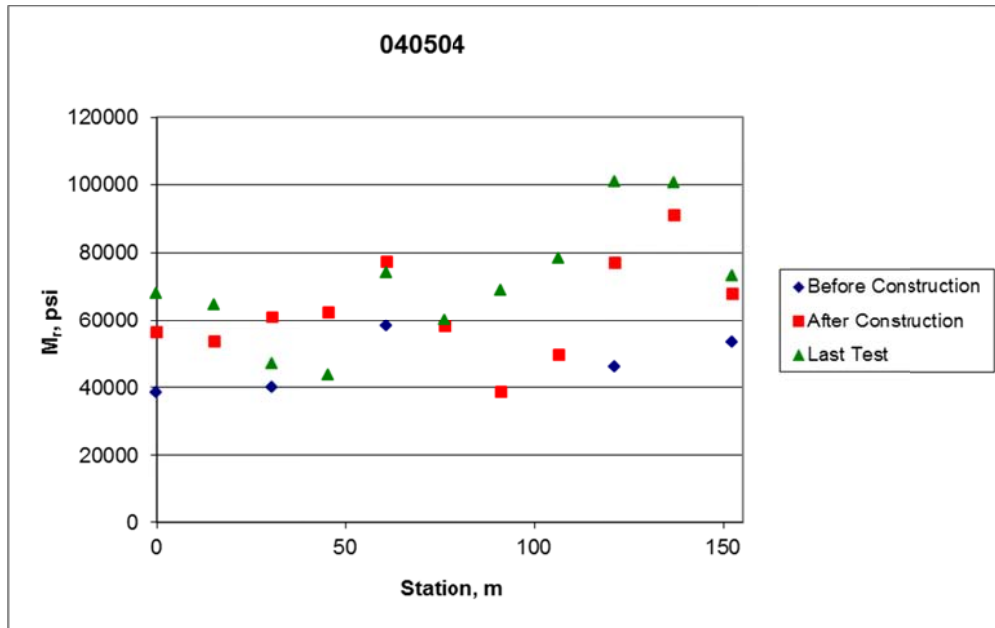


**Figure 8. Subgrade Resilient Modulus versus Station, Section 040504**

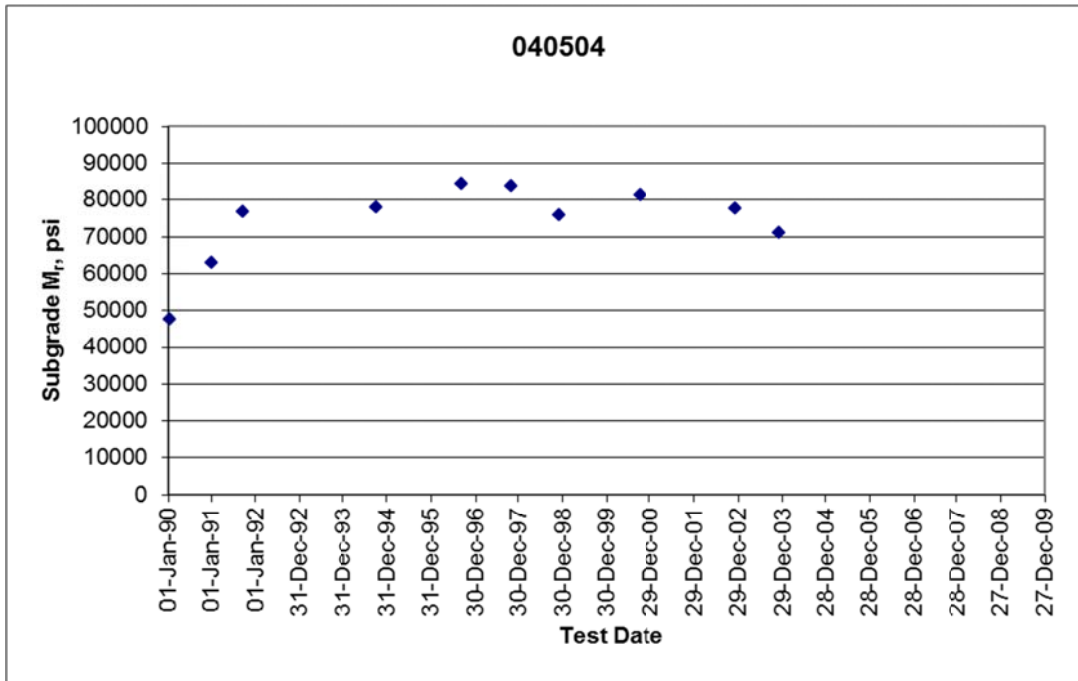


**Figure 9. Subgrade Resilient Modulus versus Date, Section 040504**

As with Section 040507, the preconstruction  $M_r$  of 47,000 psi is high, but within the reasonable range for the material type. After construction,  $M_r$  increases to approximately 80,000 psi, which is lower than was seen at Section 040507, but still above the typical range for a subgrade material.

Figures 10 and 11 show  $SN_{eff}$  for this section versus station and time. The  $SN_{eff}$  values in these figures are temperature-corrected using the methodology described earlier in this chapter.

The immediate postconstruction  $M_r$  and  $SN_{eff}$  plots both exhibit a sag around Station 100. The correlation between the plots for the last test is less apparent. The preconstruction  $SN_{eff}$  is 4.08, which is reasonable for the pavement structure. The average postconstruction  $SN_{eff}$  of 8.81 is considerably higher than expected, indicating that whatever phenomenon is affecting the response of Section 040507 is also affecting Section 040504. There appears to be a slight decrease in  $SN_{eff}$  in the final FWD test performed on December 10, 2003.

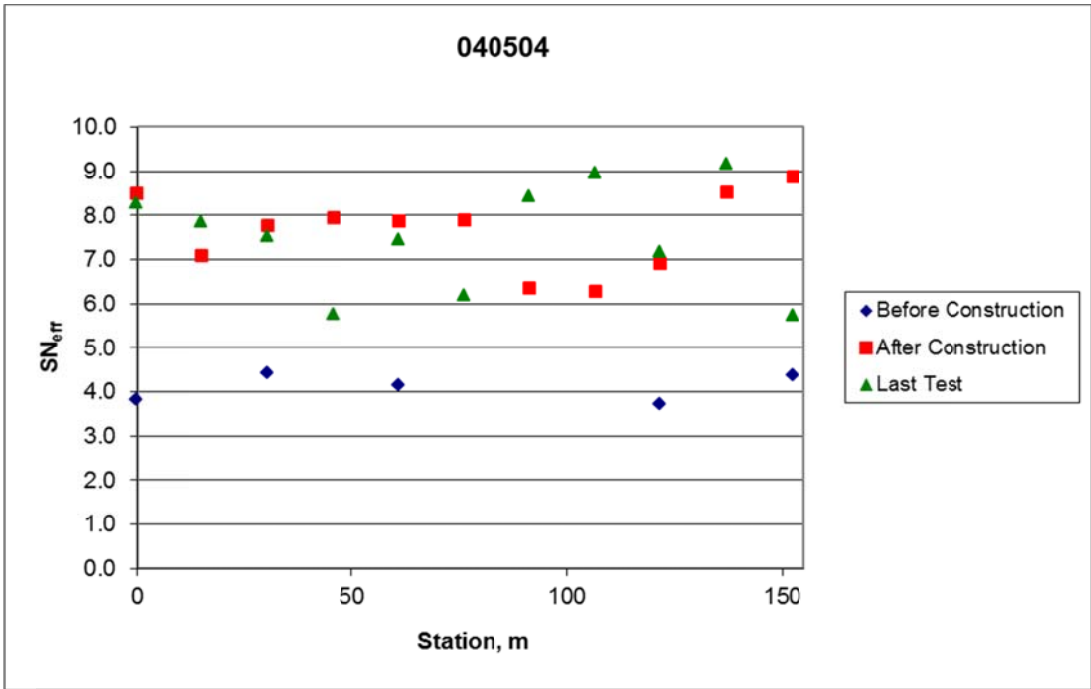


Figure 10. SN<sub>eff</sub> versus Station, Section 040504

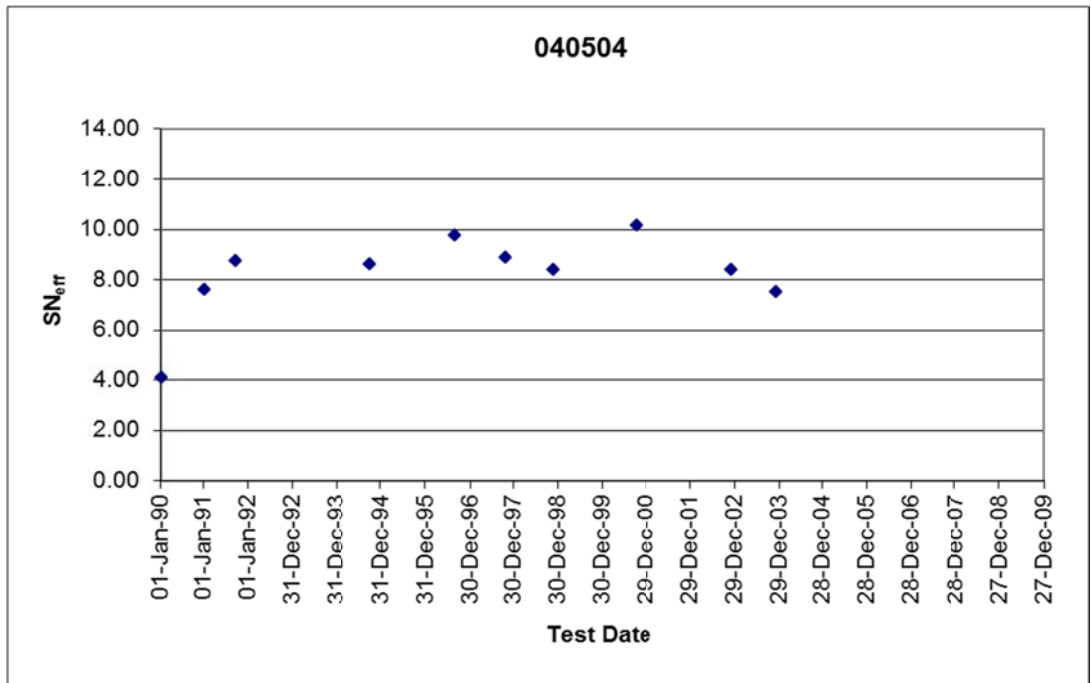


Figure 11. SN<sub>eff</sub> versus Date, Section 040504

### Section 040503

Section 040503 is in the minimal surface preparation, thick recycled overlay cell of the experimental matrix. According to the experimental design, the structure should be identical to Section 040504 except for the inclusion of recycled asphalt pavement (RAP) in the overlay material. The pre- and postconstruction layer structure as listed in Table TST\_L05B of the LTPP database is shown in Table 15.

**Table 15. Layer Structure, Section 040503**

Construction No.	Layer No.	Material Type	Thickness (inches) <sup>1</sup>
1	4	OGFC	0.8
	3	HMAC	4.2
	2	AB, 4.8% passing #200	16.6
	1	A-2-4, Clayey sand with gravel	
2 – 5 <sup>2</sup>	5	Recycled HMAC overlay	4.7
	3	HMAC	4.2
	2	AB, 4.8% passing #200	16.6
	1	A-2-4, Clayey sand with gravel	

1 Depth of milling: 0.8 inch.

2 Does not include fog seals, which are considered structurally insignificant.

Construction was from May 1 to 8, 1990, and consisted of milling 0.8 inch of the original pavement and overlaying with 4.7 inches of recycled HMA placed in two lifts.

Compared to Section 040504, the thickness of AC material is 0.2 inch less, with the difference divided evenly between the original pavement and the overlay. The thickness of AB is 1 inch less.

$M_r$  calculated using the AASHTO 1993 procedure is shown in Figures 12 and 13. Figure 12 shows  $M_r$  versus station for the preconstruction, postconstruction, and final tests. Figure 13 shows the average  $M_r$  for each test date.

The subgrade at Section 040503 exhibits different behavior than at Sections 040507 and 040504 in both the  $M_r$  versus station and  $M_r$  versus date plots. In the  $M_r$  versus station plot, there is a distinct trend in all three data sets, with  $M_r$  being higher at the beginning of the section than at the end. In addition, while the immediate postconstruction increase in  $M_r$  is uniform across the section, it then decreases over time, primarily at the end of the section. The  $M_r$  versus date plot shows a consistent increase in  $M_r$  to a rather high postconstruction value, but  $M_r$  then decreases to nearly the preconstruction value.

Figures 14 and 15 show  $SN_{eff}$  for this section versus station and time. The  $SN_{eff}$  values in these figures are temperature-corrected using the methodology described earlier in this chapter.

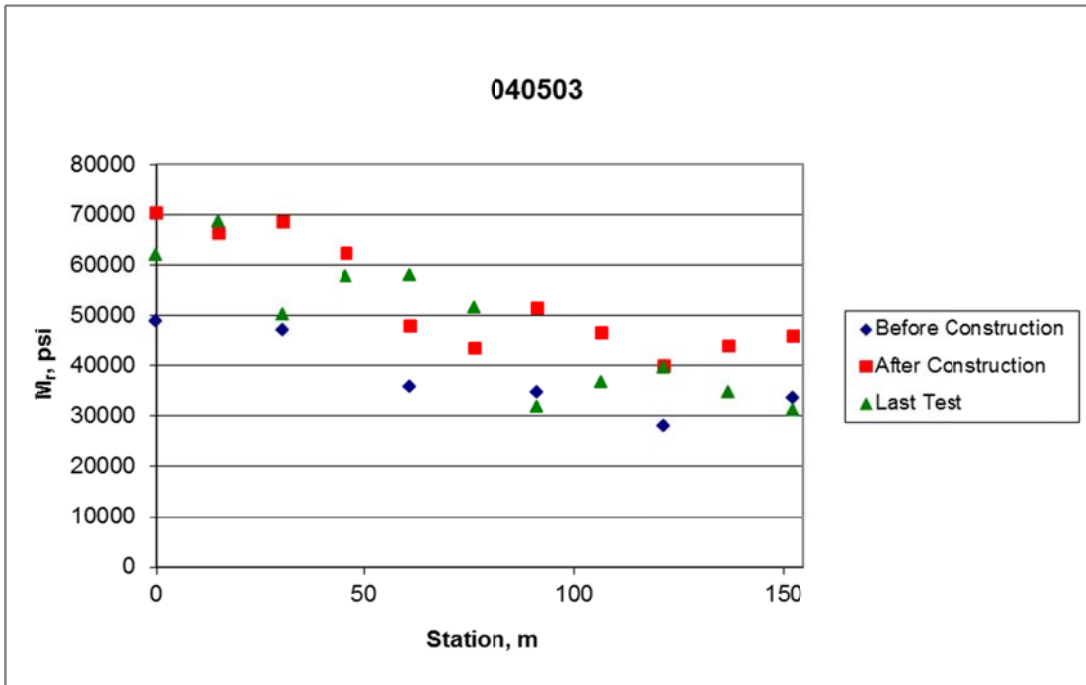


**Figure 12. Subgrade Resilient Modulus versus Station, Section 040503**

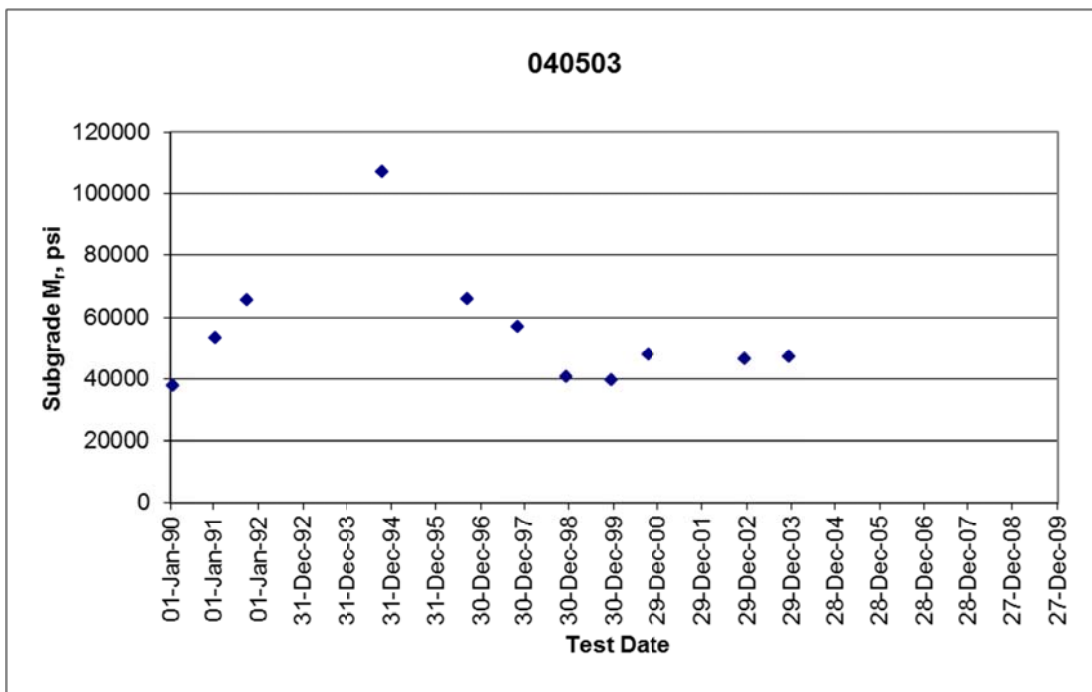


**Figure 13. Subgrade Resilient Modulus versus Date, Section 040503**

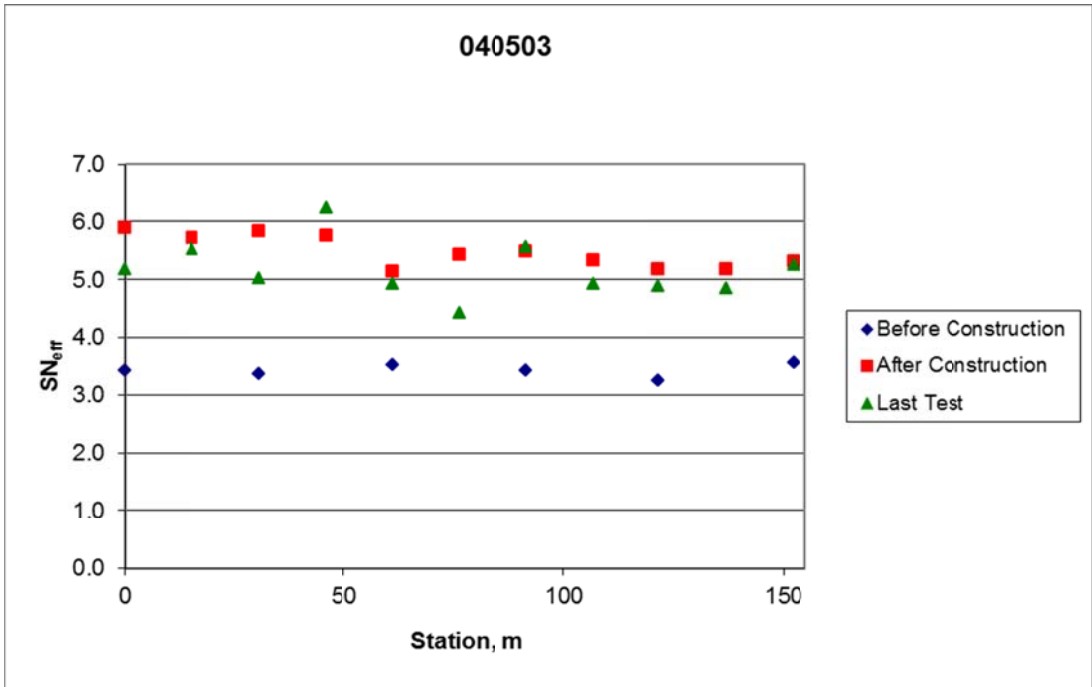


Figure 14. SN<sub>eff</sub> versus Station, Section 040503

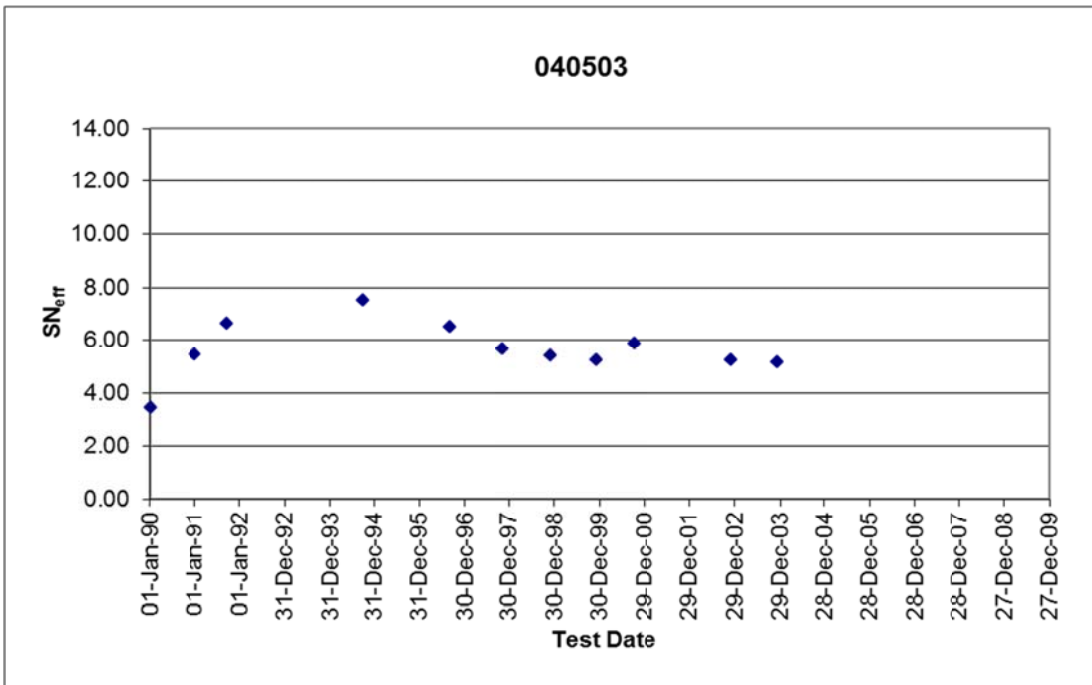


Figure 15. SN<sub>eff</sub> versus Date, Section 040503

The  $SN_{eff}$  versus station plot does not show the same trend as the  $M_r$  versus station plot, indicating that  $SN_{eff}$  and  $M_r$  are independent. The immediate postconstruction  $SN_{eff}$  is 5.47, which is reasonable for the pavement section. However, it increases to a peak of 7.50 on October 18, 1994, which is higher than would be considered reasonable. It then decreases back to a value consistent with the immediate postconstruction value. This is a similar trend as is visible in the  $M_r$  versus time plot.

### Section 040508

Section 040508 is in the intensive surface preparation, thick recycled overlay cell of the experimental matrix. According to the experimental design, it should differ from Section 040503 only in the depth of the mill-and-fill. It should differ from Section 040507 only in the use of recycled material in the AC overlay. The pre- and postconstruction layer structure as listed in Table TST\_L05B of the LTPP database is shown in Table 16.

**Table 16. Layer Structure, Section 040508**

Construction No.	Layer No.	Material Type	Thickness (inches) <sup>1</sup>
1	4	OGFC	0.7
	3	HMAC	4.7
	2	AB, 7.9% passing #200	15
	1	A-2-4, Silty gravel with sand	
2 – 7 <sup>2</sup>	6	Recycled HMAC overlay	4.1
	5	Recycled HMAC overlay	2.4
	3	HMAC	2.7
	2	AB, 7.9% passing #200	15
	1	A-2-4, Silty gravel with sand	

1 Depth of milling: 2.7 inches.

2 Does not include fog seals, which are considered structurally insignificant.

Construction was performed on April 21 to May 3, 1990, and consisted of milling 2.7 inches of the original AC surface and placing 6.5 inches of recycled HMAC in three lifts. Fog seals were applied on May 28, 1998, and April 16, 2003. Crack sealing was performed on May 1, 2002.

Compared to Section 040503, the postconstruction thickness of AC is 0.3 inch greater, and more of it is new overlay. The thickness of AB is 1.6 inches less. Compared to Section 040507, the postconstruction thickness of AC is the same, but the thickness of AB is 5.7 inches less.

$M_r$  calculated using the AASHTO 1993 procedure is shown in Figures 16 and 17. Figure 16 shows  $M_r$  versus station for the preconstruction, postconstruction, and final tests. Figure 17 shows the average  $M_r$  for each test date.

The  $M_r$  versus station plot shows a high degree of variability and a weak trend, with  $M_r$  increasing from the beginning to the end of the section. Unlike in most of the other sections, the preconstruction data also exhibits a high degree of variability. The  $M_r$  versus date plot shows an increase in  $M_r$  that persists for a longer duration than is observed at the other sites.  $M_r$  then declines to a level that is more typical for a subgrade material.

Figures 18 and 19 show  $SN_{eff}$  for this section versus station and time. The  $SN_{eff}$  values in these figures are temperature-corrected using the methodology described earlier in this chapter.

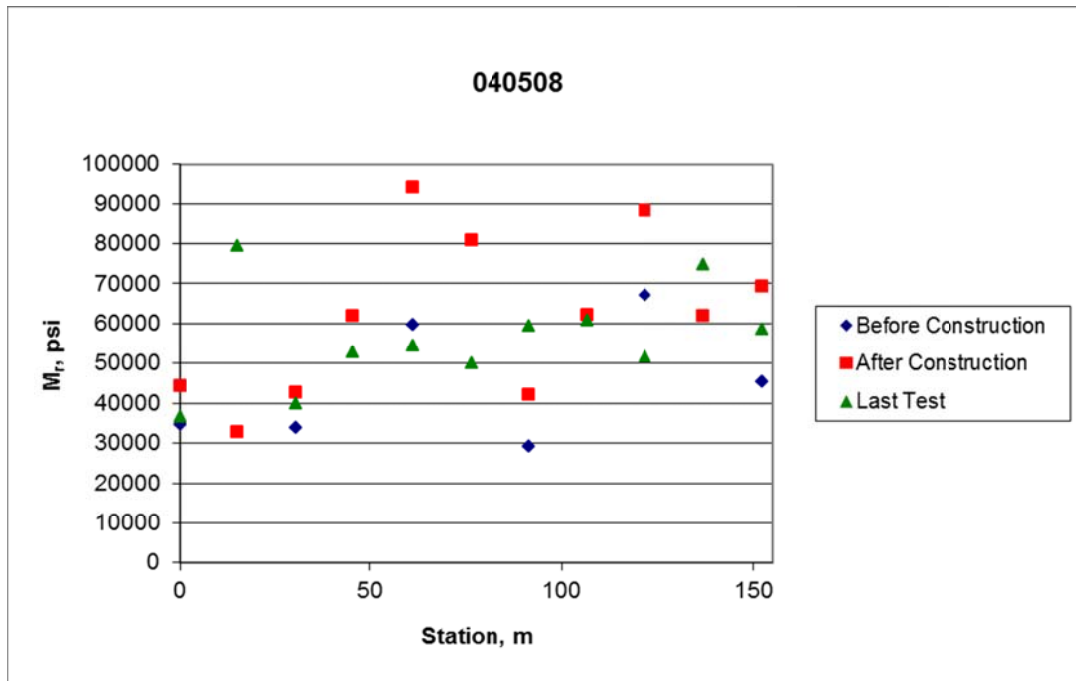


Figure 16.  $M_r$  versus Station, Section 040508

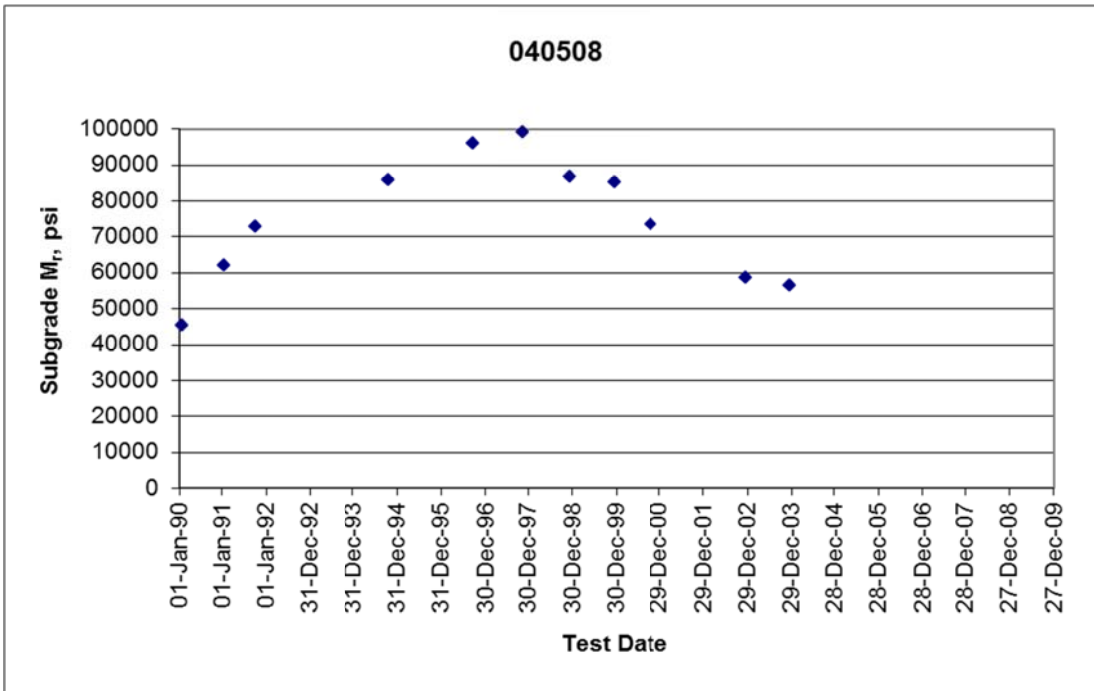


Figure 17.  $M_r$  versus Date, Section 040508

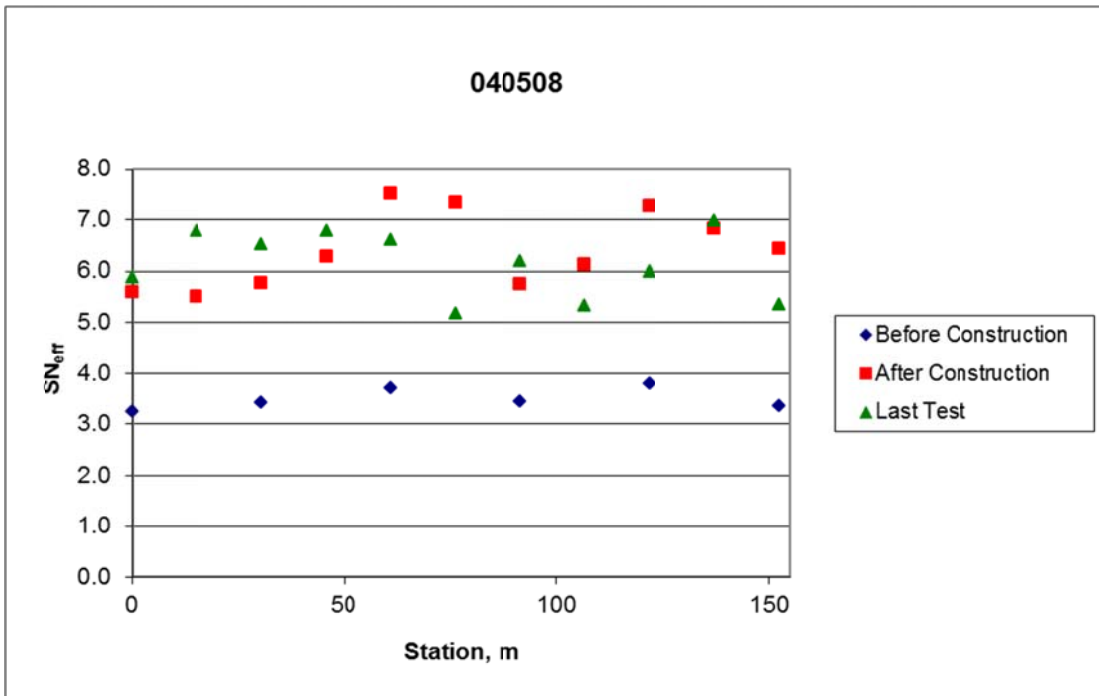
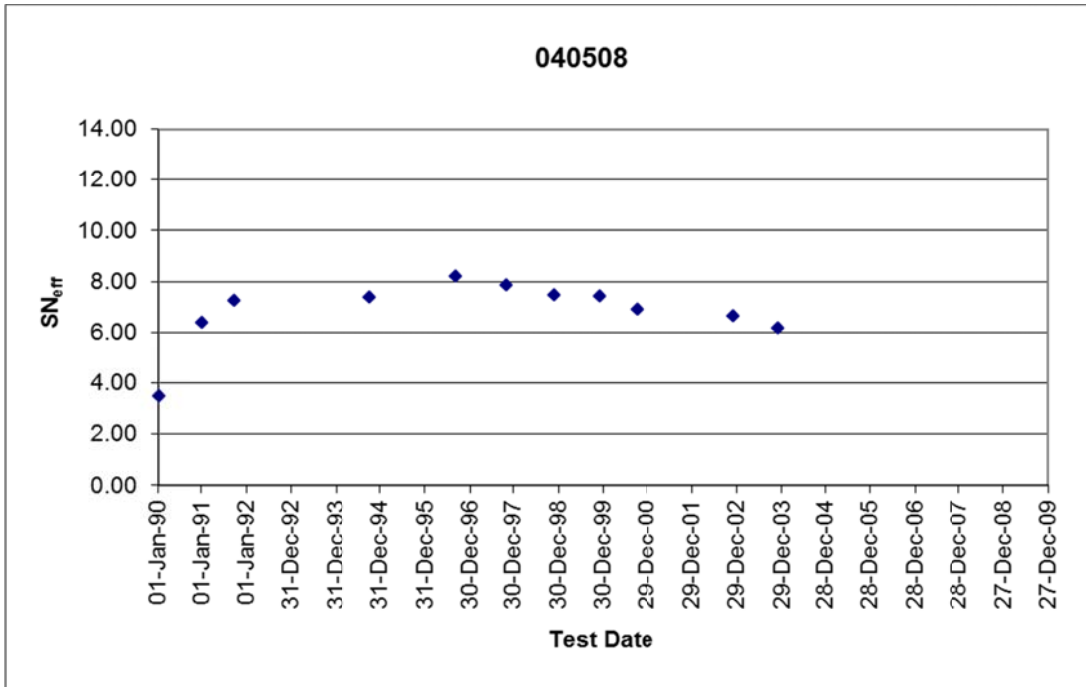


Figure 18.  $SN_{eff}$  versus Station, Section 040508



**Figure 19. SN<sub>eff</sub> versus Date, Section 040508**

The SN<sub>eff</sub> versus station plot shows less variability than the M<sub>r</sub> versus station plot, although for the immediate postconstruction and final data sets, the high and low points are coincident. The SN<sub>eff</sub> versus date plot shows an initial increase and then a gradual decrease. The peak SN<sub>eff</sub>, at six years after construction, is 8.20, which is higher than would be expected given the pavement section. The SN<sub>eff</sub> calculated from the final test at this section is 6.15, which is still somewhat higher than would be expected.

**Section 040509**

Section 040509 is in the intensive surface preparation, thin recycled overlay cell of the experimental matrix. According to the experimental design, the major difference between this section and Section 040508 should be the thickness of the overlay. The pre- and postconstruction layer structure as listed in Table TST\_L05B of the LTPP database is shown in Table 17.

Construction was performed from May 1 to 3, 1990. Construction consisted of milling 2.8 inches of the original surface and placing 3.8 inches of recycled HMAC in two lifts. The section also received fog seals on May 28, 1998, and April 16, 2003, and crack sealing on May 1, 2002.

Compared to Section 040508, the thickness of AC is 2.7 inches less. The thickness of AB is 0.2 inch less.

**Table 17. Layer Structure, Section 040509**

Construction No.	Layer No.	Material Type	Thickness (inches) <sup>1</sup>
1	4	OGFC	0.7
	3	HMAC	4.7
	2	AB, 7.9% passing #200	14.8
	1	A-1-b, Silty sand with gravel	
2 – 5 <sup>2</sup>	6	Recycled HMAC overlay	1.3
	5	Recycled HMAC overlay	2.6
	3	HMAC	2.6
	2	AB, 7.9% passing #200	14.8
	1	A-1-b, Silty sand with gravel	

1 Depth of milling: 2.8 inches.

2 Does not include fog seals, which are considered structurally insignificant.

$M_r$  calculated using the AASHTO 1993 procedure is shown in Figures 20 and 21. Figure 20 shows  $M_r$  versus station for the preconstruction, postconstruction, and final tests. Figure 21 shows the average  $M_r$  for each test date.

Similar trends for  $M_r$  versus station are seen in the pre- and postconstruction data. Variability with station decreases in the final data set. The  $M_r$  versus date data show an increase in  $M_r$  and then a return to approximately preconstruction  $M_r$  levels, which occurs at about seven years after construction.

Figures 22 and 23 show  $SN_{eff}$  for this section versus station and time. The  $SN_{eff}$  values in these figures are temperature-corrected using the methodology described earlier in this chapter.

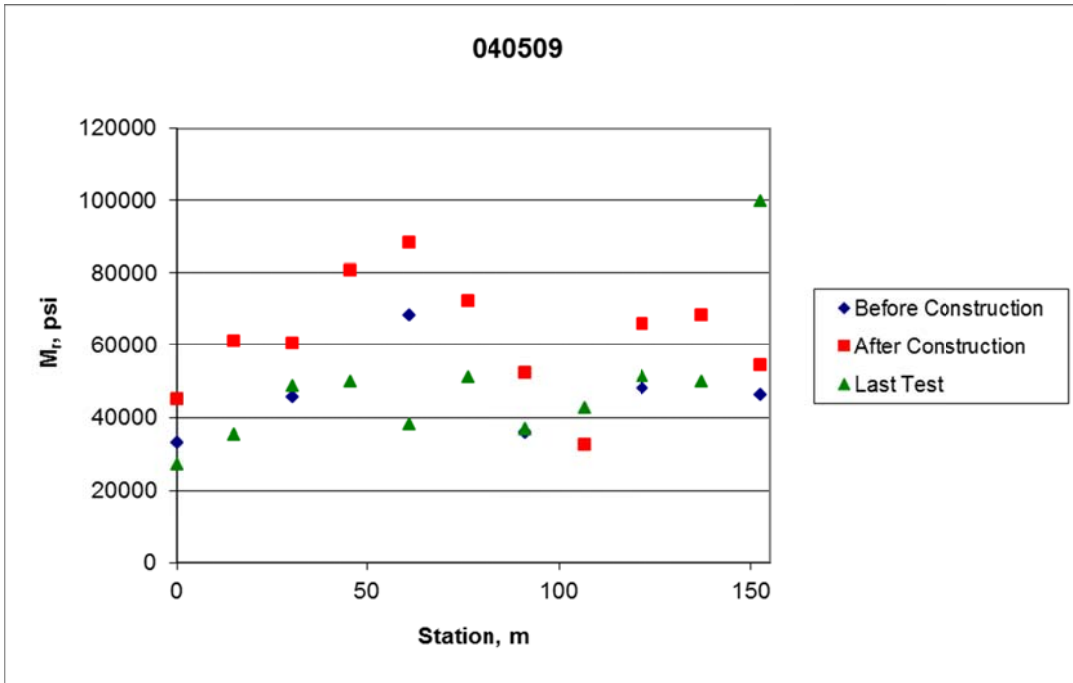


Figure 20. M<sub>r</sub> versus Station, Section 040509

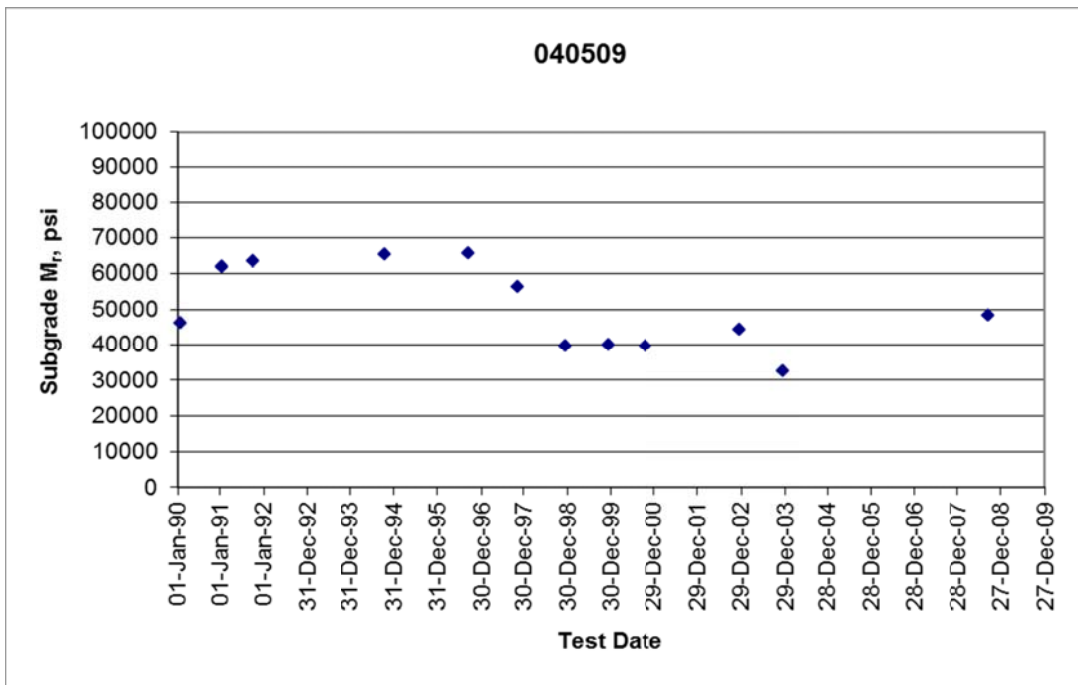


Figure 21. M<sub>r</sub> versus Date, Section 040509

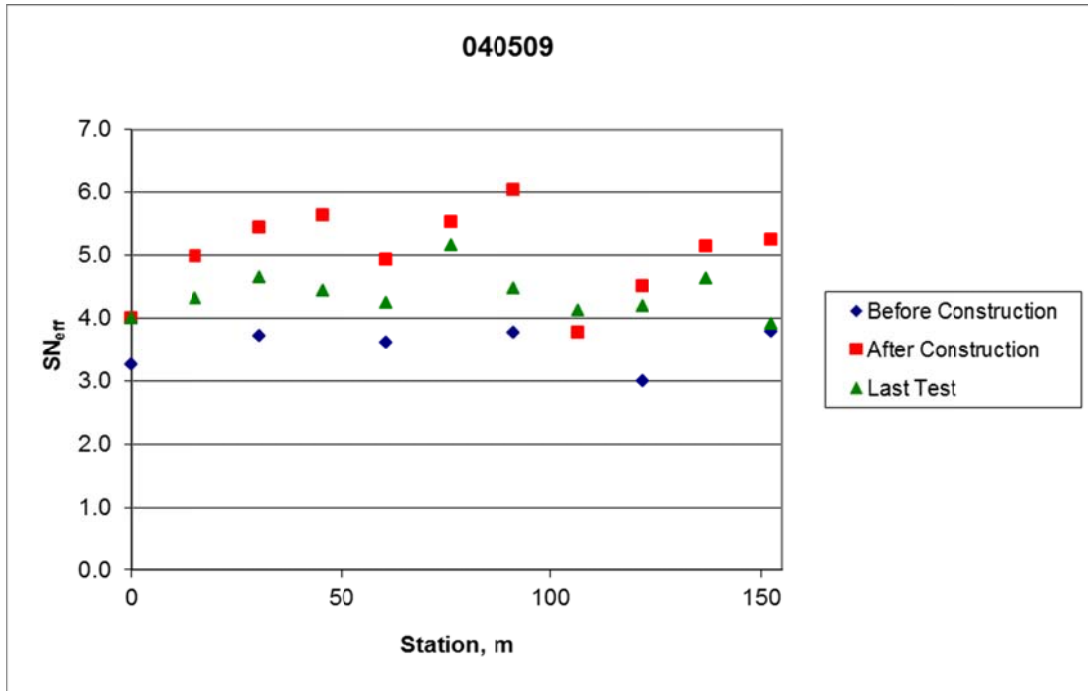


Figure 22. SN<sub>eff</sub> versus Station, Section 040509

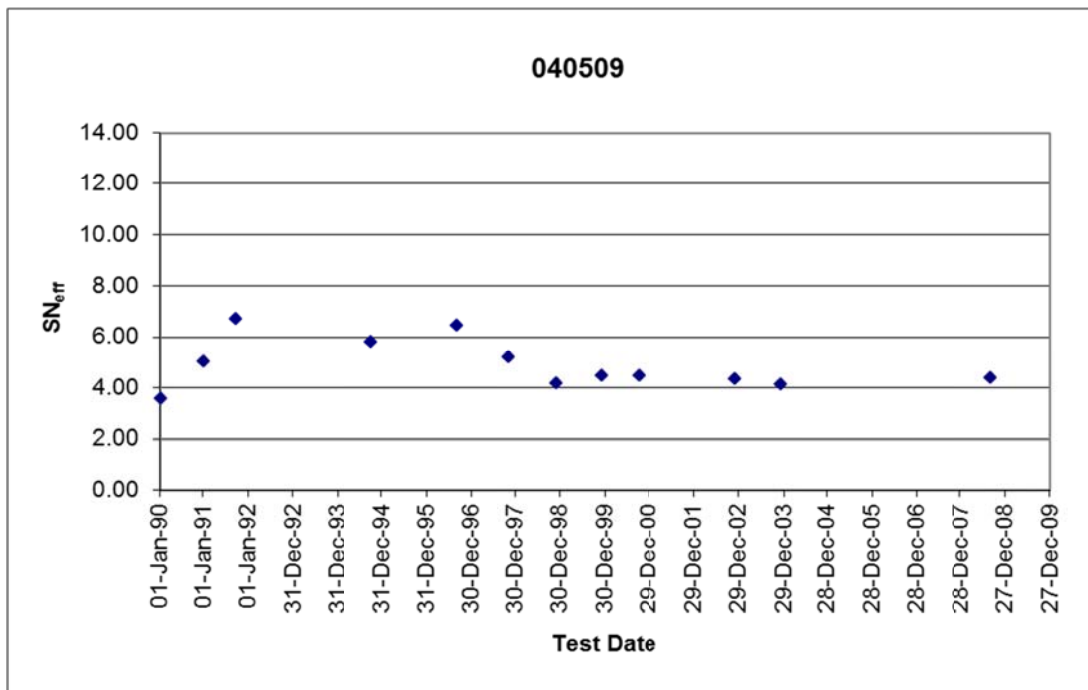


Figure 23. SN<sub>eff</sub> versus Date, Section 040509

The trends seen in the SN<sub>eff</sub> versus station plot are not the same as those seen in the M<sub>r</sub> versus station plot, indicating that SN<sub>eff</sub> and M<sub>r</sub> are independent. However, the SN<sub>eff</sub> versus date and M<sub>r</sub> versus date

plots show a similar trend, with an increase over the first two years after construction and then a decrease approximately seven years after construction. The peak  $SN_{eff}$  value is 6.68, which is higher than would be expected for this pavement section. After 1998, the average  $SN_{eff}$  value is 4.29, which is reasonable.

### Section 040502

Section 040502 is in the minimal surface preparation, thin recycled overlay cell of the experimental matrix. According to the experimental design, the major difference between this section and Section 040509 should be the thickness of the mill-and-fill. The pre- and postconstruction layer structure as listed in Table TST\_L05B of the LTPP database is shown in Table 18.

**Table 18. Layer Structure, Section 040502**

Construction No.	Layer No.	Material Type	Thickness (inches) <sup>1</sup>
1	4	OGFC	0.9
	3	HMAC	4.2
	2	AB, 7% passing #200	14.7
	1	A4, Clayey sand with gravel	
2 – 6 <sup>2</sup>	5	Recycled HMAC overlay	2.7
	3	HMAC	3.7
	2	AB, 7% passing #200	14.7
	1	A4, Clayey sand with gravel	

1 Depth of milling: 1.4 inches.

2 Does not include fog seals, which are considered structurally insignificant.

Construction was performed from May 1 to 8, 1990, and consisted of milling 1.4 inches of the original surface and placing a 2.7-inch overlay in one lift. Fog seals were applied on May 28, 1998, August 23, 2001, and April 16, 2003. Crack sealing was performed on May 1, 2002.

Compared to Section 040509, the thickness of AC is 0.1 inch less, although less of it is new overlay. The thickness of AB is also 0.1 inch less.

$M_r$  calculated using the AASHTO 1993 procedure is shown in Figures 24 and 25. Figure 24 shows  $M_r$  versus station for the preconstruction, postconstruction, and final tests. Figure 25 shows the average  $M_r$  for each test date.

Unlike the previous sections, Section 040502 does not show a significant increase in  $M_r$  after construction, and in fact the overall trend of  $M_r$  over time is downward.

Figures 26 and 27 show  $SN_{eff}$  for this section versus station and time. The  $SN_{eff}$  values in these figures are temperature-corrected using the methodology described in the previous section.

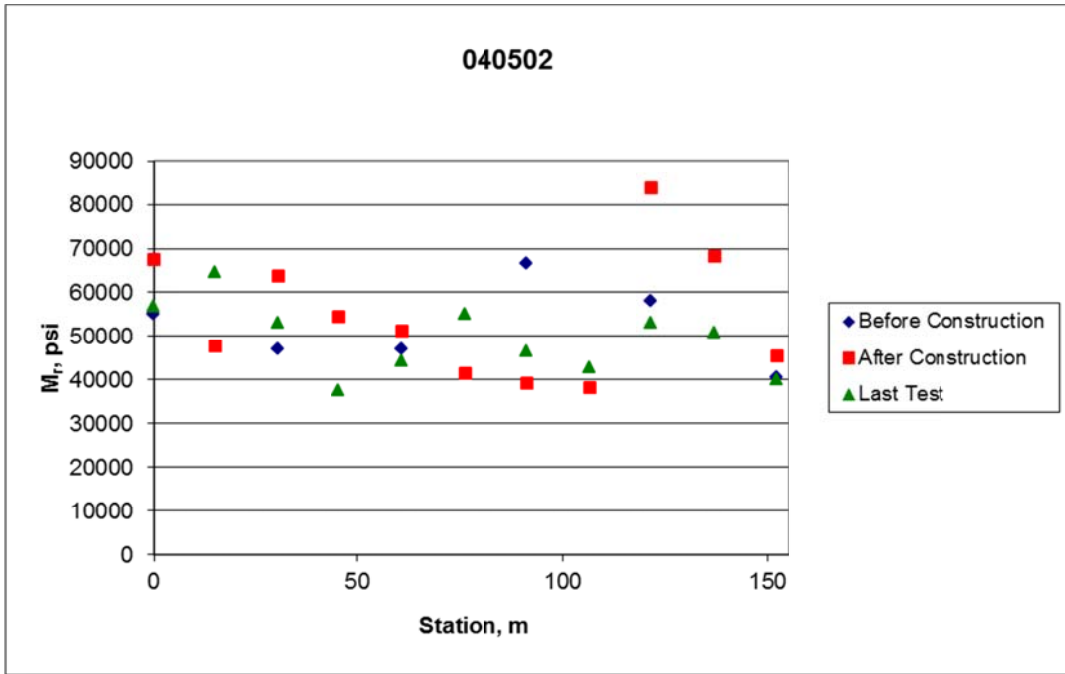


Figure 24.  $M_r$  versus Station, Section 040502

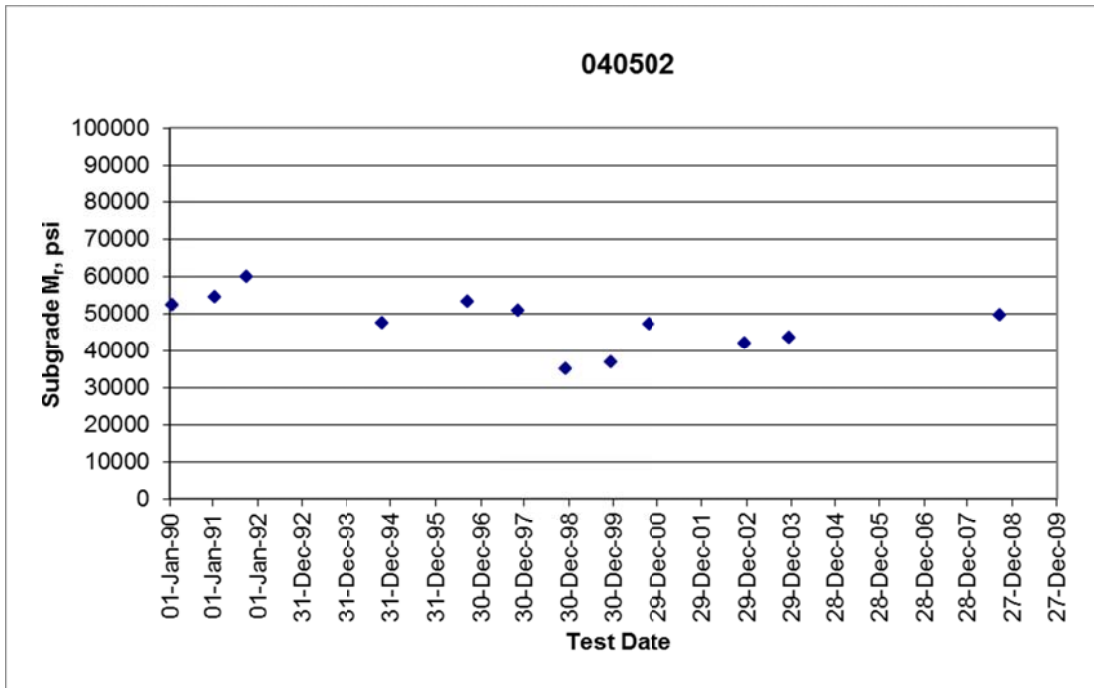


Figure 25.  $M_r$  versus Date, Section 040502

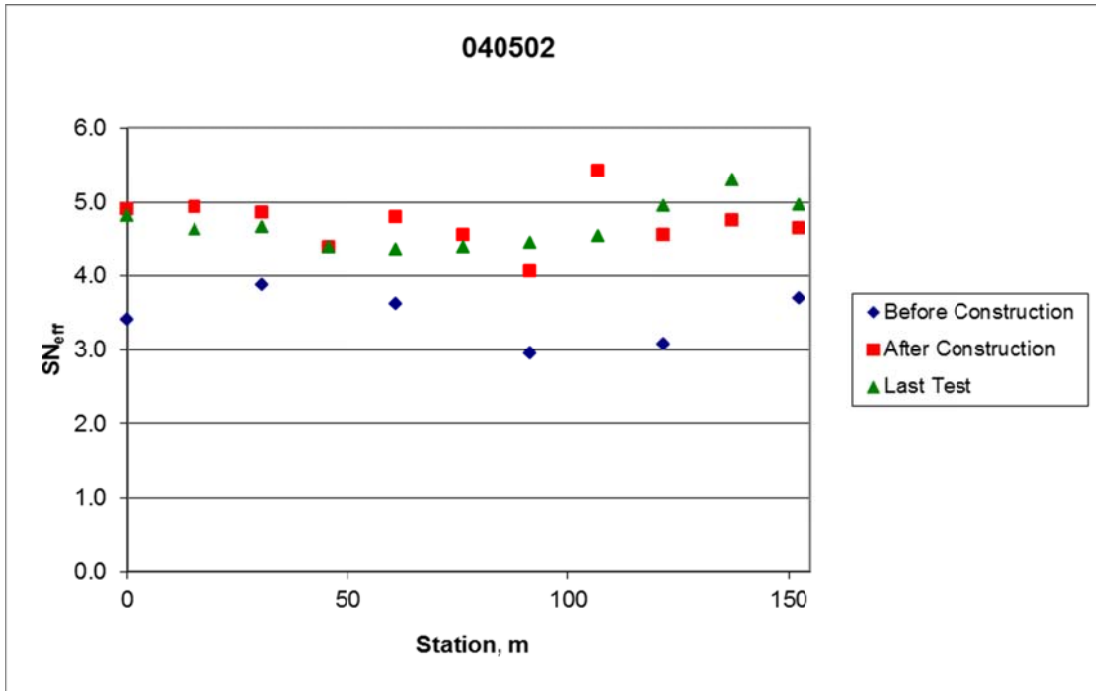


Figure 26. SN<sub>eff</sub> versus Station, Section 040502

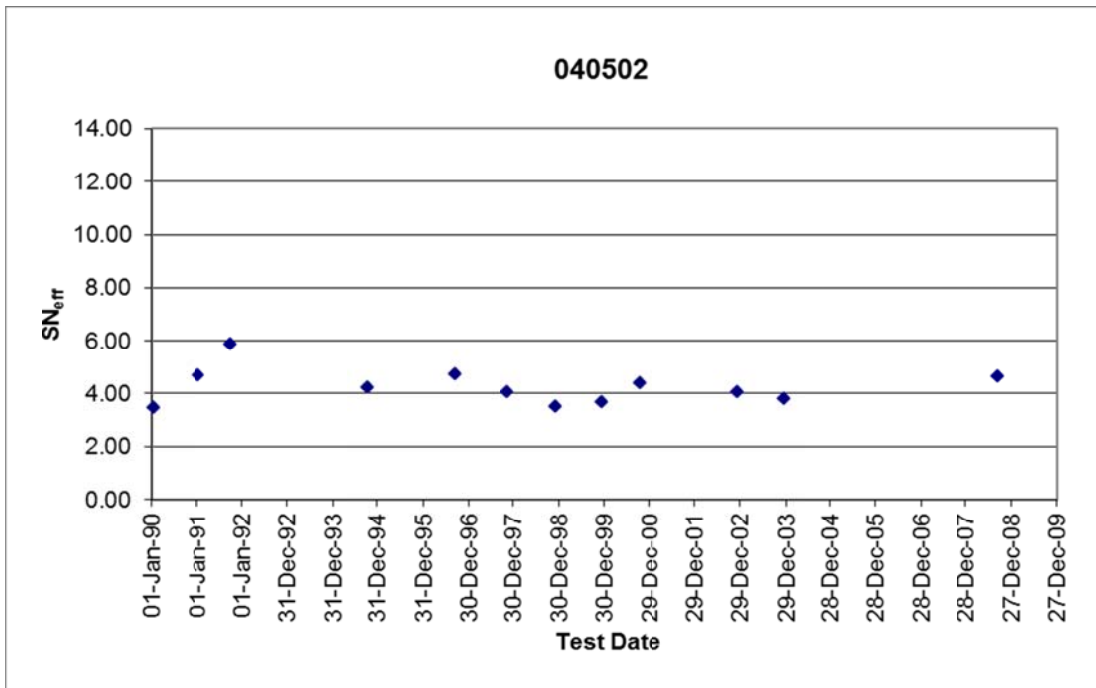


Figure 27. SN<sub>eff</sub> versus Date, Section 040502

The  $SN_{eff}$  versus date plot shows an initial increase to 5.86 at 17 months after construction.  $SN_{eff}$  then declines to an average of 4.12, which is reasonable for this pavement section. The decline may be due to pavement deterioration; however, the data set is lacking points between October 1991 and October 1994, when this may have occurred.

### Section 040506

Section 040506 is in the intensive surface preparation, thin virgin overlay cell of the experimental matrix. The major difference between this section and Section 040509 should be the use of virgin HMA instead of recycled HMA. The pre- and postconstruction layer structure as listed in Table TST\_L05B of the LTPP database is shown in Table 19.

**Table 19. Layer Structure, Section 040506**

Construction No.	Layer No.	Material Type	Thickness (inches) <sup>1</sup>
1	4	OGFC	0.9
	3	HMAC	4.0
	2	AB, 7% passing #200	12.8
	1	A4, Clayey sand with gravel	
2 – 7 <sup>2</sup>	6	Virgin HMA overlay	2.4
	5	Virgin HMA overlay	2.8
	3	HMAC	3
	2	AB, 7% passing #200	12.8
	1	A4, Clayey sand with gravel	

1 Depth of milling: 1.9 inches.

2 Does not include fog seals, which are considered structurally insignificant.

Compared to Section 040509, the thickness of AC is 1.7 inches greater, and the new overlays do not include recycled material. The thickness of AB is 2 inches less.

Construction was performed from May 16 to 24, 1990, and consisted of milling 2.9 inches of the original AC surface and placing 5.2 inches of HMA in two lifts. The section received fog seals on May 28, 1998, August 23, 2001, and April 16, 2003. Crack sealing was performed on May 1, 2002. Patching was performed on August 1, 2007.

$M_r$  calculated using the AASHTO 1993 procedure is shown in Figures 28 and 29. Figure 28 shows  $M_r$  versus station for the preconstruction, postconstruction, and final tests. Figure 29 shows the average  $M_r$  for each test date.

This section exhibits a postconstruction increase in  $M_r$ , followed by a gradual decrease. The increase in average postconstruction  $M_r$  is predominantly due to high  $M_r$  in the first half of the section. The  $M_r$  in the second half of the section is closer to the preconstruction value.

Figures 30 and 31 show  $SN_{eff}$  for this section versus station and time. The  $SN_{eff}$  values in these figures are temperature-corrected using the methodology described earlier in this chapter.

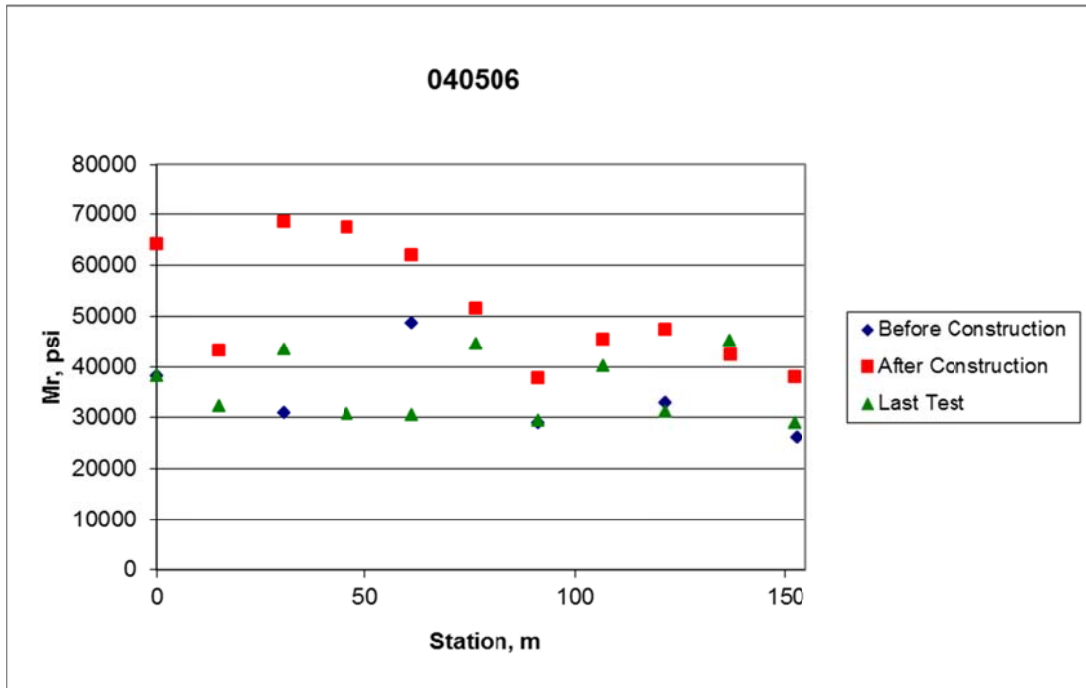


Figure 28.  $M_r$  versus Station, Section 040506

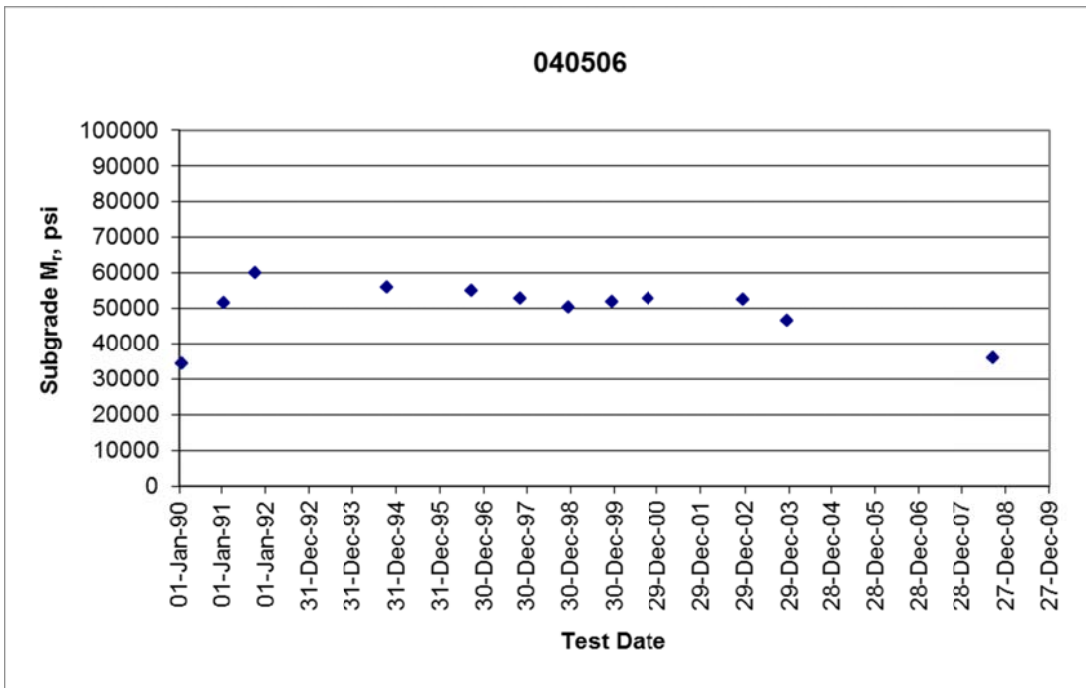


Figure 29.  $M_r$  versus Date, Section 040506

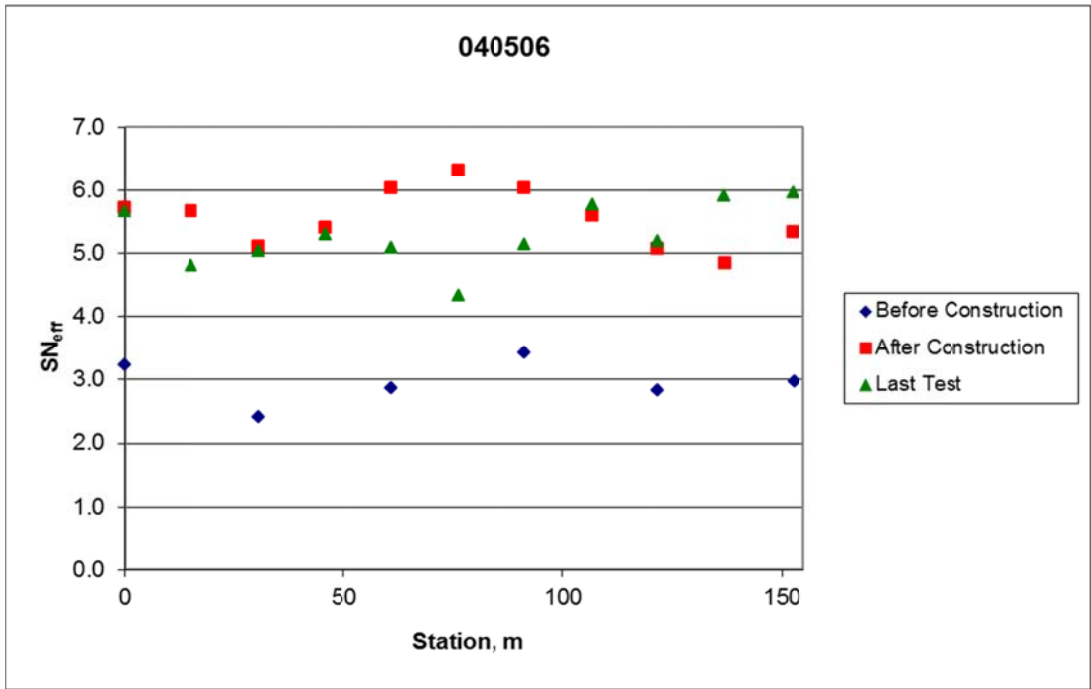


Figure 30. SN<sub>eff</sub> versus Station, Section 040506

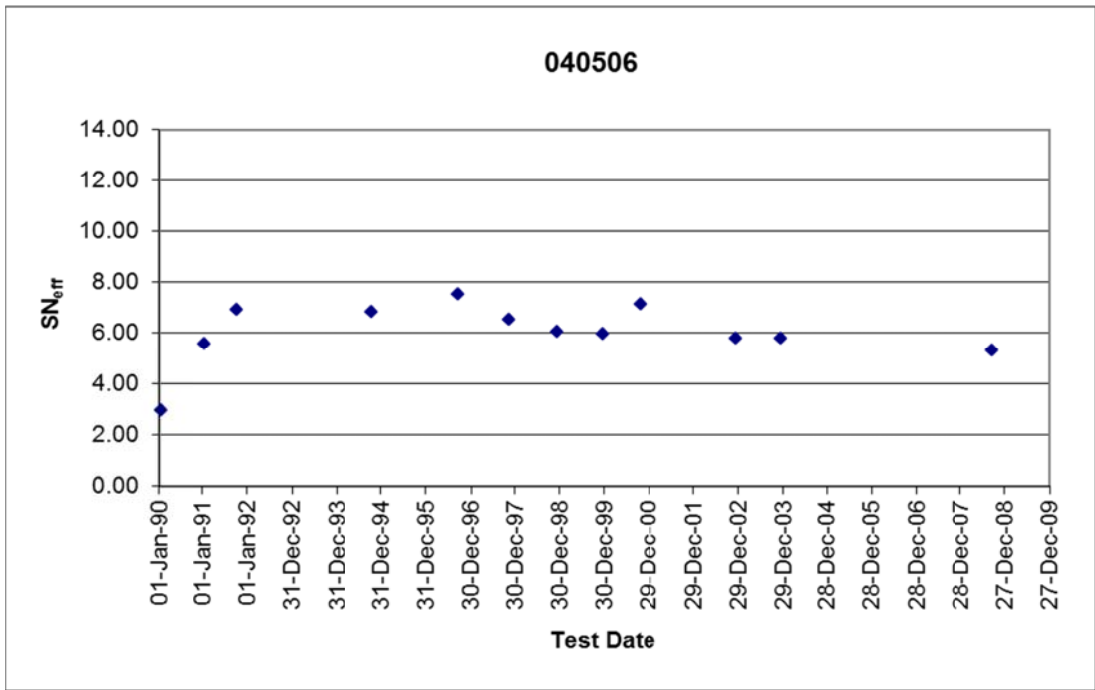


Figure 31. SN<sub>eff</sub> versus Date, Section 040506

The  $SN_{eff}$  versus date data show an increase in  $SN_{eff}$  to an average of 6.89 at 17 months after construction, and then a decrease to 5.27 at 18 years after construction. The  $SN_{eff}$  versus station data show that most of the decrease in  $SN_{eff}$  occurred between the stations at 80 m and 100 m.

### Section 040505

Section 040505 is in the minimal surface preparation, thin virgin overlay cell of the experimental matrix. According to the experimental design, the major difference between this section and Section 040506 should be the depth of the mill-and-fill. The major difference between this section and Section 040502 should be the use of virgin material for the overlay. The pre- and postconstruction layer structure as listed in Table TST\_L05B of the LTPP database is shown in Table 20.

**Table 20. Layer Structure, Section 040505**

Construction No.	Layer No.	Material Type	Thickness (inches) <sup>1</sup>
1	4	OGFC	0.9
	3	HMAC	4.1
	2	AB, 7% passing #200	12.8
	1	A4, Clayey sand with gravel	
2 – 6 <sup>2</sup>	5	Virgin HMAC overlay	2.8
	3	HMAC	4.1
	2	AB, 7% passing #200	12.8
	1	A4, Clayey sand with gravel	

1 Depth of milling: 1.2 inches.

2 Does not include fog seals, which are considered structurally insignificant.

Construction was performed from May 3 to 24, 1990, and consisted of milling 0.9 inch of the existing material and placing 2.8 inches of HMAC in one lift. The section received fog seals on May 28, 1998, August 23, 2001, and April 16, 2003. Crack sealing was performed on May 1, 2002.

Compared to Section 040506, the postconstruction thickness of AC is 1.3 inches less. The thickness of AB is the same. Compared to Section 040502, the postconstruction thickness of AC is 0.5 inch greater, and the thickness of AB is 1.9 inches less.

$M_r$  calculated using the AASHTO 1993 procedure is shown in Figures 32 and 33. Figure 32 shows  $M_r$  versus station for the preconstruction, postconstruction, and final tests. Figure 33 shows the average  $M_r$  for each test date.

The postconstruction  $M_r$  is highly variable with respect to station, and consistently shows a soft spot in the middle of the section. Average  $M_r$  increases for the first 17 months after construction, then returns to the preconstruction value approximately eight years after construction, and then gradually increases again.

Figures 34 and 35 show  $SN_{eff}$  for this section versus station and time. The  $SN_{eff}$  values in these figures are temperature-corrected using the methodology described earlier in this chapter.

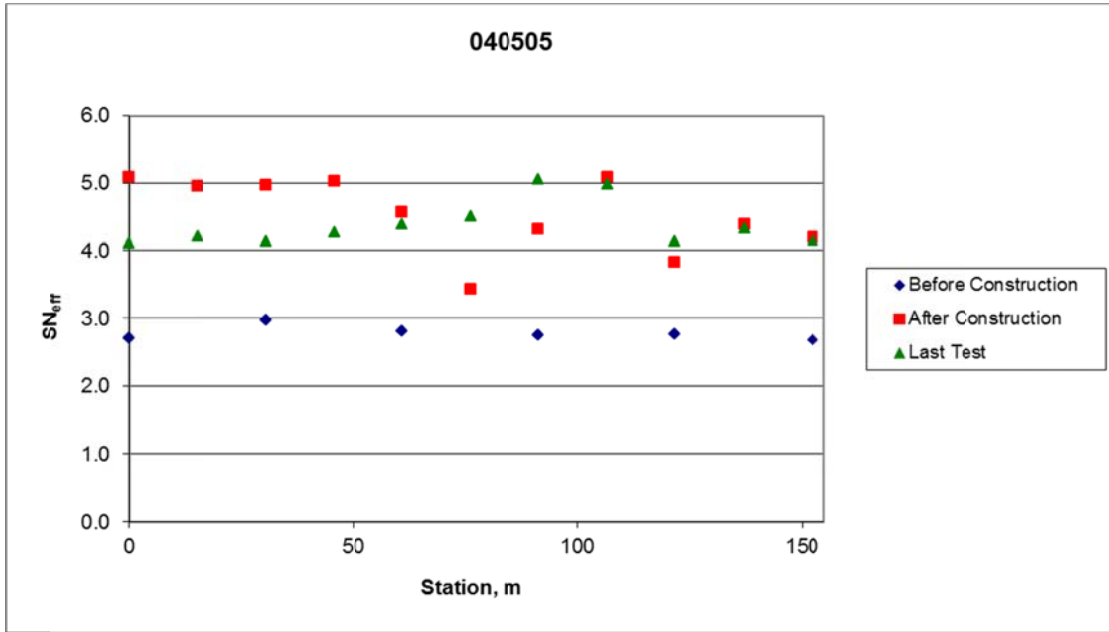


Figure 32.  $M_r$  versus Station, Section 040505

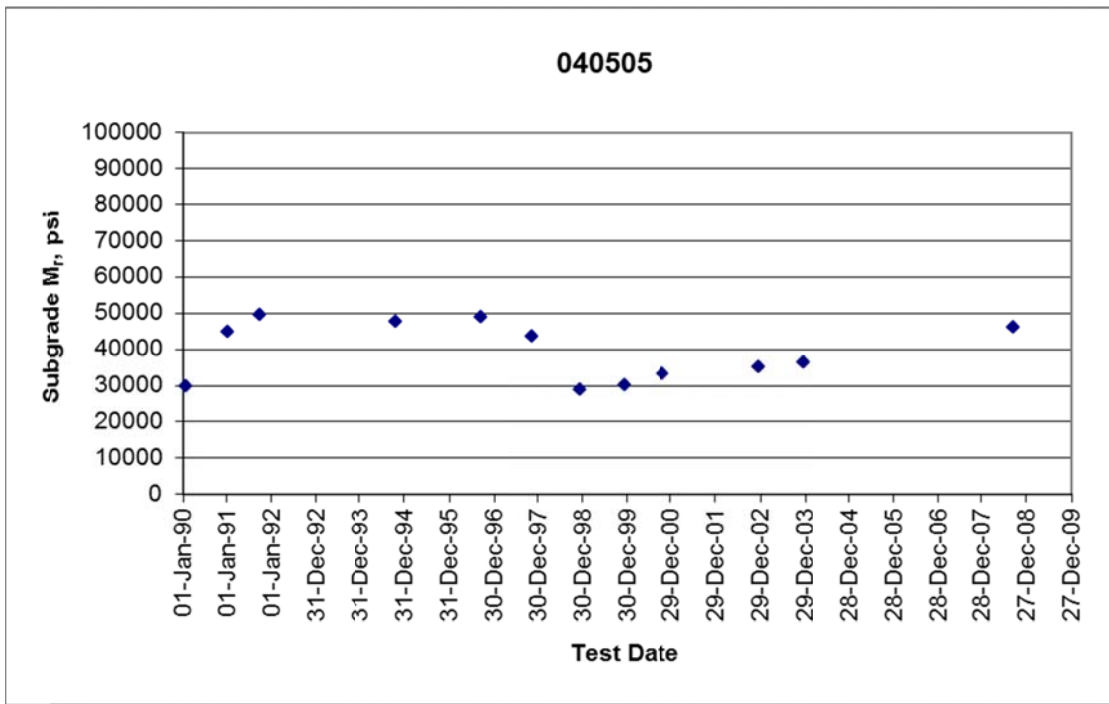


Figure 33.  $M_r$  versus Date, Section 040505

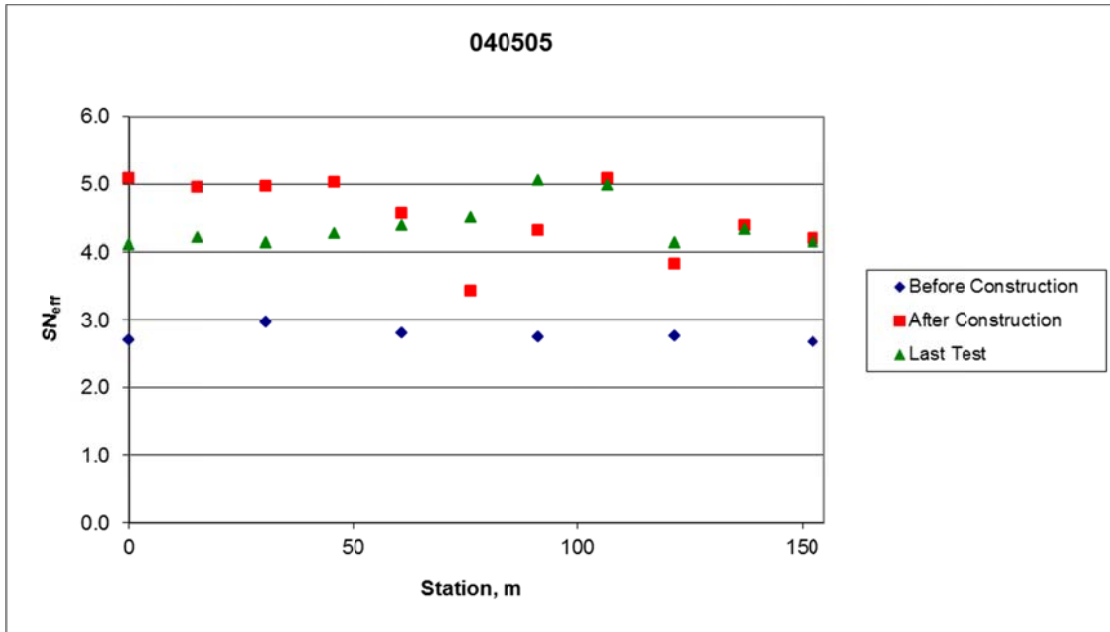


Figure 34. SN<sub>eff</sub> versus Station, Section 040505

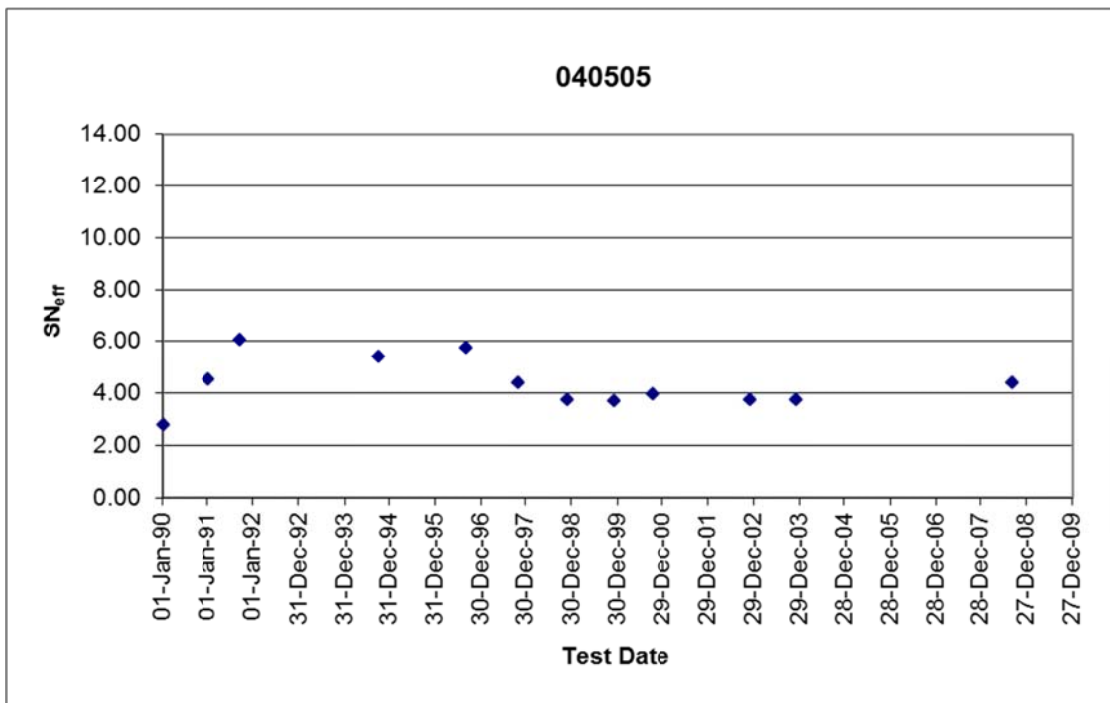


Figure 35. SN<sub>eff</sub> versus Date, Section 040505

The immediate postconstruction test results show a low  $SN_{eff}$  in the center of the section, corresponding to the low  $M_r$  value.  $SN_{eff}$  increases over time in this localized area, even as the average  $SN_{eff}$  throughout the section decreases.

### Section 040559

Section 040559 is a supplemental section, constructed using intensive surface preparation and an “inverted” overlay consisting of recycled AC over virgin AC. The pre- and postconstruction layer structure as listed in Table TST\_L05B of the LTPP database is shown in Table 21.

**Table 21. Layer Structure, Section 040559**

Construction No.	Layer No.	Material Type	Thickness (inches) <sup>1</sup>
1	4	OGFC	1.0
	3	HMAC	4.2
	2	AB, 7% passing #200	13.2
	1	A-2-4, Silty sand with gravel	
2 – 6 <sup>2</sup>	6	Recycled HMAC overlay	3
	5	Virgin HMAC overlay	3
	3	HMAC	1.7
	2	AB, 7% passing #200	13.2
	1	A-2-4, Silty sand with gravel	

1 Depth of milling: 3.5 inches.

2 Does not include fog seals, which are considered structurally insignificant.

Construction was performed from May 16 to 25, 1990, and consisted of milling 3.5 inches of the original AC surface and placing a 3-inch recycled overlay on a 3-inch virgin overlay. Fog seals were applied on May 28, 1998, August 23, 2001, and April 16, 2003. Crack sealing was performed on May 1, 2002.

$M_r$  calculated using the AASHTO 1993 procedure is shown in Figures 36 and 37. Figure 36 shows  $M_r$  versus station for the preconstruction, postconstruction, and final tests. Figure 37 shows the average  $M_r$  for each test date.

Figures 38 and 39 show  $SN_{eff}$  for this section versus station and time. The  $SN_{eff}$  values in these figures are temperature-corrected using the methodology described earlier in this chapter.

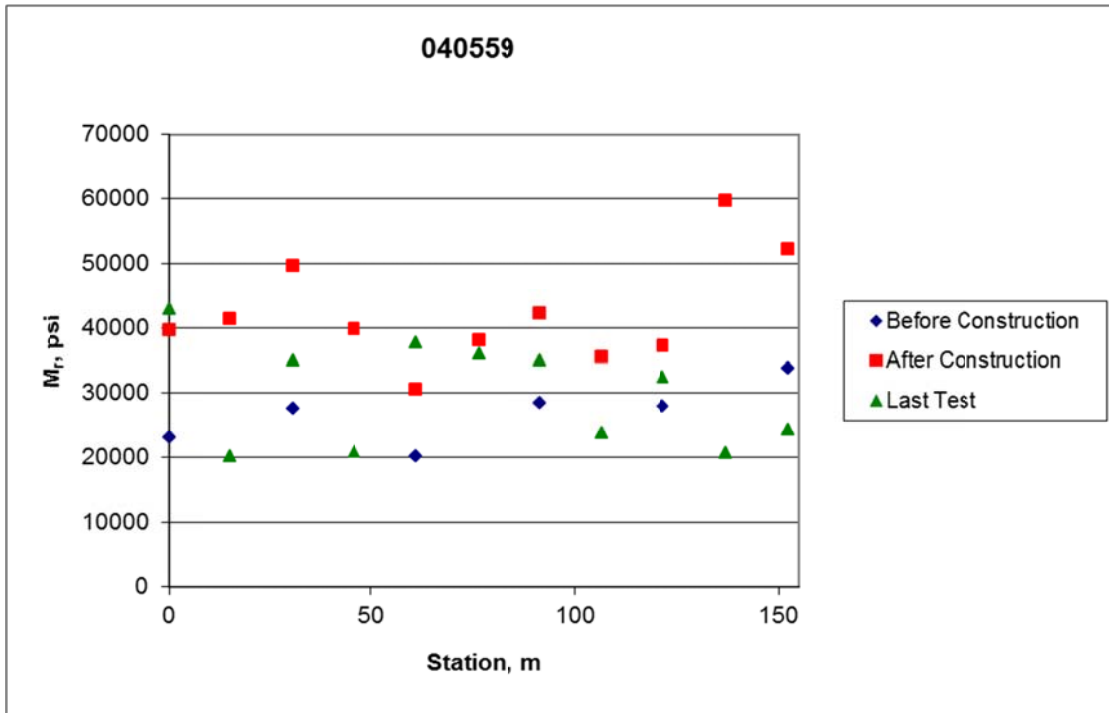


Figure 36.  $M_r$  versus Station, Section 040559

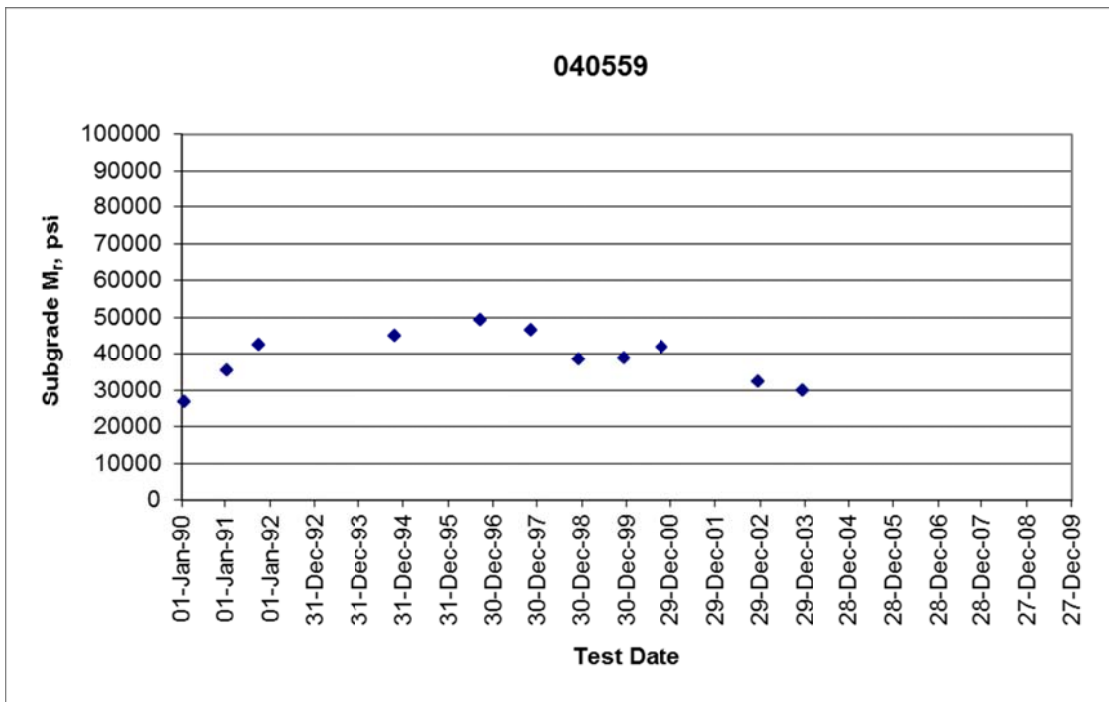


Figure 37.  $M_r$  versus Date, Section 040559

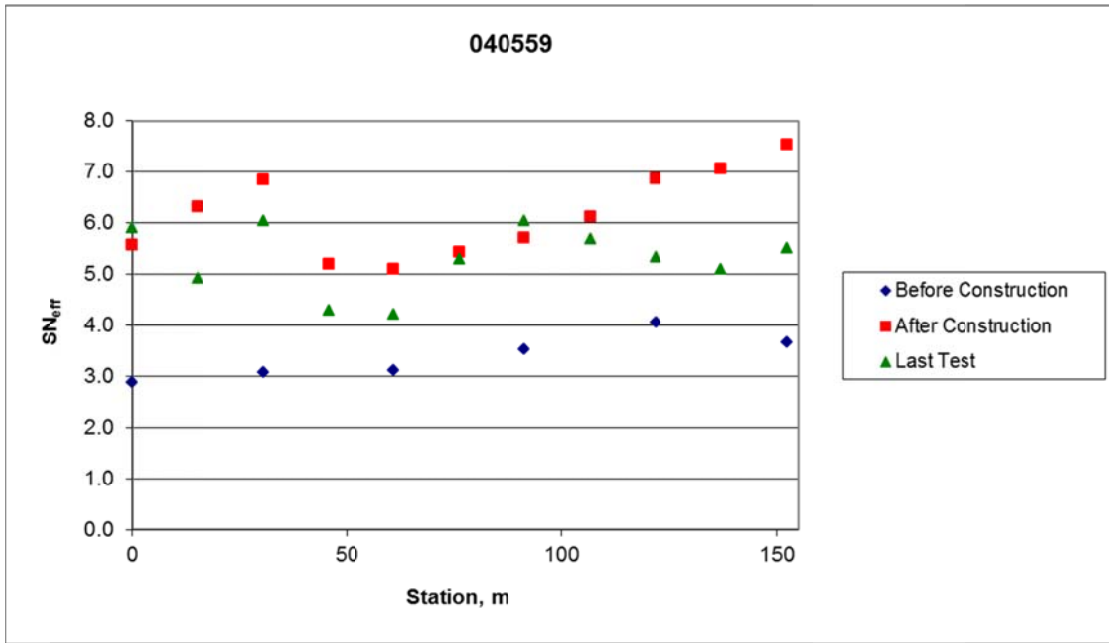


Figure 38. SN<sub>eff</sub> versus Station, Section 040559

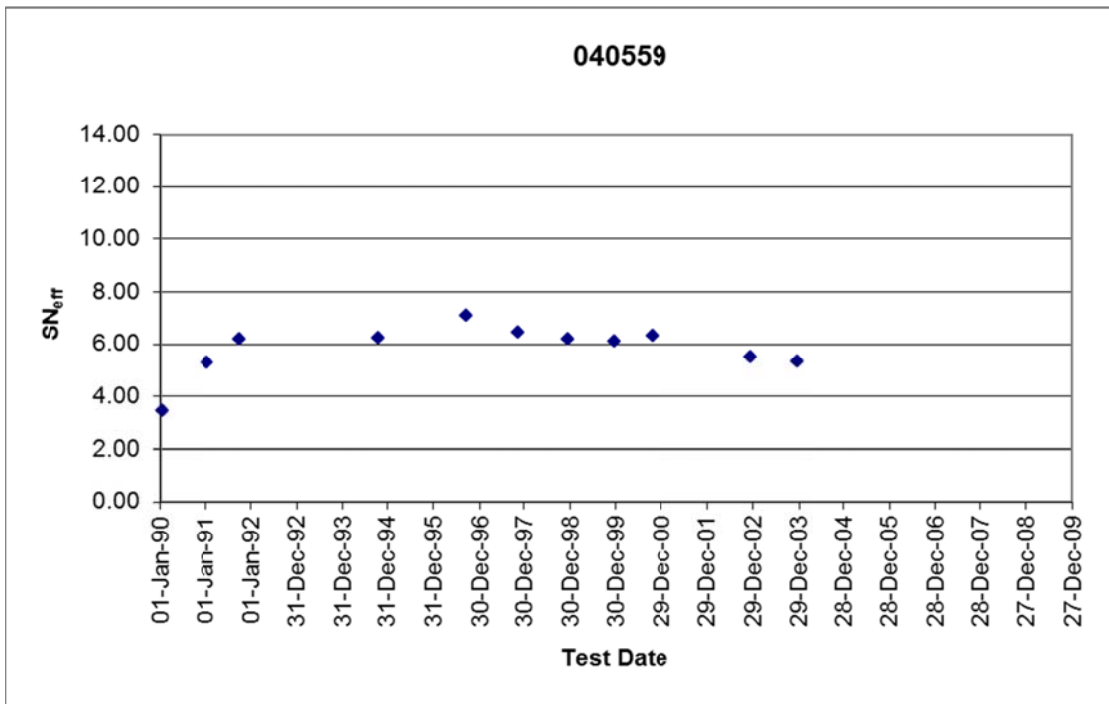


Figure 39. SN<sub>eff</sub> versus Date, Section 040559

## Section 040560

Section 040560 is a supplemental test section, consisting of minimal surface preparation and a thin overlay of asphalt rubber asphalt concrete (ARAC). The pre- and postconstruction layer structure as listed in Table TST\_L05B of the LTPP database is shown in Table 22.

**Table 22. Layer Structure, Section 040560**

Construction No.	Layer No.	Material Type	Thickness (inches) <sup>1</sup>
1	4	OGFC	0.9
	3	HMAC	4.1
	2	AB, 7% passing #200	14.0
	1	A-2-4, Silty sand with gravel	
2 – 6 <sup>2</sup>	5	ARAC	2.2
	3	HMAC	4.1
	2	AB, 7% passing #200	14.0
	1	A-2-4, Silty sand with gravel	

1 Depth of milling: 0.9 inch.

2 Does not include fog seals, which are considered structurally insignificant.

Construction was performed from May 4 to June 13, 1990, and consisted of milling 0.9 inch of the existing AC surface and placing a 2.2-inch overlay of ARAC. Fog seals were applied on May 28, 1990, August 23, 2001, and April 16, 2003. Crack sealing was performed on May 1, 2002.

$M_r$  calculated using the AASHTO 1993 procedure is shown in Figures 40 and 41. Figure 40 shows  $M_r$  versus station for the preconstruction, postconstruction, and final tests. Figure 41 shows the average  $M_r$  for each test date.

The  $M_r$  versus station plots are quite similar for the pre- and postconstruction data. The final data set is also similar for the first half of the section, but is significantly higher for the second half of the section. The  $M_r$  versus date trend is more stable than the other test sections.

Figures 42 and 43 show  $SN_{eff}$  for this section versus station and time. The  $SN_{eff}$  values in these figures are temperature-corrected using the methodology described earlier in this chapter.

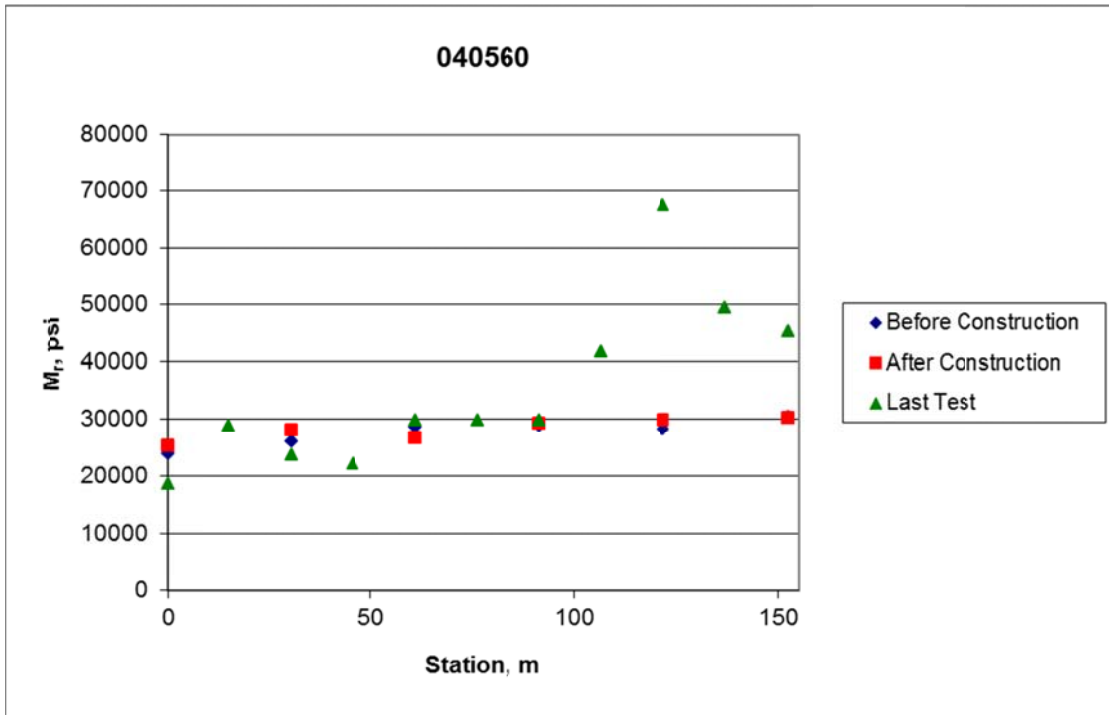


Figure 40.  $M_r$  versus Station, Section 040560

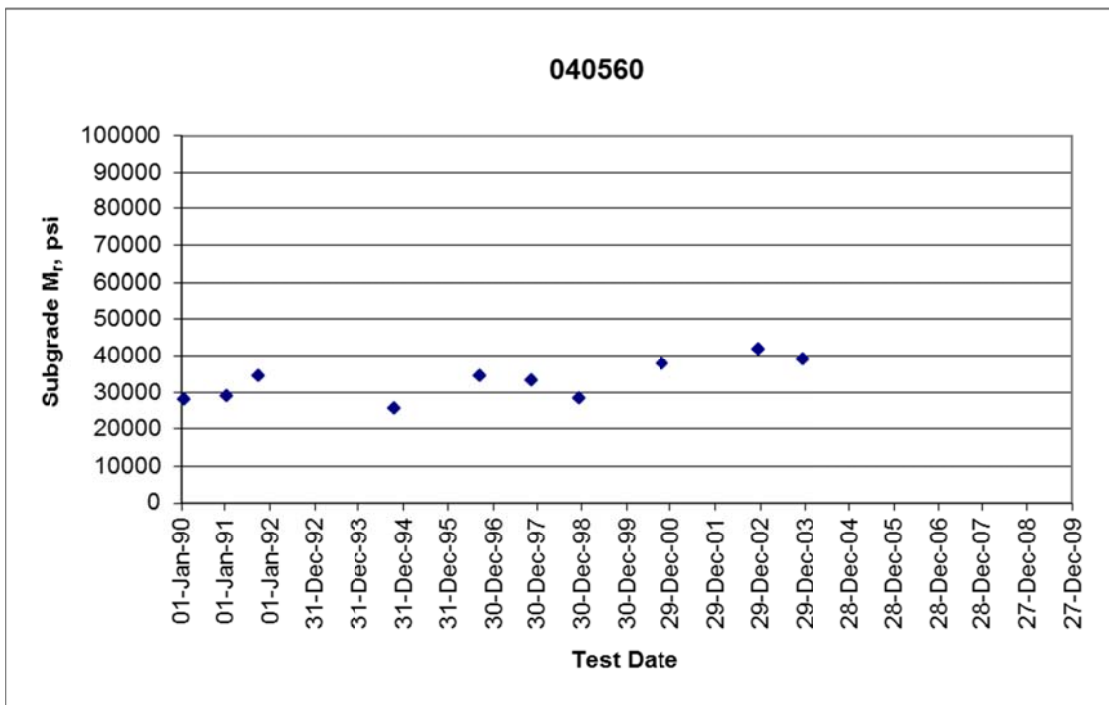


Figure 41.  $M_r$  versus Date, Section 040560

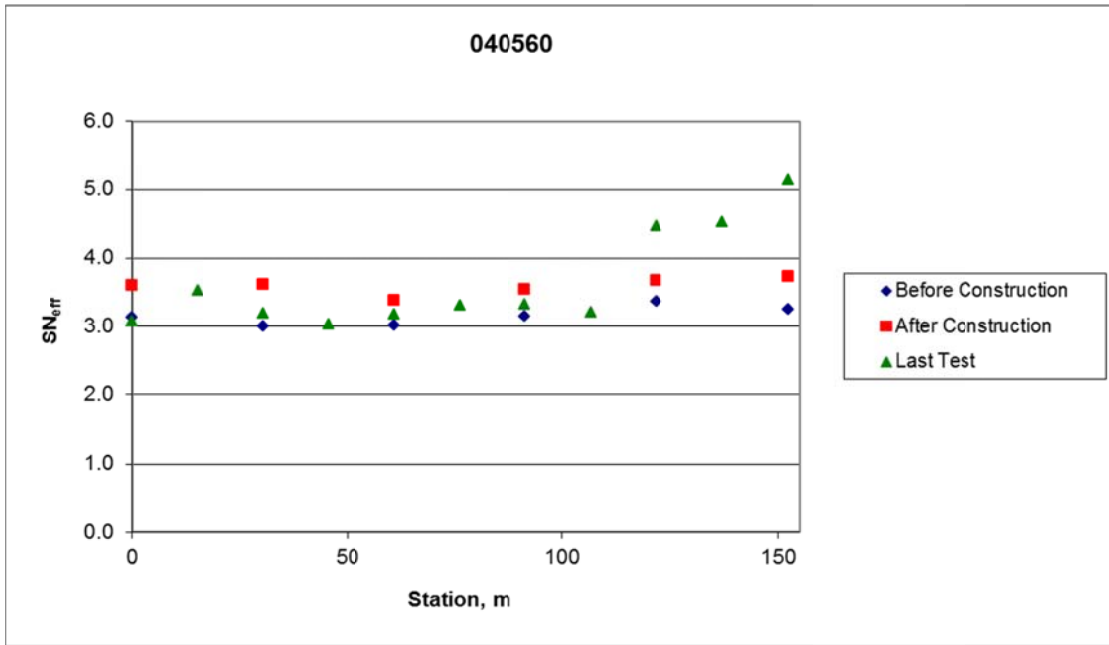


Figure 42. SN<sub>eff</sub> versus Station, Section 040560

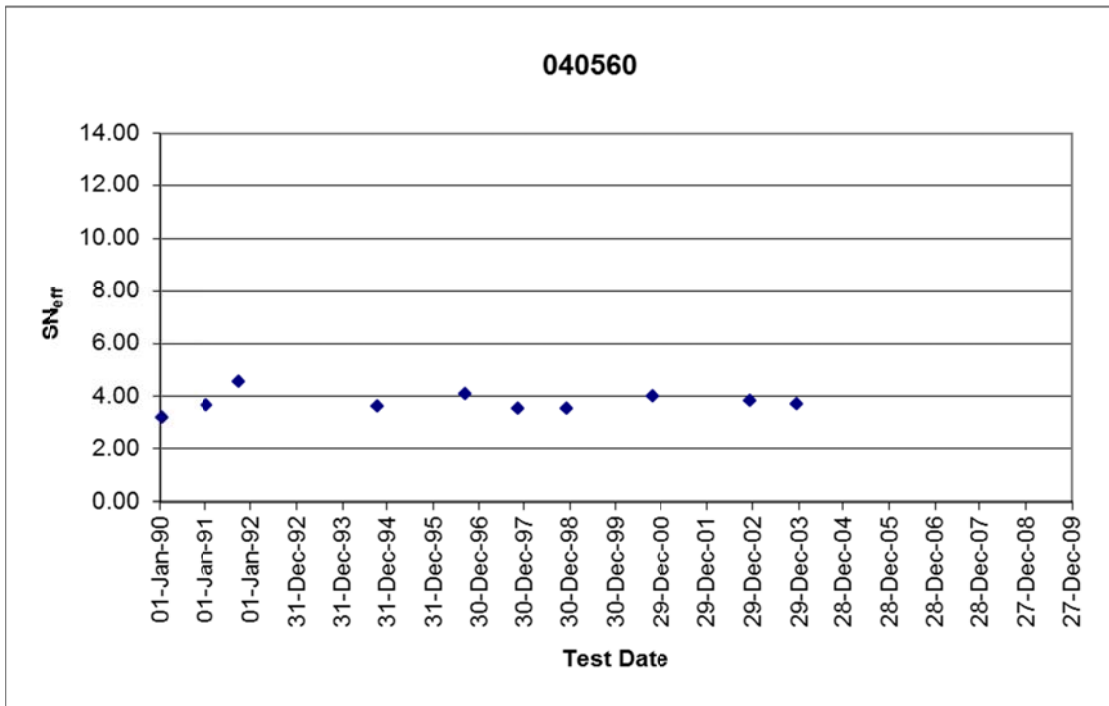


Figure 43. SN<sub>eff</sub> versus Date, Section 040560

The  $SN_{eff}$  versus station data show a slight and consistent increase in  $SN_{eff}$  at each test point between pre- and postconstruction. The final test shows a return to preconstruction  $SN_{eff}$  for most of the section, but an increased  $SN_{eff}$  at the end of the test section.  $SN_{eff}$  versus date data is relatively stable.

**Section 040501**

Section 040501 is the control section. No construction activities were performed on this section, and it was removed from the study on October 1, 1996, due to excessive deterioration. The pre- and postconstruction layer structure as listed in Table TST\_L05B of the LTPP database is shown in Table 23.

**Table 23. Layer Structure, Section 040501**

Construction No.	Layer No. <sup>1</sup>	Material Type	Thickness (inches)
1	4	OGFC	0.9
	3	HMAC	4.1
	2	AB, 5.1% passing #200	14.2
	1	A-2-4, Clayey sand with gravel	

1 Does not include fog seals, which are considered structurally insignificant.

$M_r$  calculated using the AASHTO 1993 procedure is shown in Figures 44 and 45. Figure 44 shows  $M_r$  versus station for the preconstruction, postconstruction, and final tests. Figure 45 shows the average  $M_r$  for each test date.

The  $M_r$  versus station data is quite consistent between the pre- and postconstruction data. However, there is a significant increase in  $M_r$  in the final data set.

Figures 46 and 47 show  $SN_{eff}$  for this section versus station and time. The  $SN_{eff}$  values in these figures are temperature-corrected using the methodology described earlier in this chapter.

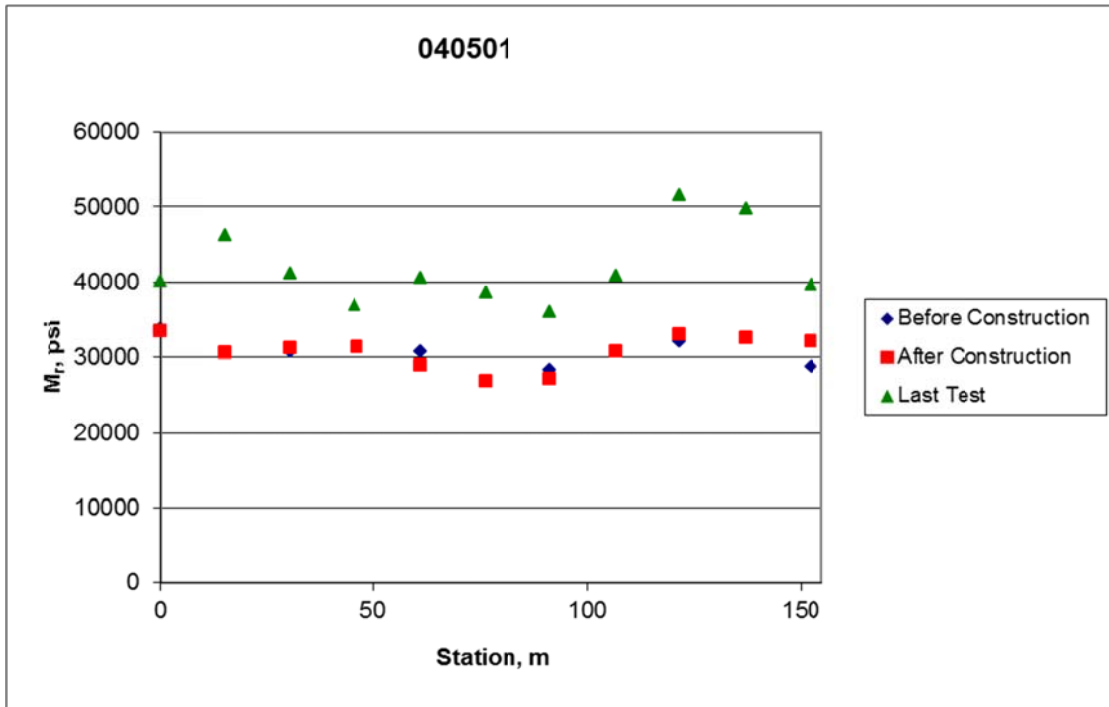


Figure 44.  $M_r$  versus Station, Section 040501

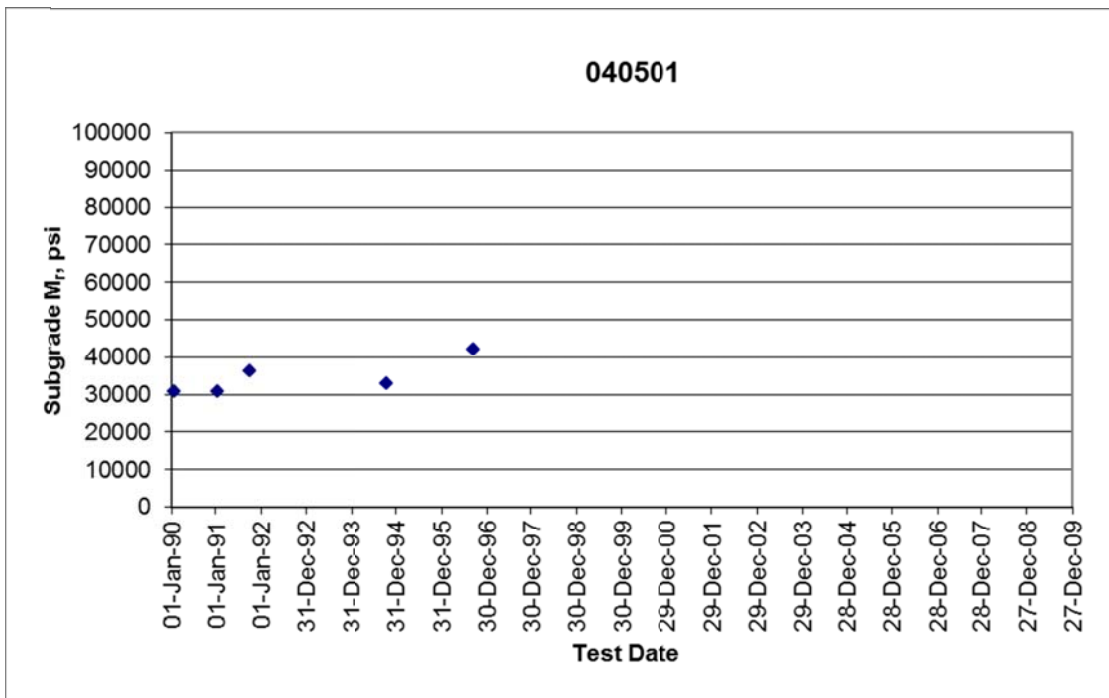


Figure 45.  $M_r$  versus Date, Section 040501

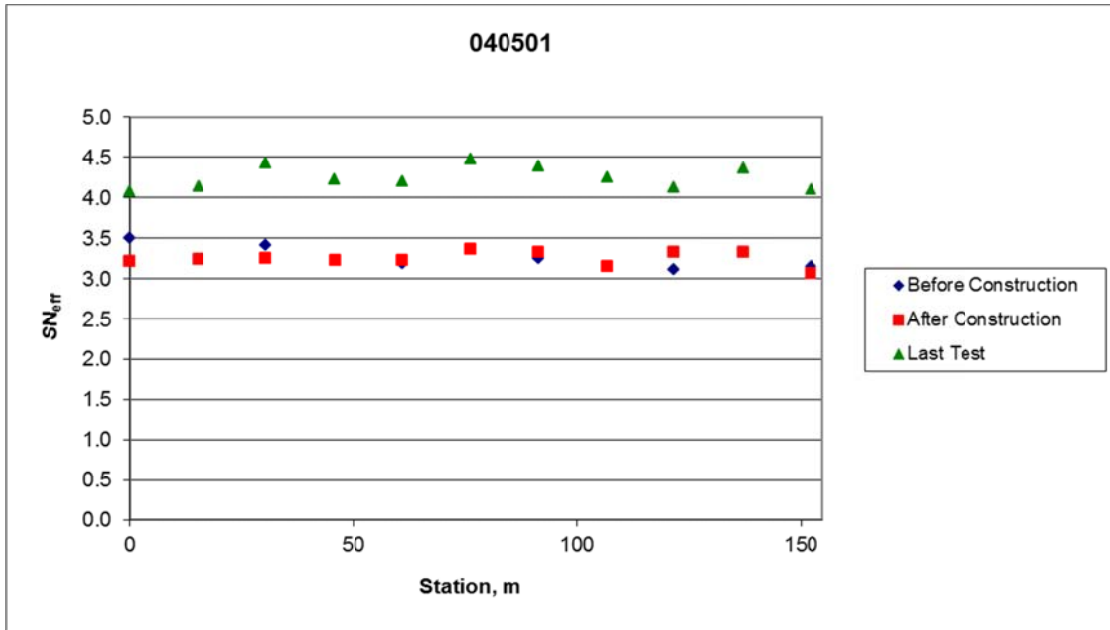


Figure 46. SN<sub>eff</sub> versus Station, Section 040501

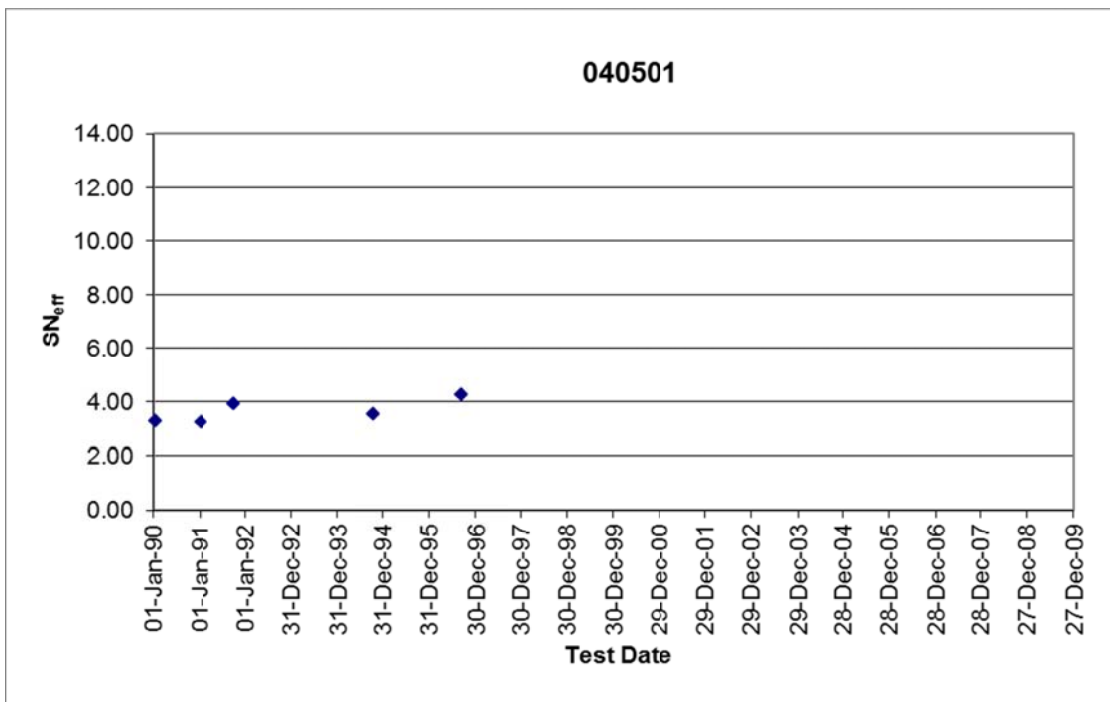


Figure 47. SN<sub>eff</sub> versus Date, Section 040501

As with  $M_r$ ,  $SN_{eff}$  is quite consistent between the pre- and postconstruction data sets, but increases thereafter.

### Summary of Structural Number Data by Experimental Factor

This experiment has three project-level factors: overlay material (recycled versus virgin mix), overlay thickness (thick versus thin), and level of surface preparation (intensive versus minimal). The other experimental factors, including climate, traffic, and subgrade, can only be investigated by comparing multiple projects.

Changes in  $SN_{eff}$  according to the three experimental factors are summarized in Tables 24, 25, and 26.  $SN_{eff}$  is expressed in terms of increase from the preconstruction  $SN_{eff}$  for both the postconstruction results and final results. Increase in  $SN_{eff}$  was chosen as the dependent variable in order to minimize the effect of preconstruction variability. The postconstruction data set used is from October 1991. The January 1991 data consistently show results intermediate between the preconstruction data and the October 1991 data. While this could be measurement bias or bias due to inaccuracies in the temperature correction algorithm, this may also reflect stiffness gain due to aging of the AC binder. Further investigation of this effect is hampered by a lack of data between October 1991 and October 1994. The October 1991 data was chosen as the best representation of  $SN_{eff}$  after initial aging but before significant traffic damage. The final results are from the December 2003 data set. Some sections also have data from September 2008, but it cannot be used for comparison purposes because this data is not available for all sections.

**Table 24.  $SN_{eff}$  Increase by Overlay Material**

Cell	Sections	Postconstruction		Final Test	
		Virgin	Recycled	Virgin	Recycled
Intensive, Thick	040507 vs. 040508	5.57	3.77	5.84	2.68
Intensive, Thin	040506 vs. 040509	3.96	3.15	2.82	0.54
Minimal, Thick	040504 vs. 040503	4.68	3.22	3.42	1.73
Minimal, Thin	040505 vs. 040502	3.28	2.41	0.93	0.35
Average:		4.37	3.14	3.25	1.33

**Table 25.  $SN_{eff}$  Increase by Overlay Thickness**

Cell	Sections	Postconstruction		Final Test	
		Thick	Thin	Thick	Thin
Virgin, Intensive	040507 vs. 040506	5.57	3.96	5.84	2.82
Virgin, Minimal	040504 vs. 040505	4.68	3.28	3.42	0.93
Recycled, Intensive	040508 vs. 040509	3.77	3.15	2.68	0.54
Recycled, Minimal	040503 vs. 040502	3.22	2.41	1.73	0.35
Average:		4.31	3.20	3.42	1.16

**Table 26. SN<sub>eff</sub> Increase by Level of Surface Preparation**

Cell	Sections	Postconstruction		Final Test	
		Intensive	Minimal	Intensive	Minimal
Virgin, Thick	040507 vs. 040504	5.57	4.68	5.84	3.42
Virgin, Thin	040506 vs. 040505	3.96	3.28	2.82	0.93
Recycled, Thick	040508 vs. 040503	3.77	3.22	2.68	1.73
Recycled, Thin	040509 vs. 040502	3.15	2.41	0.54	0.35
Average:		4.11	3.40	2.97	1.61

As expected, the thick overlays perform better than the thin overlays, and the sections with intensive preparation perform better than those with minimal preparation. However, there is some bias introduced by Section 040506, which was built significantly thicker than the other sections in the thin cells and therefore exaggerates the performance of virgin mixes, thin overlays, and intensive surface preparation. Removing it (and its partner sections) from the analysis yields the results shown in Table 27.

**Table 27. Summary of SN<sub>eff</sub> Increase by Experimental Factor**

Factor A	Factor B	Postconstruction SN <sub>eff</sub> Increase			Final Test SN <sub>eff</sub> Increase		
		Factor A	Factor B	Difference	Factor A	Factor B	Difference
Virgin	Recycled	4.51	3.13	31%	3.40	1.59	53%
Thick	Thin	3.89	2.95	24%	2.61	0.61	77%
Intensive	Minimal	4.16	3.44	17%	3.02	1.83	39%

These results show that at the time of the final test, overlay thickness has the strongest influence on SN<sub>eff</sub> among the factors investigated. Overlay material (virgin versus recycled mix) is still a stronger factor than level of surface preparation. The strength of each experimental factor increases over time.

**BACKCALCULATION**

Backcalculation was performed for all data collected at the project using MODCOMP version 6E (release date November 10, 2012). Specific results for each section are discussed in the sections that follow; however, some general points are relevant to all sections.

Data for each test location, date, and drop height were averaged prior to backcalculation. This has the effect of reducing the data analysis requirements by a factor of four (as typically four drops are performed at each drop height). In theory, this process also reduces the effect of random error on the analysis results, which is beneficial because of the low deflections throughout this project.

For all analyses, the subgrade was split into two layers: an upper layer that was 24 inches thick, representing the seasonally affected portion of the subgrade, and a lower semi-infinite deep subgrade. In some sections, the response of these two subgrade layers was quite similar; in others it was quite different.

When possible, the individual AC layers were analyzed separately. This was generally not possible for layers less than 2 inches thick, especially the OGFC that existed preconstruction. Because of the well-known “thin layer effect,” backcalculation is typically unreliable for layers that do not significantly contribute to the stiffness of the entire structure. Put differently, moduli can only be determined from deflections if the deflections are reasonably sensitive to those moduli. The modulus of a sufficiently thin layer can vary widely without causing a significant difference in the surface deflections. MODCOMP 6E displays error codes to warn the user of layers whose backcalculated modulus is insensitive to the measured deflections, and these error codes were considered in establishing the layer structures.

Only results with a root mean square error (RMSE) of less than 5 percent are presented here. This RMSE threshold is somewhat high for typical backcalculation; however, this data set includes many modeling difficulties, and a higher threshold would result in very few data points for some sections and test dates. Some results with an RMSE of less than 5 percent were also rejected due to unreasonable moduli.

All of the moduli of AC layers have been temperature-corrected to 77° F (25° C) using the following LTPP-derived equation unless otherwise stated (Lukanen et al. 2000).

$$E_{ref} = E_{calc} \times 10^{k(T_{ref} - T_{calc})} \quad (\text{Eq. 6})$$

Where  $E_{ref}$  = modulus at the reference temperature  
 $E_{calc}$  = backcalculated modulus  
 $k$  = -0.0195 for testing in the wheel path, -0.021 for testing in the midlane  
 $T_{ref}$  = reference temperature (°C)  
 $T_{calc}$  = AC temperature corresponding to backcalculated modulus (°C)

All temperatures are based on the measured AC mid-depth temperature where available. For tests where the mid-depth temperature was not available, the BELLS2 estimation procedure was followed.

In general, the backcalculated moduli are often not within the reasonable range for their respective material types, especially for the AC and upper subgrade layers. Potential reasons for these results are discussed later in this chapter.

**Section 040507**

Section 040507 is in the intensive maintenance, thick virgin overlay cell of the experimental matrix. The layer models used for backcalculation of all data are shown in Table 28.

**Table 28. Layer Models for Backcalculation, Section 040507**

Date Range	Layer	Layer Type	Thickness (inches)	Seed Modulus (ksi)	Poisson's Ratio
1/18/1990	1	AC	5	500	0.35
	2	AB	20.7	10	0.50
	3	Subgrade	24	35	0.45
	4	Subgrade	Semi-infinite	35	0.45
1/14/1991-12/10/2003	1	AC overlay	6.8	500	0.35
	2	AC original	2.4	500	0.35
	3	AB	20.7	10	0.50
	4	Subgrade	24	35	0.45
	5	Subgrade	0	35	0.45

The postconstruction layer model splits out the AC overlay and remaining original AC layer for comparison. The original AC layer (Layer 2) is only 2.4 inches thick after milling, and it is beneath 6.8 inches of stiff material, which makes the backcalculated modulus relatively insensitive to the surface deflections. The backcalculated moduli for the original AC layer (Layer 2) should therefore be used with caution.

Backcalculation results are shown in Table 29. The results shown are for drop height 4 only. Drop height 4 was chosen for this table because it generally has the highest number of acceptable backcalculation results. The number of acceptable backcalculation results is given as N;  $N_{\text{rejected}}$  is the number of unacceptable backcalculation results. The AB layer (Layer 3 in the table) showed significant nonlinearity, which is not apparent from the data in this table. Nonlinearity of this layer is discussed later in this chapter.

The AC layers (Layers 1 and 2) exhibit highly variable moduli, and the moduli are higher than is typical for AC materials. Some of this may be explained by deficiencies in the temperature correction methodology, as discussed later in this chapter. The upper subgrade (Layer 4 in Table 29) also exhibits extremely high moduli, especially for the testing on December 10, 2003. Reasons for this phenomenon are discussed later.

**Table 29. Backcalculation Results, Section 040507**

Test Date	Lane Position	Average Layer Modulus (ksi)					Average RMSE (%)	N	N <sub>rejected</sub>
		1	2	3	4	5			
1/18/1990	OWP		228 <sup>1</sup>	19 <sup>1</sup>	33 <sup>1</sup>	34 <sup>1</sup>	2.1	1	5
	ML		719 <sup>1</sup>	30 <sup>1</sup>	41 <sup>1</sup>	44 <sup>1</sup>	1.8	4	2
1/14/1991	OWP	1962	1146	36	268	67	1.3	11	0
	ML	1635	2422	31	923	58	1.1	11	0
10/2/1991	OWP	1044	6139	87	283	83	2.4	11	0
	ML	1316	7402	80	414	81	1.8	11	0
10/18/1994	OWP	1775	2370	89	385	87	1.3	11	0
	ML	2038	2717	114	459	87	1.3	10	1
9/11/1996	OWP	1612	5000	122	354	94	1.4	11	0
	ML	1790	5030	185	306	98	1.6	11	0
11/12/1997	OWP	1816	2431	77	593	87	2.9	8	3
	ML	1783	3326	126	605	93	1.7	8	3
12/9/1998	OWP	1449	1164	70	677	87	1.2	10	1
	ML	1844	1861	71	829	86	0.9	10	1
12/13/1999	OWP	1878	1461	71	154	83	1.8	10	1
	ML	1729	2159	75	51	89	1.3	11	0
10/16/2000	OWP	3147	1325	21	459	88	1.0	5	6
	ML	3293	2465	142	712	89	2.0	10	1
12/10/2002	OWP	2553	142	197	195	82	2.8	2	9
	ML	2338	1353	152	221	117	3.2	3	8
12/10/2003	OWP	2337	715	65	2068	83	2.1	9	2
	ML	2283	1064	90	2323	110	2.9	9	2

1 Preconstruction layer numbers shifted to align with postconstruction model.

## Section 040504

Section 040504 is in the intensive maintenance, thick virgin overlay cell of the experimental matrix. The layer models used for backcalculation of all data are shown in Table 30.

**Table 30. Layer Models for Backcalculation, Section 040504**

Date Range	Layer	Layer Type	Thickness (inches)	Seed Modulus (ksi)	Poisson's Ratio
1/18/1990	1	AC	5	500	0.35
	2	AB	17.6	10	0.50
	3	Subgrade	24	35	0.45
	4	Subgrade	Semi-infinite	35	0.45
1/15/1991-12/10/2003	1	AC overlay	4.8	500	0.35
	2	AC original	4.3	500	0.35
	3	AB	17.6	10	0.50
	4	Subgrade	24	35	0.45
	5	Subgrade	0	35	0.45

Backcalculation results are shown in Table 31. Results are for drop height 4 only. Drop height 4 was chosen for this table because it generally has the highest number of acceptable backcalculation results. The number of acceptable backcalculation results is given as N;  $N_{\text{rejected}}$  is the number of unacceptable backcalculation results.

**Table 31. Backcalculation Results, Section 040504**

Test Date	Lane Position	Average Layer Modulus (ksi)					Average RMSE (%)	N	N <sub>rejected</sub>
		1	2	3	4	5			
1/18/1990	OWP		256 <sup>1</sup>	50 <sup>1</sup>	57 <sup>1</sup>	55 <sup>1</sup>	3.5	1	4
	ML		457 <sup>1</sup>	26 <sup>1</sup>	60 <sup>1</sup>	54 <sup>1</sup>	2.9	2	3
1/15/1991	OWP	1665	486	42	185	61	1.0	11	0
	ML	2151	942	26	758	56	1.1	11	0
10/2/1991	OWP	868	1821	86	267	78	2.1	11	0
	ML	1144	2707	102	215	78	1.2	11	0
10/18/1994	OWP	1536	2127	86	447	80	1.3	11	0
	ML	1937	866	74	275	78	1.2	11	0
9/11/1996	OWP	1583	2105	120	277	86	1.3	11	0
	ML	2382	3288	123	368	85	1.3	11	0
11/12/1997	OWP	1908	1186	86	289	84	2.9	4	7
	ML	1134	1964	86	447	80	1.3	11	0
12/9/1998	OWP	1710	785	48	411	74	1.0	11	0
	ML	1814	1292	43	1248	73	1.1	8	3
12/9/1999	OWP	No data							
	ML	1957	2243	75	434	81	1.1	10	1
10/16/2000	OWP	3250	1613	90	365	79	1.7	10	1
	ML	4075	2872	82	599	76	1.9	7	4
12/10/2002	OWP	5607	1092	403	772	66	3.5	2	9
	ML	3858	624	194	197	94	2.4	2	9
12/10/2003	OWP	2214	547	59	133	67	1.8	5	6
	ML	1989	917	19	2773	55	1.4	5	6

1 Preconstruction layer numbers shifted to align with postconstruction model.

**Section 040503**

Section 040503 is in the minimal surface preparation, thick recycled overlay cell of the experimental matrix. The layer models used for backcalculation of all data are shown in Table 32.

Backcalculation results are shown in Table 33. Results are for drop height 4 only. Drop height 4 was chosen for this table because it generally has the highest number of acceptable backcalculation results. The number of acceptable backcalculation results is given as N; N<sub>rejected</sub> is the number of unacceptable backcalculation results.

**Table 32. Layer Models, Section 040503**

Date Range	Layer	Layer Type	Thickness (inches)	Seed Modulus (ksi)	Poisson's Ratio
1/18/1990	1	AC	5	500	0.35
	2	AB	16.6	10	0.50
	3	Subgrade	24	35	0.45
	4	Subgrade	Semi-infinite	35	0.45
1/15/1991-12/10/2003	1	AC overlay	4.7	500	0.35
	2	AC original	4.2	500	0.35
	3	AB	16.6	10	0.50
	4	Subgrade	24	35	0.45
	5	Subgrade	0	35	0.45

**Table 33. Backcalculation Results, Section 040503**

Test Date	Lane Position	Average Layer Modulus (ksi)					Average RMSE (%)	N	N <sub>rejected</sub>
		1	2	3	4	5			
1/18/1990	OWP		267 <sup>1</sup>	19 <sup>1</sup>	23 <sup>1</sup>	44 <sup>1</sup>	1.9	1	5
	ML		763 <sup>1</sup>	25 <sup>1</sup>	41 <sup>1</sup>	41 <sup>1</sup>	3.1	4	2
1/15/1991	OWP	672	279	17	56	48	1.1	11	0
	ML	1012	613	15	54	47	0.8	11	0
10/2/1991	OWP	580	753	44	83	66	1.1	11	0
	ML	698	1543	53	65	64	0.6	11	0
10/18/1994	OWP	541	1240	110	105	112	0.3	1	0
	ML	1910	1414	72	100	78	0.8	11	0
9/11/1996	OWP	613	961	33	90	62	2.1	11	0
	ML	1829	2050	59	109	69	1.5	11	0
11/12/1997	OWP	893	442	20	94	51	2.9	11	0
	ML	1229	1399	19	170	57	2.7	7	4
12/9/1998	OWP	1225	184	22	41	40	1.2	11	0
	ML	1089	747	15	541	36	1.1	9	2
12/13/1999	OWP	1025	225	19	36	39	1.2	11	0
	ML	531	1188	8	359	35	1.3	8	3
10/16/2000	OWP	1912	340	25	128	46	2.3	11	0
	ML	2133	1167	21	26	46	1.7	10	1
12/11/2002	OWP	1794	2	171	77	27	3.6	1	10
	ML	2071	339	360	193	44	3.4	3	8
12/10/2003	OWP	1083	434	15	91	48	2.6	5	6
	ML	1228	955	4	410	32	1.9	7	4

<sup>1</sup> Preconstruction layer numbers shifted to align with postconstruction model.

## Section 040508

Section 040508 is in the intensive surface preparation, thick recycled overlay cell of the experimental matrix. The layer models used for backcalculation of all data are shown in Table 34.

The postconstruction layer model splits out the AC overlay and remaining original AC layer for comparison. The original AC layer (Layer 2) is only 2.7 inches thick after milling, and is beneath 6.5 inches of stiff material, which makes the backcalculated modulus relatively insensitive to the surface deflections. The backcalculated moduli for the original AC layer (Layer 2) should therefore be used with caution.

Backcalculation results are shown in Table 35. Results are for drop height 4 only. Drop height 4 was chosen for this table because it generally has the highest number of acceptable backcalculation results. The number of acceptable backcalculation results is given as  $N$ ;  $N_{\text{rejected}}$  is the number of unacceptable backcalculation results. The AB layer (Layer 3 in Table 35) showed significant nonlinearity, which is not apparent from the data in this table. Nonlinearity of this layer is discussed later in this chapter.

**Table 34. Layer Models, Section 040508**

Date Range	Layer	Layer Type	Thickness (inches)	Seed Modulus (ksi)	Poisson's Ratio
1/18/1990	1	AC	5.4	500	0.35
	2	AB	15	10	0.50
	3	Subgrade	24	35	0.45
	4	Subgrade	Semi-infinite	35	0.45
1/15/1991-12/10/2003	1	AC overlay	6.5	500	0.35
	2	AC original	2.7	500	0.35
	3	AB	15	10	0.50
	4	Subgrade	24	35	0.45
	5	Subgrade	0	35	0.45

**Table 35. Backcalculation Results, Section 040508**

Test Date	Lane Position	Average Layer Modulus (ksi)					Average RMSE (%)	N	N <sub>rejected</sub>
		1	2	3	4	5			
1/18/1990	OWP		331 <sup>1</sup>	23 <sup>1</sup>	30 <sup>1</sup>	43 <sup>1</sup>	2.6	6	0
	ML		692 <sup>1</sup>	19 <sup>1</sup>	25 <sup>1</sup>	43 <sup>1</sup>	2.4	3	3
1/15/1991	OWP	871	507	69	79	64	1.1	11	0
	ML	810	1120	33	75	60	0.6	11	0
10/2/1991	OWP	545	5208	60	133	75	1.4	11	0
	ML	628	6772	75	126	74	0.9	11	0
10/19/1994	OWP	1095	1289	49	185	88	1.1	11	0
	ML	1021	2585	52	189	89	0.8	10	1
9/12/1996	OWP	977	3019	87	247	100	2.3	11	0
	ML	1108	5713	82	258	97	1.7	11	0
11/12/1997	OWP	1440	481	750	219	110	3.0	8	3
	ML	1109	3055	53	416	105	2.9	6	4
12/9/1998	OWP	1465	809	112	318	87	1.1	11	0
	ML	1474	2276	30	432	90	1.1	10	1
12/13/1999	OWP	1281	1202	36	200	84	1.2	10	1
	ML	1741	1195	50	189	77	1.2	9	2
10/17/2000	OWP	1800	425	75	96	76	1.8	10	1
	ML	1484	1240	77	81	67	1.8	9	2
12/11/2002	OWP	2179	282	29	122	59	2.2	3	8
	ML	1582	823	49	81	54	3.0	3	8
12/10/2003	OWP	1429	337	38	29	56	0.9	4	7
	ML	7270	1205	16	42	46	2.1	4	7

1 Preconstruction layer numbers shifted to align with postconstruction model.

**Section 040509**

Section 040509 is in the intensive surface preparation, thin recycled overlay cell of the experimental matrix. The layer models used for backcalculation of all data are shown in Table 36.

**Table 36. Layer Models, Section 040509**

Date Range	Layer	Layer Type	Thickness (inches)	Seed Modulus (ksi)	Poisson's Ratio
1/18/1990	1	AC	5.4	500	0.35
	2	AB	14.8	10	0.50
	3	Subgrade	24	35	0.45
	4	Subgrade	Semi-infinite	35	0.45
1/15/1991-12/10/2003	1	AC overlay	3.9	500	0.35
	2	AC original	2.6	500	0.35
	3	AB	14.8	10	0.50
	4	Subgrade	24	35	0.45
	5	Subgrade	0	35	0.45

Backcalculation results are shown in Table 37. Results are for drop height 4 only. Drop height 4 was chosen for this table because it generally has the highest number of acceptable backcalculation results. The number of acceptable backcalculation results is given as N; N<sub>rejected</sub> is the number of unacceptable backcalculation results. The AB layer (Layer 3 in Table 37) showed significant nonlinearity, which is not apparent from the data in this table. Nonlinearity of this layer is discussed later in this chapter.

**Table 37. Backcalculation Results, Section 040509**

Test Date	Lane Position	Average Layer Modulus (ksi)					Average RMSE (%)	N	N <sub>rejected</sub>
		1	2	3	4	5			
1/18/1990	OWP		233 <sup>1</sup>	31 <sup>1</sup>	59 <sup>1</sup>	38 <sup>1</sup>	0.7	1	5
	ML		817 <sup>1</sup>	33 <sup>1</sup>	50 <sup>1</sup>	43 <sup>1</sup>	2.1	3	3
1/16/1991	OWP	745	655	34	120	59	1.3	10	1
	ML	1291	1146	46	87	57	1.1	11	0
10/2/1991	OWP	480	703	72	257	63	1.6	10	1
	ML	703	6342	107	185	69	1.8	11	0
10/19/1994	OWP	1592	1290	81	162	67	1.0	10	1
	ML	1886	1252	107	142	69	1.3	11	1
9/12/1996	OWP	1246	3103	68	170	68	2.2	9	2
	ML	1010	7211	109	135	74	2.3	11	0
11/13/1997	OWP	1094	1018	43	77	50	3.1	6	5
	ML	1009	1380	46	40	52	2.2	7	3
12/10/1998	OWP	625	330	25	37	36	1.5	9	2
	ML	1096	492	22	45	32	1.3	9	2
12/13/1999	OWP	1257	430	26	33	39	0.9	11	0
	ML	1375	1326	27	122	35	1.1	11	0
10/17/2000	OWP	2290	400	17	56	36	1.7	11	0
	ML	3047	571	23	42	35	1.5	8	3
12/11/2002	OWP	1281	383	53	69	43	2.7	7	4
	ML	1245	281	61	49	44	2.2	6	5
12/11/2003	OWP	488	481	21	44	31	1.9	5	6
	ML	1878	491	40	50	40	1.9	6	5
9/15/2008	OWP	1148	1759	20	43	42	2.5	7	4
	ML	2130	2634	24	39	41	2.5	6	5

<sup>1</sup> Preconstruction layer numbers shifted to align with postconstruction model.

## Section 040502

Section 040502 is in the minimal surface preparation, thin recycled overlay cell of the experimental matrix. The layer models used for backcalculation of all data are shown in Table 38.

Backcalculation results are shown in Table 39. Results are for drop height 4 only. Drop height 4 was chosen for this table because it generally has the highest number of acceptable backcalculation results. The number of acceptable backcalculation results is given as N;  $N_{\text{rejected}}$  is the number of unacceptable backcalculation results. The AB layer (Layer 3 in Table 39) showed significant nonlinearity, which is not apparent from the data in this table. Nonlinearity of this layer is discussed later in this chapter.

**Table 38. Layer Models, Section 040502**

Date Range	Layer	Layer Type	Thickness (inches)	Seed Modulus (ksi)	Poisson's Ratio
1/18/1990	1	AC	5.1	500	0.35
	2	AB	14.7	10	0.50
	3	Subgrade	24	35	0.45
	4	Subgrade	Semi-infinite	35	0.45
1/16/1991-9/15/2008	1	AC overlay	2.7	500	0.35
	2	AC original	3.7	500	0.35
	3	AB	14.7	10	0.50
	4	Subgrade	24	35	0.45
	5	Subgrade	Semi-infinite	35	0.45

**Table 39. Backcalculation Results, Section 040502**

Test Date	Lane Position	Average Layer Modulus (ksi)					Average RMSE (%)	N	N <sub>rejected</sub>
		1	2	3	4	5			
1/18/1990	OWP		438 <sup>1</sup>	34 <sup>1</sup>	44 <sup>1</sup>	48 <sup>1</sup>	3.9	3	3
	ML		516 <sup>1</sup>	30 <sup>1</sup>	59 <sup>1</sup>	45 <sup>1</sup>	3.9	5	1
1/16/1991	OWP	584	396	49	98	56	1.5	9	2
	ML	1603	271	81	82	53	1.9	8	3
10/3/1991	OWP	692	833	92	155	67	1.6	8	3
	ML	1078	1401	130	145	60	1.4	8	3
10/19/1994	OWP	579 <sup>2</sup>		21	31	44	2.2	9	2
	ML	917		35	27	42	1.7	10	1
9/12/1996	OWP	720		32	43	53	2.4	10	1
	ML	975		31	32	46	3.2	9	2
11/13/1997	OWP	403		21	52	46	3.0	3	8
	ML	738		15	74	39	2.4	4	7
12/10/1998	OWP	180		16	31	33	2.2	4	7
	ML	400		11	59	31	3.4	4	7
12/14/1999	OWP	251		9	153	33	3.2	1	10
	ML	390		15	69	29	3.6	5	6
10/17/2000	OWP	614		17	35	42	4.0	4	7
	ML	1090		16	61	36	2.9	5	6
12/11/2002	OWP	826		25	41	46	3.5	2	9
	ML	479		16	59	36	3.9	1	10
12/11/2003	OWP	369		14	73	54	4.7	1	10
	ML	251		21	47	36	3.2	2	9
9/15/2008	OWP	737		26	41	47	3.1	7	4
	ML	1919		33	55	45	3.3	4	7

1 Preconstruction layer numbers shifted to align with postconstruction model.

2 AC layers combined beginning 10/19/1994 due to insensitivity of Layer 2.

**Section 040506**

Section 040506 is in the intensive surface preparation, thin virgin overlay cell of the experimental matrix. The layer models used for backcalculation of all data are shown in Table 40.

Backcalculation results are shown in Table 41. Results are for drop height 4 only. Drop height 4 was chosen for this table because it generally has the highest number of acceptable backcalculation results. The number of acceptable backcalculation results is given as N; N<sub>rejected</sub> is the number of unacceptable backcalculation results.

**Table 40. Layer Models, Section 040506**

Date Range	Layer	Layer Type	Thickness (inches)	Seed Modulus (ksi)	Poisson's Ratio
1/19/1990	1	AC	4.9	500	0.35
	2	AB	12.8	10	0.50
	3	Subgrade	24	35	0.45
	4	Subgrade	Semi-infinite	35	0.45
1/16/1991-9/15/2008	1	AC overlay	5.7	500	0.35
	2	AC original	3.0	500	0.35
	3	AB	12.8	10	0.50
	4	Subgrade	24	35	0.45
	5	Subgrade	Semi-infinite	35	0.45

**Table 41. Backcalculation Results, Section 040506**

Test Date	Lane Position	Average Layer Modulus (ksi)					Average RMSE (%)	N	N <sub>rejected</sub>
		1	2	3	4	5			
1/19/1990	OWP	No acceptable results						0	6
	ML		244 <sup>1</sup>	46 <sup>1</sup>	28 <sup>1</sup>	29 <sup>1</sup>	1.1	1	5
1/16/1991	OWP	1314	218	78	162	54	1.1	11	0
	ML	1005	464	27	162	48	1.3	9	2
10/3/1991	OWP	1174	1045	70	137	64	1.9	10	1
	ML	1299	2136	71	174	63	1.5	10	1
10/19/1994	OWP	1509	938	64	139	59	1.0	9	2
	ML	2051	745	100	176	57	0.8	10	1
9/12/1996	OWP	1230	3090	61	128	57	1.9	8	3
	ML	1545	5179	83	263	58	1.4	10	1
11/13/1997	OWP	1748	835	26	150	59	1.9	2	9
	ML	1693	1934	47	315	65	3.3	2	9
12/10/1998	OWP	1289	692	25	287	51	1.0	4	7
	ML	1318	697	32	296	54	0.7	8	3
12/14/1999	OWP	764	298	16	33	30	2.2	10	1
	ML	1451	403	61	222	56	1.0	10	1
10/17/2000	OWP	2710	963	32	223	57	1.7	6	5
	ML	2953	1916	47	357	48	2.6	6	5
12/12/2002	OWP	1703	112	149	380	45	2.1	6	5
	ML	1163	866	51	274	55	2.4	7	4
12/11/2003	OWP	1444	1209	17	562	56	1.9	3	8
	ML	1326	1351	35	160	49	1.1	8	3
9/15/2008	OWP	1529	1577	5	277	31	1.2	10	1
	ML	1345	2484	7	516	30	1.1	10	1

1 Preconstruction layer numbers shifted to align with postconstruction model.

## Section 040505

Section 040505 is in the minimal surface preparation, thin virgin overlay cell of the experimental matrix. The layer models used for backcalculation are shown in Table 42.

Backcalculation results are shown in Table 43. Results are for drop height 4 only. Drop height 4 was chosen for this table because it generally has the highest number of acceptable backcalculation results. The number of acceptable backcalculation results is given as N;  $N_{\text{rejected}}$  is the number of unacceptable backcalculation results. The AB layer (Layer 3 in Table 43) showed significant nonlinearity, which is not apparent from the data in this table. Nonlinearity of this layer is discussed later in this chapter.

**Table 42. Layer Models, Section 040505**

Date Range	Layer	Layer Type	Thickness (inches)	Seed Modulus (ksi)	Poisson's Ratio
1/19/1990	1	AC	5	500	0.35
	2	AB	12.8	10	0.50
	3	Subgrade	24	35	0.45
	4	Subgrade	Semi-infinite	35	0.45
1/16/1991-9/15/2008	1	AC overlay	2.8	500	0.35
	2	AC original	4.1	500	0.35
	3	AB	12.8	10	0.50
	4	Subgrade	24	35	0.45
	5	Subgrade	Semi-infinite	35	0.45

**Table 43. Backcalculation Results, Section 040505**

Test Date	Lane Position	Average Layer Modulus (ksi)					Average RMSE (%)	N	N <sub>rejected</sub>
		1	2	3	4	5			
1/19/1990	OWP		271 <sup>1</sup>	19 <sup>1</sup>	34 <sup>1</sup>	26 <sup>1</sup>	3.5	2	4
	ML		483 <sup>1</sup>	12 <sup>1</sup>	85 <sup>1</sup>	34 <sup>1</sup>	4.7	2	4
1/16/1991	OWP	847	419	41	75	46	1.5	11	0
	ML	1222	654	41	191	45	2.6	11	0
10/3/1991	OWP	860	938	100	103	53	2.2	11	0
	ML	1123	1646	95	153	56	1.8	10	1
10/19/1994	OWP	1946	749	67	66	50	1.3	11	0
	ML	2045	7186	72	92	51	1.7	10	1
9/12/1996	OWP	1863	1052	87	43	51	2.3	10	1
	ML	1465	2995	72	54	50	2.5	9	2
11/13/1997	OWP	1028	694	35	42	41	3.1	6	5
	ML	1015	1452	17	65	40	2.6	9	2
12/10/1998	OWP	2898	198	69	60	29	1.8	9	2
	ML	3675	342	43	30	31	1.6	11	0
12/14/1999	OWP	670	395	16	34	30	2.3	9	2
	ML	769	708	24	53	36	1.5	4	7
10/18/2000	OWP	2213	342	28	36	36	2.1	8	3
	ML	2305	1497	18	148	35	1.8	5	6
12/12/2002	OWP	3188	12	12	37	27	1.8	1	10
	ML	1036	308	40	29	30	3.1	3	8
12/11/2003	OWP	568	289	22	33	31	2.6	4	7
	ML	694	544	42	35	35	1.8	6	5
9/15/2008	OWP	1567	712	24	36	41	2.0	8	3
	ML	916	1764	40	64	47	1.8	8	3

1 Preconstruction layer numbers shifted to align with postconstruction model.

### Section 040559

Section 040559 is a supplemental section, constructed using intensive surface preparation and an inverted overlay consisting of recycled AC over virgin AC. The layer models used for backcalculation are shown in Table 44.

Only 1.7 inches of original pavement was left after milling, which is too thin a layer to model. Therefore, the remaining original pavement was combined with the virgin overlay for backcalculation.

Backcalculation results are shown in Table 45. Results are for drop height 4 only. Drop height 4 was chosen for this table because it generally has the highest number of acceptable backcalculation results. The number of acceptable backcalculation results is given as N; N<sub>rejected</sub> is the number of unacceptable backcalculation results.

**Table 44. Layer Models, Section 040559**

Date Range	Layer	Layer Type	Thickness (inches)	Seed Modulus (ksi)	Poisson's Ratio
1/19/1990	1	AC	5.2	500	0.35
	2	AB	13.2	10	0.50
	3	Subgrade	24	35	0.45
	4	Subgrade	Semi-infinite	35	0.45
1/16/1991-12/12/2003	1	Rec. overlay	3	500	0.35
	2	Vir. overlay	4.7	500	0.35
	3	AB	13.2	10	0.50
	4	Subgrade	24	35	0.45
	5	Subgrade	Semi-infinite	35	0.45

**Table 45. Backcalculation Results, Section 040559**

Test Date	Lane Position	Average Layer Modulus (ksi)					Average RMSE (%)	N	N <sub>rejected</sub>
		1	2	3	4	5			
1/19/1990	OWP		359 <sup>1</sup>	36 <sup>1</sup>	27 <sup>1</sup>	28 <sup>1</sup>	2.3	4	2
	ML		614 <sup>1</sup>	27 <sup>1</sup>	51 <sup>1</sup>	27 <sup>1</sup>	2.3	5	1
1/16/1991	OWP	1177	946	24	49	37	0.9	6	0
	ML	1407	1078	31	56	36	0.7	6	0
10/3/1991	OWP	683	1520	59	78	45	0.8	11	0
	ML	704	1553	77	81	45	0.9	11	0
10/20/1994	OWP	2862	1298	50	118	47	0.7	11	0
	ML	2664	1415	78	96	78	0.4	11	0
9/13/1996	OWP	788	3321	84	110	52	1.1	11	0
	ML	822	4602	164	98	54	1.2	11	0
11/14/1997	OWP	2297	1700	40	123	48	2.7	9	2
	ML	3829	2515	133	286	48	2.1	9	2
12/10/1998	OWP	3773	1194	22	356	38	0.8	11	0
	ML	2145	2147	44	553	41	0.9	11	0
12/14/1999	OWP	2058	1230	50	76	42	0.8	11	0
	ML	3318	1497	173	94	43	0.9	11	0
10/18/2000	OWP	4790	1365	62	75	46	1.4	8	3
	ML	7242	2048	113	67	42	1.7	10	1
12/12/2002	OWP	7503	1159	80	138	32	2.6	5	6
	ML	9844	1707	34	85	35	1.4	7	4
12/12/2003	OWP	6157	438	51	56	34	0.9	9	2
	ML	2994	855	47	19	31	0.9	8	3

1 Preconstruction layer numbers shifted to align with postconstruction model.

## Section 040560

Section 040560 is a supplemental test section, consisting of minimal surface preparation and a thin overlay of asphalt rubber asphalt concrete (ARAC). The layer models used for backcalculation are shown in Table 46.

Backcalculation results are shown in Table 47. Results are for drop height 4 only. Drop height 4 was chosen for this table because it generally has the highest number of acceptable backcalculation results. The number of acceptable backcalculation results is given as  $N$ ;  $N_{\text{rejected}}$  is the number of unacceptable backcalculation results. The AB layer (Layer 3 in Table 47) showed significant nonlinearity, which is not apparent from the data in this table. Nonlinearity of this layer is discussed later in this chapter.

**Table 46. Layer Models, Section 040560**

Date Range	Layer	Layer Type	Thickness (inches)	Seed Modulus (ksi)	Poisson's Ratio
1/19/1990	1	AC	5	500	0.35
	2	AB	14	10	0.50
	3	Subgrade	24	35	0.45
	4	Subgrade	Semi-infinite	35	0.45
1/16/1991- 12/12/2003	1	ARAC	2.2	500	0.35
	2	Original AC	4.1	500	0.35
	3	AB	13.2	10	0.50
	4	Subgrade	24	35	0.45
	5	Subgrade	Semi-infinite	35	0.45

**Table 47. Backcalculation Results, Section 040560**

Test Date	Lane Position	Average Layer Modulus (ksi)					Average RMSE (%)	N	N <sub>rejected</sub>
		1	2	3	4	5			
1/19/1990	OWP		289 <sup>1</sup>	21 <sup>1</sup>	33 <sup>1</sup>	29 <sup>1</sup>	2.4	2	3
	ML		418 <sup>1</sup>	27 <sup>1</sup>	32 <sup>1</sup>	28 <sup>1</sup>	3.5	7	0
1/16/1991	OWP	802	382	12	29	28	1.5	7	0
	ML	1744	879	24	27	31	1.6	7	0
10/3/1991	OWP	747	1053	16	36	35	2.3	13	0
	ML	907	1960	23	40	37	1.4	11	0
10/20/1994	OWP	2342	338	9	69	24	2.4	4	0
	ML	5457	787	73	50	30	2.1	9	4
9/13/1996	OWP	1838	663	14	35	33	2.6	11	2
	ML	2770	2070	18	59	35	2.2	12	1
11/14/1997	OWP	3431	180	21	54	37	3.4	4	9
	ML	5489	702	142	83	38	2.4	6	7
12/10/1998	OWP	3994	69	33	22	28	2.4	7	5
	ML	5532	318	15	63	27	1.7	11	2
11/18/2000	OWP	7368	187	45	46	40	2.0	11	2
	ML	3446	938	16	50	32	2.2	7	6
12/12/2002	OWP	4367	101	621	66	40	2.7	8	5
	ML	7000	285	83	57	36	3.3	6	7
12/12/2003	OWP	2989	69	53	108	46	2.0	6	7
	ML	484	481	22	35	36	1.9	5	8

1 Preconstruction layer numbers shifted to align with postconstruction model.

**Section 040501**

Section 040501 is the control section; it received no overlay or other maintenance. The layer model used for backcalculation of all data is shown in Table 48.

Backcalculation results are shown in Table 49. Results are for drop height 4 only. Drop height 4 was chosen for this table because it generally has the highest number of acceptable backcalculation results. The number of acceptable backcalculation results is given as N; N<sub>rejected</sub> is the number of unacceptable backcalculation results. The AB layer (Layer 2) showed significant nonlinearity, which is not apparent from the data in this table. Nonlinearity of this layer is discussed later in this chapter.

**Table 48. Layer Model, Section 040501**

Layer	Layer Type	Thickness (inches)	Seed Modulus (ksi)	Poisson's Ratio
1	AC	5	500	0.35
2	AB	14.2	10	0.50
3	Subgrade	24	35	0.45
4	Subgrade	Semi-infinite	35	0.45

**Table 49. Backcalculation Results, Section 040501**

Test Date	Lane Position	Average Layer Modulus (ksi)				Average RMSE (%)	N	N <sub>rejected</sub>
		1	2	3	4			
1/19/1990	OWP	87	21	32	31	3.0	4	2
	ML	153	27	30	33	3.0	5	1
1/16/1991	OWP	367	17	28	32	2.7	4	7
	ML	1054	7	55	33	3.4	1	10
10/3/1991	OWP	944	22	34	37	3.2	6	5
	ML	1319	29	34	37	3.0	7	4
10/20/1994	OWP	752	19	29	33	2.4	7	4
	ML	1207	18	40	34	3.2	9	2
9/16/1996	OWP	1766	25	30	41	3.0	11	0
	ML	1800	39	33	44	3.0	11	0

The AC layer (Layer 1) exhibits extremely large variability in modulus, and generally high modulus values. The raw versus uncorrected moduli for this layer are shown in Table 50.

The measured (not temperature-corrected) data show significantly less variability and more reasonable values than the temperature-corrected data, indicating that the temperature correction methodology used is not valid for this section. Similar results were seen for the other sections. This could be due to the poor condition of the AC layer, or the use of an AC material that is not well represented in the nationwide modulus versus stiffness model used for correction. The as-measured results show no relationship to temperature, and therefore cannot be used to establish a site-specific temperature correlation.

**Table 50. Measured and Temperature-Corrected AC Moduli**

Test Date	Lane Position	AC Modulus (ksi)		AC Temperature (°F)
		Measured	Corrected	
1/19/1990	ML	437	87	54
	OWP	800	153	61
1/16/1990	ML	487	367	66
	OWP	1430 <sup>1</sup>	1054	66
10/3/1991	ML	395	944	111
	OWP	532	1319	111
10/20/1994	ML	480	752	95
	OWP	860	1207	90
9/16/1996	ML	752	1766	111
	OWP	830	1800	106

1 Based on only one test point.

The AB layer exhibits significant nonlinearity, as shown in Table 51.

**Table 51. Nonlinearity of AB Modulus**

Test Date	Lane Position	Average Layer 2 Modulus (ksi)			
		Height 1	Height 2	Height 3	Height 4
1/19/1990	OWP	15.2	20.2	18.3	21.4
	ML	16.7	18.7	21.6	26.5
1/16/1991	OWP	14.6	14.1	15.7	16.7
	ML	No data	No data	No data	6.9
10/3/1991	OWP	18.3	17.6	22.0	22.4
	ML	18.5	20.5	24.9	29.2
10/20/1994	OWP	14.7	15.8	17.5	18.9
	ML	12.1	15.4	17.7	18.4
9/16/1996	OWP	15.0	15.9	19.7	25.1
	ML	25.2	26.7	33.1	39.2

The relationship between modulus and drop height is most apparent for the 1994 and 1996 data sets. These data sets also have the highest rates of basin convergence ( $N/N_{\text{rejected}}$ ). Layer 2 exhibits an increase in modulus with drop height (i.e., stress-hardening), which is typical for AB materials. This behavior is typically modeled with a bulk-stress model of the following form:

$$E = k_1 \times \Theta^{k_2} \quad (\text{Eq. 7})$$

Where  $E$  = modulus (psi)  
 $k_1, k_2$  = regression coefficients  
 $\Theta$  = bulk stress (psi)

Nonlinear backcalculation was performed using MODCOMP 6E. The layer model shown in Table 48 was used, with the additional required inputs shown in Table 52.

**Table 52. Nonlinear Layer Parameters**

Layer	Layer Type	Unit Weight (pcf)	Coefficient of Lateral Earth Pressure
1	AC	145	0.0
2	AB	135	0.5
3	Subgrade	125	0.5
4	Subgrade	125	0.5

Nonlinear backcalculation was only performed for the 1994 and 1996 data sets, as the modulus versus drop height results for the other data sets using linear backcalculation indicated that nonlinear backcalculation was unlikely to be successful. Results are shown in Table 53. MODCOMP reported all these regressions to be statistically significant.

**Table 53. Nonlinear Backcalculation Results**

Test Date	Lane Position	Average Regression Coefficient	
		$k_1$ (psi)	$k_2$
10/20/1994	OWP	10,887	0.061
	ML	12,867	0.057
9/16/1996	OWP	14,024	0.049
	ML	23,402	0.045

### Discussion of Backcalculation Results

The data presented in this report have many peculiarities of the sort that would typically be ignored in normal production FWD testing in support of pavement design. Because of the large volume of FWD testing performed on this project, both over time and across different pavement structures, we can begin to address these peculiarities.

### Deep Subgrade Modulus Increase

The deep subgrade modulus values are the most consistent and reasonable layer modulus values computed in this study. However, the phenomenon of increasing postconstruction layer modulus should be explained. Table 54 summarizes the increase in postconstruction modulus for the deep subgrade layer as determined through backcalculation, the total increase in pavement thickness, and the increase in  $SN_{eff}$  as determined through the AASHTO 1993 analysis. The postconstruction values presented in the table are from the October 1991 round of testing, as the January 1991 round of testing tends to show intermediate values.

Increase in pavement thickness and increase in  $SN_{eff}$  were chosen as potential explanations for the deep subgrade modulus increase because of their effect on the stress state of the deep subgrade. An increase in pavement thickness will increase overburden stress and therefore confining pressure, and will decrease deviator stress by spreading the load over a greater area.  $SN_{eff}$  is a function of both pavement thickness and effective pavement modulus, and therefore should better represent the decrease in deviator stress in the subgrade due to the overlay.

**Table 54. Postconstruction  $SN_{eff}$  Increase**

Section	$M_r$ Increase (%)	Thickness Increase (inches)	$SN_{eff}$ Increase (%)
040507	84	4.2	123
040504	44	4.2	115
040503	56	3.9	94
040508	74	3.8	109
040509	60	1.1	89
040502	60	1.3	70
040506	117	3.3	135
040505	65	1.9	117
040559	67	2.5	81
040560	32	1.3	43
040501	9	0	20

The increase in pavement thickness shows poor correlation to the increase in deep subgrade modulus. The increase in  $SN_{eff}$  has better correlation to the increase in deep subgrade modulus, as shown in Figure 48.

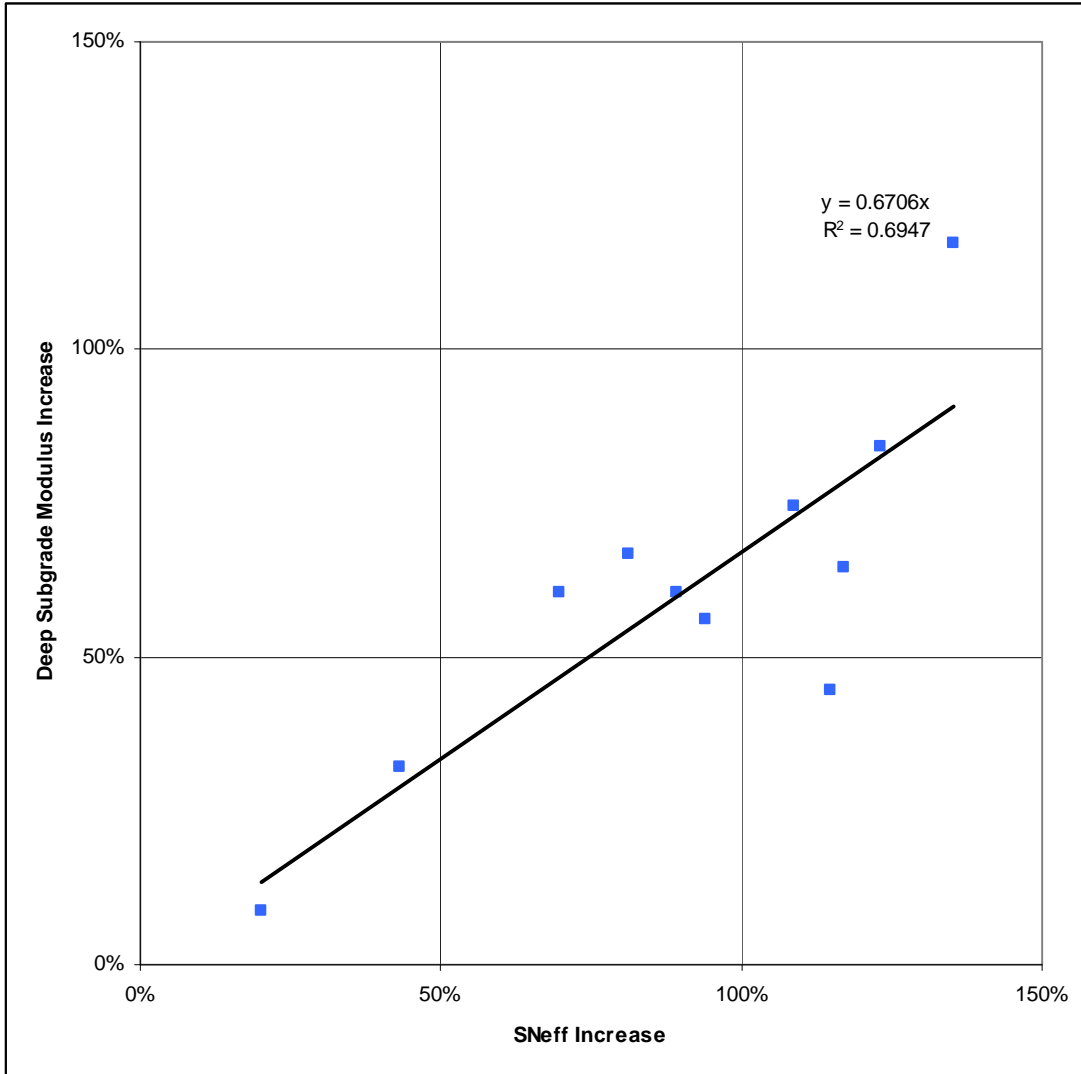


**Figure 48. Subgrade Modulus Increase versus  $SN_{eff}$  Increase**

It should be noted that backcalculation of this data set does not indicate significant nonlinear behavior for the deep subgrade. However, due to the very small deflections at the lower drop heights and the great depth to the lower subgrade, the ability of the FWD to detect nonlinearity in this layer is very limited. In addition, FWD testing at different drop heights only varies the deviator stress; there is no way to vary the confining pressure (and thereby measure its effect on modulus) without changing the pavement structure. Still, the phenomenon of increasing subgrade modulus in response to an overlay is supported by both theory and this data set, and such increases should be considered in pavement design.

The January 1991 data show subgrade modulus values intermediate between the preconstruction data and the October 1991 data. The  $SN_{eff}$  values computed from the January 1991 data are also intermediate values. These intermediate values may be due to stiffness gain from short-term aging of the AC layer.

### Upper Subgrade Stiff Layer

In many but not all tests, a very high modulus value has been backcalculated for the upper subgrade. In a few cases, the stiff layer is the base layer. In some sections, such as 040507, this stiff layer exists for all of the postconstruction data sets. In other sections, such as 040503, the stiff layer appears to come and go in different tests. This stiff layer is not seen in the control section (040501), or in any of the preconstruction data. The obvious question is whether this stiff layer actually exists, or whether it is an artifact of measurement error or error in the analysis method.

To better understand why MODCOMP calculated such high modulus for this layer, we experimented with various layer models for a single test section and date, and used the backcalculation results to develop synthetic deflection basins for comparison. The synthetic deflection basins were computed using the CHEVLAY2 program version 2.3 (release date April 20, 1997), which is used by MODCOMP for forward-calculation. The testing performed on Section 040507 on December 10, 2003, was selected because it shows the highest modulus values for the upper subgrade layer. All of the drop height 4 data was averaged to produce a single average deflection basin. This was done to reduce the effect of random error and spatial variability, which is significant because of the advanced state of deterioration of the pavement. Table 55 shows the average deflection basin along with the synthetic deflection basins generated using the backcalculation results. The backcalculation results for this average deflection basin using different layer models are shown in Table 56.

**Table 55. Measured and Synthetic Deflection Basins**

	Deflection (mils)							
	0 in	8 in	12 in	18 in	24 in	36 in	48 in	60 in
Measured	2.96	2.50	2.24	1.85	1.56	1.13	0.85	0.72
5-Layer	2.99	2.52	2.25	1.88	1.57	1.11	0.85	0.71
4-Layer	2.96	2.50	2.23	1.88	1.57	1.12	0.86	0.71
3-Layer	2.96	2.50	2.25	1.90	1.61	1.15	0.85	0.66
2-Layer	2.95	2.48	2.23	1.88	1.57	1.11	0.81	0.62

**Table 56. Backcalculation Results, Average Deflection Basin from Drop Height 4 Data**

Model Layers	Layer 1		Layer 2		Layer 3		Layer 4		Layer 5		RMSE (%)
	Thick (inches)	E (ksi)									
5	6.8	3600	2.4	3110	20.7	54	24.0	555	∞	87	0.70
4	9.2	3480	N/A		20.7	51	24.0	582	∞	87	0.71
3	9.2	3350	N/A		20.7	122	∞	110	N/A		3.39
2	9.2	3320	N/A		N/A		∞	114	N/A		5.30

In Table 56, the layer numbers were shifted to allow easier comparison of similar layer types. For example, in the five-layer model, the original AC surface and the overlay are treated as separate layers. In the other models, these two layers are combined, and the combined AC layer is represented in the Layer 1 column, with “not applicable” indicated in the Layer 2 column. Seed moduli and Poisson’s ratios were omitted for brevity because of their low sensitivity; the values used for each layer type were the same as the values used in the regular backcalculation.

The four- and five-layer models yield very similar results. The difference is that in the four-layer model, the two AC layers were combined, and the backcalculated modulus of the combined layer is a weighted average of the modulus of the two separated layers. The backcalculated moduli for the remaining layers are quite similar, as is the RMSE.

The three- and four-layer models yield very different results for the base and subgrade layers. In the three-layer model, the subgrade is treated as a homogeneous half-space, whereas in the four-layer model the subgrade is broken into an upper and lower subgrade layer. In the four-layer model, the backcalculated modulus for the upper subgrade is 582 ksi, which is exceedingly high for an unbound material. In the three-layer model, the backcalculated modulus for the combined subgrade layer is 110 ksi, which is still very high for an unbound material. The backcalculated modulus is quite similar between the two models. The RMSE for the three-layer model is 3.39 percent, which is high in general terms and quite high for an averaged deflection basin.

Figure 49 compares the measured deflection basin to the synthetic deflection basins calculated for the five- and three-layer models. The four- and two-layer models were omitted for clarity because the deflection basins for the five- and four-layer models are quite similar, as are the deflection basins for the three- and two-layer models.

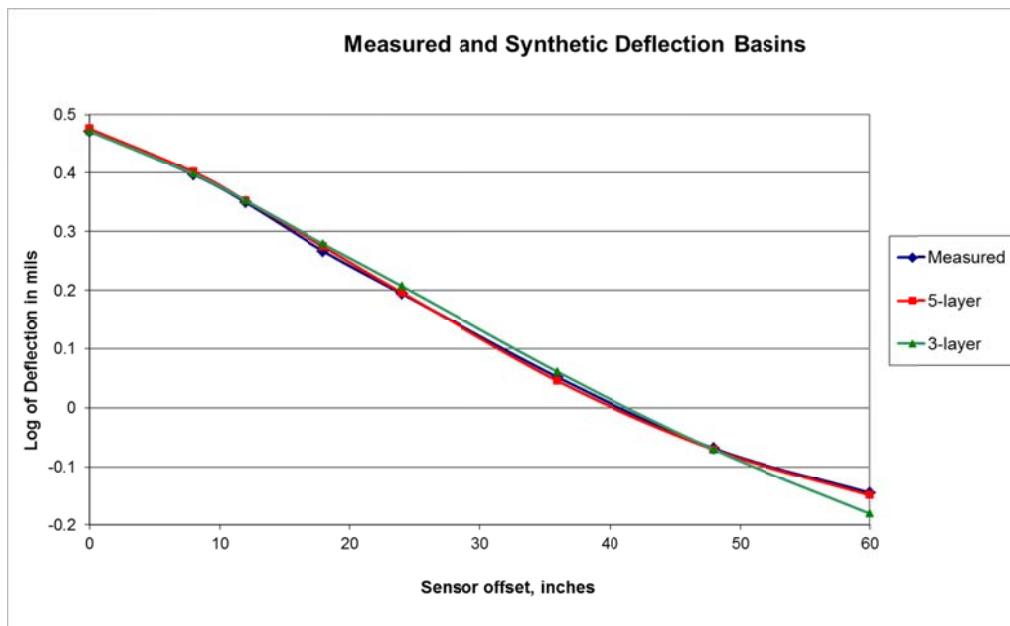


Figure 49. Measured versus Synthetic Deflection Basins

As can be seen from Figure 49 and Table 55, the models in which the upper and lower subgrades are combined (i.e., the three- and two-layer models) overpredict deflections at the 18- and 24-inch offsets, and underpredict deflections at the 60-inch offset, yielding a flatter deflection basin than the measured deflection basin and that computed by the four- and five-layer models.

This phenomenon is unlikely to be due to measurement error. Although the magnitude of the deflections is low, random error should be minimized by the large number of actual basins used to compute the average basin. Systematic error, either in deflection measurements or sensor offset, is an unlikely explanation because the phenomenon is apparent in the results for some of the sections tested on December 10, 2003, but not others.

Backcalculation, and indeed all FWD analysis procedures in common use, is subject to a number of assumptions. Among these assumptions are that pavement layers are homogeneous, isotropic and elastic, and that the pavement response to dynamic loads (e.g., moving wheel loads or FWD load pulses) is the same as its response to static loads. Since the layered elastic algorithms used in backcalculation are similar to (and in some cases the same as) those used in mechanistic pavement design methodologies such as the AASHTOWare Pavement ME Design software, problems associated with the violation of these assumptions are not limited to the analysis of FWD data, but represent fundamental limitations in our ability to understand, model, and predict the behavior of pavement systems. Indeed, the most amazing thing about pavement modeling is that it gives reasonable results most of the time.

The pavements at this test section (and indeed all pavements to one degree or another) are not homogeneous or isotropic. However, errors related to violations of modeling assumptions regarding homogeneity or isotropy should be greatest for the control section (040501), which had the greatest distress density throughout the analysis period. However, the stiff layer phenomenon does not occur for this test section, indicating that this phenomenon has other causes.

Dynamic effects have been understood to have a large influence on the analysis of deflection data since the very beginning of pavement deflection measurement. There have been numerous research projects related to incorporating dynamic effects in the analysis of FWD data; however, none of the products of these studies have met with acceptance either in the industry or in the research community at large. Beyond issues with usability and robustness, there remains the question of what to do with the results, as current pavement design tools, including the *Mechanistic-Empirical Pavement Design Guide* (NCHRP 2004), are still based on static layered-elastic analysis. (Although the MEPDG does adjust the modulus of the AC layer based on loading frequency, its response model is fundamentally static.)

Dynamic effects can be visualized using hysteresis plots. Two hysteresis plots are shown in Figures 50 and 51. The first is for Section 040507 on December 10, 2003, where the stiff layer phenomenon occurs. The second is for Section 040559 on December 12, 2003, where the stiff layer phenomenon does not occur.

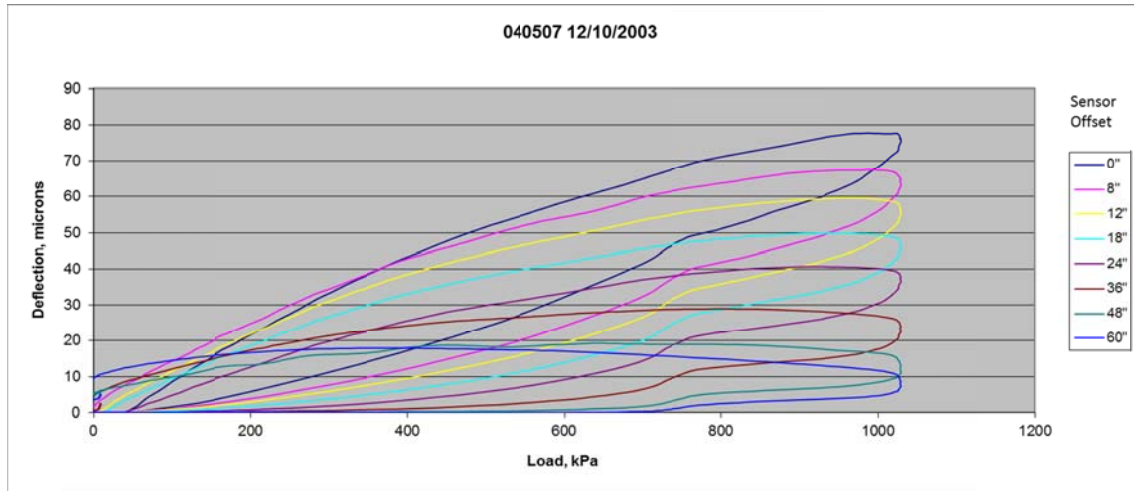


**Figure 50. Hysteresis Plot, Section 040507 (Stiff Layer Phenomenon)**

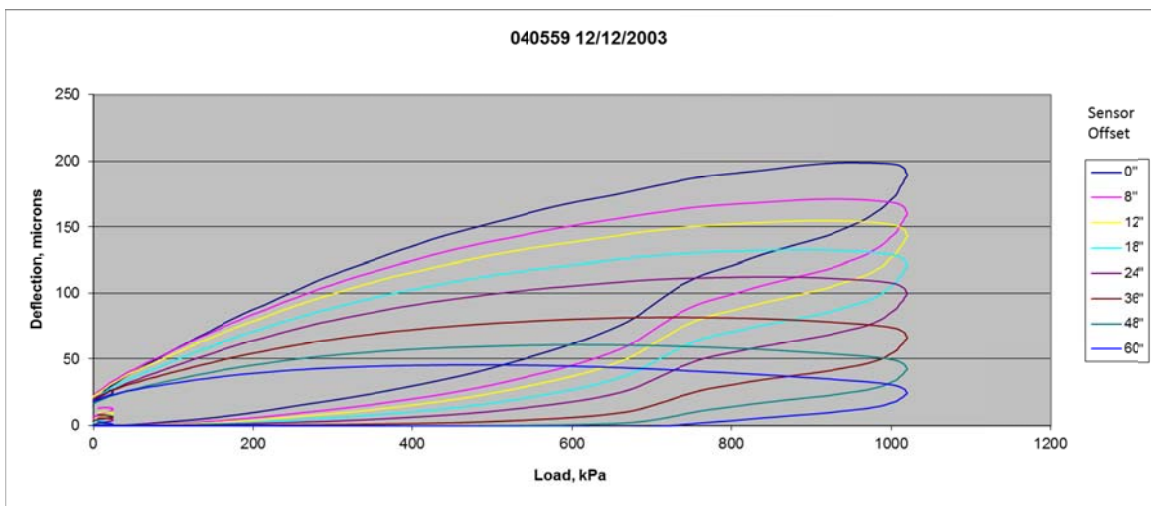


**Figure 51. Hysteresis Plot, Section 040559 (Stiff Layer Phenomenon Not Observed)**

The data for Section 040559 shows much higher damping than the data for Section 040507. The damping can be seen in the decrease in area included in the loop with increasing distance from the load plate. This lack of damping has the effect of increasing deflection measured for the outer sensors above that predicted by layered-elastic theory, and is a likely explanation for the stiff layer phenomenon.

### **DEFLECTION ANALYSIS KEY FINDINGS**

Three methods of analyzing deflection data have been presented in this section: normalized deflection, AASHTO 1993, and layered-elastic backcalculation. All three agree that the sections at this project are extremely stiff. The most sophisticated method used, layered-elastic backcalculation, generally

produced highly variable and unreasonable results, and these results should be used with extreme caution. One source of difficulty for the layered-elastic backcalculation is dynamic effects resulting from poor damping. Errors associated with these dynamic effects should be expected in any layered-elastic modeling of these pavements, including that performed by the MEPDG, although these errors may be less obvious.

The simpler AASHTO 1993 analysis procedure yielded less variable and more reasonable results, although dynamic effects should still be expected to result in a slight underprediction of  $M_r$ . Despite this, the  $SN_{eff}$  calculated for Sections 040507 and 040504 is still significantly higher than expected based on assumed layer coefficients.

The FWD data show significant variability in preconstruction  $SN_{eff}$  among the sections. The preconstruction  $SN_{eff}$  in Section 040507 was 61 percent greater than in Section 040505. These results are supported by coring results, which show similar variability in AB thickness. Analyses of the differential performance of the sections based solely on the difference in construction methods are therefore questionable.

Based on the increase in  $SN_{eff}$  from the preconstruction testing, thicker overlays performed better than thin overlays, virgin AC materials performed better than recycled materials, and intensive surface preparation performed better than minimal surface preparation. In the testing performed 17 months after construction, the virgin overlays had a 31 percent greater increase in  $SN_{eff}$  than the recycled overlays. The thick overlays had a 24 percent greater increase in  $SN_{eff}$  than the thin overlays. The intensive surface preparation sections had a 17 percent greater increase in  $SN_{eff}$  than the minimal surface preparation sections.

By the time of the final test, 163 months after construction, the thickness of the overlay had become the most important factor. At that time, the thick overlays had a 77 percent greater increase in  $SN_{eff}$  than the thin overlays. The virgin overlays had a 55 percent greater increase in  $SN_{eff}$  than the recycled overlays. The intensive surface preparation sections had a 39 percent greater increase in  $SN_{eff}$  than the minimal surface preparation sections.

## CHAPTER 3. SPS-5 DISTRESS ANALYSIS

This chapter describes the analyses and evaluations of distress data collected on the Arizona SPS-5 project using LTPP manual survey techniques (Miller and Bellinger 2003). Surface distress provides powerful information about the nature and extent of pavement deterioration, which can be used to quantify performance trends as well as to investigate the contribution of design features on service life.

All 11 SPS-5 test sections were constructed consecutively and exposed to the same traffic-loading, climate, and subgrade conditions, which allowed for direct comparisons between layer configurations and design features without confounding effects introduced by different in situ conditions.

### AC DISTRESS TYPES

Multiple distress types can cause deterioration in asphalt surfaces (Huang 1993), such as:

- **Fatigue cracking:** A series of interconnecting cracks caused by repeated traffic loading. Cracking initiates at the bottom of the asphalt layer where tensile stress is the highest under the wheel load. With repeated loading, the cracks propagate to the surface.
- **Longitudinal wheelpath (WP) cracking:** Cracking parallel to the centerline occurring in the WP. This cracking can be the early stages of fatigue cracking or can initiate from construction-related issues such as paving seams and segregation of the mix during paving. In the latter case, cracking is typically very straight (with no meandering).
- **Longitudinal non-wheelpath (NWP) cracking:** Cracking parallel to the centerline occurring outside the WP. This cracking is not load-related and can initiate from paving seams or where segregation issues occurred during paving. Cracking can also be caused by tensile forces experienced during temperature changes. Pavements with oxidized or hardened asphalt are more prone to this type of cracking.
- **Transverse cracking:** Cracking that is predominantly perpendicular to the pavement centerline. Cracking starts from tensile forces experienced during temperature changes. Pavements with oxidized or hardened asphalt are more prone to this type of cracking.
- **Block cracking:** Cracking that forms a block pattern and divides the surface into approximately rectangular pieces. Cracking initiates from tensile forces experienced during temperature changes. This distress type indicates that the AC has significantly oxidized or hardened.
- **Raveling:** Wearing away of the surface caused by dislodging of aggregate particles and loss of asphalt binder. Raveling is caused by moisture stripping and asphalt hardening.
- **Bleeding:** Excessive bituminous binder on the surface that can lead to loss of surface texture or a shiny, glass-like, reflective surface. Bleeding is a result of high asphalt content or low air void content in the mix.
- **Rutting:** A surface depression in the WPs. Rutting can result from consolidation or lateral movement of material due to traffic loads. It can also signify plastic movement of the asphalt mix because of inadequate compaction, excessive asphalt, or a binder that is too soft given the climatic conditions.

Table 57 summarizes these flexible pavement distress types and their associated failure mechanisms.

**Table 57. Flexible Pavement Distress Types and Failure Mechanisms**

Distress Type	Failure Mechanism	
	Traffic/Load Related	Climate/Materials Related
Fatigue cracking	✓	
Longitudinal WP cracking	✓	
Longitudinal NWP cracking		✓
Transverse cracking		✓
Block cracking		✓
Raveling		✓
Bleeding		✓
Rutting	✓	✓

## RESEARCH APPROACH

Investigators began the analysis by reviewing all of the distress data collected at each test section to identify suspect or inconsistent information. They used photos and distress maps to verify quantities reported in the database. Because of the subjective nature of the data collection technique (raters had to select distress type and severity based on a set of rules), variation is expected in distress data.

Most LTPP distress data are reported at three severity levels: low, moderate, and high. Inconsistencies between severity levels (within one distress type) are one of the largest sources of variability in distress data (Rada et al. 1999). In addition, conducting analyses on three separate severity levels for each distress type becomes an increasingly complex process with results that are difficult to interpret. To reduce variability and to consolidate the information for analyses, the quantities from the three severity levels were summed into one composite value for the research presented.

In addition to the structural and environmental distress factors used to assess SPS-5 section performance, investigators also incorporated rutting, patching, and other surface defects (i.e., potholes, bleeding, and raveling) into the analyses. Rutting data reported in this study were generated using a wire line reference.

The experimental design of the SPS-5 project is such that replicate data were not collected. Therefore, standard statistical comparisons (i.e., *t* tests) to determine the significance of findings could not be conducted. Instead, the evaluation consisted of graphical comparisons between test sections from data collected at the same time.

## OVERALL PERFORMANCE TREND OBSERVATIONS

While gathering pavement distress data for this research, investigators became aware of a few significant trends impacting the project's overall pavement performance. These observations were clearly driving issues for this project and were intrinsically important to the distress performance.

Section 040501, the test section that did not receive an overlay, performed the worst of all SPS-5 sections. Within six years, this section had deteriorated to a level that required reconstruction and, therefore, it was taken out of the experiment.

All minimum preparation, 2-inch overlay sections (040502, 040505, and 040560) showed evidence of structurally related distress within seven years after construction, with Sections 040502 and 040505 accumulating fatigue to over half of the section area by the end of the study. These sections also exhibited pumping eight years after construction.

In general, test sections receiving an intensive surface preparation before overlay treatment performed much better than the other test sections in the project. Test sections with virgin AC overlays also performed better when compared to the recycled AC sections (040504 to 040503).

Compared to the rest of the SPS-5 test sections, Section 040507 exhibited significantly smaller amounts of damage accumulation. The pavement structure for this section is composed of 20.7 inches of granular base, 2.4 inches of existing inlay AC, 2.7 inches of new inlay AC, and 4.1 inches of overlay AC.

In general, the extent of distresses in all the sections increased over time except for Section 040502, which quickly became distressed and only the severity of distresses increased over time.

Table 58 lists the dates when surveys were performed at each test section. Figures 52 through 62 illustrate the overall structural and environmental performance trends for each section. These trends are relatively consistent and within the expected range of variation. Drops in the distress graph typically indicate the distress propagating into a different distress (i.e., longitudinal WP cracking forming into fatigue cracking). The maintenance work (i.e., fog seal and crack sealing) performed on the project did not significantly mask the severity and extent of distresses. Nonetheless, distress comparisons formulated in this analysis focused primarily on the extent of distress. Appendix B provides the complete work history of each site.

**Table 58. MDS Dates by Section**

<b>Survey Date</b>	<b>0501</b>	<b>0502</b>	<b>0503</b>	<b>0504</b>	<b>0505</b>	<b>0506</b>	<b>0507</b>	<b>0508</b>	<b>0509</b>	<b>0559</b>	<b>0560</b>
01/15/1991	✓										
10/18/1994- 10/20/1994	✓	✓	✓	✓	✓	✓	✓	✓	✓	✓	✓
09/12/1996- 09/12/1996		✓				✓		✓	✓		
11/13/1997- 11/13/1997					✓	✓					
12/09/1998- 12/10/1998		✓	✓	✓	✓	✓	✓	✓		✓	✓
12/13/1999- 12/14/1999		✓	✓	✓	✓	✓		✓	✓	✓	✓
10/16/2000- 10/18/2000		✓	✓	✓	✓	✓	✓	✓	✓	✓	✓
11/28/2001- 11/30/2001		✓	✓	✓		✓	✓	✓	✓	✓	✓
12/10/2002- 12/12/2002		✓	✓	✓	✓	✓	✓	✓	✓	✓	✓
12/10/2003- 12/12/2003		✓	✓	✓	✓		✓		✓	✓	
12/07/2004- 12/08/2004		✓	✓	✓	✓	✓	✓	✓	✓		
12/05/2005- 12/05/2005			✓	✓			✓	✓	✓		
09/15/2008- 09/15/2008		✓			✓	✓			✓		

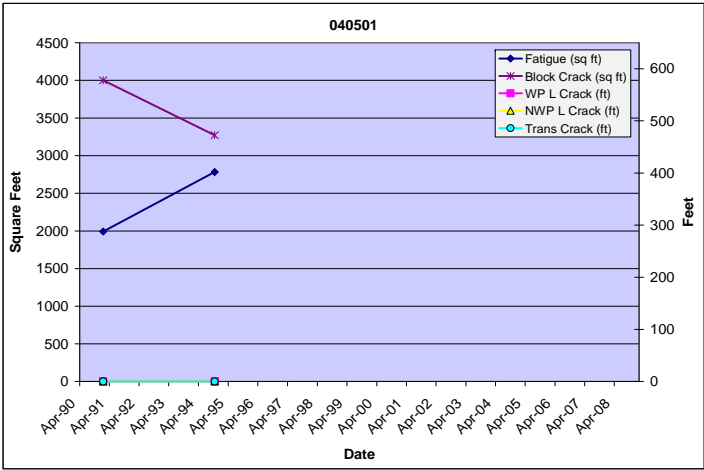


Figure 52. Structural and Environmental Distress Trends in Section 040501

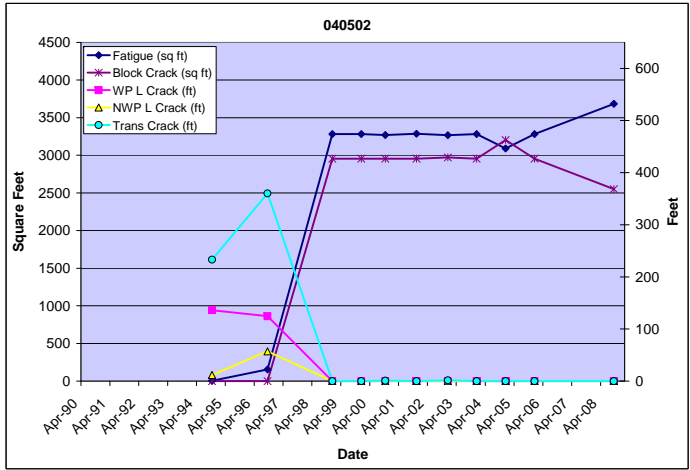


Figure 53. Structural and Environmental Distress Trends in Section 040502

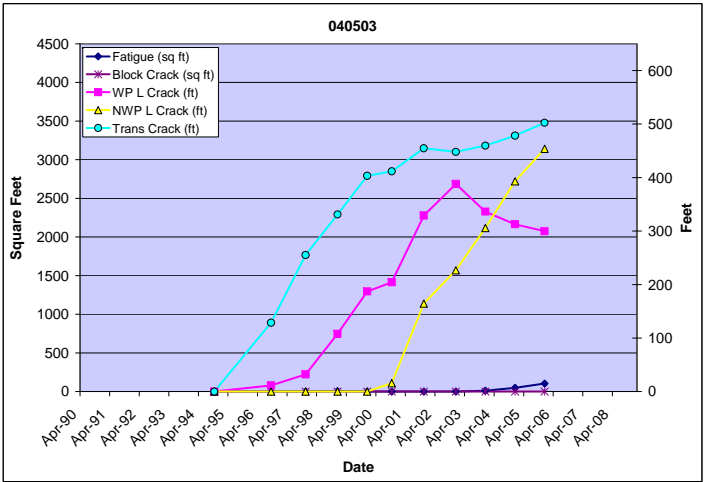


Figure 54. Structural and Environmental Distress Trends in Section 040503

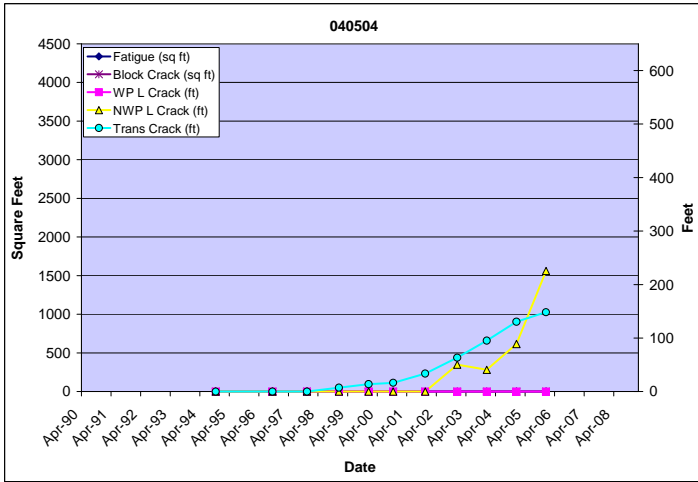
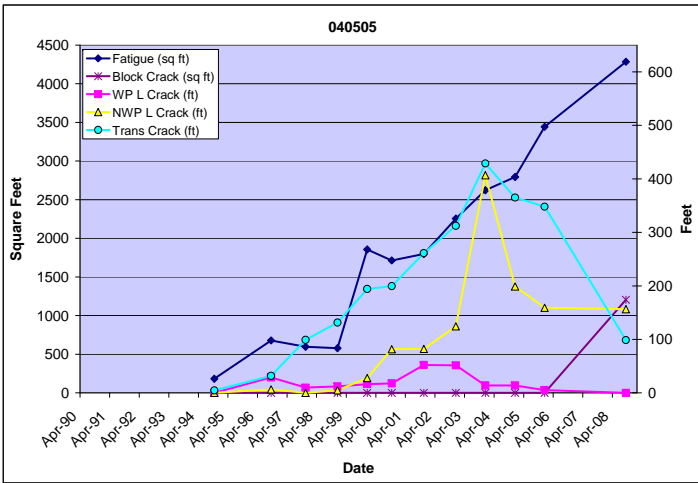
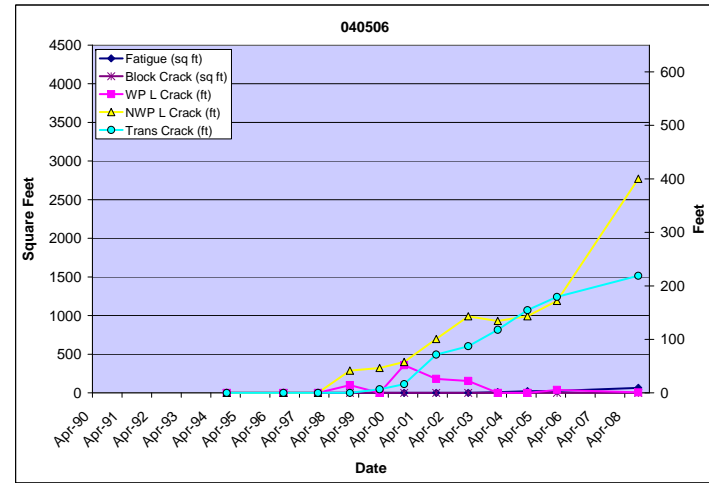


Figure 55. Structural and Environmental Distress Trends in Section 040504



**Figure 56. Structural and Environmental Distress Trends in Section 040505**



**Figure 57. Structural and Environmental Distress Trends in Section 040506**

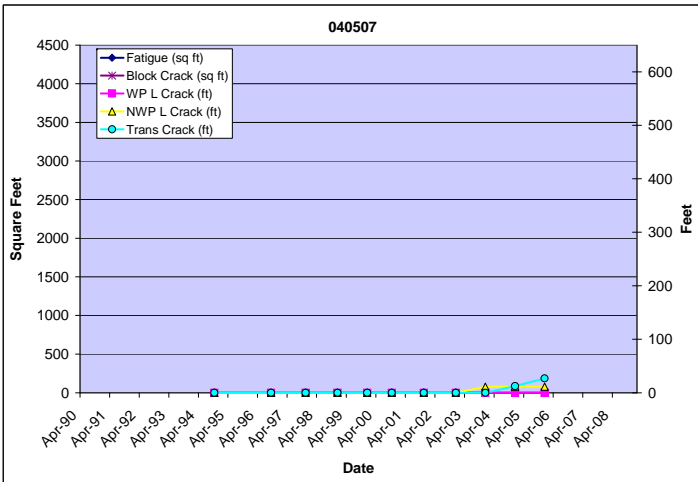


**Figure 58. Structural and Environmental Distress Trends in Section 040507**

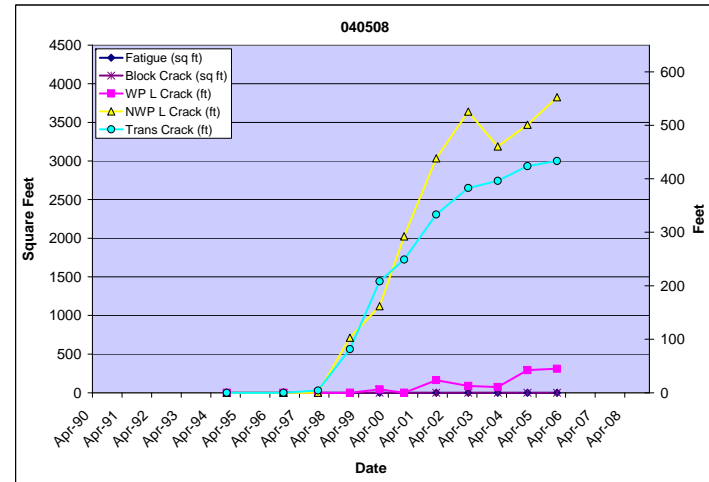


**Figure 59. Structural and Environmental Distress Trends in Section 040508**

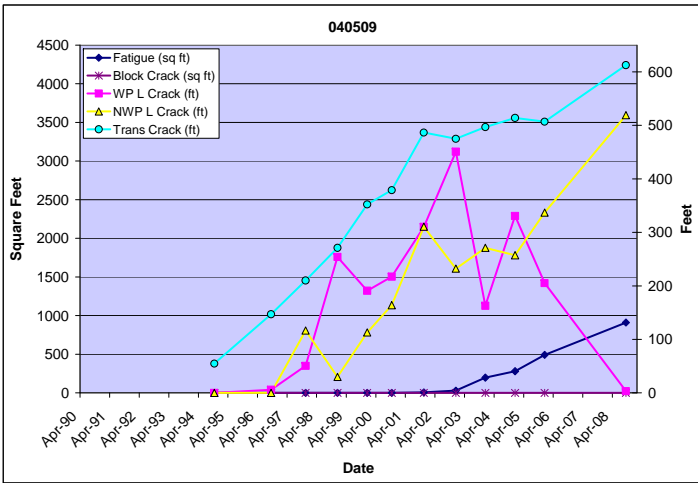


**Figure 60. Structural and Environmental Distress Trends in Section 040509**

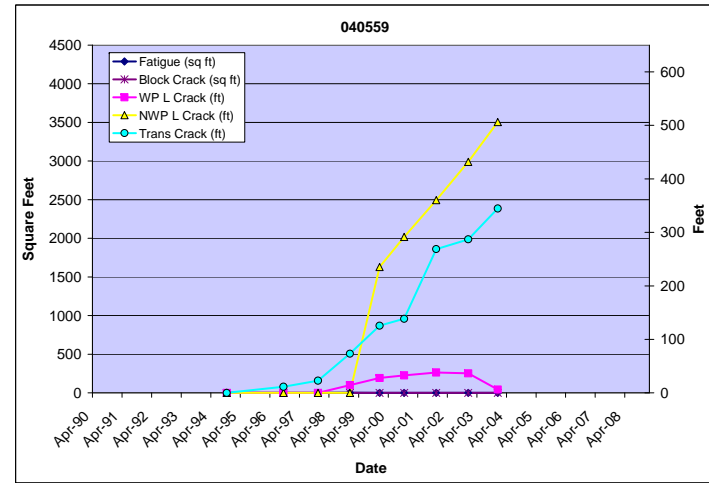


**Figure 61. Structural and Environmental Distress Trends in Section 040559**

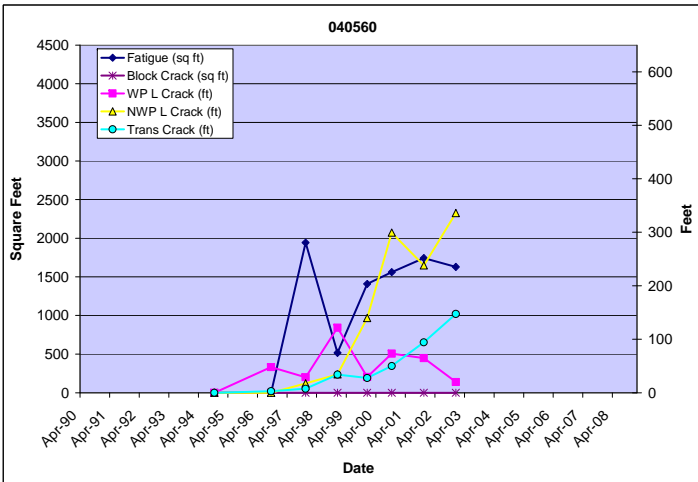


**Figure 62. Structural and Environmental Distress Trends in Section 040560**

## Performance Comparisons

Investigators conducted in-depth analyses and comparisons all of the SPS-5 test sections. Figure 63 summarizes the structural distress and Figure 64 summarizes the environmental distress for each section. Results in both distress charts are based on the data collected in December 2002, the last date that every section was surveyed manually.

Figure 65 summarizes the structural distresses and Figure 66 summarizes the environmental distresses for each core section. Results in both distress charts are based on the data collected in December 2005, the last date that every core section was surveyed manually.

Figure 67 summarizes rutting in each section in 2002, while Figure 68 summarizes rutting in each core section in 2005. In 2008, investigators conducted a forensic study on Sections 040502, 040505, 040506, and 040509. After excavating trenches, investigators found rutting mainly in the top AC layer; virtually no rutting was detected in the lower layers. The average rut depth of both trenches was 6.5 mm (Nichols Consulting Engineers, unpublished data, 2010).

All sections exhibited less than 10 mm of rutting after more than seven years in service, which is below the level required to trigger improvements in most pavement management systems. Sections 040502 and 040509 exhibited large amounts of localized rutting; however both sections had other distresses that would have triggered improvements in most pavement management systems. Therefore, rutting was not the driving factor in the overall condition of the pavement.

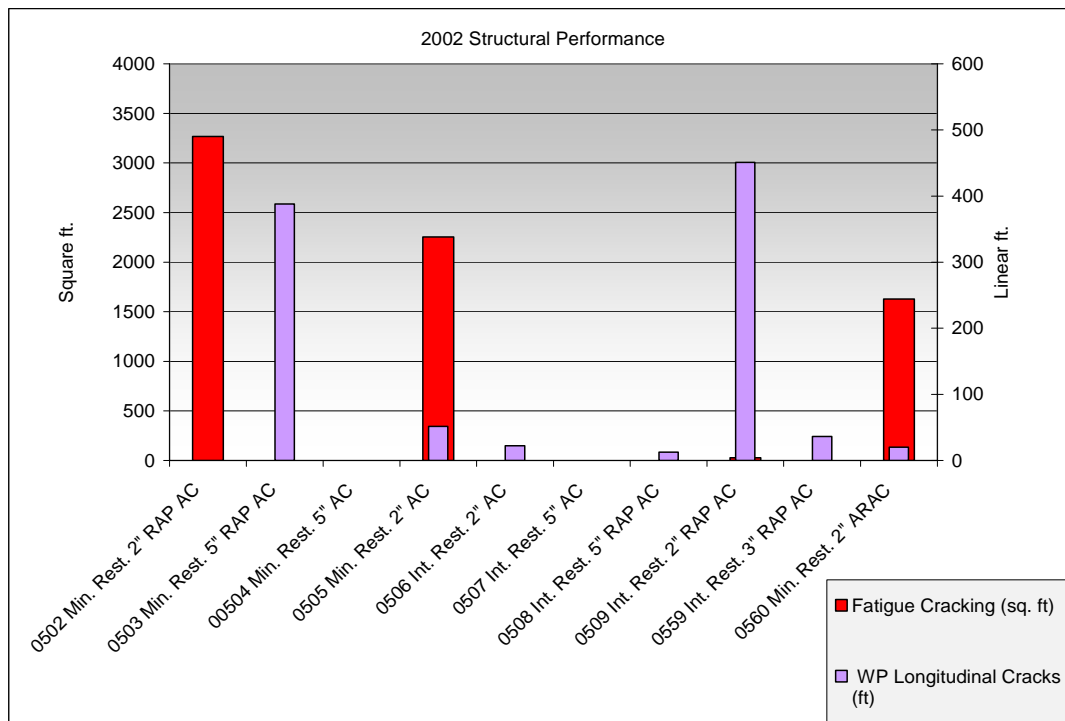
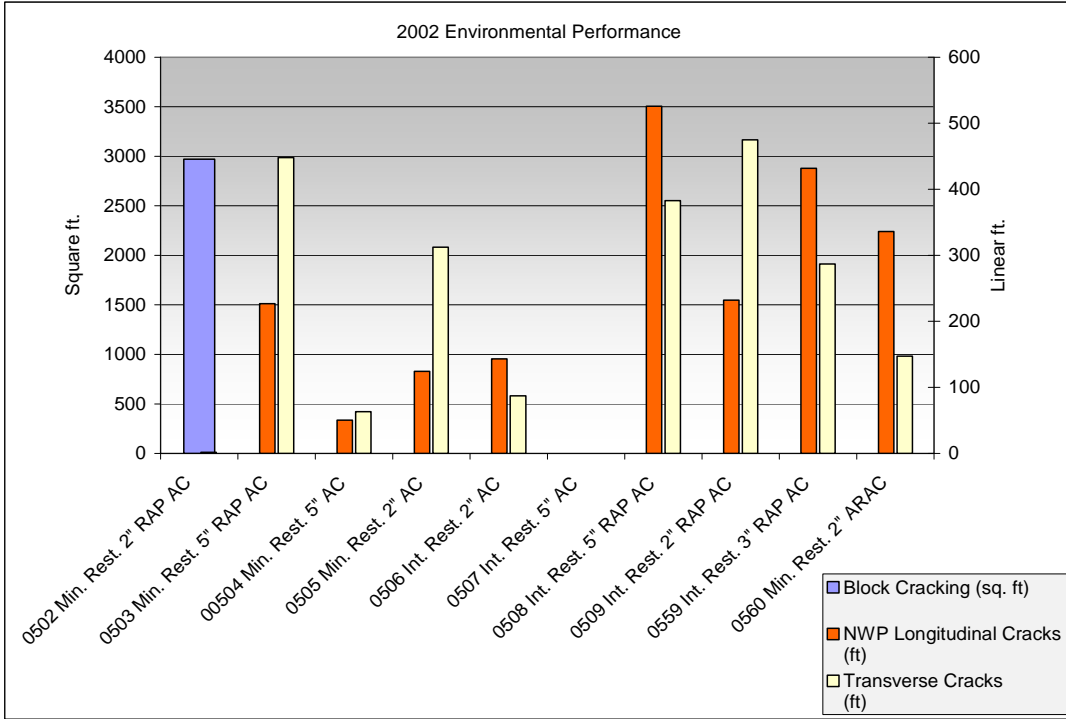
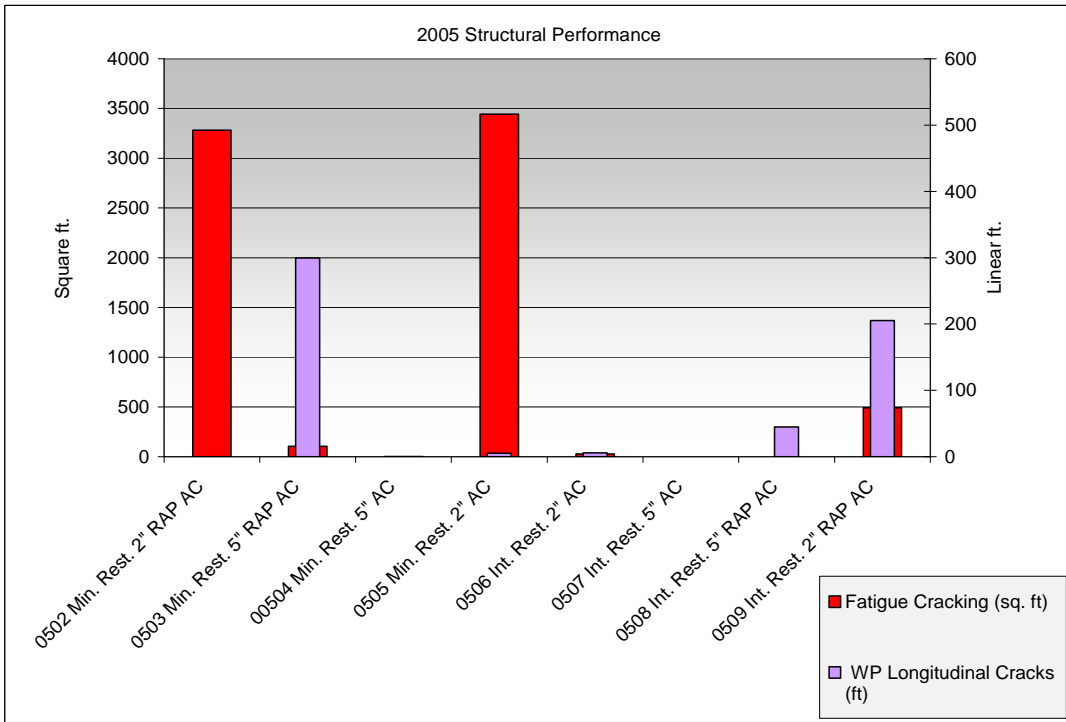


Figure 63. 2002 Structural Performance of All SPS-5 Sections



**Figure 64. 2002 Environmental Performance of All SPS-5 Sections**



**Figure 65. 2005 Structural Performance of SPS-5 Core Sections**

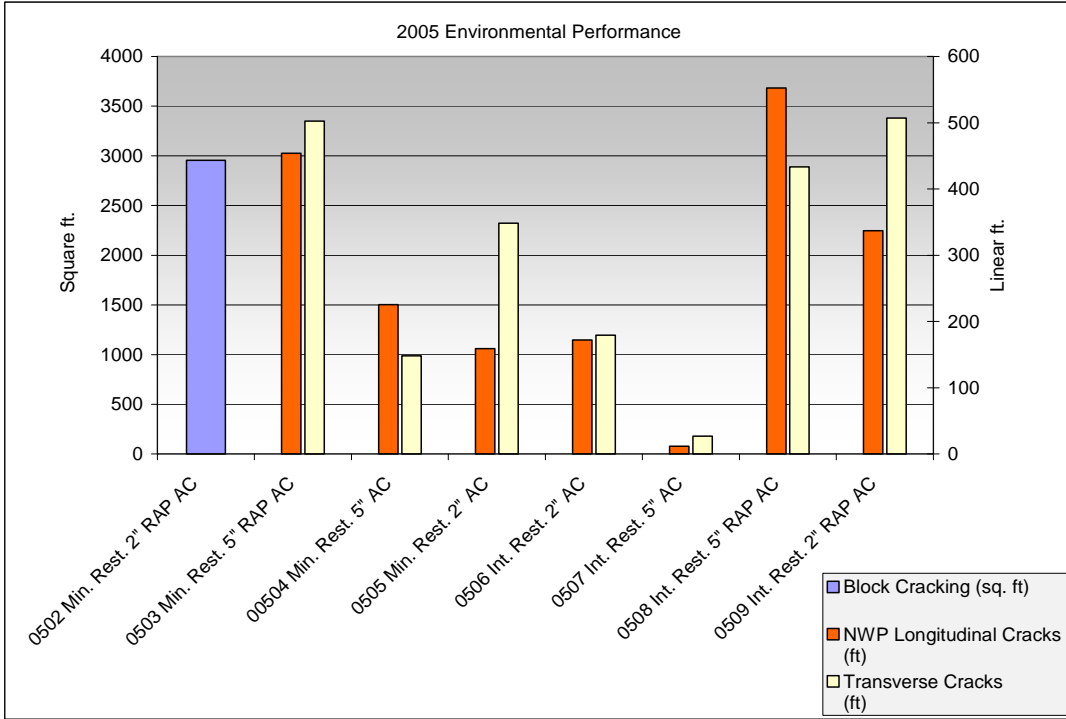


**Figure 66. 2005 Environmental Performance of SPS-5 Core Sections**

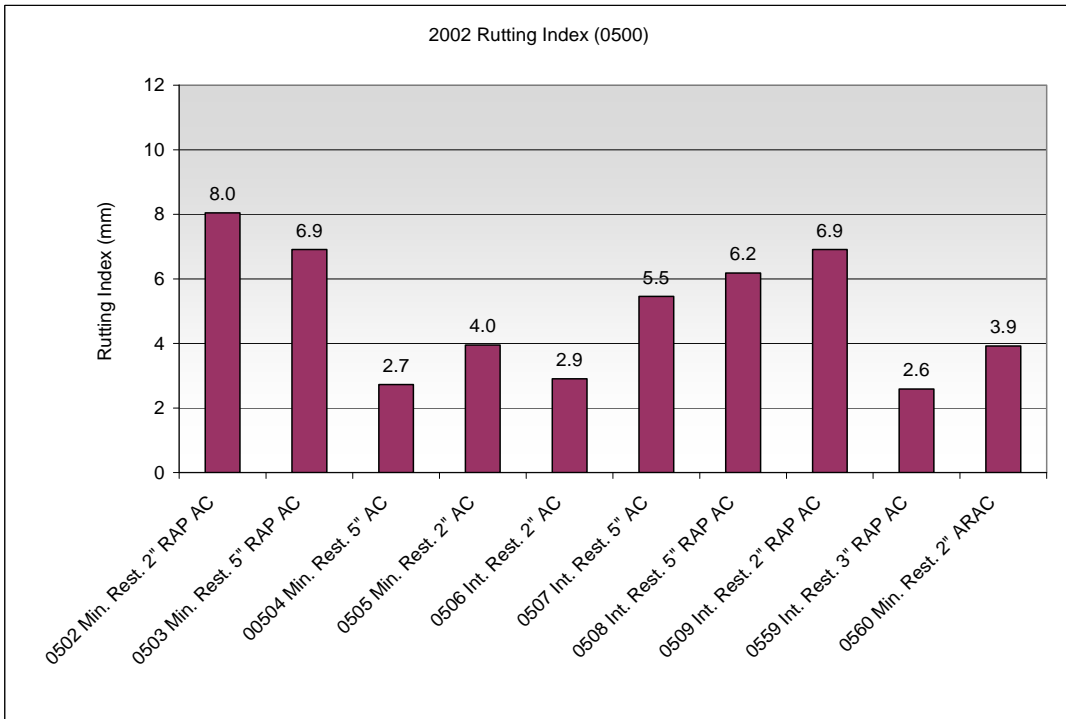


**Figure 67. 2002 Rutting Index Summary of All SPS-5 Sections**

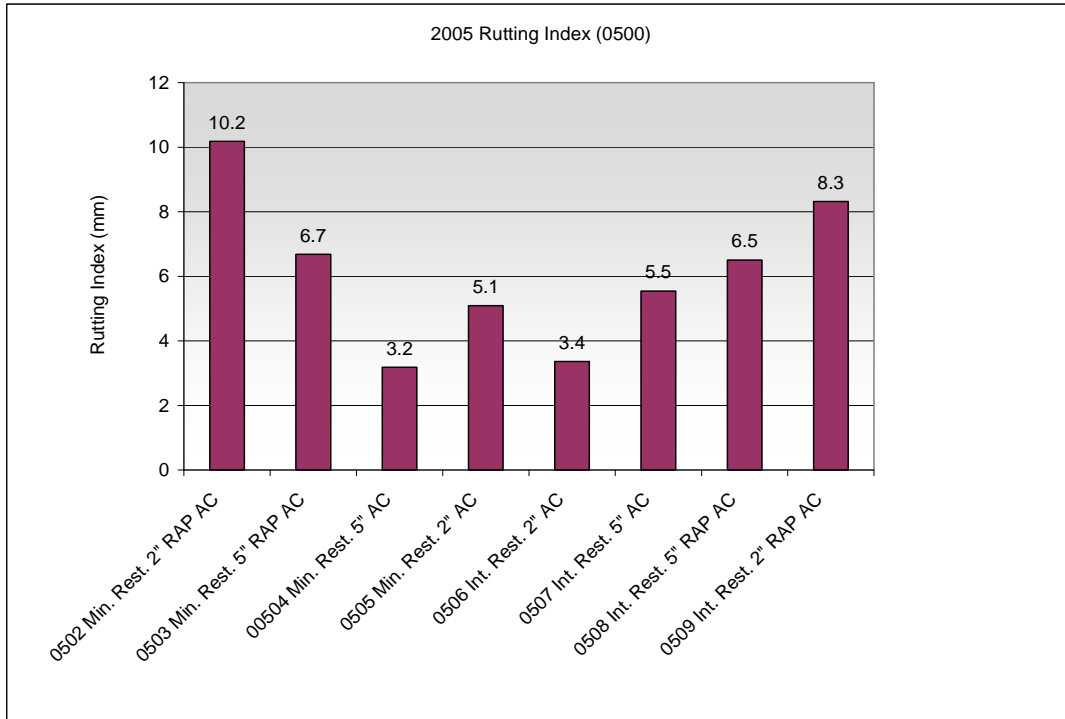


**Figure 68. 2005 Rutting Index Summary of SPS-5 Core Sections**

In the experimental design of the SPS-5 project, the milled layer was to be replaced with the same overlay material used in the section before overlay placement. From an LTPP perspective, this thickness is not considered to be part of the overlay thickness. However, this additional material does appear to affect the structural performance of the sections. Fatigue cracking, the standard measure of pavement performance, seems to have a direct correlation with the thickness of the AC material. Figure 69 shows that sections where the total thickness of all AC layers (new and existing) was greater than 6 inches had a greater resistance to fatigue cracking than sections with total AC layer thicknesses less than 6 inches (based on limited observations of the eight core sections). Sections 040505 and 040502, in which the total AC material thickness was less than 6 inches, incurred fatigue cracking in over half the total area of the sections.

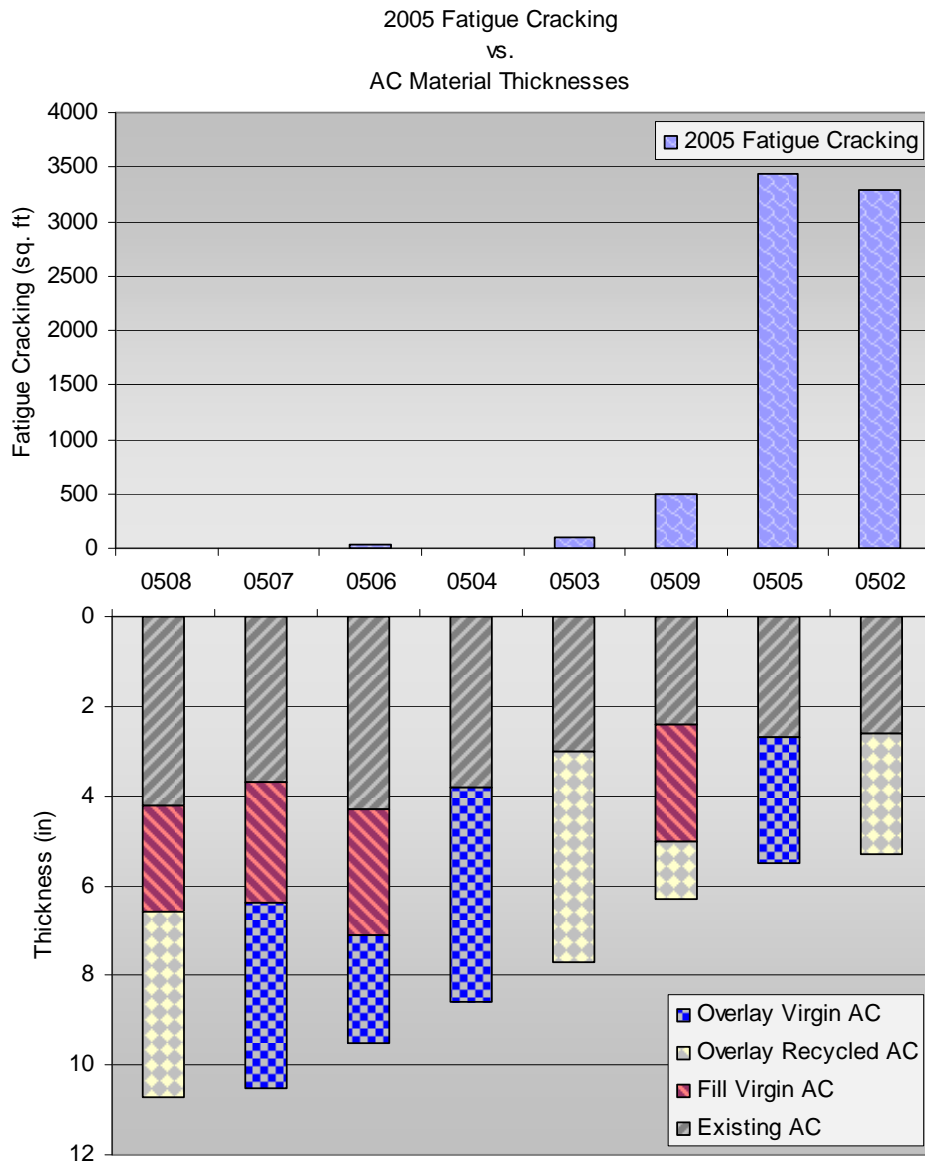


**Figure 69. Fatigue Cracking and AC Material Thicknesses**

There is a debate in the paving community between top-down and bottom-up cracking. The classic fatigue cracking model looks at bottom-up cracking resulting from repeated tensile stresses at the bottom of the AC pavement. However, increasingly evidence suggests that some of the WP cracking initiates at the surface of the pavement and progresses downward, particularly in thicker pavement sections (Al-Qadi et al. 2008; Uhlmeier et al. 2000).

Forensic sampling of Sections 040502, 040505, 040506, and 040509 determined whether the crack mechanism was primarily top-down or bottom-up cracking. AC core samples from the sections and trench excavations in Sections 040506 and 040509 were visually inspected. In general, the core samples exhibited medium to high severity cracks initiated at the pavement surface and extending to the inlay

layer, showing a top-down cracking pattern. Visual inspection of the trenches revealed no reflective cracks (i.e., cracks from underlying pavement layers propagating to surface layers) at the bottom of the AC slab layer, reconfirming the crack mechanism as top-down cracking.

The following observations of the SPS-5 sections are based on structural and environmental distress trends (illustrated in Figures 63 and 64). General (structural and environmental) and specific distress trends are discussed along with probable causes for sudden increases and decreases within the identified distress trends.

#### *Section 040501 (Control Section)*

Section 040501 only received the required routine maintenance needed to keep the section in a safe and functional condition. The section had 1992 ft<sup>2</sup> of fatigue cracking in 1991 and 4000 ft<sup>2</sup> of block cracking. In 1994, fatigue cracking spread into areas that had block cracking, which resulted in 2781 ft<sup>2</sup> of fatigue cracking and 3272 ft<sup>2</sup> of block cracking. This section was placed out of study in October 1996 because of significant deterioration. At the time it was taken out of study, the entire section exhibited moderate severity block and fatigue cracking.

#### *Section 040502 (Minimum Preparation, 2-Inch Recycled Asphalt Pavement (RAP) Overlay)*

Section 040502 performed very poorly against structural and environmental distresses. Distresses began to appear in 1994 and peaked in 1998, when the primary distresses of fatigue and block cracking had spread throughout the entire section. Investigators observed very little fatigue cracking and some WP longitudinal cracking in 1994. In the following years, the WP longitudinal cracking progressed into fatigue cracking. In 1999, the fatigue had spiked to 3282 ft<sup>2</sup>, existing in both WPs, and remained constant until the end of the study. Some rater variability between fatigue cracking and block cracking caused a slight increase and respective decrease between the two distresses in 2004. In 2008, fatigue cracking spread in block cracked areas and peaked at 3684 ft<sup>2</sup>. No block cracking, some longitudinal NWP cracking, and substantial transverse cracking was observed in 1994. Longitudinal NWP and transverse cracking continued to increase until 1999 when both distresses dropped to zero and block cracking spiked up to 2955 ft<sup>2</sup>. Block cracking then remained fairly constant until a slight drop in 2008 because of the spread of fatigue cracking into block cracked areas. This section also exhibited large amounts of pumping and rutting that increased over time.

#### *Section 040503 (Minimum Preparation, 5-Inch RAP Overlay)*

Section 040503 performed poorly against environmental distresses, with large amounts of transverse and longitudinal cracking, but little or no fatigue or block cracking. The primary structural distress, longitudinal WP cracking, appeared in 1996 and steadily increased to 388 ft in 2002, after which some longitudinal WP cracking progressed into fatigue cracking. By 2008, fatigue cracking had increased to 104 ft<sup>2</sup>. Transverse cracking appeared in 1996, increased to 455 ft in 2001, and then gradually increased to 502 ft in 2008. Longitudinal NWP cracking appeared in 2000 and steadily increased to 454 ft in 2008. Investigators did not observe block cracking at this section. Minimal pumping was observed in 2005, and the section had average rut resistance compared to the other sections.

*Section 040504 (Minimum Preparation, 5-Inch AC Overlay)*

Section 040504 performed well against structural and environmental distresses throughout the study. Investigators observed very little fatigue or longitudinal WP cracking. Transverse cracking steadily increased from 7 ft in 1998 to 148 ft in 2005. Longitudinal NWP cracking appeared in 2002 at 50 ft and increased to 225 ft in 2005.

*Section 040505 (Minimum Preparation, 2-Inch AC Overlay)*

Section 040505 performed poorly against structural and environmental distresses. Distresses were minor in 1994, but steadily increased until the end of the study. Fatigue cracking was the primary distress observed by the end of the study, with some transverse, longitudinal NWP, and block cracking also recorded. The primary structural distress, fatigue cracking, consistently increased from 1994 to 2008 and peaked at 4285 ft<sup>2</sup>. No block cracking was observed from 1994 to 2005, but suddenly increased to 1206 ft<sup>2</sup> in 2008. Transverse and longitudinal NWP cracking steadily increased to a peak in 2003 at 429 ft and 407 ft, respectively. Transverse and longitudinal NWP cracking dropped to 100 ft and 156 ft, respectively, in 2008 because of the spread of fatigue cracking and block cracking. The section also exhibited large amounts of pumping and moderate rut resistance, and performed better than its recycled counterpart, Section 040502.

*Section 040506 (Intensive Preparation, 2-Inch AC Overlay)*

Section 040506 performed well against structural distresses but poorly against environmental distresses. Distresses rated as longitudinal WP cracking propagated into fatigue cracking in 2003. Fatigue cracking then steadily increased from 10 ft<sup>2</sup> in 2003 to 64 ft<sup>2</sup> in 2008. Longitudinal NWP and transverse cracking steadily increased throughout the study period. Longitudinal NWP cracking appeared in 1998 at 42 ft and increased to 400 ft in 2008; transverse cracking was observed at 7 ft in 1999 and increased to 219 ft in 2008. Minimal pumping was observed in 2008.

*Section 040507 (Intensive Preparation, 5-Inch AC Overlay)*

Section 040507 performed well against structural and environmental distresses throughout the study. Only longitudinal NWP and transverse cracking were observed at this section. Longitudinal NWP cracking appeared from 2003 to 2005 at an average of 11 ft; transverse cracking appeared from 2004 to 2005 at an average of 20 ft. The section exhibited no pumping and had average rut resistance.

*Section 040508 (Intensive Preparation, 5-Inch RAP Overlay)*

Section 040508 performed well against structural distresses but poorly against environmental distresses. In 1999, investigators observed longitudinal WP cracking that increased to 45 ft in 2008. No fatigue cracking was observed at this section throughout the study. Investigators observed transverse cracking in 1997 and longitudinal NWP cracking in 1998. Both distresses steadily increased and in 2005, 433 ft of transverse and 552 ft of longitudinal NWP cracking were observed. No block cracking was observed at this section throughout the study, and the section had below average rut resistance compared to other test sections.

*Section 040509 (Intensive Preparation, 2-Inch RAP Overlay)*

Section 040509 performed moderately well against structural distresses but poorly against environmental distresses. Longitudinal WP and NWP cracking and transverse cracking quickly increased soon after the study started. Longitudinal WP cracking appeared in 1996 at 6 ft and increased steadily to its peak of 451 ft in 2002. In the following years, longitudinal WP cracking dropped as it turned into fatigue cracking. In 2008, investigators observed 3 ft of WP longitudinal WP cracking and 910 ft<sup>2</sup> of fatigue cracking. Outliers of this trend for longitudinal cracking include a spike in 1998 and a drop in 2003, both of which were attributed to rater variability. Transverse cracking was observed in 1994 at 55 ft and steadily increased to 613 ft<sup>2</sup> in 2008. Longitudinal NWP cracking appeared in 1997 at 116 ft<sup>2</sup> and steadily increased to 519 ft<sup>2</sup> in 2008. No block cracking was observed at this section. Section 040509 exhibited the second poorest resistance to rutting, and pumping was observed in 2005 and 2008.

*Section 040559 (Intensive Preparation, 3-Inch RAP Overlay [Inverted])*

Section 040559 performed well against structural distresses but poorly against environmental distresses. Longitudinal WP cracking appeared in 1998 at 14 ft and steadily increased to a peak of 38 ft in 2001. Longitudinal WP cracking remained constant at 36 ft in 2002 and then dropped to 6 ft in 2003 due to rater variability. Only 3 ft<sup>2</sup> of fatigue cracking appeared at this section (in 1998). Transverse cracking appeared in 1996 at 1 foot and steadily increased to 344 ft in 2003. Longitudinal NWP cracking spiked at 235 ft in 1999 and steadily increased to 506 ft in 2003. No block cracking was observed at this section, and the section exhibited similar environmental performance as Sections 040509 and 040508. The performance of this section cannot be compared to conventional noninverted sections because such a section was not constructed for this study.

*Section 040560 (Minimum Preparation, 2-Inch ARAC Overlay)*

Section 040560 performed moderately poor against both structural and environmental distresses. The ARAC design experienced low stability. A mix with a stability value of 1100 lb was used in construction, 300 lb less than the target range (Hossain et al. 1996). The spike in fatigue cracking in 1997 was attributed to rater variability. The observed fatigue cracking reached 1954 ft<sup>2</sup> in 2002, which was only surpassed by Sections 040502 and 040505. Transverse cracking was observed in 1996 and increased steadily over time from 3 ft to 176 ft in 2002. Longitudinal NWP cracking was observed in 1997 and increased rapidly to 403 ft in 2002. Pumping was observed in 1998 until the final survey in late 2002. When the project began in 1990, the initial cost of this section was similar to the 5-inch overlay sections.

**DISTRESS ANALYSIS KEY FINDINGS**

The distress data captured at the project provided valuable insight into pavement performance, design, management, and construction. Highlights from the SPS-5 distress analysis follow.

### **Best and Worst Performers**

Section 040507, the thick (5-inch) virgin AC overlay with intensive preparation, performed the best among all of the SPS-5 test sections. Compared to Section 040507, Sections 040504 and 040506 both performed as well in structural distresses but worse in environmental distresses.

Section 040502, the thin (2-inch) recycled AC overlay with minimal preparation, performed the worst among all of the SPS-5 test sections, excluding the control section. Section 040502 reached the peak of its pavement distress (fatigue and block cracking throughout the entire section) nine years after rehabilitation, after which the distresses remained relatively constant. Section 040505 also reached an equal amount of structural distress by the end of the study, 19 years after the rehabilitation.

### **Core Section Performance by Rehabilitation Feature**

Sections with intensive surface preparation (040506, 040507, 040508, and 040509) performed better in structural distresses than pavements with minimal surface preparation (040502, 040503, and 040505). Section 040504 was the exception to this trend as the section performed well despite receiving only minimal surface preparation. Section 040504 received a thick virgin AC overlay, which contributed to its superior structural performance.

Sections with thick overlays (040503, 040504, 040507, and 040508) performed better in structural distresses than pavements with thin overlays (040502, 040505, and 040509). Section 040506 was the exception to this trend as the section performed well despite receiving only a thin overlay. However, total combined thickness of all AC layers (existing and new) ranks Section 040506 as the third thickest of the eight core sections (despite being a thin overlay section). Also, the virgin asphalt and intensive preparation contributed to Section 040506's superior structural performance.

Sections with virgin AC overlays (Sections 040504, 040506, and 040507) performed better in both structural and environmental distresses than pavements with recycled AC overlays (Sections 040502, 040503, and 040509). Section 040505 was an exception to this trend as the section performed poorly in fatigue cracking despite using a virgin AC overlay. Section 040505 received minimal surface preparation and a thin overlay, which contributed to its relatively poor structural performance. Section 040508 was also an exception to the trend as the section performed well despite receiving a recycled AC overlay. Section 040508 also received intensive surface preparation and a thick AC overlay, which contributed to its superior structural performance.

Sections that received two of three rehabilitation methods (Sections 040504, 040506, and 040508) that improve performance (i.e., intensive preparation, virgin AC, and 5-inch overlay) performed better than sections that received only one of these three rehabilitation methods (Sections 040503, 040505, and 040509).

### **Core Section Performance by Distress Type**

Tables 59 and 60 show the comparisons made between sections with respect to relative performance against structural and environmental distresses, respectively.

**Table 59. Core Section Performance Against Structural Distresses**

	040502	040503	040504	040505	040506	040507	040508	040509
040502*	■	✗	✗	☒	✗	✗	✗	✗
040503*	✓	■	✗	✓	✗	✗	✗	☑
040504*	✓	✓	■	✓	☑	N/A	☑	✓
040505*	☑	✗	✗	■	✗	✗	✗	✗
040506*	✓	✓	☒	✓	■	N/A	☑	✓
040507*	✓	✓	N/A	✓	N/A	■	N/A	✓
040508*	✓	✓	☒	✓	☒	N/A	■	✓
040509*	✓	☒	✗	✓	✗	✗	✗	■

\*Did section perform better?

Yes, significantly – ✓

No, significantly – ✗

Yes, slightly – ☑

No, slightly – ☒

N/A – Section performed equally

**Table 60. Core Section Performance Against Environmental Distresses**

	040502	040503	040504	040505	040506	040507	040508	040509
040502*	■	✗	✗	✗	✗	✗	✗	✗
040503*	✓	■	✗	✗	✗	✗	☑	☒
040504*	✓	✓	■	☑	N/A	✗	✓	✓
040505*	✓	✓	☒	■	☒	✗	✓	✓
040506*	✓	✓	N/A	☑	■	✗	✓	✓
040507*	✓	✓	✓	✓	✓	■	✓	✓
040508*	✓	☒	✗	✗	✗	✗	■	☒
040509*	✓	☑	✗	✗	✗	✗	☑	■

\*Did section perform better?

Yes, significantly – ✓

No, significantly – ✗

Yes, slightly – ☑

No, slightly – ☒

N/A – Section performed equally

Comparisons were made between sections receiving only one of three rehabilitation methods (Sections 040503, 040505, and 040509) that improve performance (i.e., intensive preparation, virgin AC, and 5-inch overlay). Key findings follow:

- **Structural distresses:** Section 040503 (5-inch overlay) performed better than Section 040509 (intensive surface preparation). Both Sections 040503 and 040509 performed significantly better than Section 040505 (virgin AC overlay), suggesting that overlay thickness had a greater effect

on performance against structural distresses than surface preparation, which had a greater effect on performance against structural distresses than virgin AC. However, total thickness of the combined (new and existing) AC material layer may have contributed to this trend.

*5-inch overlay > intensive surface preparation > virgin AC*

- **Environmental distresses:** Section 040505 (virgin AC overlay) performed better than Section 040509 (intensive surface preparation). Both Sections 040505 and 040509 performed significantly better than Section 040503 (5-inch overlay), suggesting that the use of virgin AC had a greater effect on performance against environmental distresses than surface preparation, which had a greater effect on performance against environmental distresses than overlay thickness.

*virgin AC > intensive surface preparation > 5-inch overlay*

Comparisons were made between sections receiving two of the three rehabilitation methods (Sections 040504, 040506, and 040508) that improve performance (i.e., intensive preparation, virgin AC, and 5-inch overlay). Key findings follow:

- **Structural distresses:** Section 040504 (5-inch overlay and virgin AC overlay) performed better than Section 040508 (5-inch overlay and intensive surface preparation). Both Sections 040504 and 040508 performed better than Section 040506 (intensive surface preparation and virgin AC overlay). From this, it can be concluded that the use of thick overlay had a greater effect on performance against structural distresses than the use of virgin AC overlay, which had a greater effect on performance against structural distresses than surface preparation. However, total thickness of the combined (new and existing) AC material layer may have contributed to this trend.

*5-inch overlay > virgin AC > intensive surface preparation*

- **Environmental distresses:** Section 040504 (5-inch overlay and virgin AC overlay) performed better than Section 040506 (intensive surface preparation and virgin AC overlay). Both Sections 040504 and 040506 performed better than Section 040508 (5-inch overlay and intensive surface preparation). From this, it can be concluded that the use of virgin AC had a greater effect on performance against environmental distresses than overlay thickness, which had a greater effect on performance against environmental distresses than surface preparation.

*virgin AC > 5-inch overlay > intensive surface preparation*

The conclusions from these comparisons are that (1) sections with thick overlays will perform better against structural distresses than sections with thin overlays regardless of other design features and (2) sections with virgin AC overlays will perform better against environmental distresses than sections with recycled overlays regardless of other design features.

## **Evaluation of Supplemental Sections**

The inverted section (040559) performed well against structural distress (comparable to other sections with 5-inch overlays) and poorly against environmental distress (comparable to other sections using recycled AC overlays). Section 040559 is most comparable to Section 040508, which had a similar pavement structure, with varying AC layer thickness. While Section 040508 had more existing AC and recycled AC material and greater total combined AC layer thickness, Section 040559 had more new virgin AC material. Section 040559 performed slightly worse than Section 040508 against structural distress, but slightly better than Section 040508 in environmental distresses.

Section 040560, the ARAC overlay section, had poor to moderate performance in this study. This could be due to the problems encountered in the mix design, as ARAC has exhibited better performance in other SPS experiments, such as the Arizona SPS-6 project. Its performance against structural distresses was better than sections using thin overlay and minimal surface preparation (Sections 040502 and 040505) and worse than all the other core sections. Its performance against environmental distresses was better than sections using recycled AC overlay (Sections 040502, 040503, 040508, and 040509) and worse than sections using virgin AC overlays (Sections 040504, 040505, 040506, and 040507).

## **Additional Observations**

- Sections with thicker combined (new and existing) AC material layer experienced significantly higher resistance to fatigue cracking. Sections with at least 6 inches of AC material performed better than thinner sections in regard to fatigue cracking resistance.
- All sections exhibited less than 11 mm of rutting during the monitoring period. Rutting was not a critical distress and did not have a significant impact in the structural performance of all sections.
- With no replicate sections, there is limited ability to assess potential variability independent of actual performance.



## CHAPTER 4. SPS-5 ROUGHNESS ANALYSIS

This chapter provides the results of profile and roughness analyses for the LTPP SPS-5 site. The information presented characterizes the surface roughness of the test sections over time and links the observations to records of pavement distress and its development. Investigators collected road profile measurements from this site about once per year since the winter after the site was opened to traffic. This study analyzed the profiles in detail by calculating their roughness values, examining the spatial distribution of roughness within them, viewing them with post-processing filters, and examining their spectral properties. These analyses provided details about the initial roughness of the road and also provided a basis for quantifying and explaining the changes in roughness with time.

### PROFILE DATA SYNCHRONIZATION

Profile data were collected at the Arizona SPS-5 site on 14 dates, from February 5, 1990, through March 24, 2006 (Table 61). Raw profile data were available for visit 00 and visits 03 through 13. In each visit for which raw data were available, investigators made a minimum of seven repeat profile measurements. Since raw data were not available for visits 01 and 02, whenever possible, profiles for these visits were extracted from the public database. Visit 00 took place before the original rehabilitation and visit 01 took place just after the original rehabilitation. Investigators removed Section 040501 from the study after visit 03 because it was in extremely poor condition.

**Table 61. Profile Measurement Visits of the SPS-5 Site**

Visit	Date	Time	Repeats	Sections
00	Feb. 5, 1990	17:18	7	040501-040509, 040559-040560
01	Sept. 21, 1990	21:56	—	040501-040509
02	Jan. 15, 1992	17:50-18:49	—	040504, 040507
03	Feb. 22, 1993	13:54	9	040501-040509, 040559-040560
04	Feb. 3, 1997	09:34-10:44	9	040502-040509, 040559-040560
05	Dec. 9, 1997	14:04-14:55	7	040502-040509, 040559-040560
06	Dec. 11, 1998	12:54-13:35	7	040502-040509, 040559-040560
07	Nov. 11, 1999	11:30-12:06	7	040502-040509, 040559-040560
08	Dec. 1, 2000	10:53-11:46	9	040502-040509, 040559-040560
09	Nov. 15, 2001	10:49-11:38	9	040502-040509, 040559-040560
10	Nov. 4, 2002	12:02-13:10	9	040502-040509, 040559-040560
11	Feb. 6, 2004	15:24-16:35	9	040502-040509, 040559-040560
12	Dec. 14, 2004	12:49-14:00	9	040502-040509, 040559-040560
13	March 24, 2006	11:54-12:48	9	040502-040509, 040559-040560

## **DATA EXTRACTION**

Profiles of individual test sections were extracted directly from the raw measurements for two reasons: First, profiles were collected in visits 04 through 09 at a 0.98-inch sample interval and in visits 10 through 13 at a 0.77-inch sample interval. These data appeared in the database after the application of an 11.8-inch moving average and decimation to a sample interval of 5.91 inches. The raw data contained the more detailed profiles. Second, this study depended on consistency of the profile starting and ending points with the construction layout and consistency of the section limits with time. In particular, a previous quality check revealed that some profiles were shifted (Evans and Eltahan 2000).

Researchers used the raw data to synchronize all of the profiles to each other through their entire history. Three indicators were available for this purpose: (1) the site layout from the construction report, (2) event markers in the raw profiles from the start and end of each section, and (3) automated searching for the longitudinal offset between repeat measurements.

## **CROSS CORRELATION**

A helpful way to refine the synchronization of profile measurements is to search for the longitudinal offset between repeat profile measurements that provides the best agreement by inspecting filtered profile plots. However this approach is very time-consuming. Visual assessment is also somewhat subjective when two profiles do not agree well, which is often the case when measurements are made a year or more apart. In this study, investigators used an automated procedure rather than visual inspection to find the longitudinal offset between measurements.

The procedure, which is based on a customized version of cross correlation (Karamihas 2004), designates a basis measurement that is considered to have the correct longitudinal positioning. A candidate profile is then searched for the longitudinal offset that provides the highest cross correlation to the basis measurement. A high level of cross correlation requires a good match of profile shape, the location of isolated rough spots, and overall roughness level. Therefore, the correlation level is often only high when the two measurements are synchronized. When the optimal offset is found, a profile is extracted from the candidate measurement with the proper overall length and endpoint positions. For the remainder of this discussion, this procedure will be referred to as automated synchronization.

In this application, investigators performed cross correlation after the IRI filter was applied to the profiles rather than using the unfiltered profiles, which helped assign the proper weighting to relevant profile features. In particular, it increased the weighting of short-wavelength roughness that may be linked to pavement distress. This enhanced the effectiveness of the automated synchronization procedure. The long-wavelength content within the IRI output helped ensure that the longitudinal positioning was nearly correct, and the short-wavelength content was able to leverage profile features at isolated rough spots to fine-tune the positioning.

### **Synchronization of Visits 03 Through 13**

For visits 03 through 13, investigators extracted profiles of individual test sections from the raw measurements using the following steps:

1. Establish a basis measurement for each section from visit 09. This was done using the event markers from a raw measurement. The first repeat measurement was used for this purpose. Event markers appeared at the start of every section, and appeared at the end of every section except Section 040505. The event marker locations were compared to the layout provided in the construction report (Hossain et al. 1996). They exhibited a linear relationship with a bias of less than 0.05 percent. Once the bias was removed, no individual section starting point in the construction report differed from the event markers by more than 5 ft.

Most of the sections were assumed to begin at the appropriate event marker and continue for 500 ft except Section 040560, which continued from the event marker for 600 ft.

2. Automatically synchronize the other eight repeats from visit 09 to the basis set.
3. Automatically synchronize the measurements from the previous visit to the current basis set.
4. Replace the basis set with a new set of synchronized measurements from the first repeat of the current visit.
5. Repeat steps 3 and 4 until visit 03 is complete.

Visits 10 through 13 were synchronized using steps 3 through 5, but going forward in time. Since Section 040501 was out of the study after visit 03, its original basis measurement was extracted from the first repeat measurement of visit 00.

### **Synchronization of Visit 00**

Visit 00 could not be synchronized by comparison to later visits because it took place before major rehabilitation was performed on most of the test sections. A basis set of measurements from visit 00 was created using the first repeat measurement. The rest of the repeats were then automatically synchronized to it. Comparison of the profiles from Section 040501, which did not receive any rehabilitation, with later visits verified that visit 00 was in line with the others.

### **Synchronization of Visit 01 and 02**

Raw data were not available for visits 01 and 02. Thus, data were extracted from the public database and automatically synchronized to profiles from visit 03. For visit 01 this was fairly successful, and most of the measurements lined up with visit 03 within 6.6 ft. Unfortunately this was not the case for visit 02. In visit 02, the profiles within the public database were extracted as if the sample interval was 6 inches. However, detailed comparisons with the profiles from other visits showed that the sample interval was actually 5.91 inches. As a result, the further along the site a section appeared, the more serious the cumulative error in the location of the section starting point became. Thus, only the data from the first

two segments along the site, Sections 040504 and 040507, could be used. The sample interval of these profiles was corrected to 5.91 inches, and their starting points were shifted slightly to maintain consistency with other visits.

### LONGITUDINAL DISTANCE MEASUREMENT

The basis set of profile measurements for visit 09, established in step 1 above, was established using the event markers in one raw profile measurement (the first repeat). The other eight repeats from visit 09 were automatically synchronized to the basis set. When the longitudinal placement of the individual sections within each measurement was compared to the layout within the basis set, the slope of the linear fit ranged from 0.9994 to 1.0000. Thus, the longitudinal distance measurement for the nine profile measurements of visit 09 was consistent within 0.06 percent—a very high level of agreement in longitudinal distance measurement.

Figure 70 shows the disagreement in longitudinal distance measurement for each visit using the original basis set as a reference. In the figure, a range of disagreement for each visit exists because up to nine repeat profile measurements were made. The variation between repeat measurements within a visit appears as the width of each bar in the figure. Since the longitudinal distance measurement was based on the rotation of a drive wheel, the variations were most likely caused by variations in speed, lateral wander, and tire inflation pressure (Karamihas et al. 1999). If tire inflation pressure were the dominant cause, the disagreement would grow more positive with each successive repeat measurement as the tire heated up because the tire-rolling radius would increase, and the profiler would register less wheel rotation for the same travel distance. This occurred in visits 04 through 09, but the effect was rarely greater than 0.10 percent of the overall distance. Also, the field procedures require the operator to warm the tire before taking measurements. Visits with very consistent longitudinal distance measurement are attributed to proper tire warm-up.

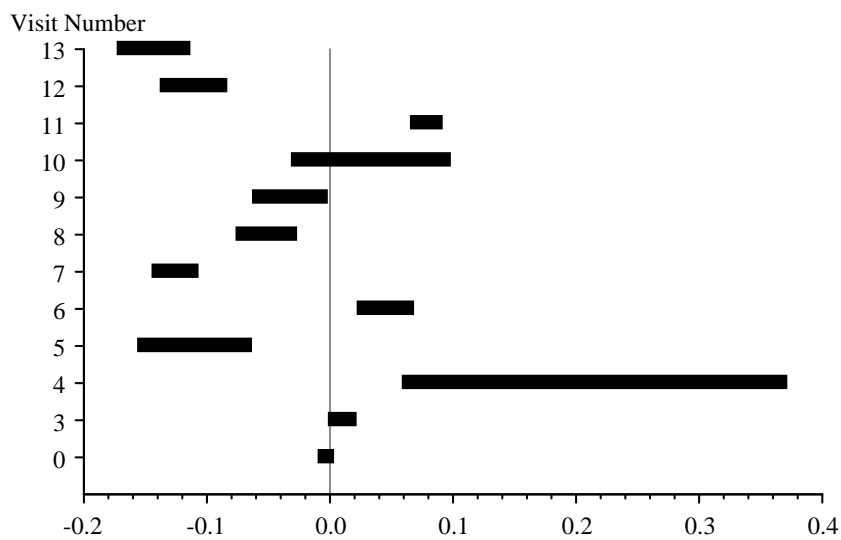


Figure 70. Consistency in Longitudinal Distance Measurement

The variation between visits in Figure 70 is caused by differences in distance measurement instrument calibration. The longitudinal distance measured by a profiler is not true horizontal distance. It always includes some additional component because the profiler must travel up and down the undulations in the road. This component can be minimized by calibrating the profiler to true horizontal distance. However, if a profiler operates on a road with grade changes and roughness that are not similar to the site used for longitudinal distance measurement calibration, some error will exist. Tire inflation pressure must also be close to the level that existed during calibration for consistent results.

Modest inconsistency in longitudinal distance measurement between visits is not critical as long as the profiles of individual sections are extracted using event markers rather than longitudinal distance from the start of each profile measurement. A high level of inconsistency, however, could interfere with comparisons between profile features and distress surveys. Errors in profile index values, such as the IRI, are also roughly of the same order as errors in longitudinal distance measurement (Karamihas et al. 1999). Figure 70 shows that longitudinal distance was measured with a very high level of agreement throughout visits 03 through 13. However in visit 04, all but one of the values for disagreement in longitudinal distance were between 0.06 and 0.13 percent. With that one value removed, Figure 70 would show an excellent level of consistency.

#### **DATA QUALITY SCREENING**

Investigators performed data quality screening to five select repeat profile measurements from each visit of each section. Among the group of available runs, investigators selected the five measurements that exhibited the best agreement with each other. In this case, agreement between any two profile measurements was judged by cross-correlating them after applying the IRI filter (Karamihas 2004). In this method, the IRI filter is applied to the profiles, and then the output signals are compared rather than the overall index. High correlation by this method requires that the overall roughness as well as the details of the profile shape that affect the IRI agree. The IRI filter was applied before correlation in this case for several reasons:

- Direct correlation of unfiltered profiles places a premium on very long wavelength content, but ignores much of the contribution of short wavelength content.
- Correlation of IRI filter output emphasizes profile features in (approximate) proportion to their effect on the overall roughness.
- Correlation of IRI filter output provides a good trade-off between emphasizing localized rough features at distressed areas in the pavement and placing too much weight on the very short-duration, narrow features (spikes) that are not likely to agree between measurements because the IRI filter amplifies short-wavelength content, but attenuates macrotexture, megatexture, and spikes.
- A relationship has been demonstrated between the cross-correlation level of IRI filter output and the expected agreement in overall IRI (Karamihas 2004).

Note: This method was performed with a special provision for correcting modest longitudinal distance measurement errors.

Each comparison between profiles produced a single value that summarized their level of agreement. When nine repeat profile measurements were available, they produced 36 correlation values. Any subgroup of five measurements could be summarized by averaging the relevant 10 correlation values. The subgroup that produced the highest average was selected, and the other repeats were excluded from most of the analyses discussed in the rest of this chapter. Since the number of available profiles ranged from six to nine, the number of measurements that were excluded ranged from one to four. Tables 62 through 72 list the selected repeats for each visit of each section and the composite correlation level produced by them.

The process for selecting five repeat measurements from a larger group is similar to the practice within LTPP except that it is based on composite agreement in profile rather than the overall index value. The correlation levels listed in Tables 62 through 72 provide an appraisal of the agreement between profile measurements for each visit of each section. When two profiles produce a correlation level above 0.82, their IRI values are expected to agree within 10 percent most (95 percent) of the time. Above this threshold, the agreement between profiles is usually acceptable for studying the influence of distresses on profile. When two profiles produce a correlation level above 0.92, they are expected to agree within 5 percent most of the time. Above this threshold, the agreement between profiles is good. Correlation above 0.92 often depends on consistent lateral tracking of the profiler and may be very difficult to achieve on highly distressed surfaces. The IRI values provided will be the average of five observations, which will tighten the tolerance even further.

**Table 62. Selected Repeats of Section 040501**

Visit	Repeat Numbers					Composite Correlation
00	1	3	4	5	6	0.649
01	1	4	6	7	8	0.608
03	2	3	4	5	6	0.751

**Table 63. Selected Repeats of Section 040502**

Visit	Repeat Numbers					Composite Correlation
00	1	3	4	5	6	0.837
01	1	2	3	4	5	0.955
03	2	4	5	6	9	0.977
04	2	3	4	6	7	0.971
05	1	2	3	4	7	0.939
06	1	4	5	6	7	0.950
07	1	2	4	5	6	0.921
08	3	4	6	8	9	0.972
09	1	4	5	7	8	0.967
10	1	4	6	7	8	0.822
11	1	2	3	6	7	0.936
12	2	3	4	5	7	0.912
13	3	4	5	7	9	0.948

**Table 64. Selected Repeats of Section 040503**

Visit	Repeat Numbers					Composite Correlation
00	1	3	4	5	7	0.717
01	1	2	3	4	5	0.945
03	2	4	5	6	7	0.963
04	2	5	6	7	8	0.963
05	2	4	5	6	7	0.937
06	1	2	3	4	5	0.952
07	1	4	5	6	7	0.966
08	2	3	5	8	9	0.982
09	1	2	3	7	9	0.966
10	1	3	5	7	9	0.901
11	2	3	5	6	7	0.918
12	1	3	4	6	9	0.937
13	1	2	3	4	5	0.938

**Table 65. Selected Repeats of Section 040504**

Visit	Repeat Numbers					Composite Correlation
00	1	4	5	6	7	0.803
01	1	2	3	4	5	0.928
02	3	4	5	6	7	0.934
03	2	4	7	8	9	0.958
04	2	3	5	7	9	0.968
05	1	2	3	4	5	0.963
06	2	3	4	6	7	0.972
07	1	2	3	4	5	0.983
08	1	4	7	8	9	0.987
09	1	3	4	6	8	0.985
10	1	2	3	4	6	0.963
11	1	2	3	4	5	0.957
12	1	3	4	5	6	0.968
13	1	4	5	6	8	0.976

**Table 66. Selected Repeats of Section 040505**

Visit	Repeat Numbers					Composite Correlation
00	1	2	3	4	5	0.928
01	1	2	3	4	5	0.945
03	1	2	3	7	8	0.963
04	1	2	5	6	8	0.958
05	1	3	5	6	7	0.912
06	3	4	5	6	7	0.939
07	1	3	4	6	7	0.923
08	1	2	3	4	5	0.922
09	1	2	4	5	6	0.947
10	2	3	4	5	9	0.835
11	2	3	4	6	7	0.887
12	2	3	4	5	8	0.827
13	1	3	5	8	9	0.877

**Table 67. Selected Repeats of Section 040506**

Visit	Repeat Numbers					Composite Correlation
00	1	3	4	5	6	0.833
01	1	2	3	4	5	0.913
03	2	3	4	5	6	0.965
04	2	3	5	7	8	0.969
05	1	2	3	4	5	0.935
06	1	3	4	5	6	0.967
07	1	2	3	5	7	0.969
08	1	4	5	6	9	0.980
09	1	5	7	8	9	0.970
10	1	2	3	6	8	0.955
11	3	6	7	8	9	0.966
12	2	3	6	7	8	0.962
13	1	2	3	5	8	0.977

**Table 68. Selected Repeats of Section 040507**

<b>Visit</b>	<b>Repeat Numbers</b>					<b>Composite Correlation</b>
00	1	2	5	6	7	0.810
01	1	2	3	4	5	0.890
02	3	4	5	6	7	0.908
03	2	3	4	5	8	0.941
04	1	2	4	7	8	0.965
05	1	3	4	6	7	0.936
06	1	3	4	5	7	0.961
07	1	2	3	4	6	0.958
08	1	4	6	8	9	0.982
09	1	2	4	6	9	0.976
10	2	4	6	7	8	0.956
11	1	4	5	7	9	0.945
12	2	3	4	5	7	0.960
13	1	3	4	5	9	0.959

**Table 69. Selected Repeats of Section 040508**

<b>Visit</b>	<b>Repeat Numbers</b>					<b>Composite Correlation</b>
00	1	3	5	6	7	0.803
01	1	2	3	4	5	0.958
03	2	5	7	8	9	0.963
04	2	3	6	7	9	0.962
05	2	3	4	6	7	0.931
06	1	3	4	5	6	0.967
07	1	2	3	4	5	0.972
08	1	2	4	5	8	0.980
09	3	6	7	8	9	0.978
10	1	3	5	6	9	0.941
11	1	2	3	4	8	0.948
12	4	6	7	8	9	0.941
13	3	5	6	8	9	0.964

**Table 70. Selected Repeats of Section 040509**

Visit	Repeat Numbers					Composite Correlation
00	1	3	4	5	6	0.848
01	1	2	3	4	5	0.943
03	2	3	4	5	6	0.967
04	2	4	5	6	9	0.976
05	2	3	5	6	7	0.924
06	3	4	5	6	7	0.967
07	1	3	5	6	7	0.971
08	2	4	5	7	8	0.962
09	1	2	3	5	7	0.958
10	1	2	6	7	8	0.838
11	1	2	3	6	7	0.886
12	1	3	4	7	9	0.822
13	3	4	5	7	9	0.929

**Table 71. Selected Repeats of Section 040559**

Visit	Repeat Numbers					Composite Correlation
00	1	2	4	5	6	0.866
03	1	2	4	7	8	0.966
04	2	4	5	7	8	0.964
05	2	3	4	5	6	0.963
06	1	3	4	5	6	0.970
07	1	2	3	4	5	0.978
08	1	3	4	7	8	0.984
09	1	3	6	7	8	0.976
10	1	2	4	5	8	0.967
11	3	4	7	8	9	0.973
12	2	3	4	5	7	0.961
13	2	3	5	6	9	0.973

**Table 72. Selected Repeats of Section 040560**

Visit	Repeat Numbers					Composite Correlation
00	1	2	5	6	7	0.789
03	1	2	5	6	9	0.946
04	1	2	4	5	9	0.914
05	1	2	4	5	6	0.873
06	1	2	4	5	6	0.882
07	1	2	3	4	5	0.883
08	2	4	6	8	9	0.880
09	2	4	7	8	9	0.919
10	1	2	5	7	9	0.731
11	2	3	4	7	9	0.832
12	1	3	4	5	6	0.815
13	2	5	6	7	8	0.874

Overall, the majority of the groups of measurements listed in Tables 62 through 72 exhibited good to excellent correlation, particularly in visits 03 through 09 and 11. Agreement was lowest overall for visit 00 and all visits of Section 040501. Any group of repeat measurements that produced a composite correlation level below 0.85 was investigated using filtered plots; these results are discussed below.

In visit 00, the profile measurements showed a lack of agreement in the shape and severity of localized distresses on many of the sections. Overall, the content within the profiles from wavelengths shorter than about 10 ft was not repeatable. This was often most serious for the right side profile. A lack of repeatability for short-wavelength content is not uncommon on pavements with significant distress. The same overall behavior was evident for visits 00, 01, and 03 of Section 040501. The correlation exhibited for these three cases was so poor that very little credence should be placed on the analysis results for Section 040501.

In visit 10, the left and right side profiles of Section 040502 included dips, often more than 0.2 inch deep, throughout the entire section. In many cases, the dips did not appear consistently in all five repeat measurements. In particular, the profiles of the last third of the section were dominated by dips that appeared in more than one repeat, but not in all five, which suggests that the profiles were affected by some type of surface distress that was not consistent across the lane width. The profile inconsistencies may have been the result of small changes in lateral tracking position of the profiler.

In visit 10, profiles of Section 040505 and Section 040509 included extraneous narrow dips and spikes that degraded their agreement. Additionally, the shape and severity of genuine narrow dips along Section 040509 were not totally consistent between repeat measurements. In visit 12 of Section 040505, narrow dips appeared with inconsistent depth and location. Profiles from visit 12 of Section 040509 included a patch of uncorrelated short-wavelength content 370 to 440 ft from the start of the section on the right and 225 to 240 ft and 310 to 380 ft from the start on the left.

In visits 10 and 11, profiles of Section 040560 included patches of uncorrelated short-wavelength content, which is typically caused by pavement distress that causes aggressive transverse variations in surface profile. Visit 12 also included dense patches of narrow dips that were not well correlated between repeat runs on the right side.

### SUMMARY ROUGHNESS VALUES

Figures 71 through 81 show the left and right IRI values for each pavement section over their monitoring period. For most of the sections, this includes 26 summary IRI values: two per visit over 13 visits (Table 61). The figures show the IRI values versus time in years. In this case, “years” refers to the number of years between the measurement date and the date that the site was opened to traffic (June 13, 1990). Fractions of a year are estimated to the nearest day.

To supplement the plots, Appendix C lists the IRI, Half-car Roughness Index (HRI), and Ride Number (RN) of each section for each visit. These roughness values are the average of the five repeat measurements selected in the data quality screening. These are not necessarily the same five repeat measurements selected within the LTPP study. Appendix C also provides the standard deviation of IRI over the five repeat measurements to help identify erratic roughness values that are the result of transverse variations in profile caused by surface distresses.

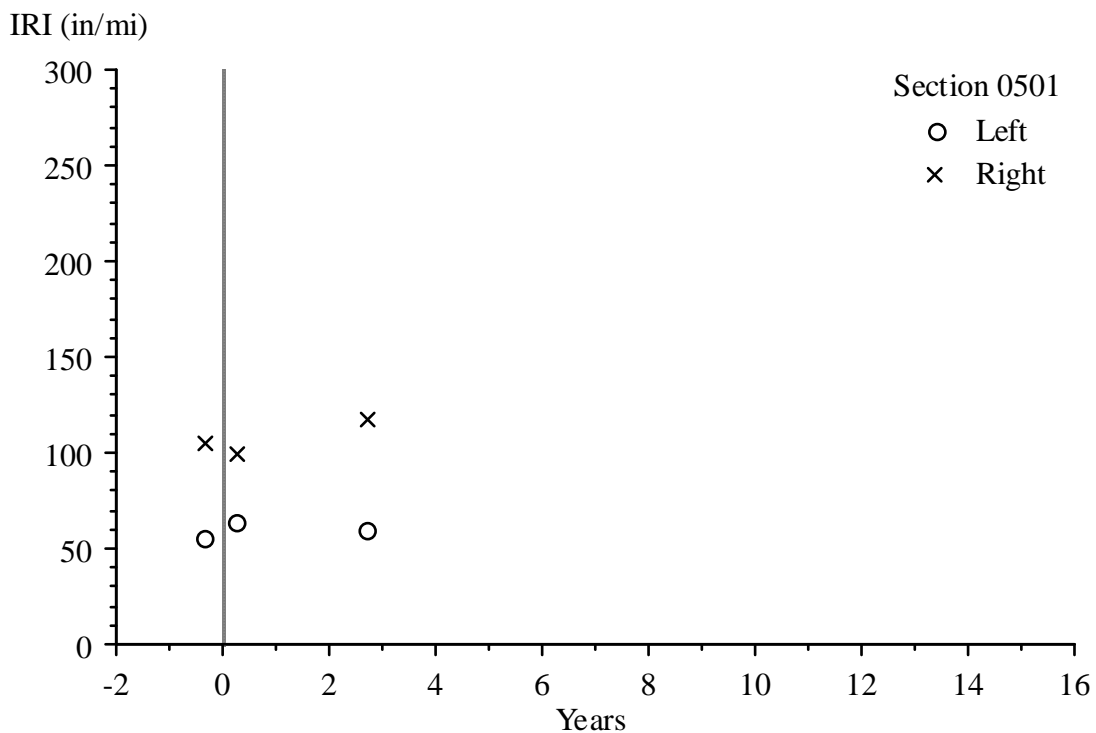


Figure 71. IRI Progression of Section 040501

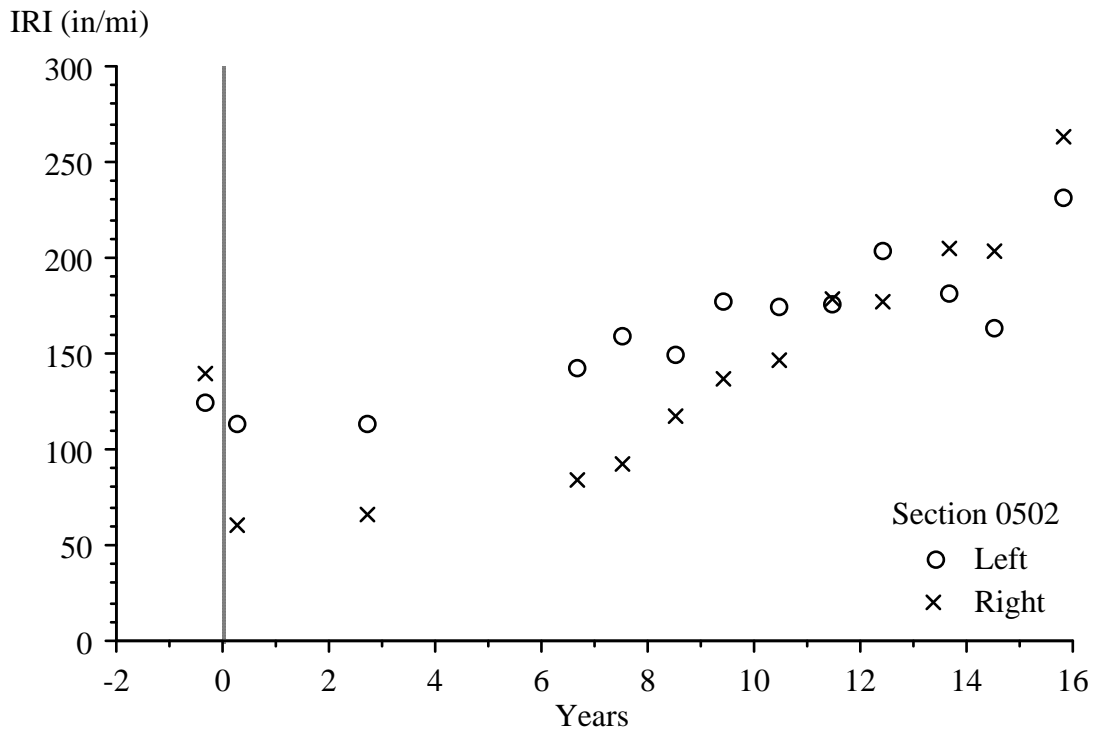


Figure 72. IRI Progression of Section 040502

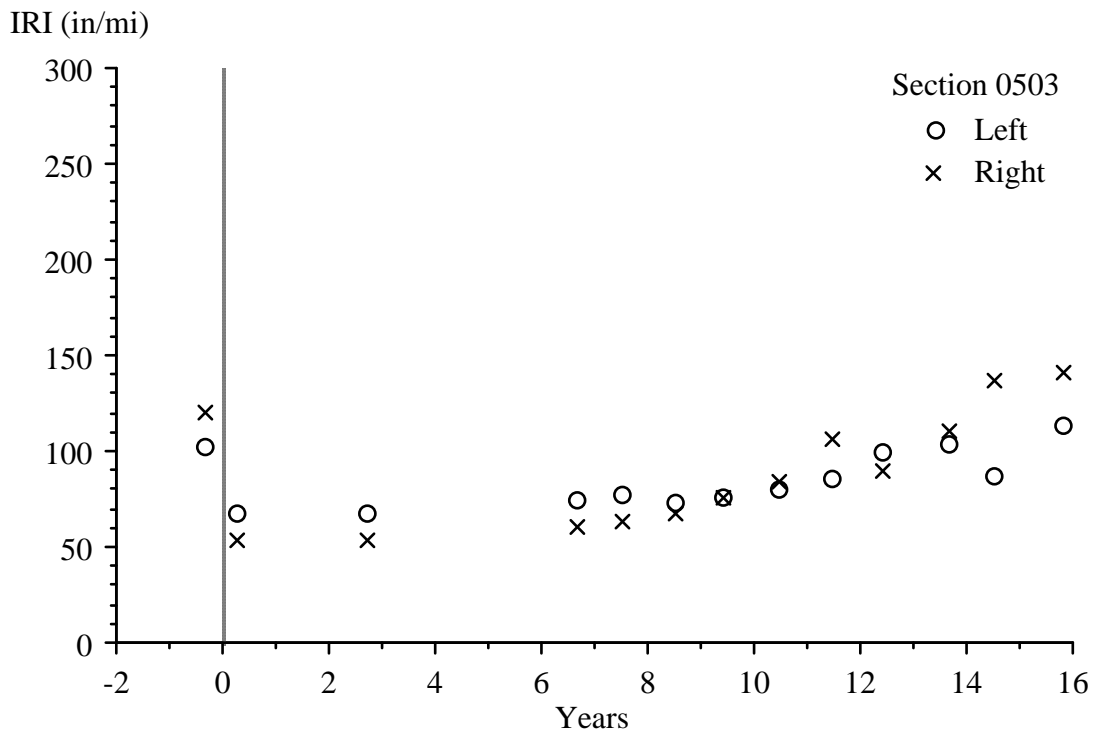


Figure 73. IRI Progression of Section 040503

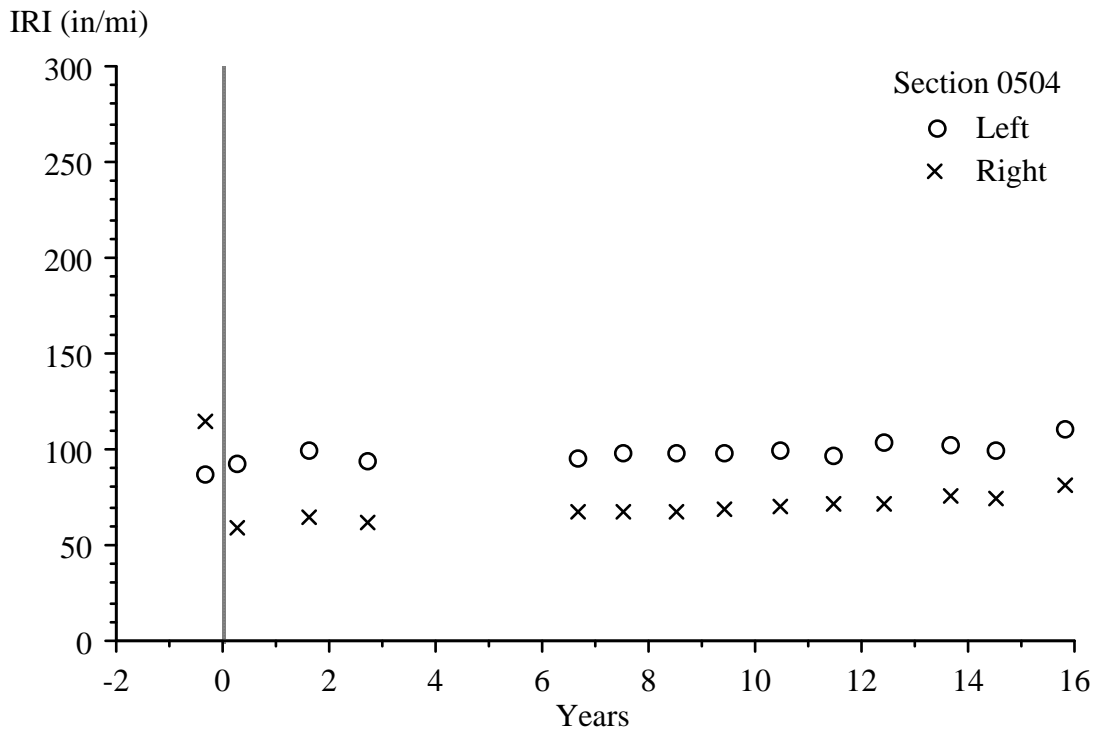


Figure 74. IRI Progression of Section 040504

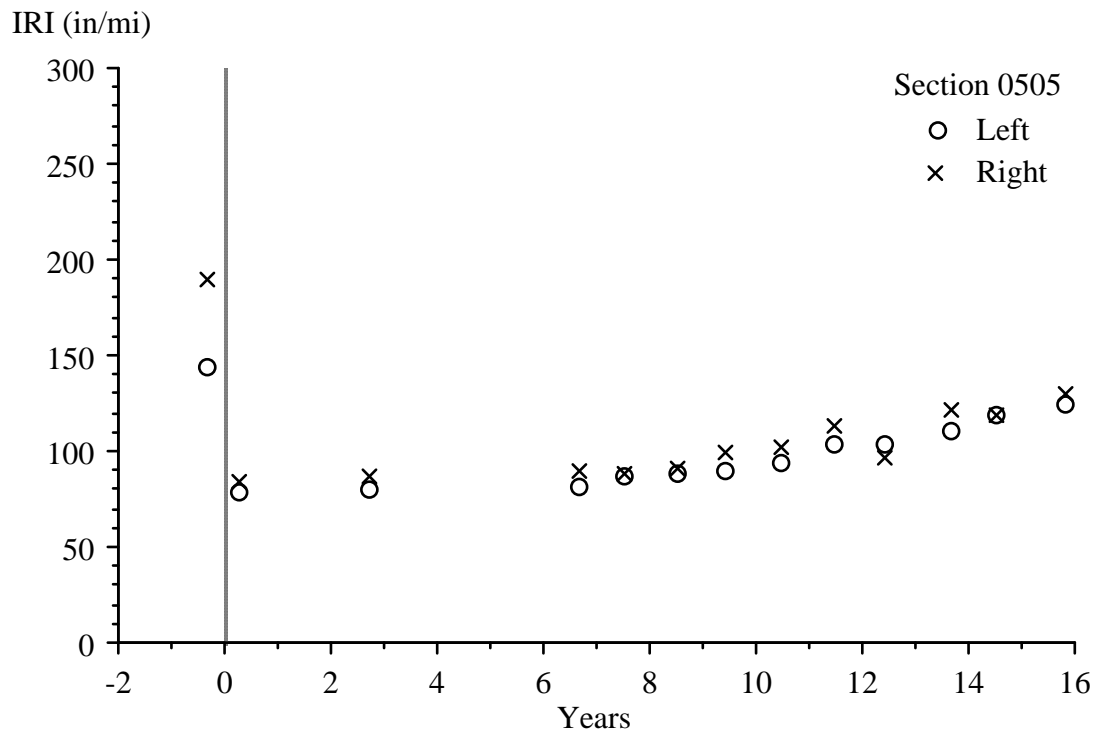


Figure 75. IRI Progression of Section 040505

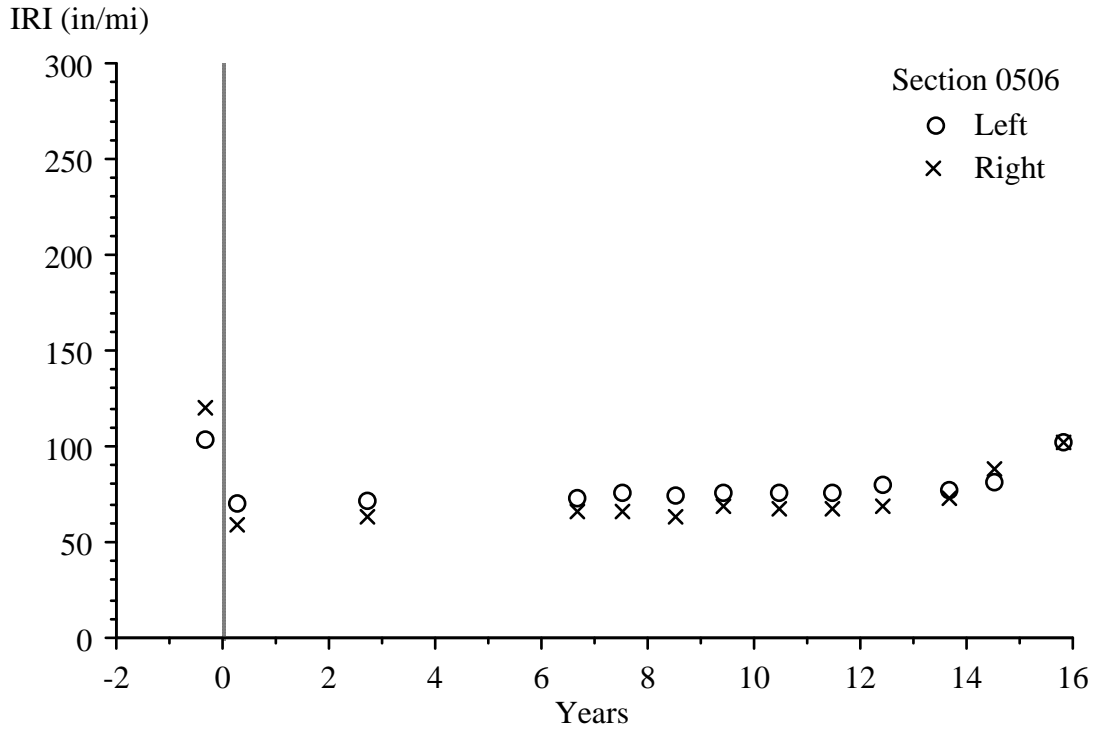


Figure 76. IRI Progression of Section 040506

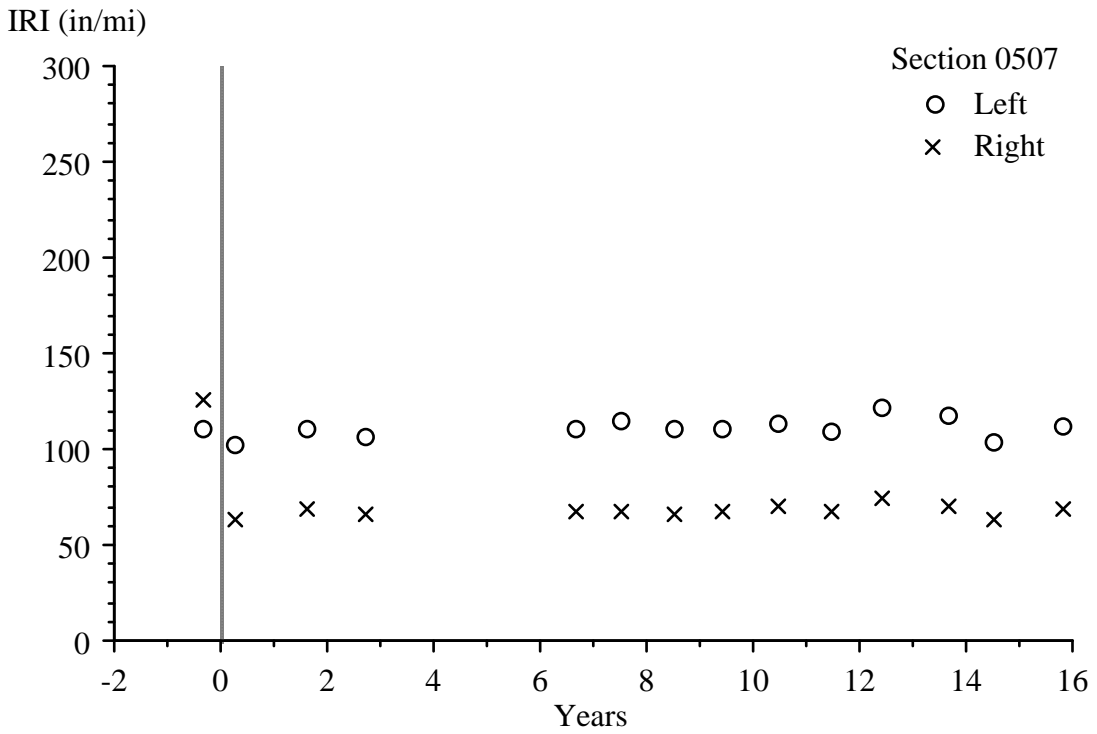


Figure 77. IRI Progression of Section 040507

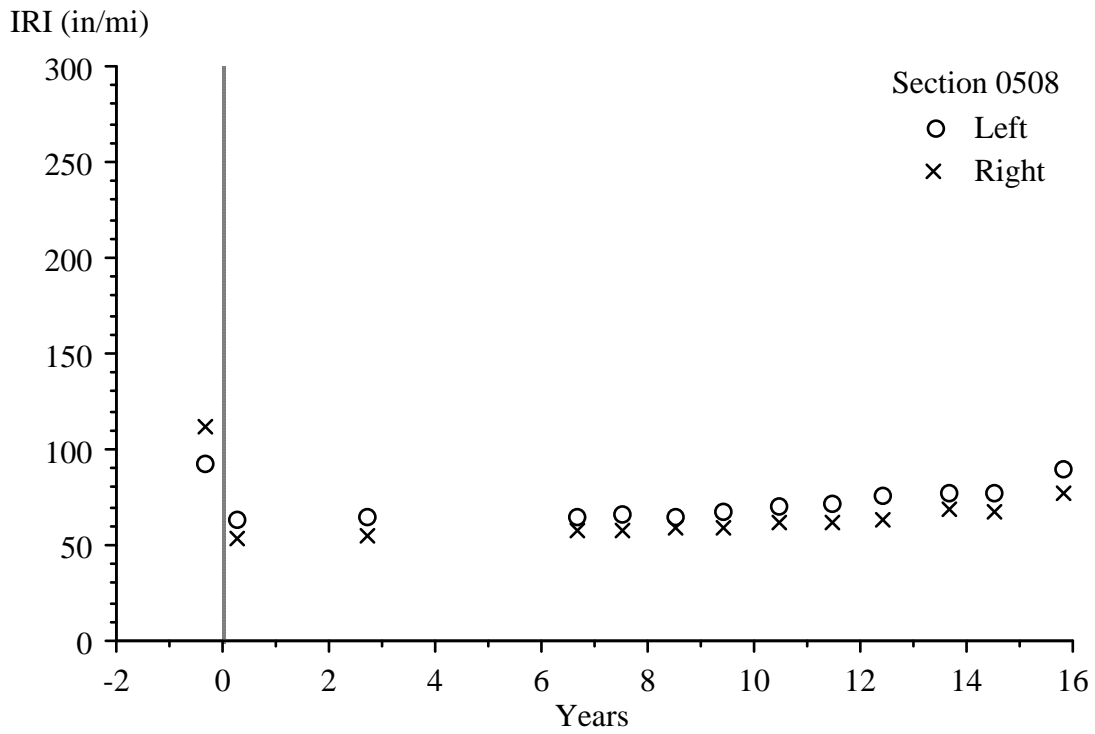


Figure 78. IRI Progression of Section 040508

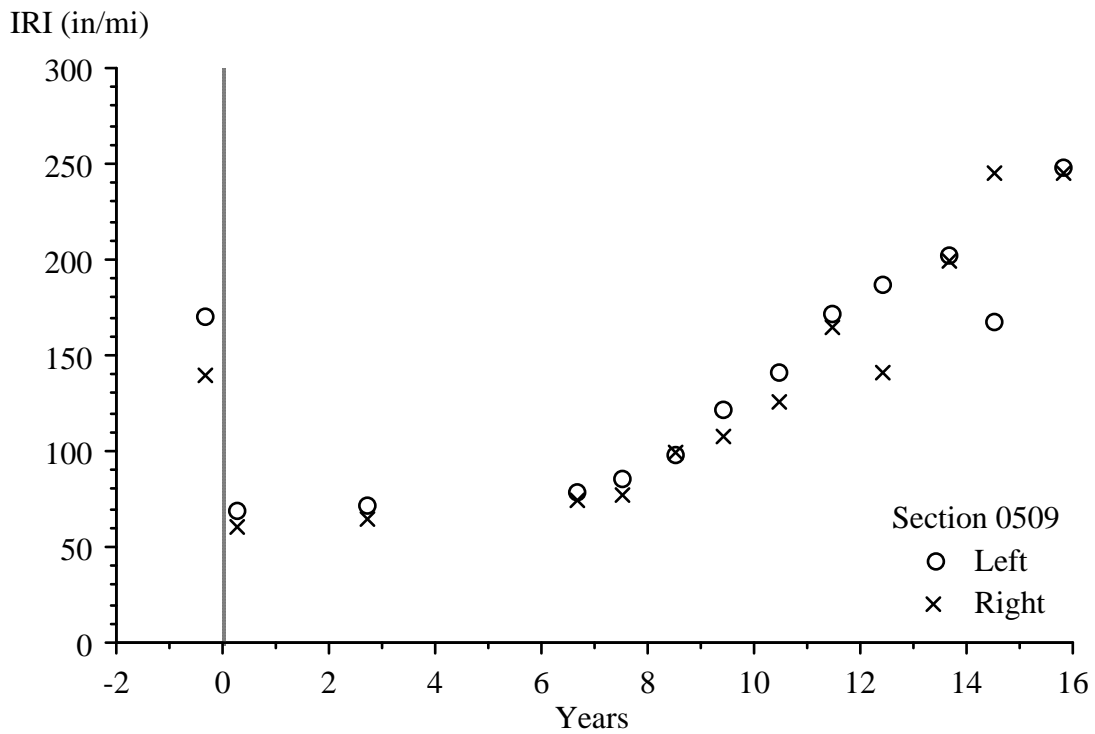


Figure 79. IRI Progression of Section 040509

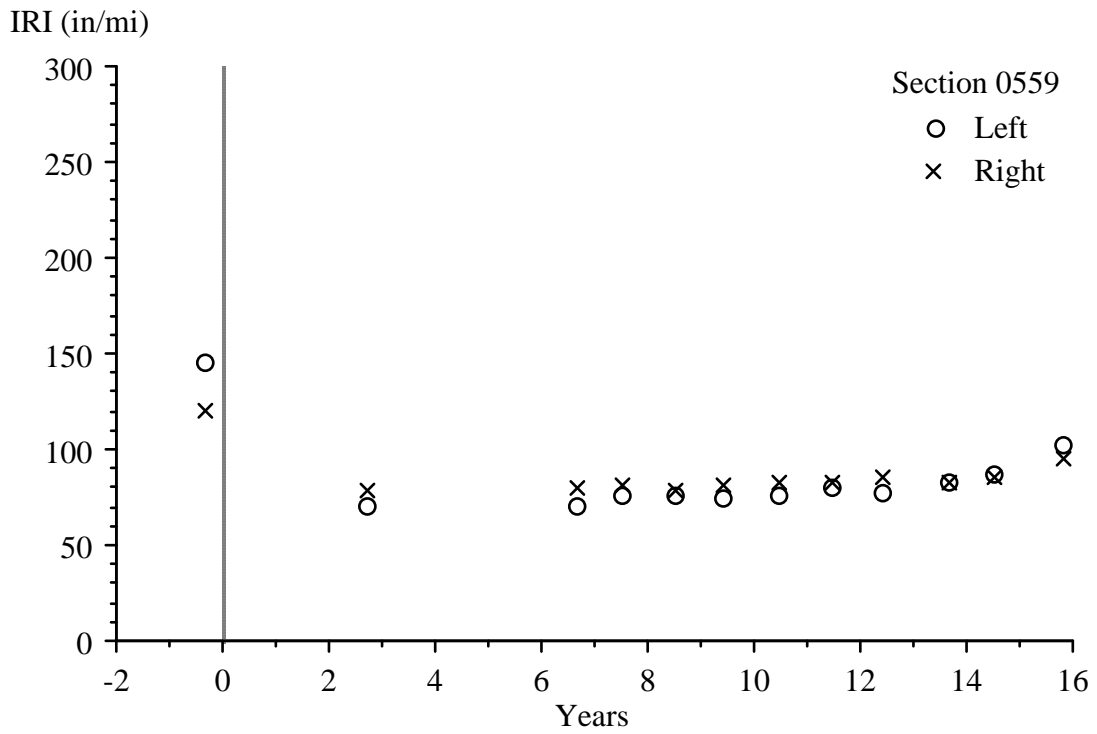


Figure 80. IRI Progression of Section 040559

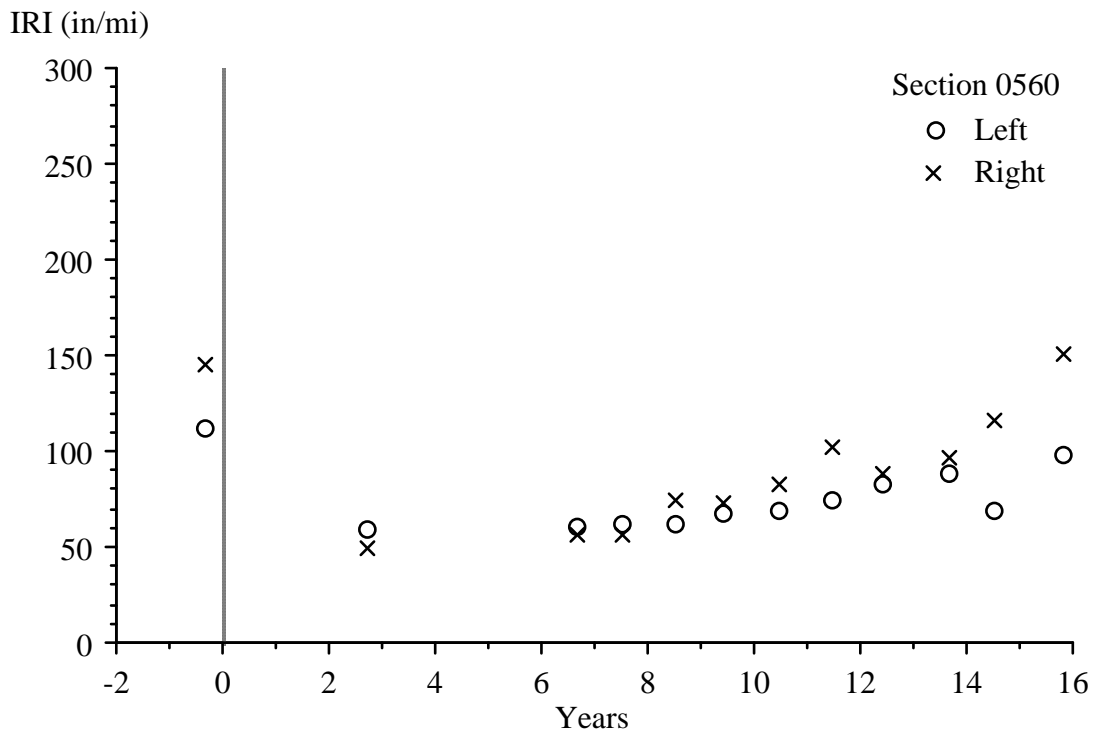


Figure 81. IRI Progression of Section 040560

These figures provide a snapshot of the roughness history of each pavement section. The remainder of this chapter characterizes the profile content that made up the roughness and explains the profile features that contributed to roughness progression.

## **PROFILE ANALYSIS TOOLS**

Investigators used various analytical techniques to study the profile characteristics of each pavement section and their change with time. These tools help study roughness, roughness distribution, and roughness progression of each section, including concentrated roughness that may be linked to pavement distress. The discussion of each analysis and plotting method is rather brief. Some examples are provided; Sayers and Karamihas (1996) provide more details about all of these methods.

### **Summary Roughness Values**

Left IRI, right IRI, Mean Roughness Index (MRI), HRI, and RN values were calculated. Appendix C provides the average value of each index for each visit of each section. The discussion of roughness in this analysis emphasizes the left and right IRI. Nevertheless, comparing the progression of HRI and RN to that of the MRI provides additional information about the type of roughness that is changing. For example, a low HRI value relative to MRI indicates roughness that exists on only one side of the lane. Further, aggressive degradation of RN without a commensurate growth in MRI signifies that the developing roughness is biased toward short-wavelength content.

### **Power Spectral Density Plots**

A power spectral density (PSD) plot of an elevation profile shows the distribution of its content within each waveband. An elevation profile PSD is displayed as mean square elevation versus wave number, which is the inverse of wavelength. A PSD plot is generated by performing a Fourier transform on a profile. The value of the PSD in each waveband is derived from the Fourier coefficients and represents the contribution to the overall mean square of the profile in that band.

Often, the wavebands used in a PSD plot are given a uniform spacing on a log scale. In this research, PSDs were typically displayed using 12 bands per octave. In other words, the center of each waveband was a factor of  $2^{1/12}$  larger than the waveband to its left on the plot and a factor of  $2^{1/12}$  smaller than the waveband to its right. This spacing provided enough detail to search for roughness that was isolated at a given wavelength, but enough averaging to eliminate spurious content that is common when PSDs are displayed using a linear wave-number scale. PSD plots were also calculated from the slope profile rather than the elevation profile, which helped to interpret the plots because the content of a slope PSD typically covers fewer orders of magnitude than an elevation PSD.

The PSD plots provided a very useful breakdown of the profile content. In particular, the plots revealed (1) cases in which significant roughness is concentrated within a given waveband; (2) the type of content that dominates the profile (e.g., long, medium, or short wavelength); (3) the effectiveness of rehabilitation in eliminating roughness over each waveband; (4) the type of roughness that increases with time; and (5) the type of roughness that is stable with time.

Figure 82 shows the PSD of Section 040502's left profile from visit 04 and visit 11. This PSD plot includes several noteworthy features:

- The plot shows the PSD of slope rather than elevation. Thus, the vertical axis has units of  $\text{slope}^2/(\text{cycles}/\text{ft})$  instead of  $\text{elevation}^2/(\text{cycles}/\text{ft})$ .
- The plot covers wave numbers from 0.01 cycle/ft to 1 cycle/ft, the range that affects IRI most.
- The spectral content from about 12 to 100 ft (wave numbers between 0.01 cycle/ft and 0.08 cycle/ft) did not change significantly with time.
- The spectral content for wavelengths shorter than 12 ft increased between visits. In fact, this progression was fairly steady from visit 04 through visit 11.
- In visit 11, the PSD grew with decreasing wavelength (increasing wave number) for wavelengths below 8 ft. This should be interpreted cautiously, however, because a single anomalous reading in the elevation profile or a single severe narrow dip would appear on a PSD plot this way. Alternatively, it may indicate uniform growth in short wavelength roughness over the entire length of the profile.
- The peak at about 0.092 cycle/ft indicates a tremendous amount of roughness with a wavelength of about 10.9 ft. The vertical axis is on a log scale, so the peak at this wavelength is actually more significant than it looks. In fact, the roughness concentrated at wavelengths near 10.9 ft is responsible for more than half of the IRI of the visit 04 profile. This content was present in the first visit after rehabilitation, which indicates that the roughness was built in rather than a result of deterioration. An inspection of right profile PSD plots shows that this periodic content is much more dominant on the left side than the right.

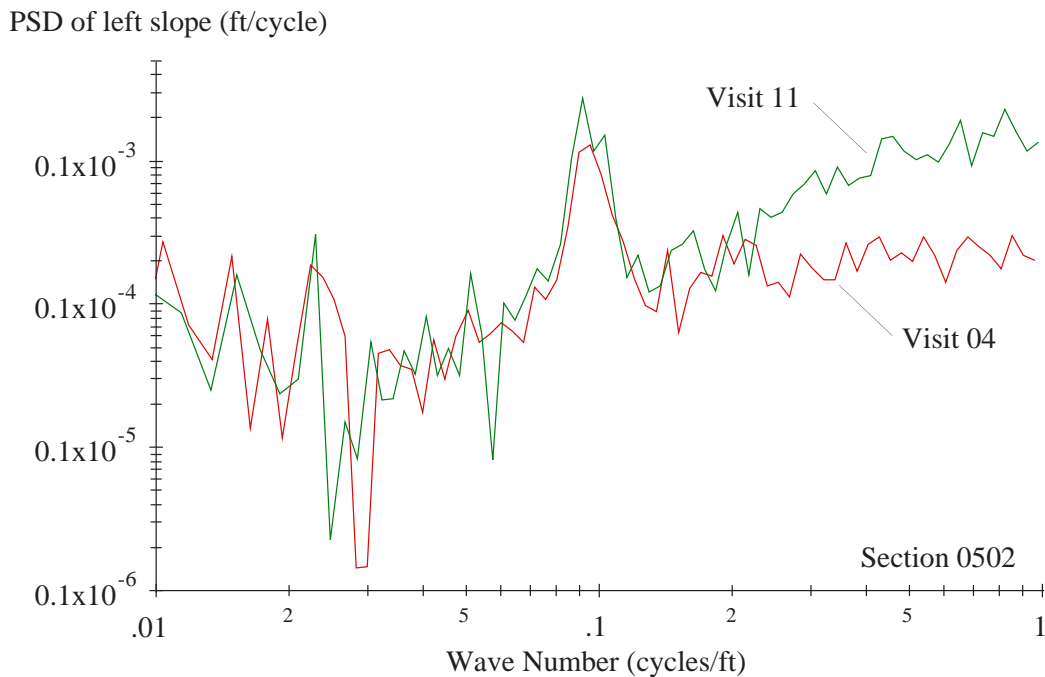


**Figure 82. PSD of Section 040502 Profiles (Left Side)**

Each of the final four observations listed above provide important information about the nature of Section 040502's roughness and its progression. However, the PSD provides no information about where the roughness exists within the section. Further, if the roughness within a profile is concentrated in a single location, the PSD plot may provide misleading information. The filtered profile plots and the roughness profiles discussed below provide a more complete assessment of the roughness on a given pavement.

The PSD plot provides insight into the filtering practices of the profiler that made the measurements. Figure 83 shows the PSD of Section 040508's left profile during visit 09 and visit 10 over the maximum range allowed by the section length and sample interval. This plot includes several noteworthy features:

- The spectral content differs for very long wavelengths (low wave numbers). This is not caused by a change in the true profile of the section. Rather, it is the result of a change in profiler and an associated change in the high-pass filtering methods (Perera and Kohn 2005).
- The spectral content shows a decreasing trend at very short wavelengths (high wave numbers). This is an artifact of the low-pass filtering applied at the time of the measurement, which is a combination of digital filtering and height sensor footprint (Karamihas 2005).
- The PSD plot for visit 09 includes a spike at a wave number of about 2.6 cycles/ft and at double that value. This is also an artifact of the measurement process, but the source is unclear. The spikes were present in all of the profiler measurements, which include all of the measurements made in visit 04 through visit 09. However, the spikes did not occur at the same wave number in each visit or in each repeat measurement within a given visit. The wave number where the left-most spike occurred ranged from about 2.04 cycles/ft to 2.72 cycles/ft.

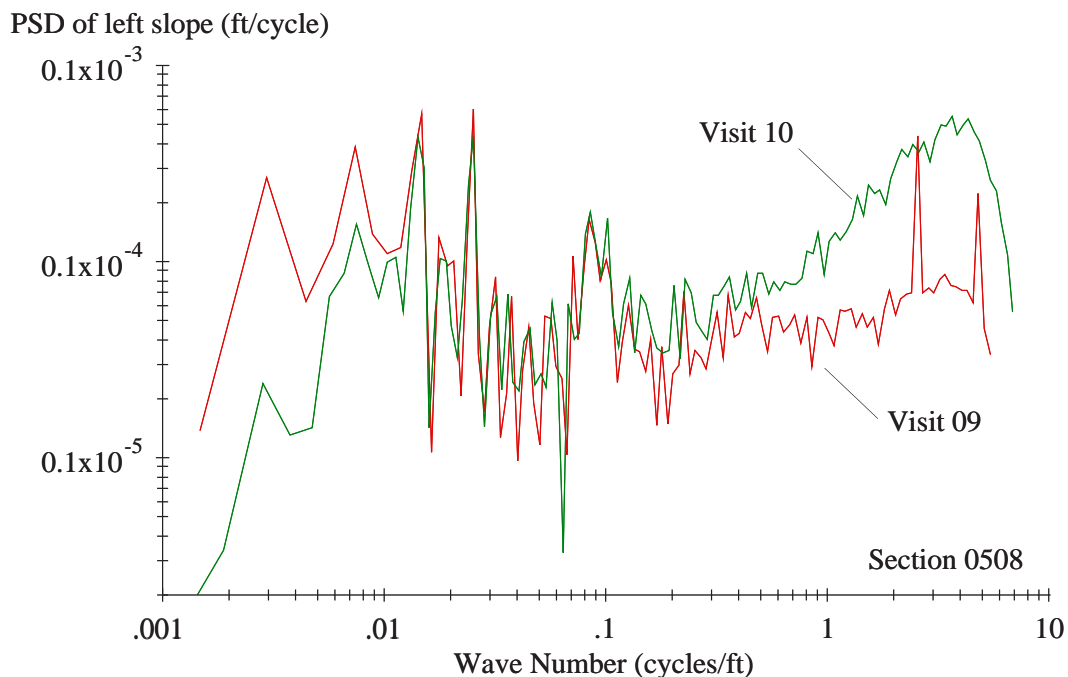


**Figure 83. PSD of Section 040508 Profiles (Left Side)**

## Filtered Profile Plots

A simple way to learn about the type of roughness that exists within a profile is to view the trace. However, certain key details of the profile are often not as obvious in a raw profile trace as they may be after the profile is filtered. For example, Figure 84 shows the raw profile trace for three visits to Section 040509 throughout its monitoring history. The plot shows that the long-wavelength content, or the trend, in each plot is quite consistent with time. On the other hand, narrow dips appear in the plots that become more prevalent and severe as time progresses.

Although the raw profile plots in Figure 84 provide very useful information about the nature of the roughness on Section 040509, a filtered plot may provide much more detail. In particular, a closer look at the narrow dips may help study their progression. Figure 85 shows a small segment of the profile after it has been high-pass filtered. An anti-smoothing moving average filter was applied with a base length of 25 ft. The anti-smoothing is performed by applying a smoothing filter and then subtracting it from the original profile. Without the filter, the overall trend in the profile masks the dip, such that it is barely visible in the trace from visit 04. When the profile is filtered, the dip and its growth with time are much more obvious.

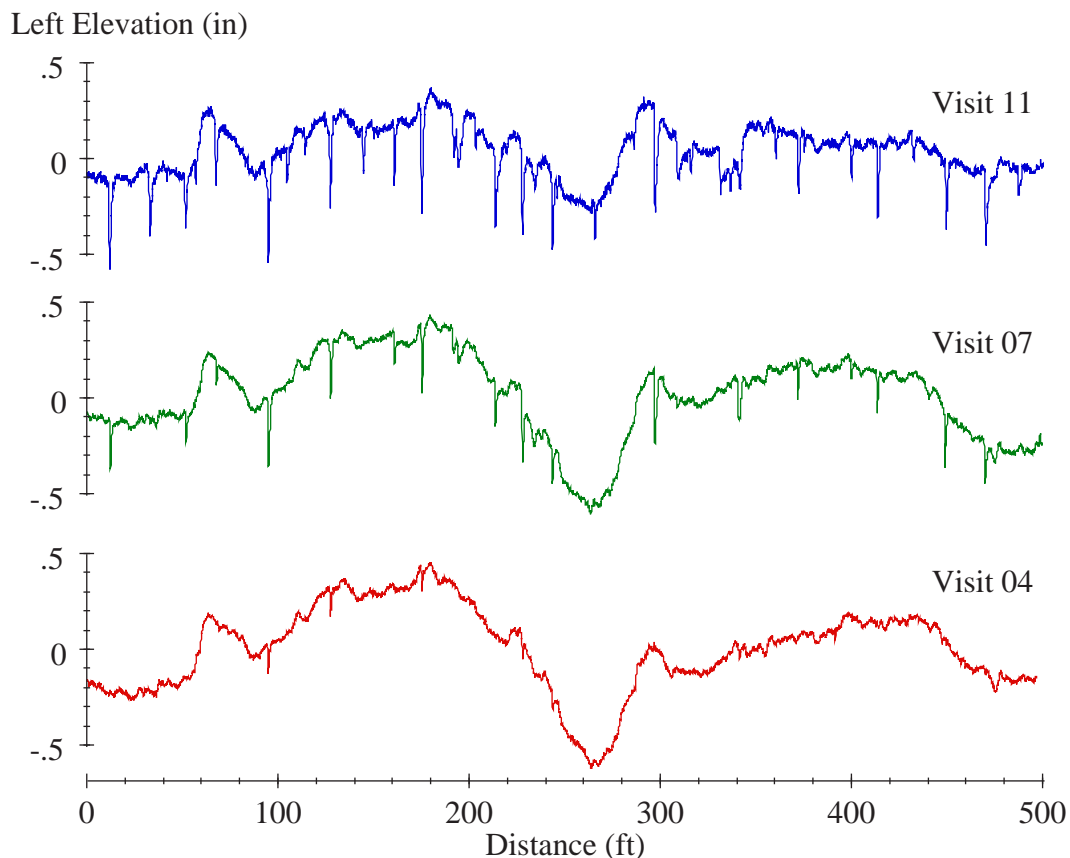


**Figure 84. Raw Profiles of Section 040509**

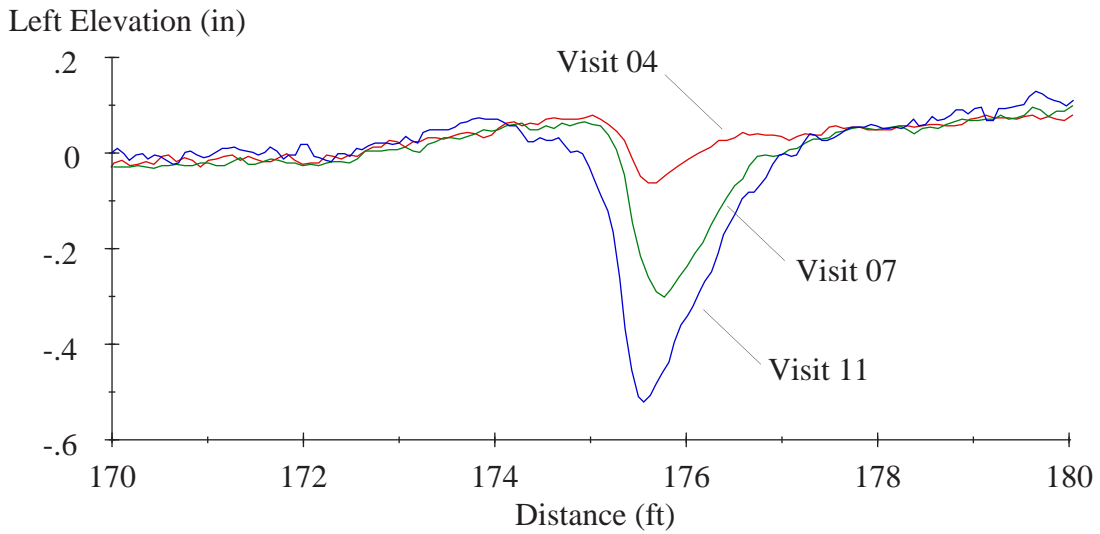


**Figure 85. Filtered Profiles of Section 040509**

In addition to a closer view of short-duration features, filtered plots help provide a clearer view of longer trends in profile. Figure 86 provides one such example. The figure shows two profile measurements of Section 040560 after they have been smoothed with a base length of 25 ft and anti-smoothed with a base length of 125 ft. One trace was collected before rehabilitation, and the other was collected several years later. On this section, the longer wavelength features displayed in the plot were not altered very much by the rehabilitation. This was not the case on every test section. On the other hand, the content within the profile in the wavelength range shorter than 25 ft was altered completely.

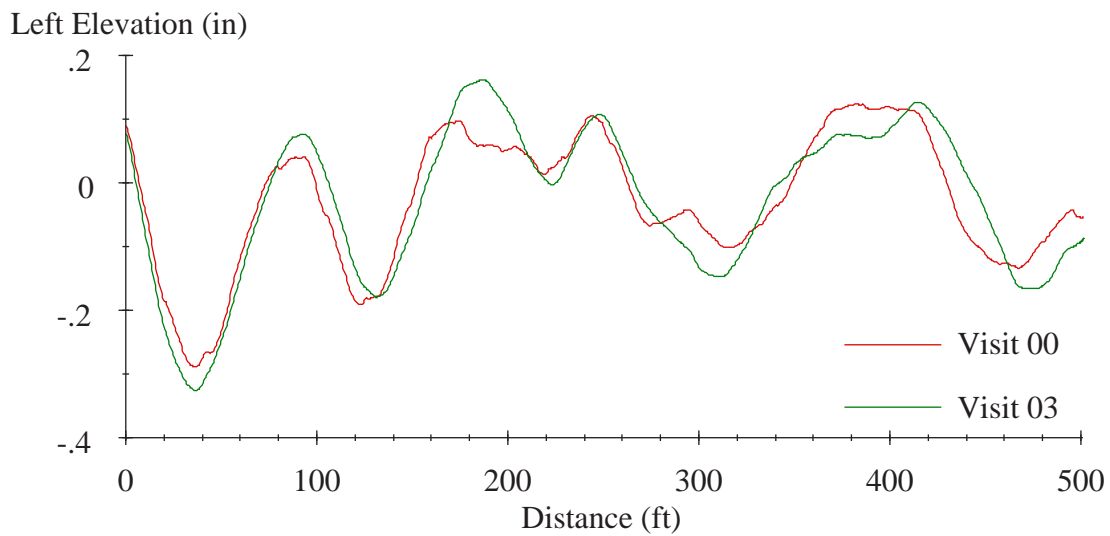


**Figure 86. Long-Wavelength Profiles of Section 040560**

Three types of filtered plots were inspected for every visit of every section:

- **Long wavelength:** A profile smoothed with a base length of 25 ft and anti-smoothed with a base length of 125 ft.
- **Medium wavelength:** A profile smoothed with a base length of 5 ft and anti-smoothed with a base length of 25 ft.
- **Short wavelength:** A profile smoothed with a base length of 1 ft and anti-smoothed with a base length of 5 ft.

These filters were used to screen the profiles for changes with time and special features of interest. The terms “long,” “medium,” and “short” are relative, and in this case pertain to the relevant portions of the waveband that affects the IRI. The long wavelength portion of the profile was typically very stable with time. However, the long wavelength profile plots of every section changed somewhat between visit 09 and visit 10—not by a change in the surface characteristics of the section, but by a change in profiler make and the associated change in filtering practices.

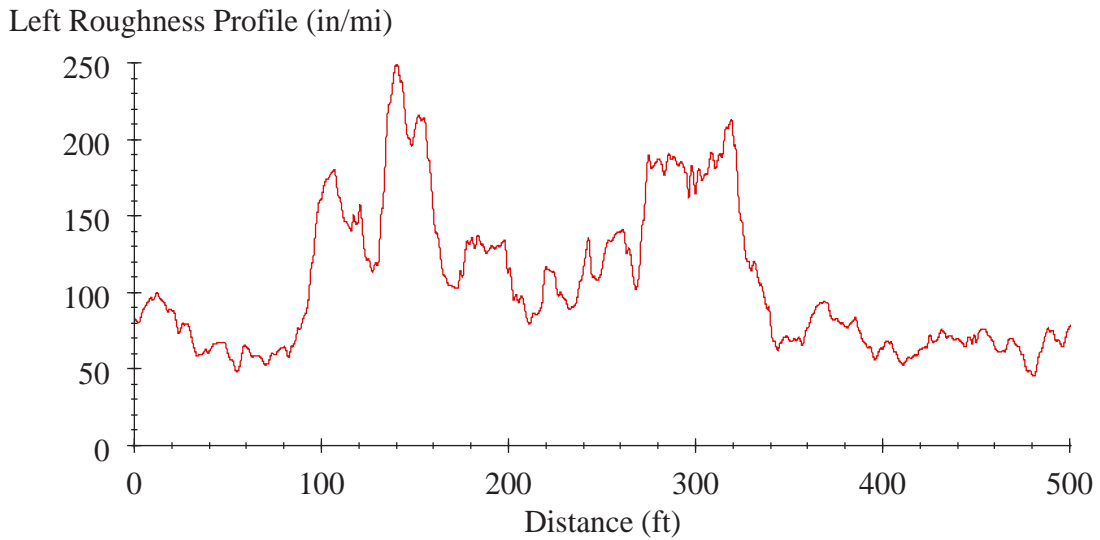
The medium-wavelength plots provided a view of the features in a profile that were likely to have a strong effect on the IRI and may change with time. The short-wavelength elevation plots also typically progressed with time, but only affected the IRI through localized roughness or major changes in content. However, the short-wavelength elevation plots helped identify and track the progression of narrow dips and other short-duration features that may have been linked to distress.

### **Roughness Profiles**

A roughness profile provides a continuous report of road roughness using a short segment length. Instead of summarizing the roughness by providing the IRI for an entire pavement section, the roughness profile shows the details of how IRI varies with distance along the section by using a sliding window to display the IRI of every possible segment of given base length along the pavement (Sayers 1990).

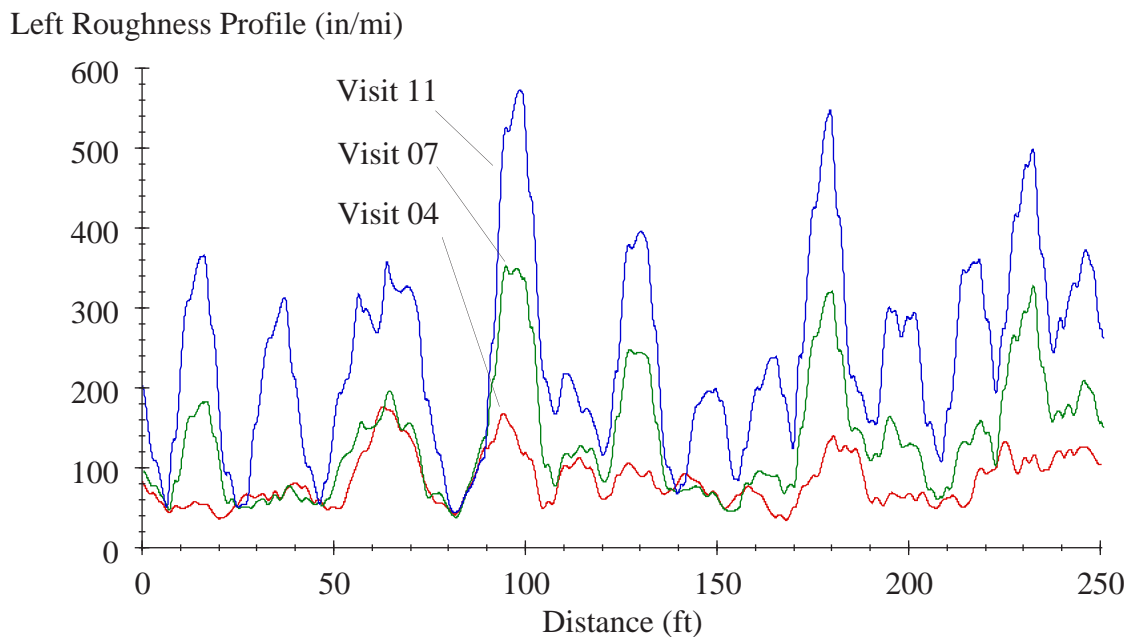
A roughness profile displays the spatial distribution of roughness within a profile. As such, it can be used to distinguish road sections with uniform roughness from sections with roughness levels that change over their length. Further, the roughness profile can pinpoint locations with concentrated roughness and estimate the contribution of a given road disturbance to the overall IRI.

Figure 87 shows an example of a roughness profile for visit 11 of Section 040503. The roughness profile was generated using a base length of 25 ft, that is, every point in the plot shows the IRI of a 25-ft segment of road, starting 12.5 ft upstream and ending 12.5 ft downstream. The plot shows that the first 100 ft and the last 150 ft of the section are very smooth. On the other hand, the area from 100 to 350 ft from the start of the section is substantially rougher.



**Figure 87. Roughness Profile of Section 040503 (25-ft Base Length)**

Figure 88 shows how a roughness profile can help find localized roughness and quantify its impact on the overall roughness of a section. The figure shows the roughness profile of Section 040509 using a 10-ft base length for visits 04, 07, and 11. With a 10-ft base length, isolated roughness is easy to identify. For example, the dips that appear at 175.5 ft increase in roughness significantly with time. In visit 11, the peak value of the roughness profile in the vicinity of the dip is 546 inches/mi. Since that value represents the roughness over just 1/50 of the segment, it suggests that the single dip contributes more than 10 inches/mi to the overall IRI of the section.



**Figure 88. Roughness Profiles of Section 040509 (10-ft Base Length)**

## **DISTRESS SURVEYS AND MAINTENANCE RECORDS**

Once the analysis and plotting were completed, all of the observations were compared to the MDS performed on each section. MDS results were available for each section starting in 1994 and covering a visit nearly every year for the rest of the monitoring history. This provided a means of relating profile features to known distresses. For the SPS-5 project, two observations were common: First, dips that grew progressively rough with time were often found in the vicinity of transverse cracks. This was the case for the dip shown in Figure 85 and the locations of peak roughness in Figure 88. Often, the first appearance of peaks within a very short interval roughness profile corresponded to the year when transverse cracks were first observed in the distress survey. The presence of the dips could typically be verified using short-wavelength elevation plots. Second, areas where cracks appeared with a very high density within a WP sometimes caused areas of isolated roughness to appear within a profile as well as areas in which the short-wavelength content within the same area was not well correlated between repeat runs.

Investigators also compared changes in profile properties to maintenance records. Crack sealing was performed on all of the sections except 040501 and 040507 in May 2002. The entire test site received a fog seal coat on May 28, 1998, and April 16, 2003. Sections 040502, 040505, 040506, 040509, 040559, and 040560 also received a fog seal on August 23, 2001.

## **DETAILED OBSERVATIONS**

Appendix D reports key observations from the roughness index progression, PSD plots, filtered profile plots, roughness profiles, and distress surveys. In many cases, similar behavior was noted for multiple sections. Those observations are repeated under every section heading where it is appropriate. However, Appendix D does not discuss changes in profile properties with time caused by changes in the profiler make.

## **PROFILE ANALYSIS KEY FINDINGS**

This section summarizes the important profile properties and the roughness progression of each section within the SPS-5 site. Several observations within this analysis were common to more than one pavement section, as described below. This section of the analysis, in conjunction with the roughness progression plots (Figures 71 through 81), provides the essential information about each pavement section.

Before rehabilitation, all 11 sections included narrow dips, typically 0.5 to 0.40 inch deep and up to 2 ft wide. The dips were usually more severe on the left side than on the right. Rehabilitation completely removed the dips within every section except for Section 040501, which was not rehabilitated.

In many of the sections, some aspects of the long wavelength roughness survived rehabilitation. Sections 040505, 040559, and 040560 had profiles after rehabilitation with very long wavelength content that was very similar to the content before rehabilitation. Sections 040502, 040503, and 040509 exhibited some similarities between the long-wavelength content before and after rehabilitation. After

rehabilitation, the content within the profiles with wavelengths greater than 30 ft rarely changed over the entire monitoring history of the site.

The change in profiler make in late 2002 affected the long-wavelength content of the profiles on every test section because the newer profiler used a high-pass filter that eliminated a little more of the profile content than the previous two devices. This had no probable effect on the measurement of localized roughness or the study of narrow bumps and dips caused by cracking and other distress. However, it did confound the study of changes in the long-wavelength content within the profiles between visits 09 and 10.

One other minor device effect within the profiles was peaks in the PSD plots with no pavement-related explanation. In visits 04 through 09 (measured by the K.J. Law T-6600) most PSD plots from the left side included a strong peak at a wavelength somewhere between 0.37 and 0.49 ft and another at a wavelength of double the first.

Sections 040502 and 040509 exhibited the most dramatic increase in IRI over their post-rehabilitation monitoring history. They both grew in roughness at an increasing rate and were both very rough by the end of the monitoring period. Both sections included transverse cracks that became more severe with time. Concentrated roughness appeared at many of the cracks within a few years of their detection by MDS measurements. The roughness appeared as narrow dips that grew in severity with time. Note that the dips were much wider than a typical crack, often 1 to 2 ft wide. Thus, some genuine depressions in the pavement were constantly developing around the cracks. Some of the dips grew to as much as 0.75 inches deep.

Sections 040503, 040505, and 040560 also exhibited a large change in roughness with time. They grew in roughness at an increasing rate, and their MRI changed by 67 inches/mi, 45 inches/mi, and 70 inches/mi, respectively, throughout their post-rehabilitation monitoring history. Section 040505 developed roughness because dips of increasing severity appeared near transverse cracks. Section 040505 developed roughness that was very similar to Sections 040502 and 040509. It had fewer rough transverse cracks, but included roughness at densely cracked areas within the WPs.

Sections 040503 and 040560 also included dips at transverse cracks. However, large, densely cracked areas, not necessarily in the transverse direction, caused a significant portion of the roughness development within the WPs. The hit-or-miss nature of their placement relative to the profiler path caused inconsistencies in the shape of rough features between repeat measurements and visits. Nevertheless, the cracks caused a consistent growth in roughness in the affected areas.

Sections 040504, 040506, 040508, and 040559 increased in roughness at a steady rate after rehabilitation until 2004. The MRI of these sections increased by no more than 15 inches/mi during their post-rehabilitation monitoring history through February 2004. These sections, particularly Section 040508, included dips near transverse cracks in earlier visits. However, the dips were usually not very severe until the final two profiling visits in late 2004 and 2006. In Sections 040506, 040508, and 040559, the roughness increased more rapidly in the last two years than during the previous 14 years because of

narrow dips near recorded transverse cracks. Section 040507 showed little roughness linked to transverse cracking.

Sections 040502, 040504, and 040507 showed little, if any, improvement in IRI on the left side after rehabilitation. In addition, the roughness of the left side after rehabilitation was much higher than the right side, and was caused by a continuous (sinusoidal) series of bumps and dips with peaks 8 to 13 ft apart and a peak-to-trough difference in elevation of up to 0.2 inch. These conditions, present on the right side and a dominant part of the left side, may have been caused by problems with the rolling process, but that could not be verified.

In May 2002 crack sealing was performed on all of the sections except Sections 040501 and 040507. Very little evidence was found that suggested this directly affected the roughness. Of course, crack sealing very well could have decelerated the deterioration of these sections. The entire test site received a fog seal coat on May 28, 1998, and April 16, 2003. Seven of the test sections (excluding Sections 040507, 040504, 040503, and 040508, the first four sections along the length of the site) at the site also received a fog seal on August 23, 2001. Fog sealing did not cause an immediate change on the IRI.

Sections 040501, 040502, and 040560 had HRI values that were 20 percent or more below the MRI values. In Section 040502, the HRI grew increasingly small with time compared to the MRI. This difference was larger than that observed on most other sections and was caused by the presence of profile features that are not consistent across the lane. Typically, this also signifies the presence of localized distress.

Table 73 summarizes the roughness behavior of each section within the SPS-5 site.

**Table 73. Summary of Roughness Behavior**

Section	040502	040503	040504	040505	040506	040507	040508	040509	040559	040560
MRI change after rehabilitation (inch/mi)	-44	-51	-24	-85	-48	-26	-44	-91	-59	-75
MRI change since rehabilitation (inch/mi)	160	67	21	45	38	11	25	183	24	70
MRI change over 7 years after rehabilitation (inch/mi)	26	7	7	6	7	9	3	18	4	5
MRI growth at an increasing rate	✓	✓		☑	☑		☑	✓		✓
MRI growth at a steady rate			✓			✓			✓	
HRI about 20% below MRI	✓			✓						✓
Left IRI much higher than right IRI			✓			✓				
Dominant periodic content, 8-13 ft	✓		✓			✓				
Very long features preserved after rehabilitation	☑	☑		✓				☑	✓	✓
Severe dips near transverse cracks	✓	✓		✓	✓		✓	✓		
Patches or roughness near dense cracking		✓		✓						✓

✓ — Yes

☑ — Somewhat

In light of the rehabilitation performed on each section, the information from Table 73 suggests the following:

- The two test sections with a 2-inch recycled overlay (Sections 040502 and 040509) exhibited the largest post-rehabilitation increase in MRI over the monitoring history by a wide margin (160 inches/mi and 183 inches/mi, respectively).
- The two test sections with a 5-inch virgin overlay (Sections 040507 and 040504) exhibited the smallest post-rehabilitation increase in MRI over the monitoring history (11 inches/mi and 21 inches/mi, respectively).
- All of the test sections except those with a 2-inch recycled overlay (Sections 040502 and 040509) increased in MRI by less than 10 inches/mi over the first seven years after rehabilitation.
- Roughness increased the most in test sections with narrow dips at transverse cracks.



## CHAPTER 5. CONCLUSIONS AND RECOMMENDATIONS

ADOT initiated this project to study the relative performance of the various SPS-5 design alternatives (including supplemental sections), which can inform future rehabilitation design decisions. Deflection, surface distress, and profile data were used as the basis for performance evaluation and were analyzed as part of the study.

The SPS-5 project offers a unique opportunity to directly compare the performance of various rehabilitated pavement structures while reducing the confounding effect of other variables such as traffic-loading, climate, and subgrade conditions. However, the findings drawn from this evaluation must be considered carefully. The experimental design did not offer replicate treatments to verify findings. The conclusions are based on one set of in situ conditions; observations from other climate or loading scenarios may differ from those noted within this report. Therefore, findings reported may be unique to the conditions and construction of this site.

Despite these issues, the data captured at the project provides valuable insight into pavement design and performance. Following is a summary of lessons learned from the performance data collected at the SPS-5 site.

### DEFLECTION ANALYSIS

- All sections in the SPS-5 project had extremely stiff pavements.
- Dynamic effects from poor damping resulted in errors in the elastic layer modeling of pavements. AASHTO 1993 analysis provided much less variable and more reasonable results.
- Calculated  $SN_{eff}$  for Section 040507 and Section 040504 were larger than expected even though dynamic effects were expected to cause a slight underprediction of  $M_r$ .
- Preconstruction  $SN_{eff}$  varied significantly among the sections, which made the analyses that compared the performance of rehabilitation methods questionable.
  - 17 months after rehabilitation:
    - Sections with virgin AC overlays had a 31 percent greater increase in  $SN_{eff}$  than sections with recycled AC overlays.
    - Sections with thick (5-inch) overlays had a 24 percent greater increase in  $SN_{eff}$  than sections with thin (2-inch) AC overlays.
    - Sections with intensive surface preparation had a 17 percent greater increase in  $SN_{eff}$  than sections with minimal surface preparation AC overlays.
  - 163 months after rehabilitation:
    - Sections with thick overlays had a 77 percent greater increase in  $SN_{eff}$  than sections with thin overlays.
    - Sections with virgin AC overlays had a 55 percent greater increase in  $SN_{eff}$  than sections with recycled AC overlays.
    - Sections with intensive surface preparation had a 39 percent greater increase in  $SN_{eff}$  than sections with minimal surface preparation.

## **DISTRESS ANALYSIS**

- Section 040507 had the best overall performance; Section 040502 had the worst overall performance.
- Sections with intensive surface preparation performed better than sections with minimal surface preparation.
- Sections with thick (5-inch) overlays performed better than sections with thin (2-inch) overlays.
- Sections with virgin AC overlays performed better than sections with minimal recycled AC overlays.
- Sections that utilized two of the following rehabilitation features performed better than sections that utilized only one of the following: thick overlay, virgin AC overlay, and intensive preparation.
- Sections that performed the best against structural distresses all had thick (5-inch) overlays. Overlay thickness had a greater effect than overlay material or surface preparation on the pavement's performance against structural distresses.
- Sections that performed the best against environmental distresses all had virgin AC overlays. Overlay material had a greater effect than overlay thickness or surface preparation on the pavement's performance against environmental distresses.
- Sections with greater total asphalt (existing and new) layer thickness showed greater resistance to fatigue cracking.
- Section 040559, the inverted section, performed well in structural distress and poorly in environmental distress, which is consistent with trends among the core sections.
- Section 040560, the ARAC overlay, performed worse in structural distresses than all sections except the two sections with thin overlays and minimal surface preparation (Section 040502 and Section 040505). Section 040559 performed worse in environmental distress than core sections with virgin AC overlays, but better than sections with recycled AC overlays.
- Rutting in all sections was considered minimal and not a critical distress.

## **PROFILE ANALYSIS**

- Rehabilitation completely removed narrow dips in every test section with the exception of the control section (Section 040501), which was not rehabilitated.
- Some aspects of long wavelength roughness survived the rehabilitation in many sections.
- Changing the profiler make in late 2002 confounded the study of changes in the long-wavelength content within the profiles between visits 09 and 10 on every test section.
- Section 040507 and Section 040504, the sections with 5-inch virgin AC overlays, exhibited the smallest post-rehabilitation increase in MRI.
- Section 040502 and Section 040509, the sections with 2-inch recycled AC overlays, exhibited the largest post-rehabilitation increase in MRI.
- Sections 040503, 040505, and 040560 also exhibited a large change in roughness over time.
- Sections 040506, 040508, and 040559 showed a steady rate of increase in roughness over the first 14 years of the study and a more rapid increase in the last few years.

- Sections 040501, 040502, and 040560 had HRI values that were 20 percent or more below the MRI values, signifying the presence of localized distress.
- MRI increased by less than 10 inches/mi over the first seven years after rehabilitation in all test sections except Sections 040502 and 040509, the sections with 2-inch recycled AC overlays.
- Roughness increased the most in test sections with narrow dips at transverse cracks.

The following recommendations are based on these findings:

- An evaluation using current recycled asphalt pavement (RAP) technologies may indicate different trends regarding RAP performance, since RAP technologies, practices, and materials have continued evolving since the time of this study.
- Pavement rehabilitation under similar in situ conditions (i.e., a dry/no-freeze climate, approximately 15 inches of granular base and 4 inches of existing AC with significant fatigue, block cracking, and traffic loading) requires at least 5 inches of new virgin AC material to prevent pavement cracking in the first seven years after rehabilitation or at least 5 inches of new recycled AC material to prevent cracking in the first four years after rehabilitation.
- Using pavement condition indicators in addition to IRI typically provides a better assessment of pavement condition for network-level decision-making.
- The effect of subgrade modulus increasing subsequent to overlay (as seen in this data set and supported theoretically) should be considered as part of pavement design.



## REFERENCES

- Al-Qadi, I. L., H. Wang, P. J. Yoo, and Samer H. Dessouky. 2008. "Dynamic Analysis and In Situ Validation of Perpetual Pavement Response to Vehicular Loading." *Transportation Research Record: Journal of the Transportation Research Board* 2087: 29–39.
- American Association of State Highway and Transportation Officials (AASHTO). 1993. *AASHTO Guide for Design of Pavement Structures*. Washington, D.C.: American Association of State Highway and Transportation Officials.
- Evans, L. D. and A. Eltahan. 2000. *LTPP Profile Variability*. Publication FHWA-RD-00-113. McLean, VA: Federal Highway Administration.
- Hossain, M., Douglas J. Lattin, and Larry A. Scofield. 1996. *SPS-5: Rehabilitation of Asphalt Concrete Pavements. Construction Report*. Phoenix: Arizona Department of Transportation. Unpublished report.
- Huang, Y. H. 1993. *Pavement Analysis and Design*. Englewood Cliffs, NJ: Prentice Hall.
- Karamihas, S. M. 2004. "Development of Cross Correlation for Objective Comparison of Profiles." *International Journal of Vehicle Design* 36(2/3): 173-193.
- Karamihas, S. M. 2005. *Critical Profiler Accuracy Requirements*. Publication UMTRI-2005-24. Ann Arbor: University of Michigan Transportation Research Institute.
- Karamihas, S. M., T. D. Gillespie, S. D. Kohn, and R. W. Perera. 1999. *Guidelines for Longitudinal Pavement Profile Measurement*. NCHRP Report 434. Washington, D.C.: National Cooperative Highway Research Program.
- Lukanen, E. O., R. Stubstad, and R. Briggs. 2000. *Temperature Predictions and Adjustment Factors for Asphalt Pavement*. Publication FHWA-RD-98-085. McLean, VA: Federal Highway Administration.
- Miller, J. S. and W. Y. Bellinger. 2003. *Distress Identification Manual for the Long-Term Pavement Performance Program*. Revised fourth edition. Publication FHWA-RD-03-031. Washington, D.C.: Federal Highway Administration.
- National Cooperative Highway Research Program (NCHRP). 2004. *Guide for Mechanistic-Empirical Design of New and Rehabilitated Pavement Structures*. Washington, D.C.: National Cooperative Highway Research Program.
- Nichols Consulting Engineers. 2010. *Long-Term Pavement Performance (LTPP) Forensic Evaluation: SPS-5 Project (040500): Casa Grande, Arizona*. Unpublished report.
- Perera, R. W., and S. D. Kohn. 2005. *Quantification of Smoothness Index Differences Related to Long-Term Pavement Performance Equipment Type*. Publication FHWA-HRT-05-054. Washington, D.C.: Federal Highway Administration.

- Rada, G. R., C. L. Wu, R. K. Bhandari, A. R. Shekharan, G. E. Elkins, and J. S. Miller. 1999. *Study of LTPP Distress Data Variability*. Publications FHWA-RD-99-074 and FHWA-RD-99-075. Washington, D.C.: Federal Highway Administration.
- Rohde, G. T., and T. Scullion. 1990. *MODULUS 4.0: Expansion and Validation of the MODULUS Backcalculation System*. Research Report No. 1123-3. Austin: Texas State Department of Highways & Public Transportation.
- Sayers, M. W. and S. M. Karamihas. 1996. *Interpretation of Road Roughness Profile Data*. Publication FHWA-RD-00-101. McLean, VA: Federal Highway Administration.
- Sayers, M. W. 1990. "Profiles of Roughness." *Transportation Research Record: Journal of the Transportation Research Board* 1260: 106-111.
- Simpson, A. L. 2001. *Characterization of Transverse Profiles*. Publication FHWA-RD-01-024. McLean, VA: Federal Highway Administration.
- Uhlmeyer, J. S., K. Willoughby, L. M. Pierce, and J. P. Mahoney. 2000. "Top-Down Cracking in Washington State Asphalt Concrete Wearing Courses." *Transportation Research Record: Journal of the Transportation Research Board* 1730: 110-116.

## APPENDIX A: CONSTRUCTION DEVIATIONS

### 040501 (Control Section):

- No deviations noted.

### 040502 (Minimum Restoration):

- There were some problems milling this section. The first passes didn't completely remove the friction course. The remaining material was stripped badly. The section was re-milled. Difficulty was also encountered working a 6-ft milling machine rather than one that could span the entire 12-ft lane.

### 040503 (Minimum Restoration):

- No deviations noted.

### 040504 (Minimum Restoration):

- No deviations noted.

### 040505 (Minimum Restoration):

- Paving began at 6:15 p.m. and ended at 7:40 p.m. However, at 6:40 p.m., the paver had reached station (local) 4+10 and stopped. There was not enough material to finish the section, and no trucks were waiting. The material quantity had been miscalculated. The hot plant had shut down and was being recalibrated for friction course for the next day. Contractor was warned to complete the section or be forced to remove what was done up to now and redo the whole section with new material later when the whole section could be done at once since no transverse joints were allowed (inside the SHRP section). A final load was delivered at 7:30 p.m. and paving continued to the end of the section. Paver stops were frequent. They were at 0+26, 0+52, 0+91, 3+32, 3+48, and 4+10 at 6:40 p.m.; 4+15 at 7:20 p.m.; 4+20 at 7:30 p.m.; and 4+98.

### 040506 (Intensive Restoration):

- Some difficulties were experienced (second lift – layer 4). The first 50 ft were paved before it was determined that the material was too shallow. Contractor removed material behind paver in WP and backed up to beginning. The first 50 ft were repaved and again, it was too shallow. The same removal was done and the first 50 ft were paved for the third time. This time the material was deep enough and paving continued. Stops were recorded at 0+15, 0+42, 4+02, local stations. Paver stops were frequent due to slow delivery of material. Paver stops made 0.5-inch to 1-inch transverse bumps that were not visible after rolling.

**040507 (Intensive Restoration):**

- No deviations noted.

**040508 (Intensive Restoration):**

- No deviations noted.

**040509 (Intensive Restoration):**

- No deviations noted.

**040559 (Intensive Restoration):**

- No deviations noted.

**040560 (Minimum Restoration, ARAC):**

- No deviations noted.

## APPENDIX B: SITE WORK HISTORY

After original construction in April through June 1990, the following maintenance activities were performed:

### **040501 (Control Section):**

- 10/01/96: Taken out of study.

### **040502 (Minimum Restoration):**

- 05/28/98: Fog seal coat (yd<sup>2</sup>).
- 08/23/01: Fog seal coat (yd<sup>2</sup>).
- 05/01/02: Crack sealing (linear feet).
- 04/16/03: Fog seal coat (yd<sup>2</sup>).
- 01/01/09: Taken out of study.

### **040503 (Minimum Restoration):**

- 05/28/98: Fog seal coat (yd<sup>2</sup>).
- 05/01/02: Crack sealing (linear feet).
- 04/16/03: Fog seal coat (yd<sup>2</sup>).
- 01/01/09: Taken out of study.

### **040504 (Minimum Restoration):**

- 05/28/98: Fog seal coat (yd<sup>2</sup>).
- 05/01/02: Crack sealing (linear feet).
- 04/16/03: Fog seal coat (yd<sup>2</sup>).
- 01/01/09: Taken out of study.

### **040505 (Minimum Restoration):**

- 05/28/98: Fog seal coat (yd<sup>2</sup>).
- 08/23/01: Fog seal coat (yd<sup>2</sup>).
- 05/01/02: Crack sealing (linear feet).

- 04/16/03: Fog seal coat (yd<sup>2</sup>).
- 01/01/09: Taken out of study.

**040506 (Intensive Restoration):**

- 05/28/98: Fog seal coat (yd<sup>2</sup>).
- 08/23/01: Fog seal coat (yd<sup>2</sup>).
- 05/01/02: Crack sealing (linear feet).
- 04/16/03: Fog seal coat (yd<sup>2</sup>).
- 08/01/07: Patch pot holes – hand spread, compacted with truck (number of holes).
- 01/01/09: Taken out of study.

**040507 (Intensive Restoration):**

- 05/28/98: Fog seal coat (yd<sup>2</sup>).
- 04/16/03: Fog seal coat (yd<sup>2</sup>).
- 01/01/09: Taken out of study.

**040508 (Intensive Restoration):**

- 05/28/98: Fog seal coat (yd<sup>2</sup>).
- 05/01/02: Crack sealing (linear feet).
- 04/16/03: Fog seal coat (yd<sup>2</sup>).
- 01/01/09: Taken out of study.

**040509 (Intensive Restoration):**

- 05/28/98: Fog seal coat (yd<sup>2</sup>).
- 08/23/01: Fog seal coat (yd<sup>2</sup>).
- 05/01/02: Crack sealing (linear feet).
- 04/16/03: Fog seal coat (yd<sup>2</sup>).
- 01/01/09: Taken out of study.

**040559 (Intensive Restoration, Inverted Design):**

- 05/28/98: Fog seal coat (yd<sup>2</sup>).
- 08/23/01: Fog seal coat (yd<sup>2</sup>).
- 05/01/02: Crack sealing (linear feet).
- 04/16/03: Fog seal coat (yd<sup>2</sup>).
- 01/01/09: Taken out of study.

**040560 (Minimum Restoration, ARAC):**

- 05/28/98: Fog seal coat (yd<sup>2</sup>).
- 08/23/01: Fog seal coat (yd<sup>2</sup>).
- 05/01/02: Crack sealing (linear feet).
- 04/16/03: Fog seal coat (yd<sup>2</sup>).
- 01/01/09: Taken out of study.

## APPENDIX C: ROUGHNESS VALUES

This appendix lists the left International Roughness Index (IRI), right IRI, mean roughness index (MRI), Half-car Roughness Index (HRI), and Ride Number (RN) values for each visit to each Specific Pavement Studies (SPS-5) project section. The roughness values are the average for five repeat runs. The five runs were selected from a group of as many as nine by automated comparison of profiles, as described in the report. Values of standard deviation are also provided for left and right IRI to reveal cases of high variability among the five measurements. However, the screening procedure used to select five repeats usually helped reduce the level of scatter.

The discussion of roughness in the report emphasizes the left and right IRI. Nevertheless, the other indexes do provide useful additional information. MRI is simply the average of the left and right IRI value. HRI is calculated by converting the IRI filter into a half-car model (Sayers 1989). This is done by collapsing the left and right profile into a single profile in which each point is the average of the corresponding left and right elevation. The IRI filter is then applied to the resulting signal. The HRI is very similar to the IRI, except that side-to-side deviations in profile are eliminated. The result is that the HRI value for a pair of profiles will always be lower than the corresponding MRI value. Comparing the HRI and MRI value provides a crude indication of the significance of roll (i.e., side-by-side variation in profile) to the overall roughness. When HRI is low compared to MRI, roll is significant. This is common among asphalt pavements (Karamihas et al. 1995). Certain types of pavement distress, such as longitudinal cracking, may also cause significant differences between HRI and MRI.

Figure C-1 compares the HRI to MRI for all of the profile measurements that are discussed in this appendix, including 670 pairs of roughness values. The figure shows a best fit line with a zero intercept and a line of equality. The slope of the line is 0.830. A typical value for asphalt pavement is about 0.85.

RN has shown a closer relationship to road user opinion than the other indexes (Sayers and Karamihas 1996). As such, it may help distinguish the segments from each other by ride quality. Further, the effect on RN may help quantify the impact of that distress on ride when the roughness of a section is dominated by a particular type of distress. In particular, a very low RN value coupled with moderate IRI values indicates a high level of short-wavelength roughness and potential sensitivity to narrow dips and noise within the profile caused by coarse surface texture.

Table C-1 provides the roughness values, including the date of each measurement and the time (in years) since the site was opened to traffic. Negative values indicate measurements that were made before rehabilitation.

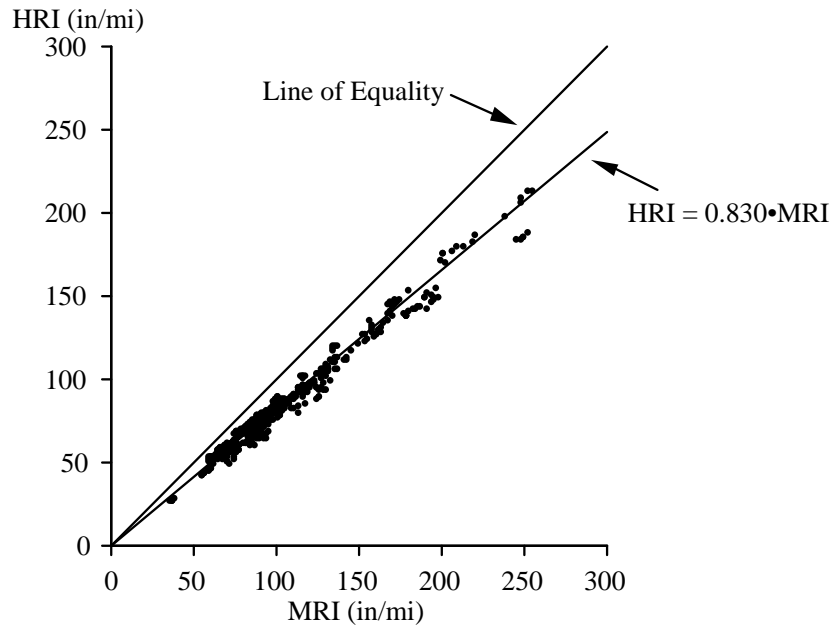


**Figure C-1. Comparison of HRI to MRI**

**Table C-1. Roughness Values**

Section	Date	Years	Left IRI (inch/mi)		Right IRI (inch/mi)		MRI (inch/mi)	HRI (inch/mi)	RN
			Avg	Std Dev	Avg	Std Dev			
040501	05-Feb-90	-0.35	55	7.1	105	10.6	80	64	3.09
040501	21-Sep-90	0.27	63	12.1	100	3.8	82	64	3.01
040501	22-Feb-93	2.70	60	4.8	118	6.6	89	71	2.77
040502	05-Feb-90	-0.35	125	6.5	140	5.8	132	106	2.41
040502	21-Sep-90	0.27	114	2.6	61	1.3	88	78	3.90
040502	22-Feb-93	2.70	114	1.5	66	0.7	90	79	3.80
040502	03-Feb-97	6.64	143	2.0	85	0.6	114	96	3.07
040502	09-Dec-97	7.49	160	4.0	93	1.4	126	105	2.81
040502	11-Dec-98	8.50	150	3.1	119	1.1	134	113	2.59
040502	11-Nov-99	9.41	178	6.7	137	1.7	157	127	2.17
040502	01-Dec-00	10.47	175	2.2	148	1.4	161	130	2.09
040502	15-Nov-01	11.43	176	2.9	179	2.2	178	139	1.85
040502	04-Nov-02	12.39	205	7.8	177	6.7	191	149	1.68
040502	06-Feb-04	13.65	182	4.3	205	1.4	194	150	1.55
040502	14-Dec-04	14.51	164	4.2	204	4.5	184	145	1.62
040502	24-Mar-06	15.78	232	7.6	264	4.5	248	186	1.02
040503	05-Feb-90	-0.35	102	4.7	121	7.4	112	84	2.70
040503	21-Sep-90	0.27	67	2.5	54	0.5	61	53	4.16
040503	22-Feb-93	2.70	68	0.6	54	0.2	61	53	4.07
040503	03-Feb-97	6.64	75	0.7	61	0.6	68	56	3.97
040503	09-Dec-97	7.49	78	0.8	63	0.5	71	59	3.82
040503	11-Dec-98	8.50	74	1.2	68	1.2	71	57	3.73
040503	11-Nov-99	9.41	76	0.4	76	1.1	76	61	3.56
040503	01-Dec-00	10.47	81	0.5	85	0.2	83	68	3.32

**Table C-1. Roughness Values (Continued)**

Section	Date	Years	Left IRI (inch/mi)		Right IRI (inch/mi)		MRI (inch/mi)	HRI (inch/mi)	RN
			Avg	Std Dev	Avg	Std Dev			
040503	15-Nov-01	11.43	86	1.5	107	1.2	96	80	2.94
040503	04-Nov-02	12.39	101	1.0	90	2.6	95	77	2.97
040503	06-Feb-04	13.65	104	2.1	111	2.1	108	90	2.76
040503	14-Dec-04	14.51	87	2.3	138	2.9	112	94	2.61
040503	24-Mar-06	15.78	114	4.2	141	2.2	128	107	2.35
040504	05-Feb-90	-0.35	87	6.5	115	6.8	101	84	2.90
040504	21-Sep-90	0.27	94	1.9	60	2.4	77	69	4.04
040504	15-Jan-92	1.59	100	2.7	65	1.3	83	73	3.98
040504	22-Feb-93	2.70	95	1.7	62	0.9	79	70	3.97
040504	03-Feb-97	6.64	96	0.5	68	0.8	82	70	3.90
040504	09-Dec-97	7.49	99	0.9	68	0.8	84	71	3.82
040504	11-Dec-98	8.50	98	0.7	68	0.8	83	71	3.85
040504	11-Nov-99	9.41	99	0.5	70	0.4	84	72	3.88
040504	01-Dec-00	10.47	100	0.6	71	0.3	86	74	3.87
040504	15-Nov-01	11.43	97	0.5	72	0.5	85	73	3.86
040504	04-Nov-02	12.39	105	1.1	73	0.6	89	76	3.67
040504	06-Feb-04	13.65	103	1.9	76	0.8	89	77	3.65
040504	14-Dec-04	14.51	101	0.5	75	1.1	88	79	3.55
040504	24-Mar-06	15.78	113	0.5	83	0.8	98	85	3.22
040505	05-Feb-90	-0.35	144	8.3	190	4.3	167	138	2.26
040505	21-Sep-90	0.27	79	1.1	84	0.8	82	71	3.95
040505	22-Feb-93	2.70	80	1.7	88	0.7	84	73	3.86
040505	03-Feb-97	6.64	82	1.2	90	0.9	86	71	3.71
040505	09-Dec-97	7.49	88	2.3	89	1.0	88	73	3.58
040505	11-Dec-98	8.50	89	1.5	91	0.3	90	74	3.43
040505	11-Nov-99	9.41	90	2.3	100	0.9	95	80	3.24
040505	01-Dec-00	10.47	95	2.2	103	0.9	99	82	3.13
040505	15-Nov-01	11.43	104	1.6	114	2.1	109	89	2.88
040505	04-Nov-02	12.39	104	4.0	98	3.4	101	80	2.86
040505	06-Feb-04	13.65	112	1.3	123	4.5	117	94	2.69
040505	14-Dec-04	14.51	119	4.2	120	4.4	119	98	2.47
040505	24-Mar-06	15.78	124	2.6	130	4.8	127	97	2.33
040506	05-Feb-90	-0.35	104	8.5	121	5.4	113	91	2.69
040506	21-Sep-90	0.27	71	2.0	59	1.8	65	58	4.09
040506	22-Feb-93	2.70	73	1.1	63	0.5	68	59	4.05
040506	03-Feb-97	6.64	74	0.9	67	0.6	70	58	3.99
040506	09-Dec-97	7.49	77	0.7	67	0.5	72	59	3.89
040506	11-Dec-98	8.50	74	0.5	64	1.0	69	58	3.95
040506	11-Nov-99	9.41	77	0.5	69	0.4	73	60	3.96
040506	01-Dec-00	10.47	76	0.3	69	0.6	72	60	3.97
040506	15-Nov-01	11.43	76	0.9	68	0.6	72	60	3.92
040506	04-Nov-02	12.39	80	0.8	69	0.7	74	61	3.83
040506	06-Feb-04	13.65	77	0.5	74	0.5	76	61	3.54
040506	14-Dec-04	14.51	82	0.6	89	0.6	85	71	2.81
040506	24-Mar-06	15.78	102	1.9	103	0.5	103	88	2.50
040507	05-Feb-90	-0.35	111	8.1	127	4.8	119	97	2.58
040507	21-Sep-90	0.27	103	5.6	63	4.6	83	74	4.01
040507	15-Jan-92	1.59	112	5.1	69	2.4	91	79	3.91

**Table C-1. Roughness Values (Continued)**

Section	Date	Years	Left IRI (inch/mi)		Right IRI (inch/mi)		MRI (inch/mi)	HRI (inch/mi)	RN
			Avg	Std Dev	Avg	Std Dev			
040507	22-Feb-93	2.70	107	1.8	66	2.3	86	76	3.93
040507	03-Feb-97	6.64	112	1.5	69	0.2	90	77	3.84
040507	09-Dec-97	7.49	115	3.8	69	1.9	92	78	3.78
040507	11-Dec-98	8.50	111	1.5	67	0.9	89	77	3.83
040507	11-Nov-99	9.41	111	1.7	68	1.3	90	77	3.85
040507	01-Dec-00	10.47	114	0.6	70	0.2	92	80	3.82
040507	15-Nov-01	11.43	110	0.5	68	0.8	89	77	3.85
040507	04-Nov-02	12.39	122	1.8	76	0.9	99	84	3.64
040507	06-Feb-04	13.65	119	1.7	71	1.3	95	81	3.69
040507	14-Dec-04	14.51	104	1.1	63	1.1	84	75	3.81
040507	24-Mar-06	15.78	113	1.4	71	0.7	92	80	3.66
040508	05-Feb-90	-0.35	93	5.0	113	3.9	103	83	2.72
040508	21-Sep-90	0.27	64	0.5	54	0.8	59	54	4.27
040508	22-Feb-93	2.70	65	0.6	55	0.5	60	54	4.21
040508	03-Feb-97	6.64	65	0.4	58	1.0	62	54	4.14
040508	09-Dec-97	7.49	67	1.0	58	0.7	62	54	3.98
040508	11-Dec-98	8.50	65	0.3	59	0.4	62	55	4.05
040508	11-Nov-99	9.41	68	0.2	60	0.4	64	56	4.11
040508	01-Dec-00	10.47	71	0.2	62	0.2	66	59	4.04
040508	15-Nov-01	11.43	72	0.5	63	0.5	67	59	3.89
040508	04-Nov-02	12.39	76	0.9	63	0.4	70	60	3.73
040508	06-Feb-04	13.65	78	1.2	69	0.6	74	64	3.57
040508	14-Dec-04	14.51	78	1.1	68	0.6	73	64	3.55
040508	24-Mar-06	15.78	90	1.1	77	0.9	84	71	3.25
040509	05-Feb-90	-0.35	171	5.1	141	5.5	156	130	2.18
040509	21-Sep-90	0.27	69	0.5	61	1.7	65	59	4.15
040509	22-Feb-93	2.70	72	0.9	65	0.6	68	61	4.06
040509	03-Feb-97	6.64	79	0.4	74	0.5	77	68	3.72
040509	09-Dec-97	7.49	87	1.0	78	1.4	83	73	3.45
040509	11-Dec-98	8.50	98	1.4	100	1.5	99	89	2.88
040509	11-Nov-99	9.41	123	1.2	108	0.4	115	102	2.49
040509	01-Dec-00	10.47	141	1.4	127	2.6	134	120	2.20
040509	15-Nov-01	11.43	173	1.5	166	5.0	169	147	1.78
040509	04-Nov-02	12.39	188	11.1	141	12.7	164	141	1.94
040509	06-Feb-04	13.65	203	7.6	200	12.2	202	175	1.62
040509	14-Dec-04	14.51	168	18.5	246	15.2	207	177	1.59
040509	24-Mar-06	15.78	249	3.1	246	15.7	248	209	1.28
040559	05-Feb-90	-0.35	146	13.4	121	2.3	134	106	2.61
040559	22-Feb-93	2.70	71	0.8	79	0.4	75	68	3.94
040559	03-Feb-97	6.64	71	1.2	81	0.3	76	67	3.91
040559	09-Dec-97	7.49	77	1.4	81	1.1	79	70	3.81
040559	11-Dec-98	8.50	76	0.7	79	0.9	78	69	3.86
040559	11-Nov-99	9.41	75	0.8	81	0.5	78	69	3.88
040559	01-Dec-00	10.47	76	0.3	83	0.5	79	71	3.83
040559	15-Nov-01	11.43	80	0.7	83	0.4	82	72	3.67
040559	04-Nov-02	12.39	77	0.7	87	1.2	82	71	3.57
040559	06-Feb-04	13.65	84	0.7	83	0.9	83	71	3.47
040559	14-Dec-04	14.51	87	1.0	86	0.7	86	74	3.37

**Table C-1. Roughness Values (Continued)**

Section	Date	Years	Left IRI (inch/mi)		Right IRI (inch/mi)		MRI (inch/mi)	HRI (inch/mi)	RN
			Avg	Std Dev	Avg	Std Dev			
040559	24-Mar-06	15.78	103	1.0	96	1.0	99	84	2.88
040560	05-Feb-90	-0.35	113	22.9	146	11.9	130	106	2.70
040560	22-Feb-93	2.70	60	0.9	50	0.6	55	44	4.14
040560	03-Feb-97	6.64	61	0.5	56	1.8	58	47	3.99
040560	09-Dec-97	7.49	63	0.7	57	5.1	60	49	3.84
040560	11-Dec-98	8.50	62	0.9	75	2.0	68	54	3.65
040560	11-Nov-99	9.41	68	0.3	74	3.7	71	52	3.54
040560	01-Dec-00	10.47	69	0.9	83	2.2	76	58	3.40
040560	15-Nov-01	11.43	74	0.8	102	1.7	88	66	3.08
040560	04-Nov-02	12.39	84	2.1	89	5.9	86	64	2.96
040560	06-Feb-04	13.65	89	0.3	97	3.1	93	67	2.80
040560	14-Dec-04	14.51	69	1.5	116	8.9	93	73	3.07
040560	24-Mar-06	15.78	99	2.9	152	3.9	125	92	2.17

**REFERENCES**

Karamihas, S. M., T. D. Gillespie, and S. M. Riley. 1995. "Axle Tramp Contribution to the Dynamic Wheel Loads of a Heavy Truck." *Proceedings of the 4th International Symposium on Heavy Vehicle Weights and Dimensions*, Ann Arbor, Michigan. C. B. Winkler (ed.). pp. 425-434.

Sayers, M. W. 1989. "Two Quarter-Car Models for Defining Road Roughness: IRI and HRI." *Transportation Research Record: Journal of the Transportation Research Board* 1215: 165-172.

Sayers, M. W. and S. M. Karamihas. 1996. "Estimation of Rideability by Analyzing Longitudinal Road Profile." *Transportation Research Record: Journal of the Transportation Research Board* 1536: 110-116.

## APPENDIX D: DETAILED OBSERVATIONS

This appendix provides detailed observations from the roughness trends, profiles, and distress surveys of each section within the Specific Pavement Studies (SPS-5) project. Investigators used power spectral density (PSD) plots, filtered elevation profile plots, and roughness profiles to monitor profile features.

Typically, roughness profiles provided the most information about the location of features that affected the IRI most, including areas of localized roughness. In this appendix, roughness profiles were displayed using a base length of either 10 ft (called a very short interval roughness profile) or 25 ft (called a short interval roughness profile) unless otherwise specified. An area has localized roughness when the short interval roughness profile reaches a peak value that is greater than 2.5 times the average IRI for the whole section. This usually prompted more careful examination of the filtered elevation profiles.

The PSD plots were less informative, since few of the profiles were dominated by periodic content.

### SECTION 040501

#### Roughness

The right side of the lane was much rougher than the left. This section was taken out of study after three visits, and no significant change in roughness occurred during that time. The average HRI for each visit was about 20 percent lower than the MRI. This is a larger difference than was observed on most other sections, which may signify the presence of localized roughness that appears in only one side of the lane.

#### PSD

The PSD plots were typical for asphalt pavement. They did not change significantly with time.

#### Filtered Elevation Profiles

- **Long wavelengths:** The long-wavelength content of the profiles was very consistent through time.
- **Medium wavelengths:** The medium-wavelength elevation plots were not consistent throughout the four visits. In addition, the profiles were not very repeatable within a given visit. Nevertheless, the overall roughness level appeared to be about the same in each profile.
- **Short wavelengths:** The short-wavelength elevation plots were not very consistent between visits or very repeatable within a given visit. The exception was the appearance of some narrow dips throughout the left side profile.

## **Roughness Profile**

A very short interval roughness profile showed that the section included multiple areas of localized roughness. However, the location where localized roughness appeared was rarely the same in multiple visits.

## **Distress Surveys**

The manual distress survey (MDS) measurements recorded block cracking, alligator cracking, and pumping in both wheel paths (WPs). This explains the difficulty with repeatability and consistency with time.

## **SECTION 040502**

### **Roughness**

Rehabilitation decreased the IRI of the left side by 9 percent and the IRI of the right side by 56 percent. The left side IRI was quite high after rehabilitation and grew at an inconsistent rate over the next 16 years. The left IRI showed a total increase of about 118 inches/mi. The right side IRI grew at a faster rate and increased by nearly 160 inches/mi.

The HRI was 11 percent below the MRI just after rehabilitation. This gap grew steadily to 25 percent by visit 13. The increasing difference between HRI and MRI indicates a lesser relationship between features in the left and right profiles, and may signify the presence of localized roughness or distress that appeared in only one side of the lane.

### **PSD**

The PSD plots for visits 00 and 01 showed a similar level of roughness for wavelengths greater than 30 ft, but major changes for wavelengths smaller than 30 ft.

Both the left and right PSDs included roughness that was concentrated at wavelengths near 10.9 ft. While this periodic roughness was present for the right side profile, it was a dominant portion of the roughness in the left side profile (see Figure 82). In fact, concentrated roughness in the waveband between 8 and 13 ft was probably responsible for the high IRI values after rehabilitation on the left side.

For the right side profile, the PSD did not change in visits 01 through 12 for wavelengths greater than 30 ft, but the range for wavelengths below 30 ft increased steadily with time. For the left profile, the PSD also did not change in visits 01 through 12, except for a steady increase in the range for wavelengths below 7 ft. (See Figure 82.) It is possible that roughness in the wavelength range from 7 to 30 ft also increased with time. However, the high content in the range from 8 to 13 ft overshadowed the progression.

## Filtered Elevation Profiles

- **Long wavelengths:** After rehabilitation, the long-wavelength content of the profiles was consistent through time. A slight change occurred between visits 09 and 10, which was caused by the change in profiler make and the associated difference in high-pass filtering techniques. Rehabilitation also changed long-wavelength elevation traces, but some aspects of the very long wavelength content were still visible.
- **Medium wavelengths:** The periodic content within the left side profiles dominated the content within the medium-wavelength profile plots. The periodic content was also visible in the right side profiles as was other roughness. The right side profiles showed a progression in localized rough features (dips) throughout the monitoring history. These features appear more clearly in short-wavelength elevation traces and unfiltered plots.

The elevation profile in the medium-wavelength roughness range after rehabilitation was not at all similar to the profile before rehabilitation.

- **Short wavelengths:** Before rehabilitation (visit 00), the profiles included narrow dips (less than 2 ft wide and 0.05 to 0.25 inches deep) throughout the section. These dips did not appear with a regular spacing.

Over the monitoring history of the section, localized roughness gradually appeared and grew in severity at several locations on each side of the lane. These were usually narrow dips (1 to 2 ft wide) that eventually grew to depths of up to 0.3 inch on the left side of the lane and up to 0.4 inch on the right side of the lane. By visit 13, more than 50 dips appeared on each side of the lane that increased the roughness of the section.

## Roughness Profile

The left side was twice as rough over the first 300 ft of the section than the last 200 ft because the first 300 ft of the section included periodic roughness with a wavelength that varied from 8 to 13 ft and amplitude of as high as 0.1 inch. The last 200 ft did not. The roughness was distributed relatively equally along the right side of the section except for increased roughness in the last 100 ft of the section in visit 13.

No localized roughness appeared in the short interval roughness profile. A very short interval (10 ft) roughness profile showed that the progression in overall roughness was due entirely to the increase in severity of the dips described above.

## Distress Surveys

The MDS measurements showed an increase in cracking on the section throughout its entire monitoring history. By 2002, it appeared that cracking covered the entire section, which explains the aggressive but unsteady increase in roughness, the frequent occurrence of narrow dips within the profiles, and the relative lack of repeatability between runs.

## SECTION 040503

### Roughness

Rehabilitation decreased the IRI of the left side by 34 percent and the IRI of the right side by 56 percent. The MRI grew at an increasing rate over the next 16 years and increased by nearly 67 inches/mi.

### PSD

The PSD plots showed very little change in content for the wavelength range from 30 to 150 ft on either side from visits 01 through 13. On the right side, the wavelength range shorter than 30 ft became steadily rougher over the monitoring history of the section. On the left side, the wavelength range shorter than 15 ft grew steadily in roughness.

PSD plots for visits 00 and 01 were somewhat similar in the wavelength range above 30 ft, but the profiles themselves were not necessarily similar over this entire range because the distribution of roughness within certain wavebands was roughly the same; but that does not necessarily indicate agreement between the profiles. Rehabilitation significantly reduced spectral content for wavelengths below 15 ft.

### Filtered Elevation Profiles

- **Long wavelengths:** After rehabilitation, the long-wavelength content of the profiles was very consistent through time. Rehabilitation also changed long-wavelength elevation traces, but some aspects of the very long wavelength content were still visible, particularly on the left side.
- **Medium wavelengths:** The elevation profile in the medium-wavelength roughness range after rehabilitation was not at all similar to the profile before rehabilitation.

Some features of the medium-wavelength elevation profiles were similar throughout the monitoring history of the section after rehabilitation. However, the roughness did appear to increase with time. In particular, several dips seemed to grow in depth over the last five visits. These features appeared more clearly in short-wavelength elevation traces and unfiltered plots.

- **Short wavelengths:** Before rehabilitation (visit 00), the left profile included narrow dips (less than 2 ft wide and 0.05 to 0.25 inch deep) throughout the section. These dips did not appear with a regular spacing and were rarely evident in the right side profile.

Over the monitoring history of the section, short-duration rough features gradually appeared and grew in severity at several locations on each side of the lane. These were usually narrow dips (1 to 2 ft wide) that eventually grew to depths of up to 0.5 inch on the left side of the lane and up to 0.8 inch on the right side of the lane. On the left side, the dips appeared 107 ft, 129 ft, 144 ft, 170 ft, 187 ft, 213 ft, 231 ft, 250 ft, 283 ft, 308 ft, 341 ft, 359 ft, 393 ft, 417 ft, 437 ft, 447 ft, and 461 ft from the start of the section. On the right side, the dips appeared at 19 ft, 43 ft, 56 ft, 77 ft, 97 ft, 144 ft, 171 ft, 187 ft, 212 ft, 219 ft, 232 ft, 249 ft, 282 ft, 308 ft, 340 ft,

359 ft, 376 ft, 397 ft, 415 ft, 434 ft, 446 ft, 463 ft, and 483 ft from the start of the section. Most of the dips first appeared in visits 04 or 05, and grew in severity over the rest of the monitoring history. The exception was the dip in the left side profile at 107 ft, which was relatively severe through the entire post-rehabilitation history of the section.

A swatch of rough pavement appeared in the right profile at 414 to 446 ft from the start of the section in visit 10. It was not nearly as rough in visits 11 through 13.

### **Roughness Profile**

A very short interval (10 ft) roughness profile showed that the progression in overall roughness was due entirely to the increase in severity of the dips described above. A short interval (25 ft) roughness profile showed that on the right side of the lane, the roughness was distributed relatively equally along the section. On the left side, increased roughness existed in the later visits from 100 to 330 ft.

Isolated roughness (not severe enough to qualify as localized roughness) appeared on the left side at 107 ft from the start of the section in visits 01 through 13. This area stood out because the dip was somewhat wider than the other dips, and it appeared much sooner than the others. The distress survey recorded an area of localized distress in the same location on the left side of the lane.

### **Distress Surveys**

All of the dips listed above appear in locations where MDS measurements reported transverse cracking. Although all of the dips correspond to transverse cracks in the distress survey, not all transverse cracks caused significant roughness in the profile measurements. Note that other sections, such as 040505, 040508, and 040559, also included dips at transverse cracks. However, the dips that occurred at cracks in this pavement section were typically much deeper and progressed in roughness much more aggressively. The swatch of rough profile on the right side from 414 to 446 ft corresponded to a large area of cracking.

## **SECTION 040504**

### **Roughness**

Rehabilitation increased the IRI of the left side by 4 percent and decreased the IRI of the right side by 49 percent. The MRI changed very little (11 inches/mi) over the next 14 years, then increased 10 inches/mi between visits 12 and 13. For all visits after rehabilitation, the left IRI was about 26 to 38 inches/mi higher than the right IRI.

### **PSD**

The PSD plots showed very little change in content for the wavelength range from 3 to 150 ft on either side from visits 03 through 12, but an increase in content shorter than 10 ft between visits 12 and 13. On the right side, very little similarity existed in spectral content between visits 00 (before rehabilitation) and 01 (after rehabilitation). On the left side, some portions of the PSD plot for visits 00 and 01 were

similar, but the profiles themselves were not because the distribution of roughness within certain wavebands was roughly the same; but that does not necessarily indicate agreement between the profiles.

Both the left and right PSDs included roughness that was concentrated at wavelengths near 12 ft. This periodic roughness was a major portion of the roughness in the left side profile and a significant source of roughness in the right side profile. In fact, the concentrated roughness in the waveband between 8 and 13 ft appeared to be responsible for the left to right difference in IRI.

### **Filtered Elevation Profiles**

- **Long wavelengths:** After rehabilitation, the long-wavelength content of the profiles was very consistent through time. Rehabilitation caused major changes in long-wavelength roughness.
- **Medium wavelengths:** Only minor changes in medium-wavelength roughness occurred from visits 01 through 13. The elevation profile in the medium-wavelength roughness range after rehabilitation was not at all similar to the profile before rehabilitation.

The periodic content within the profiles, described above, dominated the content within the medium-wavelength profile plots. In the right side profile, the amplitude of this roughness ranges from 0.04 to 0.12 inch. Over much of the section, the periodic roughness on the left side of the pavement appeared to be more than twice as severe as the right, and lagged the right side by up to 1.5 ft. The rolling process may have caused this roughness, but it would require a roller with a drum diameter of about 3.8 ft. In photo 27 from the construction report (Hossain et al. 1996), it appears that this is possible.

- **Short wavelengths:** Before rehabilitation (visit 00), the left and right profiles included narrow dips (less than 2 ft wide and 0.04 to 0.20 inch deep) throughout the section. These dips were 3 to 25 ft apart and often appeared in the same location on both sides of the lane. Rehabilitation eliminated the dips.

In most locations, short-wavelength elevation plots did not change significantly over the monitoring history of the section. Upper harmonics of the 8 to 13 ft wavelength content and associated periodic roughness dominated the content of the plots.

Over the monitoring history of the section, roughness gradually appeared 64 ft, 108 ft, 147 ft, 190 ft, 313 ft, 362 ft, 397 ft, and 498 ft from the start of the section. These were all either narrow dips (up to 3 ft wide) or narrow dips preceded by a small swell. These first began to appear in visit 04 and grew in severity with time. Their severity grew the most between visits 12 and 13.

## **Roughness Profile**

Roughness was distributed uniformly throughout the section. A very short interval (10 ft) roughness profile showed that the roughness at the dips mentioned above was not significant when compared to the periodic roughness that existed over the length of the section until visit 13.

## **Distress Surveys**

The dip locations listed above corresponded to transverse cracks recorded in the December 5, 2005, distress survey. Every transverse crack except one recorded on that date produced a dip in the profile.

## **SECTION 040505**

### **Roughness**

Rehabilitation decreased the IRI of the left side by 46 percent and the IRI of the right side by 56 percent. The MRI grew at a slightly increasing rate over the next 16 years, and increased a total of 45 inches/mi.

### **PSD**

The PSD plots showed very little change in content for the wavelength range from 15 to 150 ft in visits 01 through 13. However, the roughness at wavelengths below 15 ft steadily increased with time. PSD plots for visits 00 and 01 were similar in the wavelength range above 15 ft, but the profiles themselves were not similar for all wavelengths over 15 ft because the distribution of roughness within certain wavebands was roughly the same; but that did not necessarily indicate agreement between the profiles. Rehabilitation significantly reduced spectral content for wavelengths below 15 ft.

### **Filtered Elevation Profiles**

- **Long wavelengths:** After rehabilitation, the long-wavelength content of the profiles was very consistent through time. Rehabilitation caused only minor changes in the profile elevation plots over the long-wavelength range.
- **Medium wavelengths:** The elevation profile in the medium-wavelength roughness range after rehabilitation was not at all similar to the profile before rehabilitation. Medium-wavelength elevation profiles did not agree very well between visits. Further, rough features rarely showed steady growth in severity with time.
- **Short wavelengths:** Before rehabilitation (visit 00), the left and right profiles included narrow dips (less than 2 ft wide and 0.05 to 0.30 inch deep) throughout the section. These dips were 3 to 25 ft apart and often appeared in the same location on both sides of the lane. Rehabilitation eliminated the dips.

Over the monitoring history of the section, dips gradually appeared and grew in severity in at least 12 locations on each side of the lane. These were usually narrow dips (1 to 2 ft wide) or

wider depressed areas of pavement (i.e., dense groups of narrow dips). Some dips appeared as early as visit 04. Others did not appear until visit 11.

Patches of narrow dips appeared in the profiles of visit 09. These looked like “chatter” in the traces that covered large areas of the profile, especially in the second half of the section. The chatter was either not present or less severe in later visits.

Although the “chatter” in the profiles often appeared as very short wavelength content, they increased the IRI.

### **Roughness Profile**

The second half of the section was somewhat rougher than the first half on the right side in visits 09 and 11. Placement and severity of peaks within the very short interval (10 ft) roughness profile was not as consistent for this section as others within the SPS-5 experiment.

### **Distress Surveys**

MDS measurements indicated a tremendous amount of cracking that began to appear before visit 04. By visit 09, the cracking had consumed large areas of pavement, including major portions of both WPs. Between visits 09 and 10 (May 2002), the cracks were sealed.

The cracking history explains many of the observations listed above. Cracking caused the growth in short-wavelength roughness. When compared to other sections within the SPS-5 site, this section exhibited slight degradation in profile repeatability and inconsistency in placement of roughness because of the hit-or-miss nature of large areas of cracking within each WP. The profiler only measures two narrow tracks and does not experience precisely the same cracks, or the same aspects of each crack, equally in each pass. On the other hand, the overall IRI values were consistent between runs, and the growth in IRI was, for the most part, steady because the cracking covered a wide area of the lane, so the profiler was likely to experience about the same level of cracking in each pass, even if the roughness did not always appear in consistent locations.

The rate of increase in IRI slowed somewhat between visits 09 and 10. The crack sealing that was performed between these visits probably reduced the apparent roughness of the cracking.

## **SECTION 040506**

### **Roughness**

Rehabilitation reduced the IRI of the left side by 32 percent and the IRI of the right side by 51 percent. The MRI showed a modest increase (11 inches/mi) over the next 14 years and a steeper increase (27 inches/mi) over the next two years.

## PSD

The PSD plots showed very little change in content for the wavelength range from 2 to 100 ft on either side over visits 01 through 11, but increased in content for wavelengths shorter than 10 ft afterward. PSD plots for visits 00 and 01 were similar in the wavelength range above 20 ft, but the profiles themselves were not because the distribution of roughness within certain wavebands was roughly the same; but that does not necessarily indicate agreement between the profiles. Rehabilitation significantly reduced spectral content for wavelengths below 20 ft.

## Filtered Elevation Profiles

- **Long wavelengths:** After rehabilitation, the long-wavelength content of the profiles was very consistent through time. Rehabilitation also changed long-wavelength elevation traces, but a few aspects of the very long wavelength content were still visible.
- **Medium wavelengths:** Only minor changes in medium-wavelength roughness occurred from visits 01 through 13. The elevation profile in the medium-wavelength roughness range after rehabilitation was not at all similar to the profile before rehabilitation.
- **Short wavelengths:** Before rehabilitation (visit 00), the left and right profiles included narrow dips (less than 2 ft wide and 0.05 to 0.15 inch deep) throughout the section. These dips were 3 to 25 ft apart. They often appeared in the same location on both sides of the lane, but were much more prevalent within the left profile. Rehabilitation eliminated the dips.

Over the monitoring history of the section, roughness gradually appeared and grew in severity at some locations: about 132 ft on the right side, about 317 ft on both sides, about 369 ft on the right side, and about 419 ft on both sides. Narrow dips (1 to 2 ft wide) that were 0.10 to 0.25 inch deep caused the roughness. These began to appear in visit 09, and many of them grew in severity over the rest of the monitoring period. By visit 13, narrow dips appeared in both the left and right side profiles 22 ft, 50 ft, 89 ft, 133 ft, 164 ft, 218 ft, 250 ft, 278 ft, 317 ft, 369 ft, and 419 ft from the start of the section.

## Roughness Profile

A very short interval roughness profile showed that a few of the short-wavelength rough features on the section contributed to the roughness progression. For example, Figure D-1 shows the right roughness profile near a dip with gradually increasing severity. The roughness increases steadily with time at this location. The roughest 10-ft segment that includes the dip increases in severity from 140 inches/mi to 524 inches/mi from visits 01 through 13. Over this interval, the dip grew to a depth of 0.5 inch and a width of 3 ft. This would have an impact of over 7 inches/mi on the overall roughness of the section.

## Distress Surveys

All of the narrow dips listed above occurred in locations where distress surveys indicated the presence of transverse cracks.

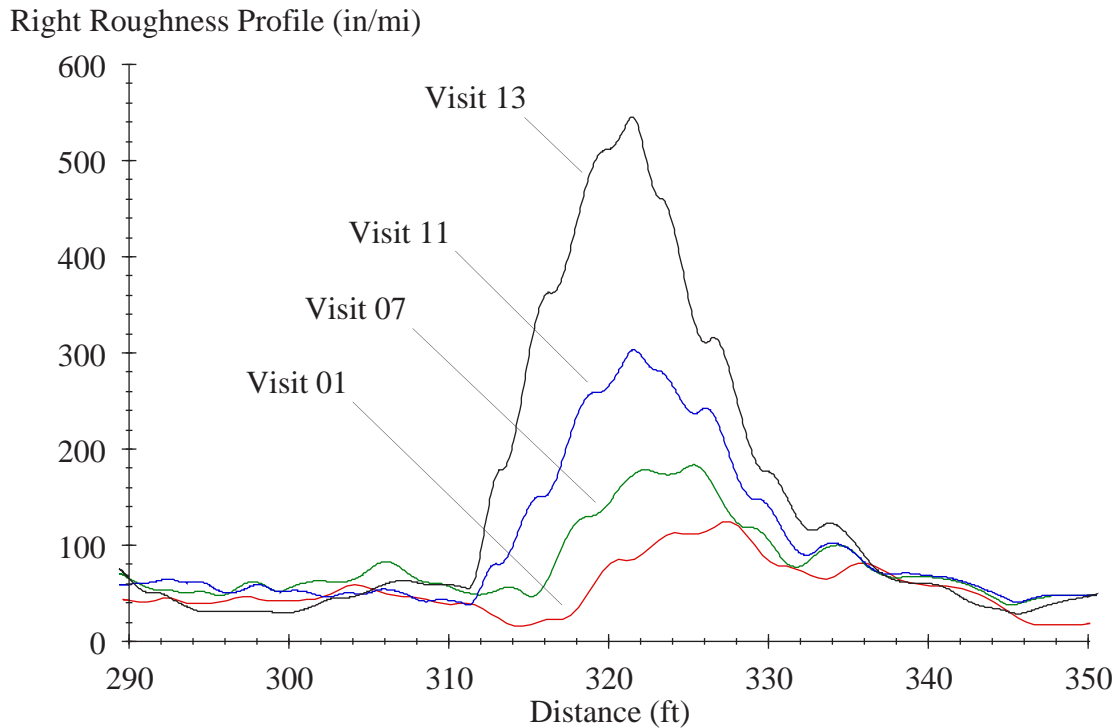


**Figure D-1. Roughness Profiles of Section 040506 (10-ft Base Length)**

## **SECTION 040507**

### **Roughness**

Rehabilitation reduced the IRI of the left side by 7 percent and the IRI of the right side by 50 percent. The MRI showed a modest, but inconsistent, increase (11 inches/mi) over the next 16 years. For all visits after rehabilitation, the left IRI is about 40 to 47 inches/mi higher than the right IRI.

### **PSD**

The PSD plots showed very little change in content for the wavelength range from 5 to 150 ft on either side over the 16 years after rehabilitation. On the right side, very little similarity existed in spectral content between visits 00 (before rehabilitation) and 01 (after rehabilitation). On the left side, some portions of the PSD plot for visits 00 and 01 were similar, but the profiles themselves were not because the distribution of roughness within certain wavebands was roughly the same; but that did not necessarily indicate agreement between the profiles.

Both the left and right PSDs included roughness that was concentrated at wavelengths near 12 ft. While this periodic roughness was significant for the right side profile, it was a major portion of the roughness in the left side profile. In fact, it appears that concentrated roughness in the waveband between 8 and 13 ft was responsible for the left to right difference in IRI.

## Filtered Elevation Profiles

- **Long wavelengths:** After rehabilitation, the long-wavelength content of the profiles was very consistent through time. Rehabilitation caused major changes in long-wavelength roughness.
- **Medium wavelengths:** Only minor changes in medium-wavelength roughness occurred from visits 01 through 13. The elevation profile in the medium-wavelength roughness range after rehabilitation was not at all similar to the profile before rehabilitation.

The periodic content within the profiles, described above, dominated the content within the medium-wavelength profile plots. Over much of the section, it appeared that the periodic roughness on the left side of the pavement was more than twice as severe as the right and lagged the right side by about 1.5 ft. The rolling process may have caused this roughness, but it would require a roller with a drum diameter of about 3.8 ft. In photo 27 from the construction report (Hossain et al. 1996), it appears that this is possible.

- **Short wavelengths:** Before rehabilitation (visit 00), the left and right profiles included narrow dips (less than 2 ft wide and 0.05 to 0.10 inch deep) throughout the section. These dips were 3 to 25 ft apart and often appeared in the same location on both sides of the lane. Rehabilitation eliminated the dips.

Short-wavelength elevation plots did not change significantly over the monitoring history of the section through visit 12. Upper harmonics of the 8 to 13 ft wavelength content and associated periodic roughness dominated the content of the plots. In visit 13, a bump appeared about 70 ft from the start of the section that was 0.25 inch high on the left side and 0.15 ft high on the right.

## Roughness Profile

Roughness was distributed uniformly throughout the section. The bump that appeared in visit 13 did not affect the roughness significantly.

## Distress Surveys

No significant localized roughness existed within the section that could be linked to distress. The distress surveys listed few cracks, although a crack was recorded about 70 ft from the start of the section.

## SECTION 040508

### Roughness

Rehabilitation reduced the IRI of the left side by 31 percent and the IRI of the right side by 51 percent. The MRI showed only a modest increase (25 inches/mi) over the next 16 years.

## PSD

The PSD plots showed very little change in content for the wavelength range from 4 to 150 ft on the left side for visits 01 through 09, and then showed an increase in roughness for wavelengths shorter than 6 ft between visits 09 and 10. The right side PSD plots did not agree as well as the left, but were consistent in the wavelength range from 10 to 150 ft for visits 01 through 13. The right side PSD plots also showed steadily increasing roughness for wavelengths shorter than 6 ft. Very little similarity existed in spectral content between visits 00 (before rehabilitation) and 01 (after rehabilitation).

## Filtered Elevation Profiles

- **Long wavelengths:** Rehabilitation also caused major changes in long-wavelength roughness, but the very long-wavelength content was not altered much in the second half of the section.
- **Medium wavelengths:** Only minor changes in medium-wavelength roughness occurred from visits 01 through 13. The elevation profile in the medium-wavelength roughness range after rehabilitation was not at all similar to the profile before rehabilitation.
- **Short wavelengths:** Before rehabilitation (visit 00), the left and right profiles included narrow dips (about 2 ft wide and 0.05 to 0.30 inch deep) throughout the section. These dips were 5 ft or more apart and appeared to have uniform spacing over some parts of the section. Rehabilitation eliminated the dips. Narrow dips did not begin to appear again until visit 08. These were all either narrow dips (up to 2 ft wide), narrow dips preceded by a small swell, or small (0.1 inch) downward steps. None of these dips appeared to correspond to localized roughness that existed before rehabilitation.

## Roughness Profile

Very short interval roughness profiles showed that few of the dips within the section added significantly to the roughness progression. Although they were easily detected in the profile, most of these features caused very little overall roughness. Two exceptions were the dips on the left profile that appeared about 15 ft and 427 ft from the section start.

## Distress Surveys

All of the dips found in profiles from the later visits appeared near locations where distress surveys indicated the presence of transverse cracks. The transverse cracking at these locations was either detected by the distress survey in the same year that evidence first appeared in the profiles or a year or two earlier. Thus, it was typical to see evidence of the cracking in the profiles for visits 09 through 13, but rarely in visits 01 through 06. The distress survey in November 1997 found very few cracks. Many cracks were listed in the distress survey that did not cause a dip in the corresponding profile.

## SECTION 040509

### Roughness

Rehabilitation decreased the IRI of the left side by 59 percent and the IRI of the right side by 57 percent. The MRI grew at an increasing rate over the next 16 years and increased 183 inches/mi.

### PSD

Rehabilitation, performed between visits 00 and 01, greatly reduced the roughness for wavelengths below 15 ft and changed the content at wavelengths above 15 ft. After rehabilitation, the PSD plots showed an aggressive growth in roughness for wavelengths below 30 ft. The content for wavelengths above 30 ft was steady with time.

### Filtered Elevation Profiles

- **Long wavelengths:** After rehabilitation, the long-wavelength content of the profiles was somewhat consistent through time. Rehabilitation changed the long-wavelength elevation plots for this section, but many of the very long wavelength traits survived the overlay.
- **Medium wavelengths:** The elevation profile in the medium-wavelength roughness range after rehabilitation was not at all similar to the profile before rehabilitation. Medium-wavelength elevation profiles showed a progression in rough features (dips) throughout the monitoring history. These features appear more clearly in short-wavelength elevation traces and unfiltered plots.
- **Short wavelengths:** Before rehabilitation (visit 00), the profiles included narrow dips (less than 3 ft wide and 0.05 to 0.35 inch deep) throughout the section. These dips were 3 to 25 ft apart and often appeared on both sides, but were relatively shallow (0.05 to 0.10 ft wide).

Over the monitoring history of the section, narrow dips gradually appeared and grew in severity in at least 20 locations on each side of the lane. These narrow dips (1 to 2 ft wide) eventually grew to depths of 0.10 to 0.75 inch. Most of these dips first appeared in visits 04 through 06, and all appeared in visit 13. On the left side, the most severe dips appeared 13 ft, 33 ft, 52 ft, 73 ft, 95 ft, 105 ft, 115 ft, 128 ft, 145 ft, 161 ft, 176 ft, 192 to 195 ft, 204 ft, 214 ft, 228 ft, 244 ft, 266 ft, 286 ft, 298 ft, 342 ft, 373 ft, 401 ft, 414 ft, 433 ft, 450 ft, and 471 ft from the start of the profile. Figure 85 shows an example of one of these dips and its progression in depth from visits 04, 07, and 11. The dips all appeared on the right side as well. On the right side, deep dips also appeared 60 ft, 113 ft, 189 ft, 322 ft, and 356 ft from the start of the profile.

### Roughness Profile

A very short interval (10 ft) roughness profile showed that the progression in overall roughness was due entirely to the increase in severity of the dips described above with time. Figure 88 illustrates this for the

first half of the section. Roughness at the dips progressed aggressively over time, but the roughness between the dips was steady.

### **Distress Surveys**

All of the dips listed above appear in locations where MDS measurements reported cracks. In most cases, these transverse cracks covered the entire width of the lane. Note that other sections, such as 040505, 040508, and 040559, also included dips at transverse cracks. However, the dips that occurred at cracks in this pavement section were typically much deeper and progressed in roughness much more aggressively.

### **SECTION 040559**

#### **Roughness**

Rehabilitation reduced the IRI of the left side by 51 percent and the IRI of the right side by 35 percent. The MRI showed only a modest increase (24 inches/mi) over the next 16 years.

#### **PSD**

The PSD plots showed an increase in roughness for wavelengths shorter than 6 ft between visits 07 and 08, and an increase in roughness for wavelengths shorter than 15 ft between visits 09 and 10. The spectral content also increased for wavelengths from 1 to 10 ft between visits 12 and 13. This was caused by localized roughness rather than periodic roughness. Rehabilitation, performed between visits 00 and 01, greatly reduced the roughness for wavelengths below 15 ft, but caused little change in the overall level of roughness for wavelengths longer than 15 ft.

#### **Filtered Elevation Profiles**

- **Long wavelengths:** Rehabilitation caused some change in long-wavelength roughness, but the very long wavelength content was barely altered.
- **Medium wavelengths:** Only minor changes in medium-wavelength roughness occurred from visits 04 through 13. The elevation profile in the medium-wavelength roughness range after rehabilitation was not at all similar to the profile before rehabilitation.
- **Short wavelengths:** Before rehabilitation (visit 00), the left profile included narrow dips (2 to 7 ft wide and 0.10 to 0.35 inch deep) throughout the section. These dips were 5 to 25 ft apart and appeared to have uniform spacing over some parts of the section. In many locations, they also appeared in the right profile, but were not as severe. Rehabilitation eliminated the dips.

Over the monitoring history of the section, roughness gradually appeared and grew in severity at several locations: (1) 70 ft, 128 ft, 150 ft, 221 ft, 291 ft, 337 ft, and 427 ft on both sides; (2) 39 ft, 106 ft, 202 ft, 248 ft, 307 ft, 357 ft, 389 ft, and 441 ft on the left side only; and (3) 28 ft and 108 ft on the right side only. These were all either narrow dips (up to 3 ft wide) or narrow dips preceded by a small swell. Most of these first appeared in visits 09 or 10. By visit 13, some

of the dips included a downward change in elevation of up to 0.4 inch from the top of the swell to the bottom of the dip.

The most severe dip occurred about 150 ft from the start of the profile on the left side. This was 5 ft wide that increased in depth throughout the monitoring history of the section until it was 0.4 inch deep. Few of the dips appeared where narrow dips existed before rehabilitation.

### **Roughness Profile**

A very short interval (10 ft) roughness profile showed that few of the rough features on the section added significantly to the roughness progression until visit 13. The dip that appeared 150 ft from the start of the section qualified as localized roughness on the left side in visit 13. A dip on the right side that was 70 ft from the start of the section nearly qualified in visit 13.

### **Distress Surveys**

The dip locations listed above correspond to sealed cracks that were recorded in the distress survey on December 12, 2003. The localized roughness in the left profile that appear 150 ft from the start of the section was near a transverse crack (at 146 to 150 ft) that was observed in all distress surveys since September 1996, which was before profiler visit 04. Further, longitudinal cracking was observed in the left WP in distress surveys starting in December 1999.

## **SECTION 040560**

### **Roughness**

Rehabilitation reduced the IRI of the left side by 45 percent and the IRI of the right side by 64 percent. The MRI grew at an increasing rate over the next 16 years, and increased 70 inches/mi overall. The average HRI for each visit was between 19 percent and 28 percent lower than the MRI. This was a larger difference than was observed on most other sections, which indicates a lesser relationship between the left and right profiles, and may signify the presence of localized roughness caused by distress that appeared in only one side of the lane.

### **PSD**

The PSD plots showed very little change in content for the wavelength range from 15 to 150 ft in visits 01 through 13. However, the roughness at wavelengths below 15 ft steadily increased with time. PSD plots for visits 00 and 01 were very similar in the wavelength range above 30 ft. Rehabilitation significantly reduced spectral content for wavelengths below 15 ft.

### **Filtered Elevation Profiles**

- **Long wavelengths:** Rehabilitation did not change the long-wavelength elevation plots for this section significantly. After rehabilitation, the long-wavelength content of the profiles was somewhat consistent through time.

- **Medium wavelengths:** Medium-wavelength elevation plots were similar throughout visits 03 through 11. However, on the left side, some features progressed in severity with time. On the right side, a large area of the section from 240 to 400 ft from the start changed properties significantly over the monitoring history, particularly from visits 07 through 11. The medium-wavelength content was significantly rougher in the right side in visits 12 and 13 than in visit 11.

The elevation profile in the medium-wavelength roughness range after rehabilitation was not at all similar to the profile before rehabilitation on the right side, but exhibited weak correlation to the profile before rehabilitation on the left side.

- **Short wavelengths:** Before rehabilitation (visit 00), the left profile included narrow dips (about 2 ft wide and 0.05 to 0.20 inch deep) throughout the section. These dips were 5 to 50 ft apart. In many locations, they also appeared in the right profile, but were not as severe. Rehabilitation eliminated the dips.

For visits 03 through 13, short-wavelength elevation plots were not very repeatable within a given visit. This seemed to get progressively worse throughout the monitoring history of the pavement, which explains some of the relatively low correlation values listed in Table 72. As such, the progression of rough features at individual locations was not consistent through time. Nevertheless, some trends were obvious. For example, patches of elevated short-wavelength content appeared and increased in severity in the right side profile from visits 03 through 06. These appeared from 65 to 85 ft, 240 to 265 ft, 280 to 295 ft, and 310 to 345 ft. In later visits, these areas became even rougher, although the details of the profile shape from the earlier visits were not evident in the later visits. In visits 11 through 13, about half of the length of the right side profile included high short-wavelength content.

### **Roughness Profile**

A very short interval (10 ft) roughness profile showed that the areas of elevated short-wavelength roughness did increase the IRI over time, particularly on the right side of the lane. However, no single area stood out as dominating the roughness of this section.

### **Distress Surveys**

Distress surveys reported a tremendous amount of cracking that began to appear before visit 04 and became progressively more prevalent and severe throughout the rest of the monitoring history. Some of the distress surveys also listed pumping in some areas. The cracking often first appeared as longitudinal cracks along a WP and progressed to large areas of cracking in later visits.

The distress history explained many of the observations listed above. The appearance and growth of patches of short-wavelength roughness over time was consistent with distress surveys. The hit-or-miss nature of profiling large areas of cracking also explained the relatively low correlation values for repeatability within a given visit to the site. The profiler only measured two narrow tracks and did not experience precisely the same cracks, or the same aspects of each crack, equally in each pass. On the

other hand, the overall IRI values showed a steady growth with time, and each area of the overall section seemed to grow in roughness steadily. This occurred because the cracking covered a wide area of the lane, so the profiler was likely to experience about the same level of cracking in each pass, even if the shape of the profile did not always appear in consistent locations.

## **REFERENCES**

Hossain, M., Douglas J. Lattin, and Larry A. Scofield. 1996. *SPS-5: Rehabilitation of Asphalt Concrete Pavements. Construction Report*. Phoenix: Arizona Department of Transportation. Unpublished construction report.





